UNIVERSIDADE DE LISBOA

FACULDADE DE CIÊNCIAS

Ciências
ULisboa

Dynamics of laminin niches during muscle development and disease

Doutoramento em Biologia
Biologia do Desenvolvimento

Andreia Marcelino Nunes

Tese orientada por:
Sólveig Thorsteinsdóttir e Marianne Deries

Documento especialmente elaborado para a obtenção do grau de doutor

2017

UNIVERSIDADE DE LISBOA

FACULDADE DE CIÊNCIAS

Dynamics of laminin niches during muscle development and disease

Doutoramento em Biologia

Biologia do Desenvolvimento

Andreia Marcelino Nunes

Tese orientada por:

Sólveig Thorsteinsdóttir e Marianne Deries

Júri:

Presidente:

- Maria Margarida de Mello dos Santos Reis Gutterres da Fonseca

Vogais:

- José António Henriques Conde Belo
- Maria José Cardoso Oliveira
- Diana Esperança dos Santos Nascimento André
- Maria Leonor Tavares Saúde
- Edgar Rodrigues Almeida Gomes
- Sólveig Thorsteinsdóttir

Documento especialmente elaborado para a obtenção do grau de doutor

Fundação para a Ciência e Tecnologia

2017

The work presented in this dissertation was developed with the support from the Fundação para a Ciência e Tecnologia, through a PhD Fellowship (SFRH/BD/86985/2012) and the Project Grant (PTDC/SAU-BID/120130/2010), Association Française contre les Myopathies Téléthon (contract nº 19959), Cure CMD, Struggle Against Muscular Dystrophy (SAM) and NIH/NIAMS Project Grant (R01AR064338-01A1).

Nota Prévia

Na elaboração da presente dissertação, e nos termos do nº1 do Artigo 45, do Regulamento de Estudos Pós-Graduados da Universidade de Lisboa, publicado no Diário da República, 2ª série, nº 65 de 30 de Março de 2012, foi usado integralmente um artigo científico publicado numa revista científica internacional indexada. Uma vez que os trabalhos referidos foram efectuados em colaboração com outros investigadores, o autor desta dissertação esclarece que participou integralmente na concepção e execução do trabalho experimental, na análise, interpretação e discussão dos resultados, assim como na redação dos manuscritos.

To my family and friends!

“Here's to the crazy ones. The misfits. The rebels. The troublemakers. The round pegs in the square holes. The ones who see things differently. They're not fond of rules. And they have no respect for the *status quo*. You can quote them, disagree with them, glorify or vilify them. About the only thing you can't do is ignore them. Because they change things. They push the human race forward. And while some may see them as the crazy ones, we see genius. Because the people who are crazy enough to think they can change the world, are the ones who do.”

Rob Siltanen

Agradecimentos/Acknowledgments

Em primeiro lugar, gostaria de agradecer à Sólveig por ter-me dado uma oportunidade quando mais precisava. Por alguma razão acreditaste em mim e eu nunca vou esquecer isso. Agradeço-te por toda a generosidade, preocupação e amizade. Não são precisas muitas palavras para dizer que foi sempre com um sorriso que fui trabalhar para o laboratório e que podia contar com o teu apoio e ajuda quando algo corria menos bem. Foste sempre uma presença serena que me trasmitiu entusiasmo e gosto por fazer Ciência. Tive uma enorme sorte de seres a minha mentora e ter aprendido contigo. Vou levar comigo tudo o que aprendi! Para finalizar, não quero deixar de agradecer todas as conversas sobre os mais variados temas e todo o carinho que sempre me transmitiste.

I would also like to thank Marianne, my co-supervisor, for your always encouraging and optimistic words, and for all the advice that you gave me throughout my PhD. Thank you for the fun times and for always bringing an easygoing mood into the lab.

I would like to thank Dean for everything he has done for me and for believing in me. Your lab is really the reflection of your personality. It was always so much fun to work in your laboratory. There was always time to go out for lunch to celebrate the good news or to go to movies in the morning session. I always felt that I was part of the group even if I was officially a collaborator.

Tive sempre imensa sorte de poder trabalhar em grupos animados e cheios de boa disposição. Gostava de agradecer em primeiro lugar ao meu grupo em Portugal. Quero agradecer a todos os membros passados do grupo com quem convivi: Raquel Vaz, Pedro Rifes, Gonçalo Pinheiro e psôr Gabriel. Quero também agradecer aos membros presentes do grupo. À Gabriela, companheira de gargalhadas nas mais disparatadas ideias, principalmente durante os lab meetings! Quero agradecer ao André e ao Luís por terem sempre piadas na carteira para manter os almoços animados. Luís, surpreendes-me sempre com a tua cultura nos mais variados temas :p... André, contemporâneo nesta saga do PhD, obrigado por teres sempre contigo esse espírito relaxado. Quero também agradecer à Marta, um membro não efectivo do nosso grupo, mas uma BDiana de coração. A diversão durante os almoços também não seria a mesma sem ti. Obrigada pela amizade e por poder contar sempre contigo para qualquer problema. Quero ainda agradecer à Inês por todo o companheirismo e amizade. Estes útimos meses foram duros, mas tu fizeste com que fossem mais fáceis e tornaste tudo mais divertido e especial com a tua companhia e carinho. Não trocava a "minha" mestranda por nenhum outro estudante e quero manter-te sempre presente, vá para onde for! Por fim, mas não de todo em último lugar, queria agradecer à Patrícia. Não só porque fazes parte do meu dia-a-dia, mas também porque fazes parte do grupo de amigos próximos. És e serás sempre

a minha “sister from another mister”, por isso, não é uma surpresa teres estado sempre presente para amparar as minhas quedas e para festejar comigo nos momentos altos. Obrigado por deixares que eu desfrute da pessoa extraordinária que és. Não importam os 20 ou vários milhares de quilómetros de distância, porque o Skype estará lá sempre para dar uma mãozinha...

I would also like to thank my american group. Merica! Everyone made me feel at home, even if I was miles away from home. The joy of everyone is contagious and I had an amazing time with everyone. I would like to thank Apurva, Ryan, Pam, Paul, Becky, Tatiana, Pamela, Vivian, Ashley, Keely and Suzann. I would like to thank Ryan for being a mentor to me and for teaching me so much in a few months. And ah, for all your attempts to mock me too... I would also like to thank Pam for her generosity and for all the help in the lab. I would like to thank Paul for his OCD with the hood and for protecting us from everything in the lab. And for creating a jungle in the lab too… I would like to thank Becky for all the help in the lab and outside of the lab. You were always ready for a good laugh in the free times. I would like to thank to my “girls”. Vivian for being a sweet and caring friend. Tats, my Portuguese carago fellow, for your energy, partnership and help. And to Pamelita, my mexican chica, for always helping and taking care of me (even in awkward situations...). Thank you for being awesome lab mates and friends. Finally, I would like to thank to my buddy Apurva for the amazing friend she is. You made so much for me that I can’t thank you enough. You truly made my experience in the States unforgettable and I want to cherish your friendship forever.

Gostava ainda de deixar um agradecimento a todas as pessoas da FCUL que sempre estiveram dispostas a ajudar quando precisei. Quero agradecer em especial à Sara Carona, Mónica Silva, Pedro Simões, Ana Neto e Inês Fragata.

Felizmente tenho uma grande lista de amigos a quem agradecer. Quero agradecer aos meus amigos Andreia Rodrigues, Ana Farinha, Alexandra, Joana, Tomás, Inês Albuquerque, Catarina Nabais, Eduardo, Catarina Dourado, Lucas, Rachel, Nelson, Raquel Silva, Andreia Margarido, Sofia Carvalho, Maggie, Diana, Inês Fragata e Josefina. Sou uma sortuda por poder contar com a vossa companhia e amizade. Agradeço à Ana Farinha pelas suas palavras sábias e meigas, à Xana pelo prazer que é estar na tua companhia e por me salvares das dorminhocas em Espanha. À Joana ornitorrinca por seres sempre uma querida e estares presente quando mais preciso. À Inês Albuquerque, pesinho de lama, por seres sempre uma presença calma, confortante e inspiradora. Catarina Nabais, por seres a minha parceira de aventura. A tua energia e espírito são contagiantes, mas mais que isso, sempre estiveste lá quando precisei de apoio. Quero agradecer ao senhor Eduardo Borboleta Marabuto, pela boa disposição e pelas suas maluqueiras! Lucas, obrigado pela tua presença dissimulada, mas atenta e generosa com que posso contar. Rachel, pela tua visão prática nos momentos em que precisei de uma perspectiva diferente. Por seres uma amiga leal e por teres estado sempre presente nos momentos

mais complicados. No fundo esses teus olhos não enganam! Obrigado, Nelson, por seres meigo e o maior tonto de sempre ao mesmo tempo! Raquel Silva, uma "defender marília" meiga, carinhosa e leal a quem posso ligar em qualquer situação, porque sei que estarás lá no momento seguinte! Obrigado à Sofia, por mudares o penteado de cada vez que nos vimos e pelo teu estilo cómico e peculiar. À Maggie, o mini caracolinho coração de manteiga, por poder contar sempre com o teu apoio preciso e prático, mesmo não estando lá todos os dias. Obrigado ao Tomás, camarada benfiquista, por todo o apoio e companhia. Finalmente, agradeço à Andreia, por seres uma amiga carinhosa e pelas conversas quotidianas e pelo apoio constante mesmo a várias centenas de quilómetros.

Por fim, não poderia deixar de agradecer à minha família que me atura desde pequena e que tem estado presente em todos os momentos da minha vida. Por terem sempre acreditado que conseguia alcançar os meus objectivos e pelas reuniões familiares animadas. Um agradecimento especial aos meus pais por terem sempre apoiado nas minhas decisões e por terem ensinado que nada se consegue na vida sem esforço e trabalho. Ensinaram-me os valores mais importantes da vida. Sou a pessoa que sou graças a tudo o que me deram e ensinaram. Em especial, um obrigado à minha mãe por ter dado tudo de si para eu poder chegar onde cheguei. Sem ti, nunca tinha chegado aqui. Agradeço também aos meus irmãos Vanessa e Jorge por estarem presentes com com o seu espírito brincalhão e com as suas "tontices". Aos meu avós Matilde e Manuel, aos meus primos Sara, João e Inês, e aos meus tios: Zé, "o brincalhão caneleiro" sempre na calha para a próxima piada, por manteres sempre a malta animada; Belinha, por seres sempre uma madrinha preocupada e por estares sempre pronta a ajudar; Nela, por teres estado sempre na linha da frente com os teus conselhos para ajudar a empurrar-me para a frente e pela confiança de que eu conseguia chegar ao fim; Nanda, o poço de ternura e mel que nunca mais acaba, sempre disposta a distribuir mimos; Xana, porque uma presença muita calma sempre com energias positivas; e ao Nelo, "o rockeiro coração de manteiga" sempre a observar, mas atento para emergências! E ao resto da família que é gigante mesmo aquela que não vejo tão frequentemente: Nazaré, Maísa, tias Elvira, Natália e Henriqueta, tios Zé e Henrique e primos Nuno, Ana Rita, Ana Luísa, Mário, entre muitos outros familiares.

Contents

Abstract

The development of skeletal and cardiac muscles are complex processes which start early in embryogenesis. Skeletal muscle cells of the trunk, limbs and tongue arise from the somite-derived dermomyotome. The myotome, the first differentiated skeletal muscle, is formed when the dermomyotome precursors enter the myogenic program and delaminate from the dermomyotome. Following stages of skeletal muscle development are marked by the formation of the embryonic and fetal myofibers. Cardiac muscle development starts when the cardiogenic progenitors in the splanchnic mesoderm are brought to the midline to form the heart tube. The heart tube then undergoes several developmentally regulated rearrangements, originating the four cardiac chambers and a myocardium capable of pumping the blood.

The main goal of this thesis was the characterization of laminin niches during muscle development. In chapter 2 and 3, we addressed the dynamics of laminin synthesis and assembly during skeletal muscle development. Our results reveal a complex assembly dynamics, which generate specific microenvironments during different phases of muscle development. We then focused our analysis on the role of laminin niches during the onset of the Merosin-deficient congenital muscular dystrophy type 1A (MDC1A) in the *dy*^{W} mouse model, and demonstrated that absence of laminin 211 in the myofiber basement membrane leads to impaired fetal muscle growth. In Chapter 4 we show the progress in the development of different techniques to unveil the mechanism by which laminin 211 signals during skeletal muscle development. In Chapter 5, we characterized the dynamics of laminin assembly during cardiac development and found that different phases of cardiac development are marked by specific laminin niches.

Together, the results presented in this thesis provide a detailed framework on laminin matrices during muscle development. This thesis also unveils an important role of laminin 211 during the fetal development of skeletal muscles.

Key-words: Laminins, Skeletal muscle development, Cardiac muscle development, Merosin-deficient congenital muscular dystrophy.

Resumo

O desenvolvimento dos músculos esquelético e cardíaco inicia-se cedo durante o desenvolvimento embrionário. Os músculos esqueléticos do tronco têm origem no dermamiótomo que contém os progenitores musculares. O miótomo forma-se quando os progenitores entram no programa miogénico e delaminam do dermomiótomo. As fases seguintes da miogénese são marcadas pela formação das miofibras embrionárias e fetais. O desenvolvimento do músculo cardíaco inicia-se quando os progenitores cardíacos na mesoderme esplancnica são levados para a linha mediana do embrião para formar o tubo cardíaco. Este tubo sofre depois vários rearranjos que permitem desenvolver um coração com quatro câmaras cardíacas.

O principal objectivo desta tese foi caracterizar os nichos de laminina ao longo do desenvolvimento do músculo esquelético e cardíaco. Nos Capítulos 2 e 3, estudámos a dinâmica da síntese e montagem das matrizes de laminina durante o desenvolvimento do músculo esquelético. Os resultados obtidos revelam a existência de microambientes de laminina específicos ao longo do desenvolvimento do músculo. Os nossos resultados demonstram ainda que a matriz de laminina 211 tem um papel no despoletar da Distrofia muscular congénita merosina negativa (MDC1A) no modelo *dy*^{W} de ratinho, uma vez que a ausência desta laminina na membrana basal da miofibra resulta num défice de crescimento do músculo.

No Capítulo 4 apresentamos o progresso no desenvolvimento de diferentes técnicas que permitam compreender o mecanismo de sinalização da laminina 211 durante o desenvolvimento do músculo esquelético. No Capítulo 5, caracterizámos as dinâmicas de montagem de matrizes de laminina ao longo do desenvolvimento do músculo cardíaco, e descobrimos que diferentes fases do seu desenvolvimento são marcadas por nichos de laminina específicos.

Em suma, os resultados apresentados nesta tese fornecem uma visão detalhada das matrizes de laminina ao longo do desenvolvimento do músculo esquelético e cardíaco e evidenciam o papel da laminina 211 no desenvolvimento fetal dos músculos esqueléticos.

Palavras-chave: Laminina, Desenvolvimento do Músculo Esquelético, Desenvolvimento do Músculo Cardíaco, Distrofia muscular congénita merosina negativa

Resumo alargado

Os músculos estriados são tecidos fulcrais não só para a capacidade de lomocoção dos animais, mas também para o correcto funcionamento de órgãos vitais, como o coração. Os músculos esqueléticos do tronco, dos membros e da língua têm origem embrionária na mesoderme paraxial, mais precisamente nos sómitos que se formam periodicamente em ambos os lados do tubo neural. A maturação dos sómitos dá origem ao dermamiótomo, um epitélio onde os progenitores musculares são mantidos. Quando a formação dos músculos, ou miogénese, é induzida, os progenitores activam o programa miogénico e delaminam para o espaço subjacente para formar os miócitos que constituem o miótomo. Durante esta fase inicial da miogénese, o miótomo cresce até ocorrer a dissociação do dermamiótomo. Posteriomente, os miócitos fundem com os mioblastos primários para formar as fibras embrionárias. Estas funcionam como suporte para a formação das fibras fetais, aquando de uma nova onda de fusão dos mioblastos fetais entre si para formar as fibras fetais. Durante esta vaga de fusões, os mioblastos fetais fundem também com as fibras embrionárias e fetais para que estas cresçam.

O desenvolvimento do músculo cardíaco é induzido quando os progenitores cardíacos localizados na mesoderme esplâncnica de ambos os lados do embrião se aproximam e se juntam na linha mediana para formar o tubo cardíaco. O tubo cardíaco sofre depois uma remodelação extensa, durante a qual o epicárdio reveste a camada exterior do miocárdio e o coração é sujeito a um processo de morfogénese até adquirir a organização final do coração adulto. Durante esta fase, o músculo cardíaco, ou miocárdio, é remodelado em trabéculas e zona compacta. As fases que se seguem englobam o desenvolvimento de todo o sistema que suporta o funcionamento do coração, tais como o desenvolvimento da vasculatura coronária, o desenvolvimento dos septos que separam as diversas câmaras cardíacas, e o desenvolvimento do sistema eléctrico de excitação cardíaca.

Diversos aspectos do desenvolvimento do músculo esquelético e cardíaco têm sido abordados na literatura, mas o papel das matrizes de laminina nestes processos é ainda pouco conhecido, e os poucos estudos realizados não fornecem uma perspectiva global das matrizes de laminina presentes durante o desenvolvimento destes dois tipos de músculo. Apesar destas lacunas, alguns destes estudos revelaram que as matrizes de laminina desempenham um papel importante durante desenvolvimento do miótomo, na homeostase do músculo esquelético no adulto, bem como durante o desenvolvimento do coração.

Nesta tese pretendemos compreender as dinâmicas de montagem das matrizes de laminina durante o desenvolvimento dos músculos esquelético e cardíaco, a fim de perceber de que forma estas matrizes modulam o desenvolvimento destes tipos de músculo durante o estabelecimento das membranas basais nos músculos. Abordamos diferentes perspectivas da montagem das matrizes de laminina, desde a expressão dos genes que codificam para as três cadeias das lamininas até à sua incorporação na membrana basal. Analisamos também o papel de lamininas durante o início da Distrofia muscular congénita merosina negativa (MDC1A) *in utero*, na qual o gene *LAMA2* se encontra mutado e a consequente ausência de lamininas com a cadeia α2. Por fim, descrevemos ainda o progresso no desenvolvimento de duas técnicas que visam fornecer diferentes metodologias para o estudo do papel das lamininas durante o desenvolvimento do músculo.

Numa primeira abordagem, esta tese teve como objectivo compreender a dinâmica dos ciclos de montagem das matrizes de laminina durante o desenvolvimento dos músculos esqueléticos epaxiais, bem como a relação desta dinâmica com o desencadear da distrofia muscular MDC1A que ocorre na ausência de lamininas 211/221. Os resultados apresentados no **capítulo 2** demonstram que o desenvolvimento do músculo esquelético ocorre em paralelo com diferentes ciclos de montagem de matrizes

de laminina, e consequentemente com o desenvolvimento de microambientes distintos em contacto com as células miogénicas. Os nossos dados evidenciam ainda que a ausência de lamininas 211/221 no modelo *dy^{W}* de ratinho para MDC1A não interfere com o decorrer miogénese no miótomo que parece prosseguir sem defeitos significativos. Isto pode possivelmente dever-se à presença da laminina 111, que parece compensar a ausência de laminina 211 no músculo adulto. Verificámos que a miogénese primária prossegue sem defeitos significativos na ausência de lamininas 211/221, o que correlaciona com uma fase da miogénese onde as matrizes de laminina não são montadas pelas células miogénicas. Em conjunto com o **capítulo 3**, revela que a ausência de lamininas incorporadas na membrana basal no músculo durante a miogénese primária não corresponde à ausência de expressão dos genes de laminina. Pelo contrário, a expressão destes genes é mantida durante toda a miogénese primária. Os dados reportados no capítulo 2 revelam que o efeito da ausência de laminina 211 na membrana basal que contacta com a miofibra e com as células estaminais musculares Pax7-positivas faz-se notar durante a miogénese fetal, quando o músculo começa a apresentar défices de crescimento, em particular no crescimento por hipertrofia. Este defeito correlaciona com a redução do número de células Pax7-positivas e Miogenina-positivas que, de acordo com os nossos dados, não conseguem assim contribuir devidamente para o normal crescimento do músculo durante esta fase do seu desenvolvimento. Este defeito correlaciona também com a activação excessiva da sinalização por STAT3, induzida provavelmente através da falta de sinalização por laminina 211-integrina α7β1, e com a redução da sinalização por Miostatina. A combinação dos efeitos da alteração destas sinalizações no contexto da ausência de laminina 211 parece inibir a expansão das células Pax7-positivas e dos mioblastos em diferenciação, o que resulta num défice de células a contribuir para o crescimento das fibras. Durante o desenvolvimento pós-natal, o defeito no tamanho das massas musculares torna-se mais evidente, com as massas deficientes para laminina 211 a evidenciarem uma incapacidade de crescimento. A sobreactivação da

sinalização por STAT3 é mantida durante esta fase, mas o estado de activação da sinalização por Miostatina é alterado para um estado de sobreactivação. Os resultados do capítulo 2 indicam ainda que a composição das matrizes de laminina influenciam a "idade" das células miogénicas. O nosso modelo de sinalização por laminina 211 sugere que a ausência de laminina 211 na membrana basal em contacto com as miofibras e as células estaminais musculares fornece os sinais característicos de fases de desenvolvimento mais tardias e, por isso, uma acumulação progressiva dos sinais que promovem a diferenciação em detrimento dos sinais que induzem a proliferação celular.

No **capítulo 3** demonstramos que ao longo da miogénese, as células estaminais musculares podem construir o seu nicho. Os nosso resultados evidenciam que as células estaminais musculares no dermamiótomo constroem de forma autónoma a membrana basal do dermamiótomo. Durante a miogénese fetal, a matriz de laminina que cobre as miofibras e as células estaminais musculares parece ser construída por células mononucleadas adjacentes às miofibras, provavelmente células estaminais musculares e/ou mioblastos em diferenciação. De facto, as células estaminais musculares produzem matrizes de laminina no início da miogénese secundária. A população de células estaminais musculares parece ser bastante heterogénea dado que algumas células montam matrizes de laminina com as cadeias α2 e α5 em simultâneo, enquanto que outras produzem apenas um tipo de matriz de laminina, e outras não produzem qualquer laminina. Esta heterogeneidade sugere que células com um repertório diferente de lamininas podem reagir de formas distintas à ausência de laminina 211 no seu nicho.

O estudo do desenvolvimento do músculo *in utero* coloca diversas barreiras técnicas que impedem a realização de alguns estudos funcionais. No **capítulo 4**, apresentamos o progresso no desenvolvimento de diferentes técnicas com vista a poder compreender melhor o mecanismo de sinalização por laminina 211 que opera durante o desenvolvimento fetal do músculo. Os resultados exploratórios apresentados neste

capítulo revelam-se promissores na utilização de injecções de laminina 111 *in utero*, uma terapia proteica com reconhecido efeito na recuperação dos defeitos da doença no adulto, como prova de princípio de que as lamininas 211/111 permitem recuperar o defeito fetal. Esta metodologia poderá ser utilizada em estudos futuros para estudar os efeitos da sinalização por laminina 211.

No **capítulo 5** evidenciamos a dinâmica de construção das matrizes de laminina durante o desenvolvimento do coração *in utero* e nas fases pós-natal e adulta. Neste capítulo demonstramos a existência de matrizes de laminina muito dinâmicas nas membranas basais cardíacas. A membrana basal na interface entre o endocárdio e o miocárdio é incialmente constituída pela combinação das matrizes de laminina 111/121, 411/421 e 511/521. Contudo, esta vai sendo progressivamente reduzida à matriz de laminina 521. Após o epicárdio envolver o coração, a membrana basal subepicardial é composta pelas matrizes de lamininas 111 e 511, sendo no entanto posteriormente substitutídas pela matriz de laminina 521. Por fim, os nosso resultados revelam a presença das matrizes de laminina 211 e 511 aquando da formação da membrana basal dos cardiomiócitos, sendo estas depois gradualmente substituídas pelas matrizes de lamininas 221 e 521 perto do fim do desenvolvimento fetal do coração.

Os capítulos desta tese ilustram a diversidade de matrizes de laminina construídas nas membranes basais presentes durante o desenvolvimento do músculo esquelético e cardíaco. O nosso estudo demonstra ainda em particular que a matriz de laminina 211 desempenha um papel fucral durante o desenvolvimento fetal dos músculos esqueléticos.

Palavras-chave: Lamininas, Desenvolvimento do músculo esquelético, Desenvolvimento do músculo cardíaco, Distrofia muscular congénita merosina negativa

List of abbreviations and acronyms

ADAM- Metalloproteinase with thrombospondin motifs

ANF- Atrial Natriuretic Factor

bHLH- Basic Helix-Loop-Helix

CXCR4- C-X-C Chemokine Receptor type 4

BDNF- Brain-Derived Neurotrophic Factor

BMP- Bone Morphogenetic Protein

DGC- Dystrophin- associated Glycoprotein Complex

DML- Dorsomedial Lip

DNA- Deoxyribonucleic Acid

E(n)- Embryonic day (number)

ECM- Extracellular Matrix

EDL- Extensor Digitorum Longus

EMT- Epithelium to Mesenchyme Transition

EGF- Epidermal Growth Factor

EGFR- Epidermal Growth Factor Receptor

EPDC- Epicardium-Derived Cell

ERK- Extracellular signal–Regulated Kinases

FAK- Focal Adhesion Kinase

Fgf- Fibroblast Growth Factor

FKRP- Fukutin-Related Protein

FLK1- Fetal Kinase Liver 1

HGF- Hepatocyte Growth Factor

ILK- Integrin-Linked Kinase

IPP- ILK, PINCH and Parvin

JAK-STAT- Janus Kinase/Signal Transducers and Activators of Transcription

LAMA2-CMD- Laminin-α2 Congenital Muscular Dystrophy

MAPK- Mitogen-Activated Protein Kinases

MESP- Mesoderm Posterior

MDC1A- Merosin-Deficient Congenital muscular dystrophy type 1A

MMP- Matrix Metalloproteinase

MyHC- Myosin Heavy Chain

MyHC-emb- Embryonic Myosin Heavy Chain

MyHC-β/slow- Myosin Heavy Chain-β/Slow

MRF- Myogenic Regulatory Factor

N-CAM- Neural Cell Adhesion Molecule

NICD- Notch Intracellular Domain

P(n)- Postnatal day (number)

PCP- Planar Cell Polarity

PINCH- Particularly Interesting Cys-His-rich

PECAM- Platelet Endothelial Cell Adhesion Molecule

PDGFR- Platelet-derived Growth Factor Receptor

POMT1- Protein O-MannosylTransferase 1

POMT2- Protein O-MannosylTransferase 2

POMGnT1- Protein O-Linked Mannose N-AcetylGlucosaminylTransferase 1

PSM- Presomitic Mesoderm

RGD- Arginine-Glycine Aspartic acid

SDF1- Stromal Cell-Derived Factor 1

Shh- Sonic Hedgehog

TAL1- T-Cell Acute Lymphocytic Leukemia 1

TBX- T-BoX

TGFβ- Transforming Growth Factor Beta

UGC- Utrophin- associated Glycoprotein Complex

V-CAM1- Vascular Cell Adhesion Molecule 1

VEGF- Vascular Endothelial Growth Factor

VEGFR- Vascular Endothelial Growth Factor Receptor

VLL- Ventrolateral Lip

Wnt- Wingless/Integrated Family Members

CHAPTER 1

Introduction

I. State of the art

1. Introduction

Striated muscles evolved during the early diversification of the animal kingdom from an ancestral actinomyosin machinery that predates muscle evolution (Steinmetz et al., 2012). They drive the blood circulation and enable the locomotion of the body. Laminins are major components of basement membranes, a specific type of extracellular matrix (ECM), which are in close contact with a number of organized tissues in the body, namely epithelia, endothelia, nerves, adipose cells and muscles (LeBleu et al., 2007; Durbeej, 2010; Domogatskaya et al., 2012). The ancestral form of trimeric laminins is believed to have arisen before the separation of the cnidaria and bilateria (Zhang et al., 2002). Laminins are crucial for the assembly of basement membranes and the absence of all laminins is incompatible with life in most, if not all, bilaterian animals (Domogatskaya et al., 2012). In this chapter I will introduce laminins and their role in basement membrane assembly and function. Moreover, I will review the development of the two types of striated muscle, cardiac and skeletal, as well as the relevance of studying laminins in these tissues.

2. Extracellular matrix

During development in multicellular organisms, individual cells interact with each other via cell-cell communication events by receiving signals from neighboring cells through paracrine factors, by engaging with adjacent cells through cell-surface bound molecules and by contacting with the cell-generated extracellular matrix. The ECM is a complex network that provides both a physical scaffold and signaling cues to cells. It comprises many different types of molecules, including glycoproteins such as laminins, fibronectin, collagens and tenascins, and polysaccharide-rich molecules such as

glycosaminoglycans and proteoglycans. These molecules are produced by a variety of cell types and are assembled extracellularly into a supramolecular matrix that connects back to cells through specific cell surface receptors (Frantz et al., 2010; Thorsteinsdóttir et al., 2011). The ECM can be divided into interstitial matrices and pericellular matrices. Interstitial matrices surround mesenchymal cells and constitute the connective tissue matrix. These matrices are composed of collagens, proteoglycans, glycosaminoglycans and contain numerous other glycoproteins and proteins such as fibronectin, tenascin and elastins among others (Frantz et al., 2010; Thorsteinsdóttir et al., 2011). Pericellular matrices are matrices that are in close proximity to cells and the most common form of pericellular matrix are the basement membranes. Basement membranes are mainly composed of laminins, collagens type IV, perlecan and nidogens. They line epithelia and endothelia, and surround neurons, fat and muscle cells (LeBleu et al., 2007; Thorsteinsdóttir et al., 2011).

2.1. Laminins

2.1.1. Laminin composition and structure

Laminins are trimeric glycoproteins composed of an α, a β and a γ chain, and are the basic building blocks of basement membranes (LeBleu et al., 2007; Durbeej, 2010; Yurchenco et al., 2015). The laminin trimer is composed of an α-helical coiled coil domain containing the three chains and three short arms corresponding to each chain (Durbeej, 2010; Hohenester and Yurchenco, 2013; Holmberg and Durbeej, 2013; Fig. 1). The short arms of α, β and γ chains vary in length but are all composed of laminin N-terminal (LN) domains separated by tandem repeats of laminin type epidermal growth factor-like (LE) domains. The C-terminal globular domain of the α chain contains five laminin G-like (LG) subdomains (Durbeej, 2010; Domogatskaya et al., 2012; Hohenester and Yurchenco, 2013;

Holmberg and Durbeej, 2013; Fig. 1). The α3A and α4 chains are distinct from other α chains because their short arms retain only one LE domain subdomain (Durbeej, 2010; Domogatskaya et al., 2012; Hohenester and Yurchenco, 2013; Holmberg and Durbeej, 2013).

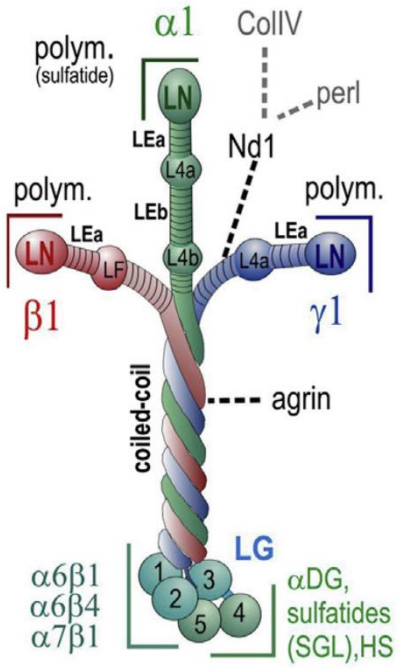

Figure 1- Laminin trimer structure. Schematic representation of laminin 111. The coiled coil domain contains the three different chains, in contrast to each N-terminal short arm which is established by each chain. The short arms are responsible for laminin self-assembly. The α chain C-terminal end consists of five globular domains which interact with cell surface receptors. Tandem LE domains are depicted in the short arm separating the LN domains. The binding sites for other basement membrane components and cell receptors are also depicted. Figure from Yurchenco, 2015.

Different combinations of α, β and γ chains generate at least 16 different laminin isoforms which are assembled into basement membranes by several cell types in multiple tissues. The current nomenclature is based on the chain composition, e.g., laminin 211 is composed of α2, β1 and γ1 chains (Aumailley et al., 2005; Table 1). The first described laminin was laminin 111 identified in the basement membrane of the murine Engelbreth-Holm-Swarm (EHS) sarcoma (Orkin et al., 1977; Timpl et al., 1979). However, the ancestral form of trimeric laminin is present in the radiata *Hydra*, and is assembled in the basement membrane separating the endoderm from the ectoderm (Zhang et al., 2002; Domogatskaya et al., 2012). The trimeric composition of *Hydra* laminin is not yet completely uncovered and doubts arise about whether the trimer is a combination of α, β and γ chains, or if the combination includes one α and two β chains (Zhang et al., 2002; Domogatskaya et al., 2012). With the appearance of Bilateria, α chain diversification led to the appearance of two branches of ancestral α chain. In the particular case of the

Vertebrata, the ancestor $\alpha_{1,2}$ originated α1 and α2 chains, whereas the $\alpha_{3,5}$ ancestor gave rise to α3 and α5 chains (Domogatskaya et al., 2012). Diversification of β and γ chains are likely to have occurred during non-vertebrate Deuterostomia evolution (Domogatskaya et al., 2012).

Current laminin nomenclature	*Old laminin nomenclature*	*Chain composition*	*Genes*
Laminin 111	Laminin- 1	α1β1γ1	*Lama1 Lamb1 Lamc1*
Laminin 121	Laminin- 3	α1β2γ1	*Lama1 Lamb2 Lamc1*
Laminin 211	Laminin- 2	α2β1γ1	*Lama2 Lamb1 Lamc1*
Laminin 221	Laminin- 4	α2β2γ1	*Lama2 Lamb2 Lamc1*
Laminin 213	Laminin- 12	α2β1γ2	*Lama2 Lamb1 Lamc3*
Laminin 212 (existence proposed)	-	α2β1γ2	*Lama2 Lamb1 Lamc2*
Laminin 222 (existence proposed)	-	α2β2γ2	*Lama2 Lamb2 Lamc2*
Laminin 311	Laminin- 6	α3Aβ1γ1	*Lama3A Lamb1 Lamc1*
Laminin 321	Laminin- 7	αA3β2γ1	*Lama3A Lamb2 Lamc1*
Laminin 332	Laminin- 5	α3Aβ3γ2	*Lama3A Lamb3 Lamc2*
Laminin 3B32	Laminin- 5B	α3Bβ3γ2	*Lama3B Lamb3 Lamc2*
Laminin 333	-	α3Aβ3γ3	*Lama3A Lamb3 Lamc3*
Laminin 411	Laminin- 8	α4β1γ1	*Lama4 Lamb1 Lamc1*
Laminin 421	Laminin- 9	α4β2γ1	*Lama4 Lamb2 Lamc1*
Laminin 423	Laminin- 14	α4β2γ3	*Lama4 Lamb2 Lamc3*
Laminin 511	Laminin- 10	α5β1γ1	*Lama5 Lamb1 Lamc1*
Laminin 521	Laminin- 11	α5β2γ1	*Lama5 Lamb2 Lamc1*
Laminin 522 (existence proposed)	-	α5β2γ2	*Lama5 Lamb2 Lamc2*
Laminin 523	Laminin- 15	α5β2γ3	*Lama5 Lamb2 Lamc3*

Table 1- Laminin nomenclature and composition. Adapted from Thorsteinsdóttir et al., 2011.

2.1.2. Laminin assembly into the basement membrane

The construction of basement membranes is a multi-step process, where laminin and collagen IV matrices are assembled separately and then incorporated into a supramolecular network (Yurchenco, 2015). Laminin trimer secretion is a two-step process, where ionic interactions first promote the formation of a βγ dimer and the subsequent addition of the α chain stabilizes the previously formed dimer (Kumagai et al., 1997; Yurchenco et al., 1997; Yurchenco, 2015). The addition of the α chain is the

determinant step as the trimer is only secreted when the α chain is added to the βγ dimer (Kumagai et al., 1997; Yurchenco et al., 1997).

Once secreted to the extracellular space, laminin is believed to polymerize according to the "three-arm interaction model" (Yurchenco et al., 1985; Hohenester and Yurchenco, 2013; Fig. 2). This model is supported by several *in vitro* reports demonstrating that laminin trimers self-assemble into polymers through a calcium dependent process, involving ternary interactions between the LN terminal domains of the α, β and γ short arms, which are subsequently stabilized by disulphide bridges (Yurchenco et al., 1985; Schittny and Yurchenco, 1990; Yurchenco and Cheng, 1993; McKee et al., 2007; Hussain et al., 2011; Hohenester and Yurchenco, 2013). These interactions promote the assembly of laminin molecules into homopolymers, but different laminin isoforms can also assemble into mixed heteropolymers (Cheng et al., 1997). Laminin isoforms in which the α chains lack most of the short arm domain, such as laminins 3A11, 3A21, 411 and 421, cannot self-assemble (Cheng et al., 1997; Domogatskaya et al., 2012).

In vivo laminin assembly seems to depend on the binding to cell surface receptors which interact with the five LG domains at the C-terminal of the α chains (McKee et al., 2007; McKee et al., 2009). However, the dependence of laminin assembly on cell surface receptors and the mechanism underlying their cross-talk is still controversial (McKee et al., 2007; McKee et al., 2009). Laminin polymerization was shown to induce clustering of integrins and dystroglycan in the cell membrane, and aggregation of intracellular cytoskeletal components (Colognato et al., 1999; Li et al., 2005a). In other studies, the production of a gal-sulfatide receptor by Schwann cells precedes laminin accumulation, and hydrolyzation of sulfatides prevents the accumulation of laminin on the cell surface (Li et al., 2005a). Conversely, dystroglycan null embryoid bodies develop a basement membrane (Li et al., 2002). Thus, these results suggest that different cell surface receptors might have different impacts on laminin assembly.

Basement membrane maturation and stability depends on the proper interconnection between different components. Laminins and collagen IV are the only basement membrane components capable of self-assembly, but the addition of perlecan and nidogen bridges allow the link between the laminin and the collagen IV networks (LeBleu et al., 2007; McKee et al., 2007; Behrens et al., 2012; Hohenester and Yurchenco, 2013). The first step in the construction of basement membranes seems to be the assembly of the laminin matrix as it precedes collagen IV accumulation on the cell surface, and occurs in the absence of assembled collagen (Smirnov et al., 2002; Li et al., 2002; Tsiper and Yurchenco, 2002; McKee et al., 2007; Yurchenco, 2015; Fig.2).

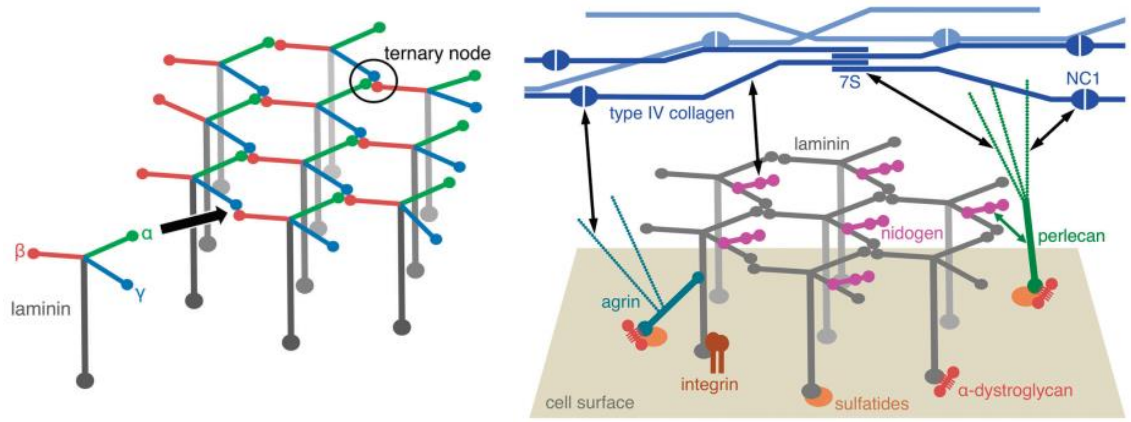

Figure 2- Laminin self-assembly into the basement membrane. Self-assembly of laminin according to the "three-arm interaction model" (left) and its incorporation into the supramolecular network of the basement membrane through interaction with other ECM components such as collagen IV, perlecan, agrin and nidogen (right). Adapted from Hohenester and Yurchenco, 2013.

2.1.3. Laminin remodeling in the basement membrane

The ECM is modified by metalloproteinases with proteolytic activity, which cleave ECM components. The two major metalloproteinase families targeting the ECM are the matrix metalloproteinase (MMP) family that is composed of 23 different proteinases, and

the metalloproteinase with thrombospondin motifs (ADAM) family which includes 19 members (Lu et al., 2011). MMPs are usually secreted molecules constituted by the prodomain, the catalytic domain and the hemopexin-containing ancillary domain. However, certain MMPs display extra domains, such as MMP2 and MMP9 which contain fibronectin type II inserts in the catalytic domain, and MMPs 14, 15, 23 and 24 which are membrane-type MMPs with a transmembrane domain and a cytoplasmic tail (Page-McCaw et al., 2007; Lu et al., 2011). Several proteinases are synthesized in an inactive form and need further cleavage of the prodomain, which normally inhibits the activity of the catalytic domain (Page-McCaw et al., 2007; Lu et al., 2011). This processing is performed by other proteinases which in the case of MMPs include the proteinases tryptase and plasmin, but also other MMPs (Lu et al., 2011). Further tuning of MMP and ADAM activity is performed by tissue inhibitor of metalloproteinases (TIMP) molecules (Sternlicht and Werb, 2001; Lu et al., 2011). Each MMPs targets specific ECM components, albeit different MMPs sharing common targets. Laminins are cleaved by MMPs 2, 3, 10, 11, 12, 13, 14, 15 and 25 (Lu et al., 2011).

ECM degradation does not solely affect the composition of the ECM, but can also release ECM fragments with biological activity as well as ECM-bound paracrine growth factors which impact cell behavior (Streuli, 1999; Page-McCaw et al., 2007; Mott and Werb, 2004). For instance, cleavage of laminin 111 into several fragments with biological activity, combined with MMP9-mediated release of VEGF (Vascular endothelial growth factor), strongly affects tumor growth and metastasis formation (Mott and Werb, 2004; Kikkawa et al., 2013). In another example, fragments generated from laminin 332 cleavage were shown to interfere with mammary gland epithelial cell migration (Koshikawa et al., 2000).

2.2. Laminin receptors

Laminins interact with several cell surface receptors through their LG domains in the C-terminal ends of the α chains. Laminins display binding affinity to integrins, dystroglycan, syndecans and Lutheran blood group glycoproteins, also called BCAM (basal cell adhesion molecule) (Durbeej et al., 2010; Hohenester and Yurchenco, 2013; Yurchenco, 2015). Different laminins have different degrees of affinity for each receptor. For example, α4-laminins bind to cell surface-bound heparin sulfate proteoglycans and sulfatides, but these laminins are poor ligands for dystroglycan and integrins (Talts et al., 2000; Nishiuchi et al., 2006). Integrin receptor binding requires the LG1-3 domains, whereas LG4-5 domains are generally responsible for binding to α-dystroglycan, heparan sulfates and sulfatides (Timpl et al., 2000; Wizemann et al., 2003; Yu and Talts, 2003; Ido et al., 2004; Suzuki et al., 2005; Durbeej, 2010; Gawlik et al., 2010; Hohenester and Yurchenco, 2013). However, α-dystroglycan also displays binding affinity to the LG1-3 domains of the α2 chain (Talts et al., 1999; Smirnov et al., 2002).

2.2.1 Integrins

2.2.1.1. Integrin structure and activation

Integrins are allosteric proteins that form heterodimers composed of non-covalently associated α and β subunits, which act as mechanosensors and mechanotransducers of the extracellular environment (Hynes, 2002; Ingber, 2006; Barczyk et al., 2010). In vertebrates, the integrin family is composed of 18 α subunits and 8 β subunits that can assemble into 24 different heterodimers (Barczyk et al., 2010). The α subunit determines integrin-ligand specificity, whereas the β subunit connects to the cytoskeleton and other intracellular proteins (Barczyk et al., 2010). Integrins can generally be grouped into collagen receptors, RGD (Arginine-Glycine Aspartic acid)-domain receptors, laminin receptors and leucocyte-specific receptors (Humphries et al., 2006; Barczyk et al., 2010). They are structurally divided into the head region and the leg region.

The head region includes the β-propeller domain and the thigh domain from the α-subunit, and the βA domain, the hybrid domain and the PSI domain from the β-subunit (Askari et al., 2009; Fig. 3). The leg region comprises the calf1 and calf2 domains from the α-subunit, and the EGF (Epidermal growth factor) domains and the β-tail domain from the β-subunit (Askari et al., 2009; Fig. 3). The intracellular β-tail domain of the β-subunit interacts directly and indirectly with several proteins which mediate the integrin-cytoskeleton linkage. These include talin, α-actinin, kindlin, FAK (focal adhesion kinase), vinculin and the IPP complex formed by ILK (integrin-linked kinase), PINCH (particularly interesting Cys-His-rich protein) and parvin proteins (Legate et al., 2006; Legate et al., 2009).

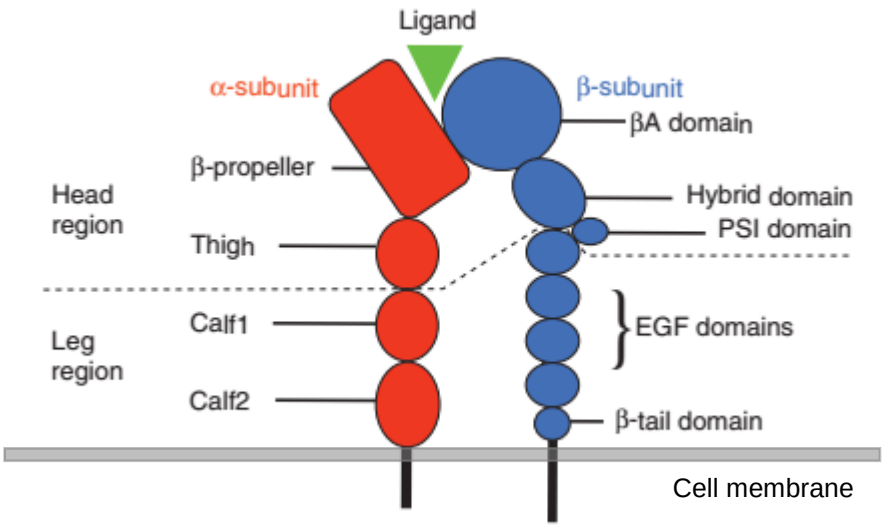

Figure 3- Integrin structure. Schematic representation of the integrin head and leg regions. The head region is formed by the α-subunit β-propeller and the thigh domains, and the βA, hybrid and PSI domains which are part of the β-subunit. The leg region includes the α-subunit calf1 and calf2 domains, and the EGF and β-tail domains of the the β subunit. Adapted from Askari et al., 2009.

Integrins are thought to adopt three major conformations which correlate with certain activation states: “inactive” of low affinity, “primed” or “active” of high affinity, and ligand occupied (Askari et al., 2009; Legate et al., 2009). The requirement of the physical extension of the integrin for its activation is still a matter of debate, but it is generally accepted that integrin activation requires the separation of the α and β cytoplasmic tails, which in turn allows the β-hybrid domain to move outwards. This rearrangement alters the βA domain conformation from a low affinity to a high affinity state (Mould et al., 2003; Rocco et al., 2008; Askari et al., 2009). Integrin activation is modulated bidirectionally through inside-out activation, which sets integrins into the “primed” or “active” high affinity state, and through outside-in activation, which is induced upon binding with their ligand and triggers the activation of multiple signaling pathways (Hynes, 2002; Askari et al., 2009; Legate et al., 2009; Fig. 4). Integrins are believed to be maintained in an inactive state, but integrin independent signals can trigger the

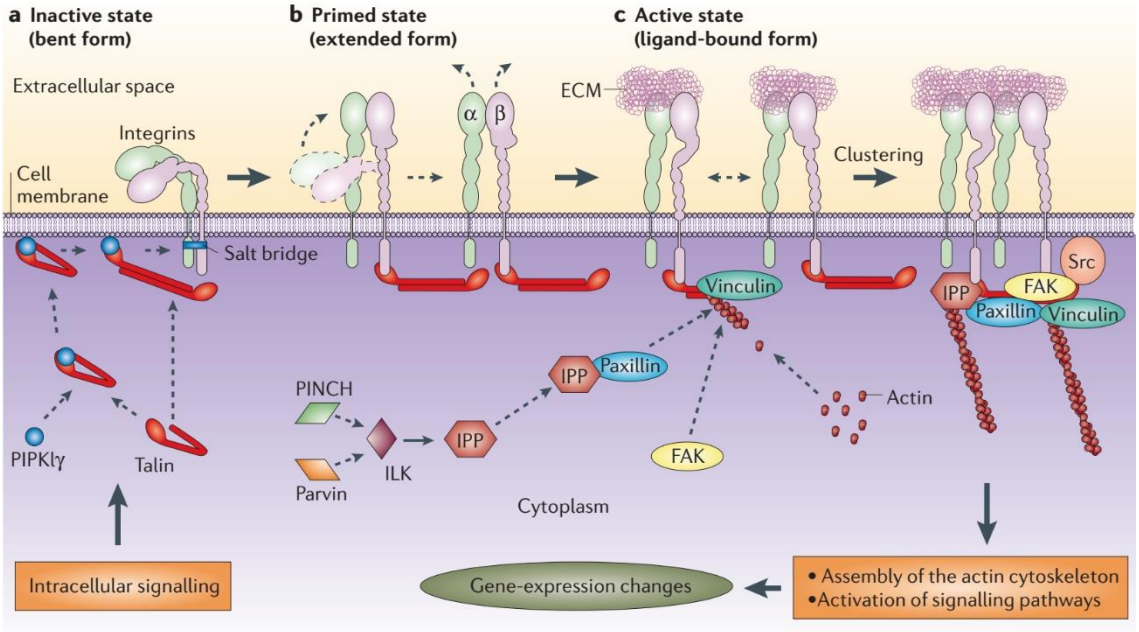

Figure 4- Integrin “inside-out” activation. Integrins can adopt different conformation/activation states: “inactive” of low affinity, “primed” or “active” of high affinity, and ligand occupied. Intracellular signaling is responsible for priming the integrins into a more extended form which allows their activation once the intracellular mediators of integrin activation such as vinculin, paxillin, the IPP complex and FAK form a complex that binds to integrins. After activation integrins bind to their ligands which induces outside-in signaling that can involve several signaling pathways. Figure from Legate et al., 2006.

recruitment of talin and kindlin to the β integrin cytoplasmic tails (Askari et al., 2009; Legate et al., 2009). Talin and kindlin mediate the separation of α and β cytoplasmic domains (Hynes, 2002; Askari et al., 2009; Legate et al., 2009). Talin also links directly to the actin cytoskeleton, but the binding of vinculin and α-actinin to the talin-actin complex is crucial to strengthen this interaction (Miyamoto et al., 1995; Gallant et al., 2005; Legate et al., 2009). Other molecules such as paxillin, FAK and Src, and the IPP complex, are also recruited to the integrin complex (Miyamoto et al., 1995; Geiger et al., 2001; Legate et al., 2006; Schwartz and DeSimone, 2008). The aggregation of all these proteins into an integrin binding complex then induces a conformational change in the integrin protein, setting it for an "active" high affinity state (Hynes, 2002; Askari et al., 2009; Legate et al., 2009; Fig. 4). The following clustering of integrins allows the exponential propagation of integrin "outside-in" activation upon the binding of the ligand. This activation is then translated into the activation of multiple signaling pathways, including that of MAPK (Mitogen-activated protein kinases), ERK (Extracellular signal–regulated kinases), Wnt (Wingless/integrated family members) and Akt associated signaling pathway, which are involved in several cellular processes such as migration, proliferation, survival and apoptosis (Hynes, 2002; Legate et al., 2006; Legate et al., 2009).

Another level of complexity in integrin signaling is provided by the cross-talk between integrins and paracrine growth factors where bidirectional signaling impacts cellular processes regulated by both signaling systems (Comoglio et al., 2003; Danen and Sonnenberg, 2003). For instance, integrin aggregation was shown to induce phosphorylation and activation of the receptor tyrosine kinases PDGFR (Platelet-derived growth factor receptor), EGFR (Epidermal growth factor receptor), and VEGFR (VEGF receptor) (Miyamoto et al., 1996; Moro et al., 1998), and to act synergistically with EGF to induce strong activation of ERK signaling (Chen et al., 1996; Renshaw et al., 1997). Additionally, the direct interaction between αvβ6 integrin and TGFβ (Transforming growth

factor β) was shown to induce FAK and paxillin phosphorylation in parallel with TGFβ1 activation in lung epithelial cells (Munger et al., 1999).

2.2.1.2. Integrins as mediators of interactions between laminins and the cytoskeleton

The major laminin binding integrins are the α3β1, α6β1, α7β1 and α6β4 integrins which present different ligand specificities and thus, different signaling outputs (Nishiuchi et al., 2006). For example, α6β1 integrin has the highest affinity for laminins 111, 332 and 511/521, while α7X1β1 isoform has high affinity for laminins 511/521 and α7X2β1 isoform displays high affinity for laminins 111 and 211/221 (Nishiuchi et al., 2006; von der Mark et al., 2007; Domogatskaya et al., 2012). Although these integrins bind to the α chain LG1-3 domain (Smirnov et al., 2002; Suzuki et al., 2005; Durbeej et al., 2010; Domogatskaya et al., 2012), β and γ chains also mediate laminin-integrin binding (Ido et al., 2008; Taniguchi et al., 2009).

2.2.2. Dystroglycan

The laminin receptor dystroglycan consists of an extracellular α subunit and a transmembrane β subunit which are non-covalently associated. α-dystroglycan is responsible for binding to the ligand, whereas the C-terminal domain of β-dystroglycan binds to the cysteine-rich domain of dystrophin, which is in turn linked to F-actin (Ervasti et al., 1993; Jung et al., 1995; Kobayashi and Campbell, 2012). The dystroglycan receptor is the product of the *DAG1* gene, which is transcribed and translated into an αβ pro-peptide, then cleaved post-translationally into the extracellular α subunit and the transmembrane β subunit (Ibraghimov-Beskrovnaya et al., 1992; Holt et al., 2000; Domogatskaya et al., 2012; Holmberg and Durbeej, 2013).

Laminin binding requires extra post-translational modifications within the mucin domain of α-dystroglycan, which are employed by the glycosyltransferase LARGE inducing glycosylation of the O-mannosyl core (Kanagawa et al., 2004; Yoshida-Moriguichi et al., 2010; Kobayashi and Campbell, 2012). Other post-translation modifications are performed by POMT1 (Protein O-Mannosyltransferase 1), POMT2 (Protein O-Mannosyltransferase 2), POMGnT1 (Protein O-Linked Mannose N-Acetylglucosaminyltransferase 1), Fukutin, and FKRP (Fukutin-related protein) glycotransferases (Kobayashi and Campbell, 2012). Compared to integrins, α-dystroglycan displays a narrower binding spectrum and presents high affinity only for laminin α1 and α2 chains (Durbeej, 2010). As mentioned previously, the laminin LG4-5 domains are the α-dystroglycan binding domains by excellence, but the α2 chain contains additional binding sites in the LG1-3 domains (Timpl et al., 2000; Suzuki et al., 2005; Durbeej, 2010; Holmberg and Durbeej, 2013).

Dystroglycan is part of the dystrophin-associated glycoprotein complex (DGC) which also includes the sarcoglycans (SG-α, β, δ and γ), the dystrobrevins, sarcospan, and the syntrophins (Allikian and McNally, 2007; Townsend, 2014; Fig.5). In addition, β-

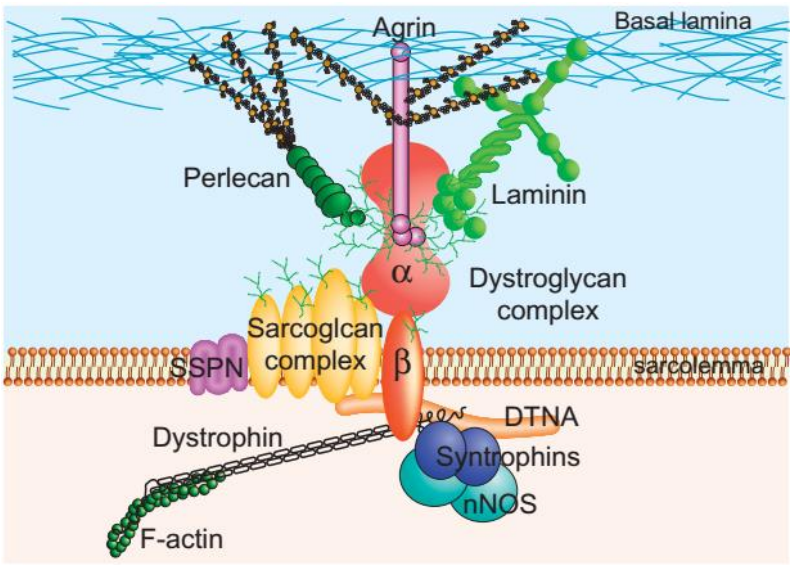

Figure 5- Dystrophin associated glycoprotein complex structure. The DGC is composed of α and β dystroglycan subunits, the sarcoglycan complex (SG-α, β, δ and γ), the dystrobrevins, sarcospan, and the syntrophins. Figure from Kobayashi and Campbell, 2012.

dystroglycan associates with the utrophin-associated glycoprotein complex (UGC) where utrophin replaces dystrophin in the linkage to the actin cytoskeleton (Rafael and Brown, 2000). Together with α7β1, the DGC and the UGC are the major laminin receptor complexes in adult skeletal muscle (Ervasti et al., 1993; Burkin and Kaufman, 1999; Rafael and Brown, 2000).

3. Cardiac development

3.1. Specification of first and second heart field progenitors

The heart is the first organ to be fully functional during embryogenesis. The presumptive myocardial cells are generated early during development, from the epiblast cells that ingress into the primitive streak to form the mesoderm (Kirby and Waldo, 2007). Cardiac development starts around E7.5 (embryonic day 7.5), when the cardiac progenitors, specified by the transcription factors Nkx2.5 and Mesp (Mesoderm posterior) 1, enter the cardiac myogenic program in the primitive streak and move antero-laterally to constitute two cardiogenic plates or cardiogenic fields, named first and second heart fields (Saga et al., 1999; Yang et al., 2002; Kirby and Waldo, 2007; Wu et al., 2008; Savolainen et al., 2009; Vincent and Buckingham, 2010; Kelly et al., 2014). They can be distinguished by *Myosin Light Chain 2a*, *Tbx5* (T-box 5) and *Hcn4* expression in the first heart field, and *Islet1*, *Tbx10*, *Fgf8* (Fibroblast growth factor) and *Fgf10* in the second heart field (Cai et al., 2003; Meilhac et al., 2004; Laugwitz et al., 2008; Vincent and Buckingham, 2010; Kelly et al., 2014; Meilhac et al., 2014). The first heart field progenitors are the first to migrate along the endoderm to form the heart tube (Kirby and Waldo, 2007; Kelly et al., 2014; Meilhac et al., 2014; Fig. 6). Afterwards, the second heart field progenitors migrate along the pharyngeal endoderm to the anterior and posterior poles of the heart tube (Vincent and Buckingham, 2010; Kelly et al., 2014; Meilhac et al., 2014; Fig. 6). Second

heart field progenitors are maintained in a proliferative state in the cardiogenic field, and differentiate once they enter the heart tube (Vincent and Buckingham, 2010). The activation of the cardiomyogenic program is mediated by the activation of *Gata4*, *Mefc2* and *Tbx5*, in response to signals such as Shh (Sonic hedgehog) and BMP (Bone morphogenetic protein) 2/Fgf 4 produced by the endoderm (Kirby and Waldo, 2007; Vincent and Buckingham, 2010). While the first heart field progenitors are the source of cells constituting the left ventricle, the second heart field progenitors will originate the atria, outflow tract, right ventricle and inflow region (Kirby and Waldo, 2007; Vincent and Buckingham, 2010; Fig. 6). These cardiogenic fields provide the progenitors for cardiomyocytes, endocardium cells and the conduction system, also termed conduction fibers or Purkinje fibers (Kirby and Waldo, 2007; Vincent and Buckingham, 2010; Meilhac et al., 2014). The heart is also colonized by neural crest cells which contribute to the outflow tract and septa that separates aorta from the pulmonary trunk (Waldo et al., 2005; Hutson and Kirby, 2007; Vincent and Buckingham, 2010).

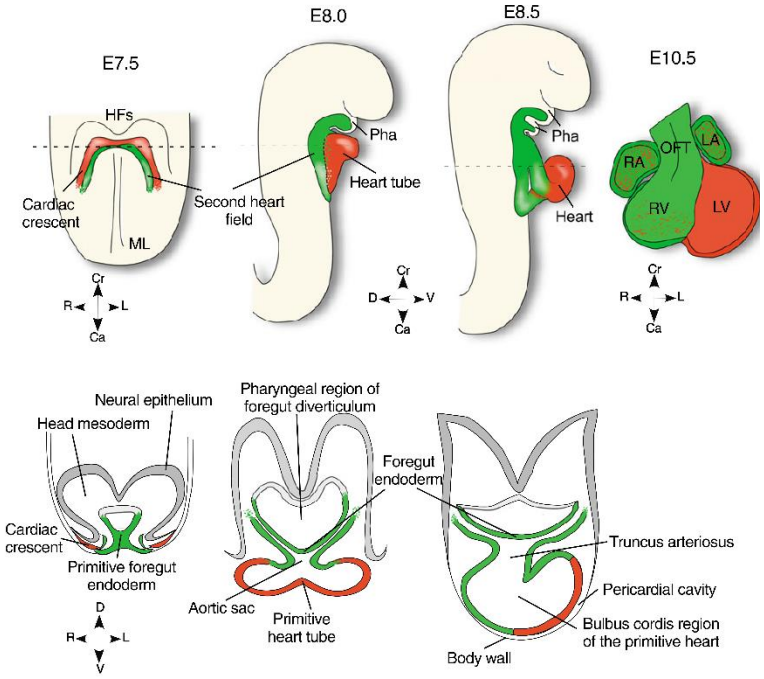

Figure 6- First and second heart field progenitor contribution to heart tube formation. First heart field progenitors form the heart tube which subsequently grows with the contribution of second heart field progenitors. The heart tube forms most of the future left ventricle, whereas the second heart field progenitors contribute mostly to the formation of outflow tract, left and right atria and right ventricle. Adapted from Laugwitz et al., 2008.

3.2. Heart tube formation and heart looping

The beating heart tube is formed by E8.0 (Kirby and Waldo, 2007; Savolainen et al., 2009), when the cardiogenic fields formed bilaterally are brought to the midline with the inward movement of the splanchnic mesoderm to form a double layered heart tube (Kirby and Waldo, 2007; Savolainen et al., 2009; Vincent and Buckingham, 2010; Kelly et al., 2014; Fig. 6 and 7). The myocardium is composed of cardiomyocytes, which are responsible for the contraction capability of the heart tube (Kirby and Waldo, 2007; Meilhac et al., 2014). The inner layer, the endocardium, is composed of endothelial cells that cover the interior of the myocardial heart tube and early in development, these endocardial cells are discriminated from the myocardium by the synthesis of TAL1 (T-Cell Acute Lymphocytic Leukemia 1), Flk1 (Fetal kinase liver 1), PECAM (Platelet endothelial cell adhesion molecule), CD34 and VE-cadherin (Drake and Fleming, 2000). In the interface between the endocardium and the myocardium is the cardiac jelly, a layer of ECM secreted by the myocardium (Kirby and Waldo, 2007; Savolainen et al., 2009). The cardiac jelly is digested by the metalloproteinase ADAMTS1 between E12.5 and E14.5 (Stankunas et al., 2008; Cooley et al., 2012; Paige et al., 2015).

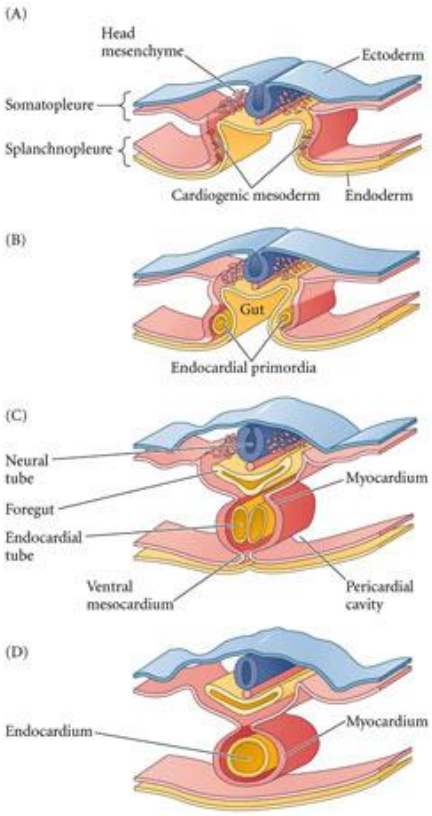

Figure 7- Heart tube formation. The heart tube is formed when the cardiogenic fields are brought to the midline with inward movement of the splanchnic mesoderm during the formation of the foregut pocket. Figure from Gilbert, 2013.

The heart changes its linear anterior-posterior conformation into the right-left conformation between E8.5 and E10.5 through a progression of bending, rotation and

torsion processes, collectively called heart looping (Kirby and Waldo, 2007; Fig. 8). During these rearrangements, the heart tube changes its linear conformation into the “C-shape” and then into the final “S-shape” (Kirby and Waldo, 2007). The initial C-shape is achieved with bending and rightward rotation of the heart tube, and then its elongation and convergence of inflow and outflow poles. Finally, during the following S-shape looping, the aorta rotates and stays between the atrioventricular valves (Kirby and Waldo, 2007). Different intrinsic and extrinsic factors are involved in the heart looping. The rightward rotation and convergence of inflow and outflow rearrangements are dependent on asymmetric divisions which allow the left side to grow faster than the right side (Linask et al., 2005; Kirby and Waldo, 2007). The cardiomyocyte proliferation during this process is in part regulated by FAK (Doherty et al., 2010). Additionally, ECM assembly and modification by MMP2, highly expressed by the endocardium, are crucial for the proper looping of the heart (Linask et al., 2005).

From E9.0 until E11.0, the proepicardium derived from the septum transversum mesenchyme in the inflow pole, starts migrating to eventually cover the external surface of the heart to form the epicardium (Moore et al., 1999; Sengbusch et al., 2002; Kirby and Waldo, 2007; Zhou et al., 2008; Vincent and Buckingham, 2010). The proepicardial and

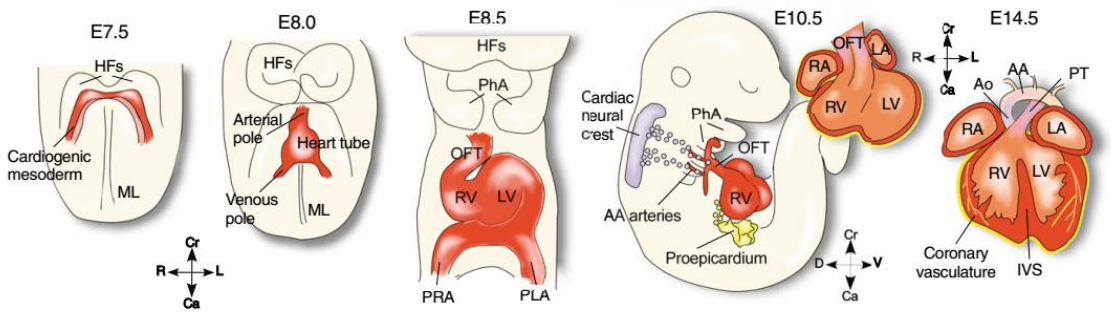

Figure 8- Cardiac development in the mouse. Cardiac development starts with the establishment of the heart fields and posterior formation and growth of the heart tube. Subsequent cardiac myogenesis and heart remodeling occurs with the heart looping, epicardium development, chamber specification and trabeculation, and development of the cardiac cushions and conduction system. Figure from Laugwitz et al., 2008.

epicardial cells are characterized by the expression of *Nkx2*.5, *Islet-1*, *Wt1* (Wilms Tumor 1) and *Tbx18* (Zhou et al., 2008; Vincent and Buckingham, 2010). Soon after the epicardium completely covers the outer myocardium, epicardial cells de-epithelialize and form a population of mesenchymal epicardium-derived cells (EPDCs). These cells invade the interior of the heart to originate myocardial fibroblasts and also the endothelial and smooth muscle cells of the coronary vasculature (Moore et al., 1999; Sengbusch et al., 2002; Kirby and Waldo, 2007; Zhou et al., 2008; Vincent and Buckingham, 2010). Strikingly, Wt1-positive epicardial cells also differentiate into cardiomyocytes during mid embryonic and fetal cardiac development (Zhou et al., 2008). The epicardium and the myocardium share a common subepicardial matrix in the interface between these two layers, which is composed of ECM molecules such as fibronectin, collagens, elastin, tenascin-X and laminins among other components (Wessels and Perez-Pomares, 2004).

3.3. Chamber specification and fetal myocardial growth

Around E10.5, the "secondary genetic program", involving factors such as ANF (Atrial natriuretic factor), Chisel, Cxn43 and Irx5, is activated to promote the development and growth of the myocardium into four different heart chambers: left and right atria, and left and right ventricle (Christoffels et al., 2000; Fig. 6 and 8). The activation of the secondary program leads to the activation of the chamber specific program, where atria are determined by the expression of myosin light chain isoform *Mlc2a*, and ventricles are specified by myosin light chain isoform *Mlc2v* expression (Small and Krieg, 2004). During this phase, the differentiation of second heart field progenitors in the myocardium is ceased and cardiomyocyte proliferation becomes the main process contributing to myocardium growth (Sedmera and Thompson, 2011; Kelly et al., 2014). The morphological changes occurring along this period are mediated by myocardial growth in the outer curvature of the heart through ballooning morphogenesis (Christoffels et al., 2000; Kelly,

et al., 2014; Paige et al., 2015). In parallel, the development of septa, cardiac cushions and Purkinje fibers allows the proper coordination between cardiac contractions and blood flow through the different chambers (Kelly et al., 2014).

After the heart loops, the myocardial wall is remodeled into the highly proliferative compact zone and the trabeculae. The development of trabeculae, or trabeculation, is crucial to increase the myocardial surface and the oxygenation of the internal wall of the myocardium (Savolainen et al., 2009; Samsa et al., 2013; Paige et al., 2015). Different signals such as Notch and neuregulin-1 from the endocardium, retinoic acid and Fgf from the epicardium, and BMP10 expressed in the trabecular myocardium, have been shown to regulate ventricular trabeculation and myocardial proliferation (Chen et al., 2004; Martin-Puing et al., 2008; Meilhac et al., 2014; Paige et al., 2015; Fig. 9). During fetal stages, the compact zone is further expanded through the proliferation of cardiomyocytes, but these start losing proliferative capacity during postnatal maturation (Martin-Puig et al., 2008; Sedmera and Thompson, 2011).

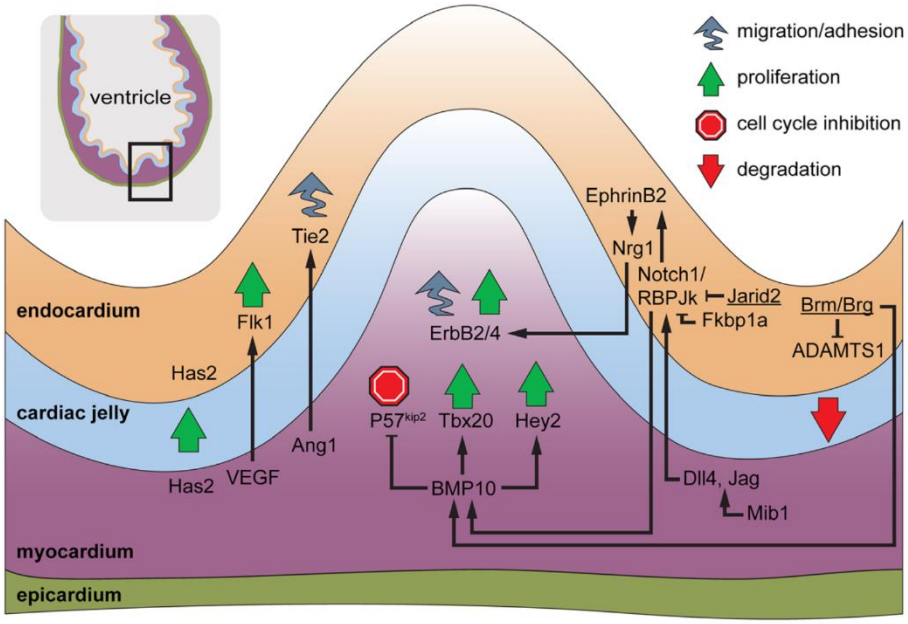

Figure 9- Myocardium trabeculation. Molecular regulation of myocardium trabeculation in the ventricle. Figure from Paige et al., 2015.

3.4. Laminins during cardiac development

Several studies have highlighted the role of different ECM components during cardiac development and repair (Dobaczewski et al., 2010; Kirby and Waldo, 2007). Laminin matrix is known to be remodeled during cardiac infraction, even though the exact role laminins play during this process is still controversial (Yabluchanskiy et al., 2013). In homeostatic conditions, laminins are assembled around cardiomyocytes (Kim et al., 1999), and seem to play critical roles during cardiac development as *Lama4* null mice and mutations in *LAMA4* in human display cardiomyopathy (Wang et al., 2006; Knöll et al., 2007). However, the role of different laminin isoforms during cardiac development remains largely unknown. At gestation week 8 during human cardiac development, β1 and β2 containing laminins can be found in the cardiomyocyte matrix (Kim et al., 1999; Roediger et al., 2010). Interestingly, α6 and α7 integrins were found to be synthesized in specific regions of the myocardium during cardiac development. In a mouse embryo stage E8.5-E9.5, integrin α6 mRNA and protein are enriched in the atrial chamber compared to the ventricle (Thorsteinsdóttir et al., 1995). During fetal stages, α6-integrins are produced by the atrial myocardium and compact myocardium of the ventricles, but is absent from the trabecular myocardium (Hierck et al., 1996). Conversely, integrin α7 mRNA (*Itga7*) is expressed in both atrial and ventricular myocardium at E13.0, but by E18, this mRNA becomes localized only at the base of trabeculae (Hierck et al., 1996). One possible outcome of the regionalized allocation of integrins is the assembly of different laminin isoforms in specific regions of the myocardium as well. Nevertheless, as noted above, information about laminin matrices in the cardiac muscle is still scarce and this hypothesis has not been formally tested.

4. From somite to skeletal muscle

4.1. Somite formation

Somites are transient embryonic segments which give rise to the axial skeleton, tendons, dermis of the back, axial vessels, brown fat cells and to all skeletal muscles of the body and the tongue (Dubrulle and Pourquié, 2004; Christ et al., 2007). They are spherical structures derived from the presomitic mesoderm (PSM), which lie on both sides of the neural plate and notochord. Somites are generated rhythmically from the anterior PSM and are composed of a layer of epitheloid cells surrounding a core of mesenchymal cells (Scaal and Christ, 2004; Martins et al., 2009). The rhythmic budding off of somites is thought to involve a posterior to anterior maturation process of the PSM cells and a molecular oscillator, the embryonic clock (Palmeirim et al., 1997; Bessho et al., 2003; Aulehla and Herrmann, 2004; Dubrulle and Pourquié, 2004; Andrade et al., 2007).

4.2. Somite derivatives

Somites undergo a process of maturation that leads to the formation of four different compartments known as sclerotome, dermomyotome, myotome and syndetome, which contain the cells responsible for the formation of the axial musculoskeletal system (Brent and Tabin, 2002; Fig. 10).

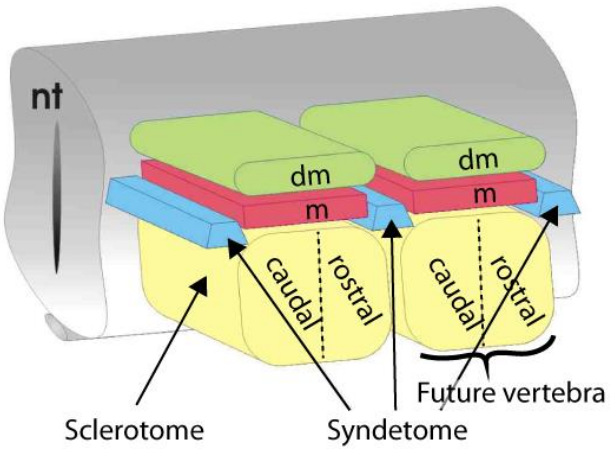

Figure 10- Somite derivatives. Scheme depicting the dermomyotome (dm; green), the myotome (m; red), the sclerotome (yellow) and the syndetome (blue). Adapted from Andrade et al., 2007.

4.2.1. Sclerotome: the source of bones and cartilage in the axial skeleton

Soon after a somite is formed, its ventral portion undergoes an epithelium to mesenchyme transition (EMT), generating the sclerotome, the precursor of the axial skeleton (Brent and Tabin, 2002). This process starts when notochord-derived Noggin (which blocks lateral mesoderm-derived BMP4) and Shh promote the expression of sclerotome-specific transcription factors such as Pax1 and Pax9 (Christ et al., 2004; Christ et al., 2007; Monsoro-Burq, 2005). Sclerotome cells then downregulate N-cadherin, decreasing cell-cell adhesion, while increasing cell motility, leading to the EMT (Brent and Tabin, 2002; Christ et al., 2007). Further maturation of the sclerotome leads to the segregation into different dorso-ventral and medio-lateral domains, which contribute to the development of different regions the vertebra and ribs (Brent and Tabin,

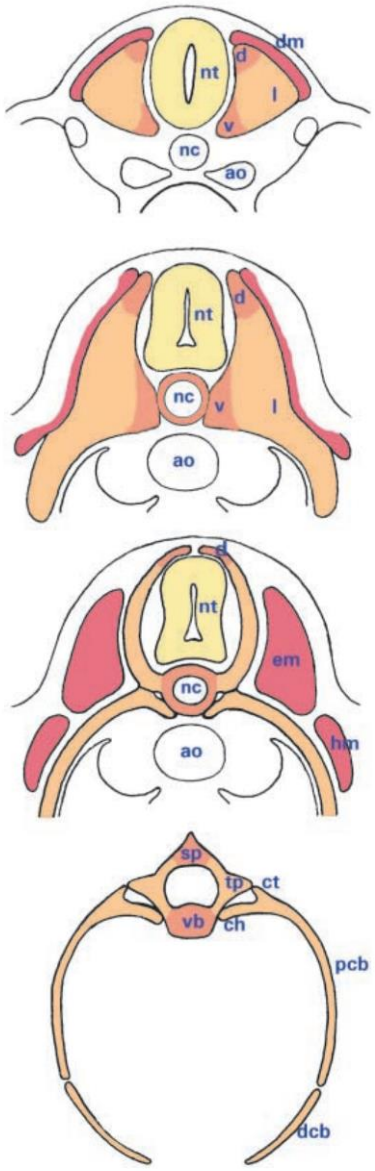

Figure 11- Sclerotome differentiation. Schematic representation of sclerotome differentiation in the avian embryo (ao: aorta; ch: costal head; ct: costal tubercle; d: dorsal sclerotome; dcb: distal costal body; dm: dermomyotome; em: epaxial muscle; hm: hypaxial muscle; l: lateral sclerotome; nc: notochord; nt: neural tube; pcb: proximal costal body; sp: spinous process; tp: transverse process; v: ventral sclerotome; vb: vertebral body). The dorsomedial part of the central sclerotome will give rise to the spinous process and the distal portion of the ribs (Brent and Tabin, 2002), while the ventromedial part develops around the notochord to generate the vertebral bodies, intervertebral discs, neural arches and proximal ribs (Christ et al., 2007; Brent and Tabin, 2002). These sclerotomal cells provide the progenitors for the formation of the distal ribs and tendons (Christ et al., 2000; Brent et al., 2003; Christ et al., 2007). Figure from Christ et al., 2000.

2002; Brent et al., 2003; Christ et al., 2007; Fig. 11). The central part of the sclerotome develops in direct contact with the myotome (Christ et al., 2007; also see section 4.2.3.). Additional sclerotome patterning occurs along the antero-posterior axis. The caudal half of one sclerotome fuses with the rostral half of the sclerotome of the adjacent somite during a process called resegmentation, which enables the formation of an articulated musculoskeletal system with the muscles attached to the bones (Saga and Takeda, 2001; Dubrulle and Pourquié, 2004; Christ et al., 2007).

4.2.2. Dermomyotome: a progenitor factory

The dorsal-most region of the somite remains epithelial and constitutes the dermomyotome (Fig. 10), whose cells are multipotent progenitors and give rise to muscle progenitors (also called muscle stem cells; see section 6.1) forming the body and limb muscles, to brown fat cells, endothelial cells, and dermal progenitors of the back (Ben-Yair and Kalcheim, 2005; Kassar-Duchossoy et al., 2005; Relaix et al., 2005; Thorsteinsdóttir et al., 2011; Deries and Thorsteinsdóttir, 2016). Dermomyotome growth depends on the maintenance of the non-differentiated and proliferative epithelial state of the dermomyotome, which are characterized by the expression of the transcription factors Pax3 and Pax7 (Kassar-Duchossoy et al., 2005; Buckingham and Relaix, 2015). Adhesion molecules such as N-CAM (Neural cell adhesion molecule) and N-cadherin, localized in apical adherens junctions (Duband et al., 1987), and Wnt6 produced by the ectoderm are critical for maintaining the epithelial state of dermomyotome (Linker et al., 2005; Cinnamon et al., 2006; Geetha-Loganathan et al., 2006; Sagar et al., 2015).The growth of the dermomyotome also depends on ectodermal Wnt3a, which has been shown to promote the proliferation of dermomyotomal cells (Galli et al., 2004; Geetha-Loganathan et al., 2006). Furthermore, BMP4 signaling (Hirsinger et al., 1997; Linker et al., 2003) as well as cues from the ECM, in particular from laminins 111 and 511 in the dermomyotome

basement membrane (Bajanca et al., 2006), are essential to prevent precocious activation of the myogenic program in dermomyotomal cells.

4.2.3. Myotome: The first differentiated skeletal muscle

Myotome development is a complex process involving multiple cellular movements and rearrangements occurring as a consequence of the activation of the myogenic program (see section 5.1.) in different regions of the dermomyotome over time. Myotome formation is a two-step process (Gros et al., 2004). During an initial phase, cells of the dorsomedial lip (DML) of the dermomyotome enter the myogenic program and delaminate

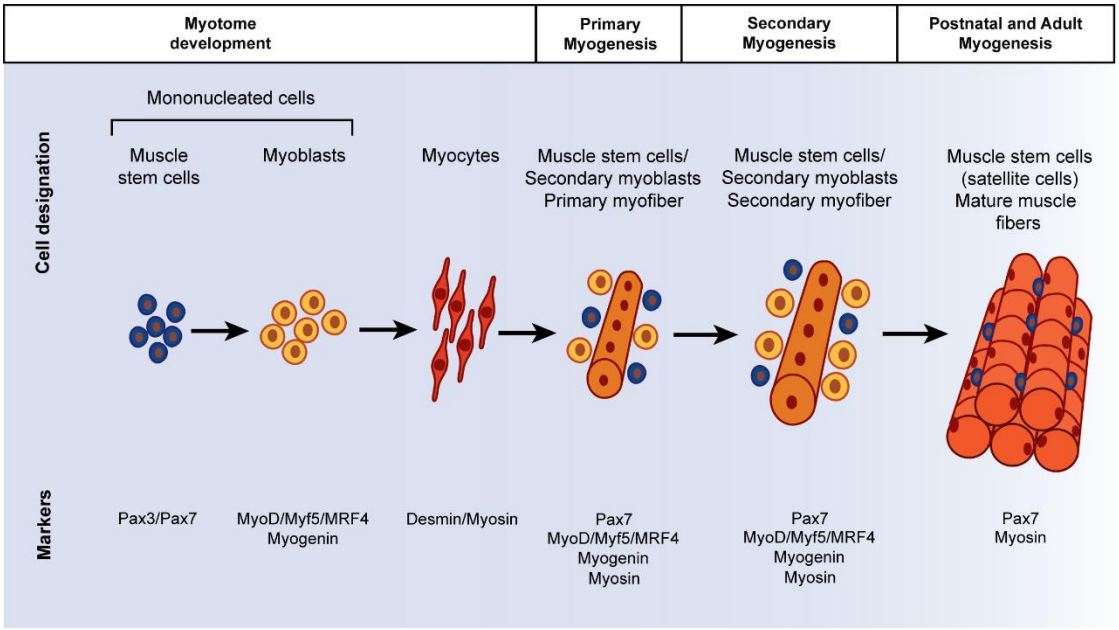

Figure 12- Overview of skeletal muscle development. Scheme depicting the different myogenic cells and the factors expressed by these cells during skeletal muscle development. The formation of the myotome begins when the dermomyotomal muscle stem cells positive for Pax3 and Pax7 are induced to differentiate into myoblasts expressing the MRFs MyoD, Myf5, MRF4 and Myogenin. These myoblasts then progress in the myogenic program and differentiate into Desmin- and Myosin-positive myocytes. During primary myogenesis, myoblasts fuse with the myocytes and with each other in axial muscles and only with each other in muscles developed from the migration of muscles stem cells to form the primary myofibers expressing Myosin, while some muscle stem Pax7-positive cells are maintained undifferentiated. Second myogenesis involved a second round of fusions between secondary myoblasts expressing MyoD, Myf5, MRF4 and Myogenin to form the secondary myofibers. The secondary myoblasts further fuse with the primary and secondary myofibers to increase their size. During postnatal development, the myofibers increase their size and muscle stem Pax7-positive cells enter into quiescence. Adapted from Deries and Thorsteinsdóttir, 2016.

into the myotomal space, where they differentiate and elongate into cells called myocytes (see Fig. 12), forming the epaxial myotome (Denetclaw et al., 1997; Venters et al., 1999; Gros et al., 2004; Rios et al., 2011; Deries and Thorsteinsdóttir, 2016). As new cells committed to myogenesis delaminate from the dermomyotome and enter the epaxial myotomal space, older myocytes get displaced ventro-laterally (Venters et al., 1999; Gros et al., 2004). During the following phase, activation of myogenesis occurs at all four lips of the dermomyotome and cells enter the myotomal space from these four lips (Venters et al., 1999; Gros et al., 2004). This contributes to the growth of the myotome in the ventral direction (hypaxial myotome) and to its medio-lateral growth, making it thicker (Gros et al., 2004; Deries and Thorsteinsdóttir, 2016; Fig. 13A). The cellular growth of the myotome is driven by the expression of myogenic regulatory factors (MRFs), transcription factors which control the progression of cells through the myogenic program (Buckingham, 2001; Buckingham and Rigby, 2014; Deries and Thorsteinsdóttir, 2016; see section 5.1).

4.2.4. Syndetome: linking bone and muscles

The syndetome is the last somite compartment to form and is the source of tendon precursors, which give rise to the tendons attaching the dorsal muscles to the vertebrae (Hollway and Curie, 2005). In the embryo, the syndetome is established in the anterior and posterior dorsal-most edges of the sclerotome, in a group of sclerotomal cells that cease the expression of sclerotome marker *Pax1* in response to myotomal Fgf8 signaling and start expressing Scleraxis, a bHLH (Basic helix-loop-helix) transcription characteristic of tendinocytes (Brent et al., 2003).

5. Skeletal muscle development

5.1. Myogenic regulatory factors

The myogenic regulatory factors, namely Myf5, MyoD, Mrf4 and Myogenin, are bHLH transcription factors essential for myogenic determination and differentiation (Buckingham, 2001; Buckingham et al., 2003; Buckingham and Rigby, 2014). Myf5, Mrf4 and MyoD act as determination factors, while Myogenin is a differentiation factor (Buckingham and Vincent, 2009; Buckingham and Rigby, 2014).

Myf5 is the first MRF to be expressed during myogenesis and is crucial for the dermomyotome progenitors to acquire the myogenic identity (Tajbakhsh et al., 1996). Myf5 and MyoD play specific roles during epaxial and hypaxial myotome development, respectively, but are able to compensate at least partially for each other's absence (Kablar et al., 1997; Kablar et al., 1998). Double *Myf5: MyoD* knock out mice can form some

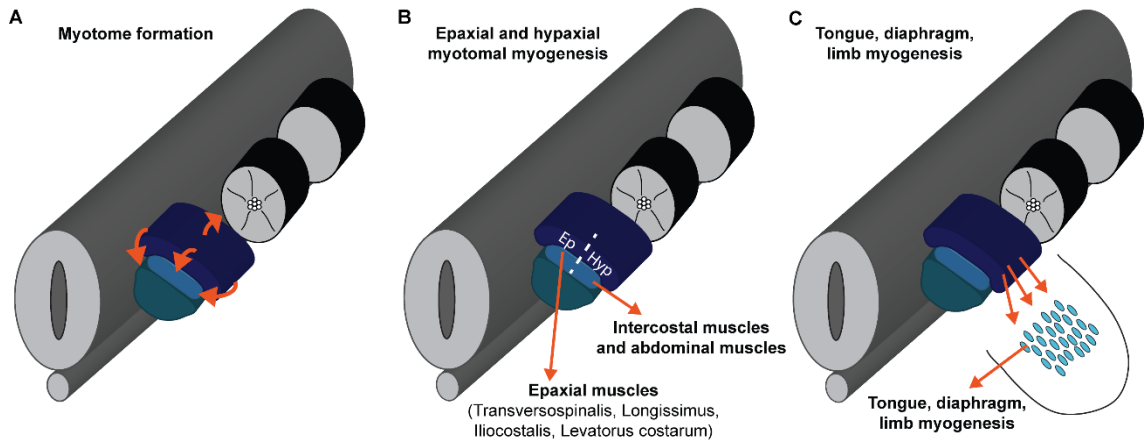

Figure 13- Myotomal and limb myogenesis. (**A**) Myotome is initially colonized by the dorsomedial lip precursors, and then grows through the addition of precursors delaminating from the four dermomyotome lips. (**B**) Epaxial myotome gives rise to the epaxial muscles (transversospinalis, longissimus, iliocostalis and levatores costarum, while the hypaxial myotome originates the intercostal and abdominal muscles. Myogenesis taking place in the epaxial myotome is the first step of epaxial myogenesis, in contrast to the myogenesis occurring in the hypaxial myotome which is only the first step of a part of the hypaxial myogenesis. (**C**) Hypaxial myogenesis also comprised the development of limb, tongue and diaphragm muscles. This process starts with the delamination and migration of the ventrolateral lip precursors towards the target sites (e.g. limb) and concludes with the myogenic differentiation at those sites.

muscles through the activation of Mrf4 (Kassar-Duchossoy et al., 2004), showing that Mrf4 can drive myogenesis by itself, albeit very incompletely. The activation of *Myf5* and *MyoD* is regulated by large and complex regulatory regions. In the case of *Myf5*, regulatory sequences span 96 Kbp and include enhancers that drive *Myf5* expression in the epaxial dermomyotome, in the branchial arches and early somites, and in the myotome (Summerbell et al., 2000; Hadchouel et a., 2003; Buckingham and Rigby, 2014). *MyoD* activation is in turn regulated by two enhancers: one controls its early expression in the myotome, and the other one regulates MyoD activation during later stages of myogenesis and in satellite cells during muscle regeneration (Tapscott, 2005).

Myogenin is crucial for terminal myogenic differentiation, because *Myogenin* knockout mice, in spite of displaying normal numbers of mononucleated muscle cells, have a dramatic reduction in the number of myofibers (Arnold and Braun, 1996). The expression of *Myogenin* is controlled by a single regulatory region throughout myogenesis (Buckingham, 2006; Yee and Rigby, 1993; Buckingham and Rigby, 2014).

5.2. Epaxial muscle development

5.2.1. Formation of the epaxial myotome

The epaxial (dorsal) and the hypaxial (ventral) regions of the myotome are induced and develop independently before giving rise to epaxial (deep back) muscles and axial hypaxial muscles (Deries and Thorsteinsdóttir, 2016; Fig. 13B). The induction of epaxial myogenesis depends on the activation of *Myf5* expression and may involve asymmetric cell divisions in the DML (Cossu et al., 2000; Gros et al., 2004; Venters and Ordahl, 2005; Bothe et al., 2007;). In fact, Shh plays a dual role in promoting proliferation and differentiation through different Gli mediators (Kahane et al., 2013). Some of these mediators, such as Gli2 and Gli3, synergize with canonical Wnt/β-catenin signaling to

induce *Myf5* activation (Borello et al., 2006). Myf5 activation in the DML is dependent on the activity of noggin in the DML, which counteracts the ectodermal derived BMP4 signal, an inhibitor of muscle differentiation (Hirsinger et al., 1997; Amthor et al., 1999). Interestingly, migrating neural crest cells expressing delta ligands have been shown to activate Notch signaling briefly in some DML cells, which induces *Myf5* expression in these cells (Rios et al., 2011; Deries and Thorsteinsdóttir, 2016).

Myotome growth is determined by the successive cycles of delamination of Myf5-positive cells from the dermomyotome and their differentiation. In the myotome, Myf5-positive myotomal myoblasts activate *Myod* while initially maintaining their proliferation (Gros et al., 2004; Buckingham, 2001; Buckingham and Rigby, 2014; Deries and Thorsteinsdóttir, 2016). During this phase, other signals such as myostatin produced by the central dermomyotome and the dorsal-most myotome induce *Myod* and the cyclin dependent kinase C*dkn1a* (encoding for p21), which force cell cycle withdraw (Manceau et al., 2008). Terminal differentiation and entry into the post mitotic state is associated with the expression of Myogenin and myosin heavy chain proteins (Pownall et al., 2002; Buckingham and Rigby, 2014).

5.2.2. The formation of the definitive epaxial muscle masses

Myotomal myogenesis is followed by the de-epithelialization and consequent dissociation of the dermomyotome. The central dermomyotome starts to de-epithelialize at E10.5, when *Paraxis* expression in the dermomyotome ceases after Wnt6 downregulation in the ectoderm (Linker et al., 2005). This dissociation is later extended to the dermomyotomal lips (Ben-Yair and Kalcheim, 2005; Kassar-Duchossoy et al., 2005; Relaix et al., 2005; Thorsteinsdóttir et al., 2011). This process leads to the release of progenitors that can migrate either ventrally as muscle stem cells that maintain the expression of Pax3 and Pax7 and intermingle with the myocytes of the myotome, or

migrate dorsally where they lose Pax3 and Pax7 and give rise to the dermal progenitors (Ben-Yair and Kalcheim, 2005; Kassar-Duchossoy et al., 2005). The pool of muscle stem cells is maintained from this stage until adulthood and give rise to the quiescent satellite cells of adult muscles (Hartley et al., 1992; Relaix et al., 2005; Kassar-Duchossoy et al., 2005; Schienda et al., 2006; Lepper et al., 2009; Tabakhsh 2009).

The myotome is a transient muscle and its epaxial part gives rise to the epaxial, or deep back, muscles which are innervated by the dorsal ramus of the spinal nerves, in contrast to the hypaxial muscles which are innervated by the ventral ramus (Deries et al., 2008). Studies in rat and mouse embryos revealed that after dermomyotome dissociation, epaxial myocytes cleave into discrete muscle masses and shift their orientation to generate the epaxial muscles during a process designated translocation (Deries et al., 2010; Fig. 14). During translocation, which spans from E11.5 to E13.0 in the mouse, the dorsal more myocytes and forming myotubes separate from the most ventral ones to form the *transversospinalis* muscle groups, while the ventral masses elongate to form the *iliocostalis* and *longissimus* muscle groups (Deries et al., 2010; Thorsteinsdóttir et al., 2011; Deries et al., 2012). The most medial muscle, the *levatores costarum* muscle is formed at the thoracic level, where it is attached to the ribs and the vertebrae. (Deries et al., 2010). During translocation, the *Scx*-positive tendon precursors are maintained between the

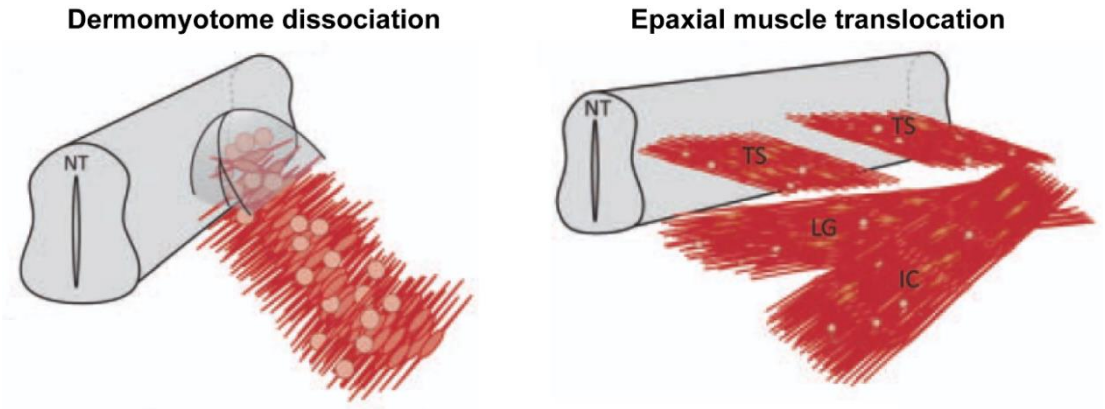

Figure 14- Dermomyotome dissociation and epaxial muscle translocation. Scheme depicting dermomyotome dissociation (left) and epaxial muscle translocation (right). Adapted from Deries et al., 2012.

translocating myocytes and within the muscle cleavage sites where they will form the tendon that attaches to the muscle (Deries et al., 2010).

5.3. Hypaxial Myogenesis

5.3.1. Formation of the hypaxial myotome

There are two types of hypaxial myogenesis and both start in the VLL (ventrolateral) lip of the dermomyotome. At limb levels, VLL cells delaminate and migrate to the forming limb buds and to the diaphragm, while maintaining Pax3 expression and only differentiate upon arrival to their target sites (Gross et al., 2000; Buckingham et al., 2003; Thorsteinsdóttir et al., 2011; Deries and Thorsteinsdóttir, 2016; Fig. 13C). Tongue muscles are formed from cervical segments in a similar fashion (Gross et al., 2000). A second hypaxial myogenesis program occurs at the remaining axial levels when cells delaminate from the VLL, activate *Myod* and form the hypaxial myotome (Kablar et al., 2003; Gros et al., 2004; Pu et al., 2013; Fig. 13B). Activation of *Myod* in the VLL may be induced by Wnt7a produced by the ectoderm (Tajbakhsh et al., 1998), and by the secretion of the BMP antagonist noggin in the hypaxial dermomyotome, that counteracts the activity of BMPs produced by the lateral mesoderm and the ectoderm (Amthor et al., 1999). The hypaxial portion of the myotome later develops in the intercostal muscles and three of hypaxial abdominal muscles (Christ et al., 1983; Cinnamon et al., 1999).

5.3.2. Limb myogenesis

Limb myogenesis requires a sequence of events that start with the delamination and migration of VLL derived muscle stem cells to the limb buds, where some of them activate the myogenic program and differentiate into myoblasts which fuse into primary myotubes to form the dorsal and ventral muscle masses (Buckingham et al., 2003). During

the initial steps of limb myogenesis, different transcription factors such as Pax3, Lbx1 and Msx1 are crucial for survival and migration of the muscle stem cells (Borycki et al., 1999; Dietrich, 1999; Buckingham et al., 2003; Buckingham and Relaix, 2015). Signaling through the tyrosine kinase receptor c-met, which binds to the hepatocyte growth factor (HGF) expressed by the mesenchyme induces the delamination of cells from the VLL and keeps the muscle stem cells in an undifferentiated state (Brand-Saberi et al., 1996; Dietrich, 1999; Scaal et al., 1999; Relaix et al., 2003). The migratory path pursued by these hypaxial muscle stem cells is defined by attractive and repulsive signals produced by the surrounding mesenchyme (Buckingham et al., 2003; Buckingham and Rigby et al., 2014). For example, migrating muscle stem cells express the CXCR4 (C-X-C chemokine receptor type 4) receptor which binds the chemoattractant stromal cell-derived factor 1 (SDF1) expressed by the mesenchyme (Vasyutina et al., 2005). In contrast, Ephrin-A5 present in the distal region of the limb acts as a repulsive signal for the migratory muscle stem cells, which express the complementary EphA4 receptor thus restricting their distribution to the more proximal limb regions (Swartz et al., 2001).

Once these muscle stem cells are in the limb, the first wave of muscle stem cell differentiation starts around E11.0 in the mouse forelimb, with the activation of Myf5 and MyoD expression (Lee et al., 2013). Simultaneously, some muscle stem cells are maintained through Notch signaling, which counteracts the activation of the myogenic differentiation program by blocking *Myod* expression (Delfini et al., 2000; Vasyutina et al., 2007). Other factors such as Shh has been shown to induce myogenesis in the early ventral limb and to promote the differentiation of slow myofibers (Hu et al., 2012). In addition, Wnt/β-catenin canonical signaling was also shown to be crucial for the normal hyperplasic muscle growth in the limb (Hutcheson et al., 2009).

5.4. Primary myogenesis

Primary (or embryonic) myogenesis starts around E11.5 in the mouse (Wigmore and Dunglison, 1998; Biressi et al., 2007). During epaxial muscle development, translocation occurs in parallel with primary myogenesis (Kelly and Zacks, 1969; Ross et al., 1987; Thorsteinsdóttir et al., 2011; Fig. 15A). The first multinucleated cells are detected in the myotome at E11.5 in the mouse (Venters et al., 1999) after dermomyotome dissociation, which releases the proliferating muscle stem cells within the muscle masses, some of which differentiate into primary myobasts (Relaix et al., 2005; Kassar-Duchossoy et al., 2005). From this stage onward, multiple fusion events between differentiating myoblasts and/or the existing myocytes quickly generate the first primary myotubes (Duxson et al., 1989; Deries et al., 2010). Primary myotubes then attach to the tendons by E14.5, and thus set up the anlagen for the subsequent phase of myogenesis (Harris et al., 1989; Duxson and Usson, 1989; Thorsteinsdóttir et al., 2011). In contrast to myogenesis in the myotome which proceeds without innervation, the beginning of primary myogenesis is marked by muscle innervation (Deries et al., 2008; Hurren et al., 2015). During myofiber maturation, the contact between the nerve and the muscle fiber is crucial to avoid degeneration (Ross et al., 1987; Ashby et al., 1993).

Primary myogenesis involves the fusion of specific myoblasts, primary (or embryonic) myoblasts, which were first defined as cells producing short fibers with few nuclei contributing solely to primary myofibers (Evans et al., 1994; Dunglison et al., 1999). More recently the gene expression profile of primary myoblasts has been further characterized and compared to that of later stage myoblasts (Biressi et al., 2007).

Primary myotubes synthesize MyHC-emb (embryonic myosin heavy chain) and MyHC-β/slow (Myosin heavy chain-β/slow) isoform at the beginning of their formation (Ecob-Prince et al., 1989; Dunglison et al., 1999; Wigmore and Evans, 2002; Schiaffino and Reggiani, 2011), but some of the primary myofibers later produce the perinatal/neonatal

fast isoform of MyHC (Myosin heavy chain) as well (Schiaffino and Reggiani, 2011). The myotubes expressing the MyHC-β/slow isoform and the perinatal/neonatal fast isoform will give rise to the adult slow-twitch or fast-twitch fibers, respectively (Schiaffino and Reggiani, 2011). The end of embryonic myosin isoform expression and the beginning of adult myosin isoform expression occurs postnatally (Wigmore and Evans, 2002).

5.5. Secondary myogenesis

During stages that follow primary myogenesis until birth, some of the remaining muscle stem cells, now designated fetal muscle stem cells (Tajbakhsh, 2009; Mourikis et al., 2012b), undergo a second wave of differentiation and fusion: the secondary (or fetal) myogenesis (Harris et al., 1989; Duxson and Udson, 1989; Evans et al., 1994; Zhang and McLennan, 1995; Dunglison et al., 1999; Thorsteinsdóttir et al., 2011; Fig. 15B). The fetal muscle stem cells only express Pax7 (Hutcheson et al., 2009). By E16.5 they migrate underneath the myofiber basement membrane in a Notch dependent process (Kassar-Duchossoy et al., 2005; Bröhl et al., 2012). Notch signaling is also necessary to maintain muscle stem cells throughout myogenesis (Mourikis et al., 2012a). In fact, committed MyoD-positive myoblasts express *Dll1* which maintains the neighboring muscle stem cells in an undifferentiatied state (Delfini et al., 2000; Schuster-Gossler et al., 2007). Moreover, in *Dll1* null fetuses, primary myotubes form but the following muscle growth is affected because very few muscle stem cells remain at E14.5 (Schuster-Gossler et al., 2007). The pace of myogenic differentiation and fusion during secondary myogenesis is also regulated by the TGFβ Myostatin signaling pathway, a well-known negative regulator of muscle growth (McPherron et al., 1997; Matsakas et al., 2010). Myostatin signaling is critical for the normal progression of secondary myogenesis as *Mstn*$^{-/-}$ fetuses display accelerated secondary myogenesis, at the expense of Pax7-positive progenitors (Matsakas et al., 2010).

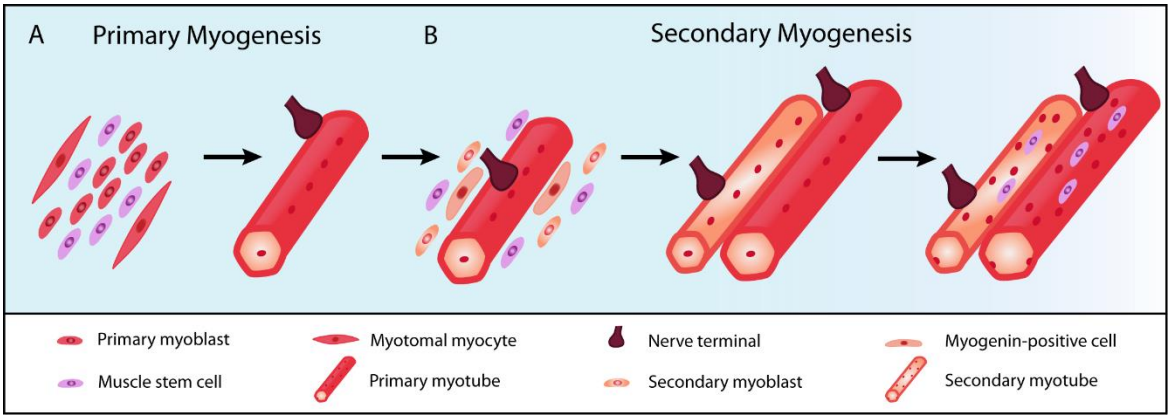

Figure 15- Primary and secondary myogenesis. (**A**) Primary myogenesis is marked by the fusion of primary myoblasts with the myotomal myocytes to form the primary myotubes. Primary myogenesis occurs concomitantly with muscle innervation (Duxson et al., 1989; Deries et al., 2010: Hurren et al., 2015). (**B**) During secondary myogenesis, secondary myoblasts fuse with each other to generate the secondary myotubes, and with the primary myotubes to increase their size (Harris et al., 1989; Duxson and Udson, 1989; Evans et al., 1994; Zhang and McLennan, 1995; Dunglison et al., 1999; Thorsteinsdóttir et al., 2011).

Secondary (fetal) myoblasts were first characterized *in vitro* as myoblasts isolated during secondary myogenesis and capable of originating long thin multinucleated myotubes in culture (Wigmore and Dunglison, 1998). They display a distinct genetic signature from that of primary myoblasts by for example expressing higher levels of the α7β1 integrin (Evans et al., 1994; Wigmore and Dunglison, 1998; Biressi et al., 2007). Secondary myotubes form with the progressive and asynchronous addition of secondary myoblasts (Harris et al., 1989), and the subsequent growth of primary and secondary myotubes occurs with the fusion of myoblasts to the end of the myotubes (Zhang and McLennan, 1995). Primary myotubes guide the longitudinal growth of secondary myotubes along their surface beneath their basement membrane through specialized adherens junctions (Kelly and Zacks, 1969; Duxson and Usson, 1989). As the secondary myotubes mature, they attach to tendons and form their own basement membrane, and at this phase, adherens junctions become restricted to the myotube extremities and to the tendons (Kelly and Zacks, 1969; Ross et al., 1987; Duxson and Usson, 1989). M-cadherin is present on the surface of both types of myotubes (Rose et al., 1994), whereas N-cadherin is primarily localized in regions where secondary myoblasts and recently formed secondary

myofibers attach to primary myofibers (Fredette et al., 1993). The sites of secondary myogenesis also seem to be controlled by other adhesion molecules such as integrins. It has been proposed that the α4β1 integrin, present on the surface of the primary and secondary myotubes, interacts with receptor V-CAM1 (Vascular cell adhesion molecule 1), which is expressed in the secondary myoblasts (Rosen et al., 1992). Secondary myofibers synthesize the embryonic and the perinatal/neonatal fast MyHC isoform, but do not produce the MyHC-β/slow isoform (Ecob-Prince et al., 1989; Dunglision et al., 1999; Wigmore and Evans, 2002; Schiaffino and Reggiani, 2011).

5.6. Postnatal myogenesis

Postnatal myogenesis is mainly characterized by the growth of muscle masses until their final adult size, which in the mouse is a hypertrophic process (Ontell and Kozeka, 1984). Until postnatal stage P21 (postnatal day 21), the hypertrophy is mostly achieved by the fusion of myoblasts with the muscle fibers as can be seen by the increase of the number of myonuclei per fiber (White et al., 2010; Lepper et al., 2011). In contrast, from P21 onwards, myofibers volume is increased without addition of myonuclei and is thus no longer a cell-mediated hypertrophy process (White et al., 2010). These changes in the nuclei contribution for myofiber growth correlates with changes in muscle stem cells identity. During this phase, myofibers also undergo maturation and start expressing the adult slow and fast-twitch myosin isoforms (also see sections 5.4. and 5.5. above).

5.7. Laminins and laminin receptors during myogenesis

Laminins are assembled early in myogenesis, with the deposition of the dermomyotomal basement membrane on the basal side of the dermomyotome and the assembly of the myotomal basement membrane (Bajanca et al., 2006; Deries et al., 2012).

Laminin deposition in the myotomal basement membrane depends primarily on laminin 111, which is crucial for the following assembly of laminin 511 (Bajanca et al., 2006; Anderson et al., 2009). These laminins play key roles during myotomal myogenesis to restrain Myf5-positive myoblasts in the myotomal compartment (Bajanca et al., 2006). Strikingly, Shh-mediated activation of myogenesis is interconnected with the assembly of laminin in the myotome basement membrane, as it has been implicated in the expression of *Lama1* and therefore, in laminin 111 assembly (Anderson et al., 2009).

At the beginning of primary myogenesis of intercostal muscles, the basement membrane is composed of laminins 211 and 511 (Patton et al., 1997). However, staining of E12.5 early epaxial muscles revealed that laminin is only found in spots within the muscle masses (Deries et al., 2012). In addition, integrins α6β1 and α7β1 are not expressed between E11.5 and E13.5 during epaxial muscle translocation (Cachaço et al., 2005). Together, these results raise the possibility that laminins might be progressively disassembled or degraded during primary myogenesis. Laminins 211/221 are expressed during fetal and adult myogenesis. Analysis of E15.0 fetal muscle revealed that the myofiber basement membrane is composed of laminins 211, 511 and 411 (Patton et al., 1997). Laminin 211 is the major laminin isoform surrounding the myofibers in the adult muscle, whereas laminin isoform 221 is characteristic of neuromuscular junctions (Patton et al., 1997; Patton, 2000). In fact, laminins 211/221 are critical for myofibers survival (Vachon et al., 1996; Laprise et al., 2003; Holmberg and Durbeej, 2013), and to regulate the autophagy-lysossome pathway (Carmignac et al., 2011) and the ubiquitin-proteasome system (Carmignac et al., 2010). Integrin β1A is synthesized throughout embryonic and fetal muscle development and downregulated after birth, whereas β1D splice variant is produced in skeletal muscle from E17.5 onwards and is maintained during adulthood (van der Flier et al., 1997; Brancaccio et al., 1998). Interestingly, the β1D integrin isoform is unable to compensate for the absence of β1A during primary myogenesis indicating a difference in integrin requirement between these two phases (Cachaço et al., 2003).

6. Adult muscle and satellite cells

6.1. Satellite cells: drivers of regeneration with a characteristic profile

Mammals display poor organ regeneration capacity when compared to other animals such as the newt and the zebrafish. However, adult mammalian skeletal muscle has regeneration capacity despite the low myonuclear turnover rate under homeostatic conditions (Chargé and Rudnicki, 2004). Upon injury, the adult muscle is capable of initiating a regeneration process to repair damaged fibers and generate new myofibers. The regeneration process is divided into the degenerative phase and the regenerative phase (Chargé and Rudnicki, 2004). During the degenerative (or inflammatory) phase, the myofiber basement membrane and the myofibrillar and cytoskeletal proteins undergo proteolysis, while macrophages infiltrate within the tissue (Chargé and Rudnicki, 2004; Yin et al., 2013). This degenerative inflammatory phase is then followed by the regenerative phase, where some of the satellite cells (quiescent muscle stem cells) are induced to differentiate and fuse to repair the damaged fibers, or to form new fibers that express the embryonic form of MyHC (Chargé and Rudnicki, 2004; Lepper et al., 2011).

Satellite cells are the main drivers of muscle regeneration in the adult (Lepper et al., 2011). These cells were initially described by electron microscopy as mononucleated cells located between the myofiber and the myofiber basement membrane (Mauro, 1961). Different studies demonstrated that satellite cells are derived from the Pax3 and Pax7-positive progenitors of the central dermomyotome and are muscle stem cells; they are maintained throughout embryonic and fetal myogenesis until they become quiescent around 2-3 weeks after birth (Hartley et al., 1992; Relaix et al., 2005; Kassar-Duchossoy et al., 2005; Schienda et al., 2006; Lepper et al., 2009; Tabakhsh, 2009). Satellite cells display several characteristic cell surface markers such as CD34 (Beauchamp et al., 2000), M-cadherin (Irintchec et al., 1994; Cornelison and Wold, 1997), V-CAM (Fukada et al., 2007), c-met (Cornelison and Wold, 1997), integrin α7β1 (Burkin and Kaufman, 1999),

dystroglycan (Cohn et al., 2002) and syndecan 3 and 4 (Cornelison et al., 2001; Fig. 16). Satellite cells are also characterized by the expression of Pax7 and the depletion of Pax7-positive cells by diphtheria toxin blocks muscle regeneration (Lepper et al., 2011; Sambasivan et al., 2011).

Satellite cells are normally maintained in a quiescent state in phase G0 of the cell cycle, with a low metabolic rate (Montarras et al., 2013; Dumont et al., 2015). The quiescent non-cycling state is characterized by the expression of different factors including the cyclin-dependent kinase inhibitor p27 and the FGF signaling antagonist Sprouty1 (Shea et al., 2010; Chakkalakal et al., 2012). Upon injury, these cells are induced to enter the cell cycle to proliferate and to increase their aerobic metabolism, increasing ATP synthesis necessary for protein synthesis during proliferation. Subsequent progress into the myogenic program allows activated satellite cells to terminally differentiate and incorporate into new or damaged fibers (Tajbakhsh, 2009; Sambasivan et al., 2011; Lepper et al., 2011; Montarras et al., 2013; Dumont et al., 2015; Fig. 17).

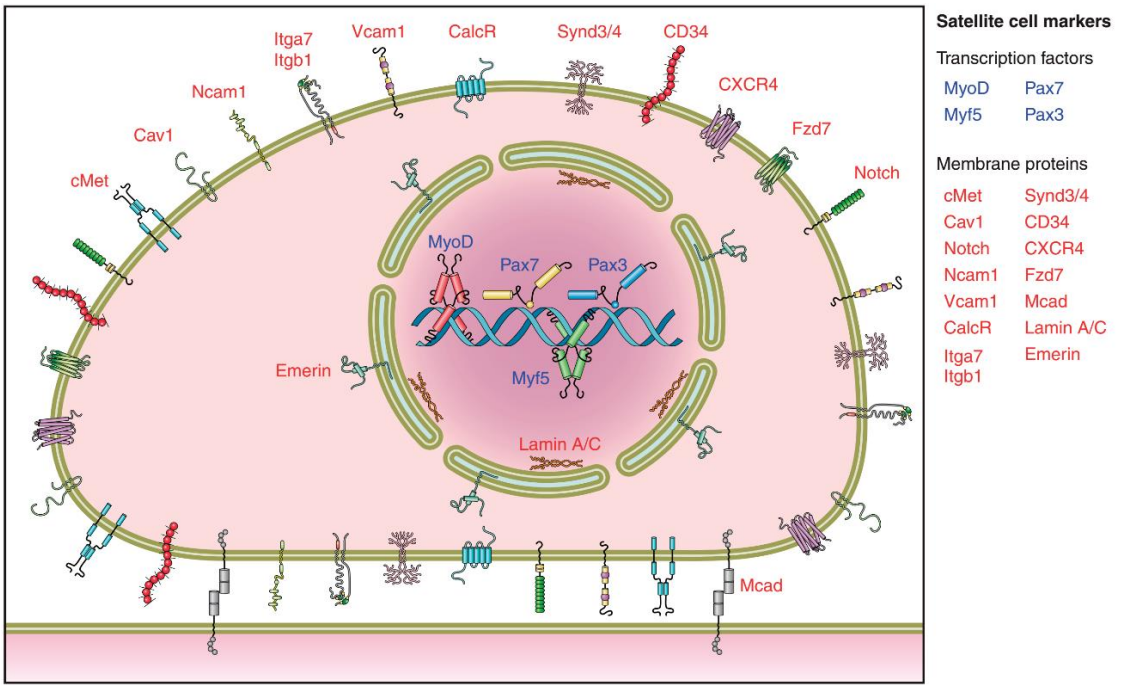

Figure 16- Satellite cell expression profile. Satellite cells express different intracellular transcription factors and cell surface markers. Adapted from Yin et al., 2013.

6.2. Self-renewal versus differentiation of satellite cells

6.2.1. Symmetric vs asymmetric divisions: polarized segregation of intracellular components

Satellite cells display an extraordinary capacity of self-renewal that enables them to maintain their pool even after several cycles of regeneration (Collins et al., 2005; Dumont et al., 2015). The balance between self-renewal and differentiation is thus crucial to maintain the satellite cell pool. *In vivo* analysis of adult EDL (Extensor digitorum longus) muscle revealed that 90% of sublaminar Pax7 cells express or have expressed *Myf5* at some point of their lives (Kuang et al., 2007). $Pax7^+/Myf5^-$ cells can divide symmetrically to expand the pool, giving rise to two $Pax7^+/Myf5^-$ daughter cells, or they divide asymmetrically into one $Pax7^+/Myf5^+$ and one $Pax7^+/Myf5^-$ daughter cell to maintain the pool, while generating committed cells (Kuang et al., 2007; Dumont et al., 2015; Fig. 17). $Pax7^+/Myf5^-$ cells lying against the basement membrane maintain Pax7 and Notch 3 production, while $Pax7^+/Myf5^+$ cells express Delta1 ligand (Delfini et al., 2000; Kuang et al., 2007). The polarized segregation of the Par complex then activates p38α/β MAPK signaling pathway, which induces MyoD in the daughter cell giving rise to the proliferating myoblasts (Troy et al., 2012). Some Pax7-positive satellite cells display high levels of Pax7 and preferentially undergo asymmetric division (Rocheteau et al., 2012). The asymmetric segregation of the older template DNA into the daughter cell is thought to maintain the satellite cell identity (Rocheteau et al., 2012). Pax7 directly regulates the expression of *Myf5* in the apical daughter cell through binding to Carm1, which is responsible for the methylation of the transcription factor Pax7 and for allowing the recruitment of ASH2L:WDR5:MLL1/2:RBBP5 histone methyltransferase complex to the regulatory region of *Myf5* locus in the committed cell (Kawabe et al., 2012).

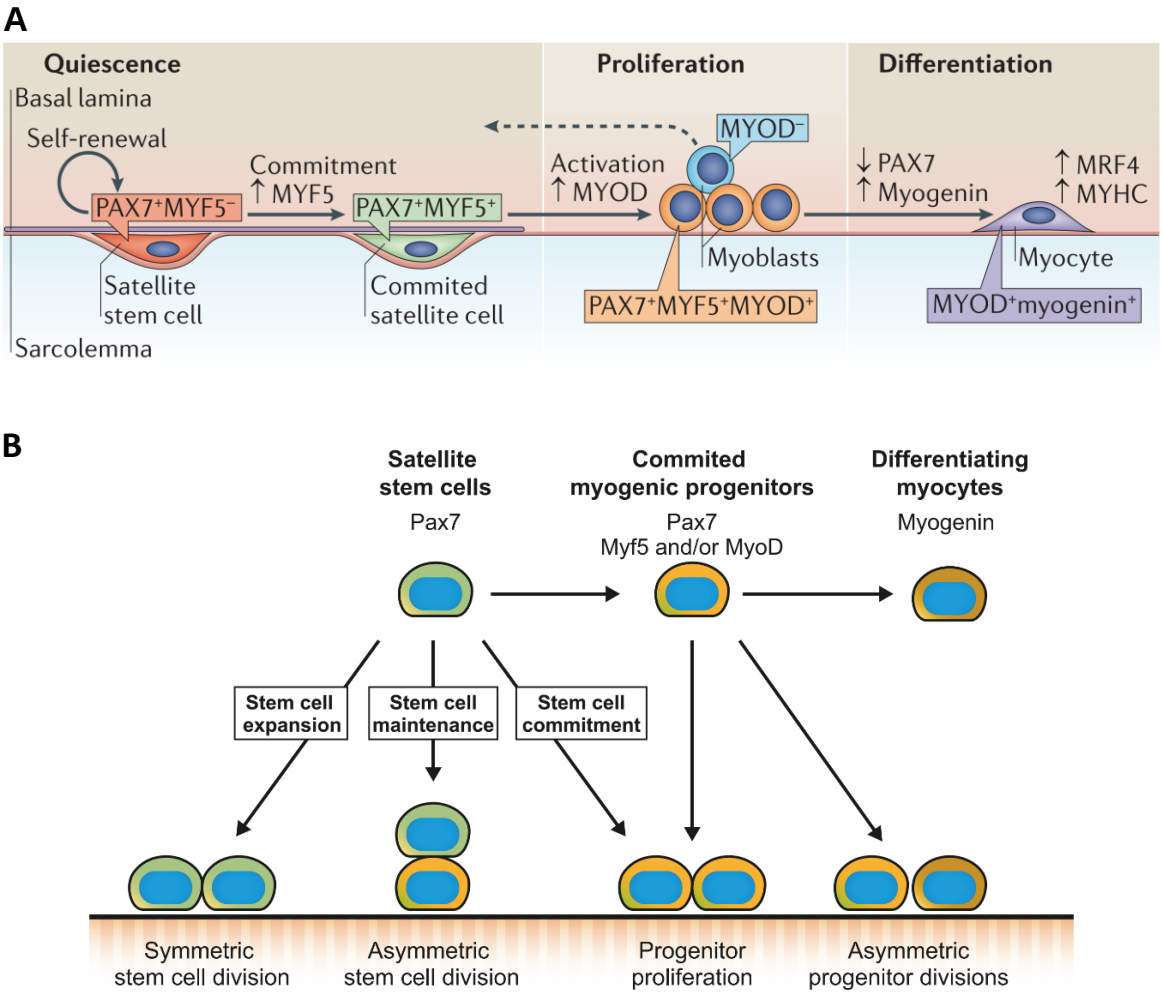

Figure 17- Muscle stem cell function during muscle regeneration. Muscle stem cells undergo different cellular states during muscle regeneration (A). Upon muscle damage, muscle cells are activated and exit their quiescent state (A). Symmetric divisions allow muscle stem cell self-renewal, while asymmetric divisions enable the generation of a daughter stem cell and another daughter committed cell (A,B). The committed cell proceeds in the myogenic program to give rise to terminal differentiated myoblasts which then fuse with the damage fiber or between each other to generate new fibers (A,B). Adapted from Wang and Rudnicki et al., 2012 and Dumont et al., 2015.

6.2.2. Extracellular environment of satellite cells: myofibers and myoblasts

The composition and stiffness (12kPa) of normal muscle extracellular matrix is known to influence self-renewal of cultured muscle satellite cells, myoblast differentiation and myotube striation (Engler et al., 2004; Boonen et al., 2009; Gilbert et al., 2010). The myofiber basement membrane provides the first cues to satellite cells as they are located

under this basement membrane after E16.5 (Kassar-Duchossoy et al., 2005). Moreover, satellite cells express several adhesion molecules and cell surface receptors such as M-cadherin and V-CAM, which allow them to interact directly with the myofiber and the ECM in homeostatic or regeneration conditions. On the other hand, myofibers secrete numerous factors which affect satellite cell function (Fig. 18). For example, myofibers secrete Wnt7a that interacts with Fz7 and synergizes with fibronectin, produced by activated satellite cells, to activate the effector Vangl2 and the Wnt PCP (Planar cell polarity) pathway, which in turn stimulate symmetric cell divisions and satellite cell self-renewal (Le Grand et al., 2009; Bentzinger et al., 2013a; Fig. 18). Wnt7a-Fzd7 signals in a Vangl2 independent manner as well, activating the Akt/mTOR pathway which in turn induces myofiber hypertrophy (von Maltzahn et al., 2011; Fig. 18).

The Janus kinase/signal transducers and activators of transcription (JAK-STAT) pathway is one of the signaling pathways involved in the dialogue between myofibers and satellite cells (Rawlings et al., 2004). In fact, the Interleukin IL-6 dependent activation of JAK2 and STAT3 signaling in C2C12 cells was shown to promote myogenic differentiation (Wang et al., 2008). Furthermore, myofibers and satellite cells are known to secrete IL-6 during cell-mediated hypertrophic growth after muscle workload, and IL-6 signals both as an autocrine and a paracrine factor in the induction of myoblast proliferation and migration (Serrano et al., 2008; Fig. 18).

During regeneration, activated satellite cells interact also with differentiating myoblasts through Notch and Myostatin signaling pathways. The activation of Notch signaling has been shown to be critical in quiescent satellite cells and proliferating myoblasts (Vasyutina et al., 2007; Mourikis et al., 2012b; Bjornson et al., 2013). Depletion of RBP-Jκ Notch mediator in satellite cells leads to spontaneous differentiation without prior cell division and therefore, the depletion of the satellite cell pool (Vasyutina et al., 2007; Bjornson et al., 2013). Likewise, double knockout of Notch target genes *Hey1* (*Hers1*)

and *HeyL* (*Hers3*) results in fewer satellite cells and fewer myofibers (Fukada et al., 2011). In other studies, overexpression of NICD (notch intracellular domain) was found to upregulate *Pax7*, while inhibiting *Myod* activation and the entry into S phase (Wen et al., 2012). In fact, interaction between Notch3 in the Pax7 muscle progenitor and Delta1 in the committed myoblast is crucial for the correct segregation of cellular components during asymmetric divisions (Delfini et al., 2000; Kuang et al., 2007; Fig. 18). Notch signaling is counteracted by canonical Wnt signaling. For instance, Wnt3a signaling was shown to antagonize Notch activity in satellite cells after an injury and to induce myogenic differentiation and lineage progression (Brack et al., 2008). In agreement with these studies, Wnt4 mediated activation of Wnt canonical signaling was shown to induce C2C12 myoblast and satellite cell differentiation (Bernardi et al., 2011).

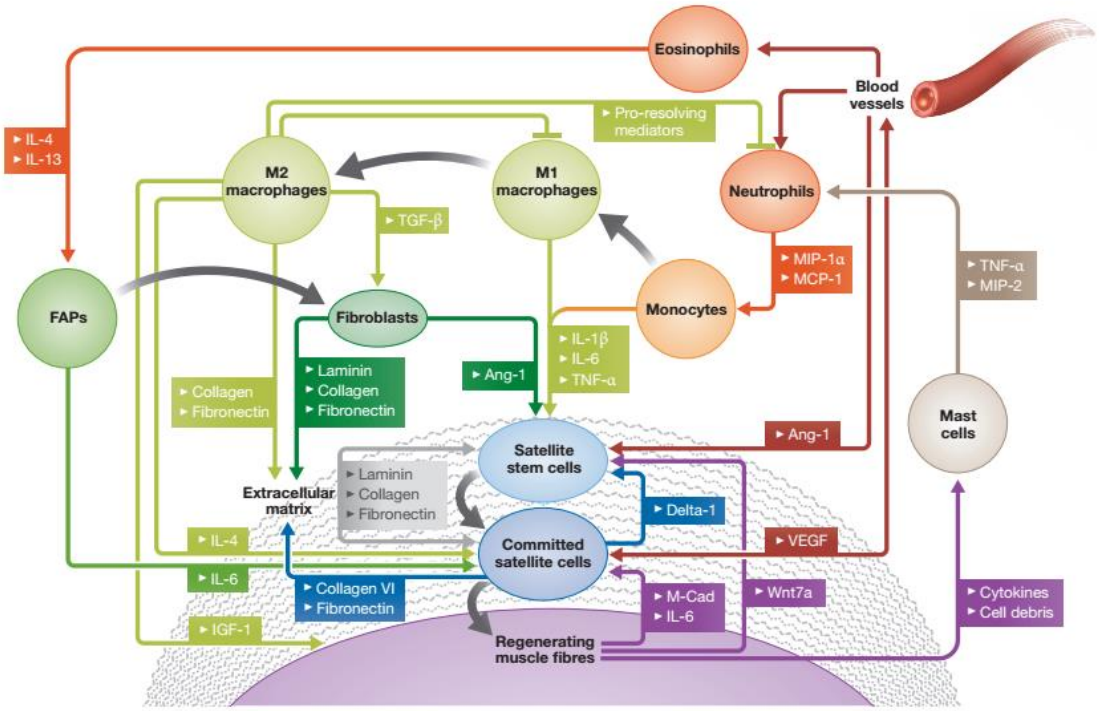

Figure 18- Satellite cell niche. Scheme depicting the different cells and extrinsic factors regulating satellite cell function. Figure from Bentzinger et al., 2013b.

Several studies have noted the negative impact of Myostatin in muscle growth as evidenced by *Myostatin* knock out mice, which display increased muscle hypertrophy and hyperplasia and, thus, larger muscles (McPherron et al., 1997; Li et al., 2005b; Marshall et al., 2008; Matsakas et al., 2010). Quiescent satellite cells and differentiating myoblasts produce Myostatin, but satellite cell activation is dependent on Myostatin downregulation and upregulation of *Mighty* (*Akirin 1*), which is negatively regulated by Myostatin (Marshall et al., 2008; Salerno et al., 2009). Mighty signals through the ActRIIB receptor, the transmembrane Alk5 and the mediators Smad 2/3, to induce MyoD and activate satellite cells (Marshall et al., 2008; Salerno et al., 2009). Several other studies have also shown that the downregulation of Myostatin is involved in the activation of MyoD and p21 (McCroskery et al., 2003; Amthor et al., 2004; Amthor et al., 2006; Marshall et al., 2008; Salerno et al., 2009; Matsakas et al., 2010). In the dermomyotome, Myostatin has an opposite effect to what was described during fetal and adult myogenesis, as overexpression of Myostatin in the dermomyotome induce MyoD and p21 (Manceau et al., 2008). It is possible that the dermomyotome muscle progenitors react differently to Myostatin signaling.

6.2.3. Extracellular environment of satellite cells: the interstitial cells

Satellite cells contact with several other cells lying in the muscle interstitium, such as immune cells, fibroblasts, fibro-adipogenic cells and nerves, and some of these are known to secrete several ECM molecules which have a role in satellite cell function (Bentzinger et al., 2013b; Fig. 18). Upon damage of muscle tissue, macrophages are promptly recruited to the injured area and interact directly with myoblasts through cell adhesion molecules such as VCAM1-integrin α4β1 and PECAM1-PECAM1 to inhibit their apoptosis (Sonnet et al., 2006; Bentzinger et al., 2013b). Macrophages produce ECM molecules such as fibronectin (Gratchev et al., 2001) and collagen VI (Schnoor et al., 2008),

which induce satellite cell self-renewal (Bentzinger et al., 2013b; Urciuolo et al., 2013). Other non-inflammatory cells such as fibroblasts normally produce several ECM molecules, including collagens I, IV and V, fibrillin and fibronectin, as well as MMPs in non-injury conditions (Chang et al., 2002; Lindner et al., 2012; Bentzinger et al., 2013b), and were shown to block the premature differentiation of satellite cells (Murphy et al., 2011; Bentzinger et al., 2013b). Although the exact role of nerves on satellite cell function remains unclear, it is known that satellite cells can interact directly with the nerve through their receptor $p75^{NTR}$, which binds to the brain-derived neurotrophic factor (BDNF) produced by the nerve (Mousavi and Jasmin, 2006). Furthermore, long-term denervation was shown to induce the separation of satellite cells from the myofibers and the respective basement membranes and their apoptosis (Schultz, 1978; Jejurikar et al., 2002; Montarras et al., 2013).

7. Merosin-deficient congenital muscular dystrophy type 1A (MDC1A)

Merosin-deficient congenital muscular dystrophy type 1A (MDC1A), or Laminin-α2 congenital muscular dystrophy (LAMA2-CMD), is a fatal neuromuscular disease characterized by severe neonatal hypotonia associated with joint contracture, inability to stand or walk and progressive muscle wasting (Gawlik and Durbeej, 2011). These patients display white-matter abnormalities, dysmyelinating neuropathy, seizures, scoliosis and they also experience feeding difficulties, limited eye movement and often need respiratory assistance (Jones et al., 2001; Gawlik and Durbeej, 2011). Congenital muscular dystrophies comprise several different pathologies with an estimated prevalence of 7 in 100 000 births (Gawlik and Durbeej, 2011). MDC1A corresponds to approximately 40% of cases of congenital muscular dystrophies in Europe (Allamand and Guicheney, 2002; Gawlik and Durbeej, 2011). The prevalence of MDC1A is estimated at 0.89/100,000 although there are regional variations (Mostacciuolo et al., 1996). It is an autosomal recessive disease, initially

described by Tomé et al. with the discovery of human patients without laminin α2 chain (Tomé et al., 1994). Since then, different mutations have been reported in the human *LAMA2* gene, which is located on chromosome 6q22-23, and comprises 260 kb corresponding to 64 exons (Helbling-Leclerc et al., 1995; Guicheney et al., 1997; Naom et al., 1997; Allamand and Guicheney, 2002). The disease pathology is marked by histological alterations such as variation in fiber size, inflammation, interstitial fibrosis and adipose tissue expansion (Miyagoe-Suzuki et al., 2000; Gawlik and Durbeej, 2011; Holmberg & Durbeej, 2013). No treatment is currently available for this devastating disease.

Laminin 211 is the predominant laminin isoform in the basement membrane surrounding adult muscle fibers. It is also present in the peripheral nervous system, while laminin 221 localizes specifically to neuromuscular junctions. Laminin 211 is important for myofibers survival (Vachon et al., 1996; Laprise et al., 2003), and for the regulation of the autophagy-lysosome pathway and the ubiquitin-proteasome system (Carmignac et al., 2010; Carmignac et al., 2011). Laminin-α2 deficiency also leads to impaired muscle regeneration (Kuang et al., 1999) and peripheral neuropathy (Occhi et al., 2005).

Several mouse models for MDC1A with different levels of severity and disruption in *LAMA2* gene have been used to study this disease. One of those models is *dy/dy* mutant mice, which have an unknown spontaneous mutation that results in reduced expression of an apparently normal α2 chain, and also display moderate muscular dystrophy (Guo et al., 2003; Gawlik and Durbeej, 2011). In contrast, dy^{W}/dy^{W} mutants are knockout mice with severely reduced expression of a truncated α2 chain, which is devoid of the laminin N-terminal domain. This mutation is lethal at 10 to 15 weeks of age and these mice display severe muscular dystrophy (Guo et al., 2003; Gawlik and Durbeej, 2011). The most severe mouse model for MDC1A is the mouse line dy^{3K}/dy^{3K}, which is a knockout with complete deficiency of α2 chain. This mutation is lethal at 4 weeks of age because of a severe muscular dystrophy (Guo et al., 2003; Gawlik and Durbeej, 2011). Humans and mice with

laminin α2 deficiency are already born with muscle defects (Gawlik and Durbeej, 2011), but the onset of this disease *in utero* is currently unknown.

Different treatments have been tested in laminin α2-deficient mice to counteract the absence of these laminins. For instance, overexpression of laminin α1 chain (Gawlik et al., 2004), α7 integrin (Doe et al., 2011), and intraperitoneal injection of laminin 111 ameliorates disease pathology and promotes regeneration (Rooney et al., 2012; Van Ry et al., 2013). Other therapies such as providing insulin growth factor 1 (Secco et al., 2013), mini-agrin (Bentzinger et al., 2005; Qiao et al., 2005; Meinen et al., 2011) and cytotoxic T cell Gal-Nac transferase (Xu et al., 2007), have also been tested in mouse models, and improved on muscle pathology as well.

II. Aims and Objectives

The foregoing State of the art highlighted the laminin diversity and the current knowledge about laminins during cardiac and skeletal muscle development. The main body of work performed in muscle development has provided valuable data unveiling the role of autonomous and paracrine mechanisms. Growing interest in the ECM has provided new insightful information about the impact of ECM as a signaling factor. However, the reviewed literature still denotes the lack of knowledge about the role of laminin isoforms during muscle development. Crucial questions such as “Why so many laminins?”, “Do different laminins function as a backup system?” or “What is the role of each laminin?” lead this work to study the impact of laminin matrices during cardiac and skeletal muscle development.

In **chapter 2**, we begin to characterize the dynamics of laminin assembly in epaxial muscles during their development *in utero*. Previous studies have described some laminin matrices in a few phases of skeletal muscle development (Patton et al., 1997; Cachaço et

al., 2005; Bajanca et al., 2006). Nevertheless, these studies did not provide a comprehensive overview of the laminin matrices during skeletal muscle development (Thorsteinsdóttir et al., 2011). Therefore, we provide a global perspective of laminin matrix assembly during skeletal muscle development. In addition, we study the role of laminin 211 along the entire myogenesis using *dy^{W} Lama2* deficient mice, a mouse model for MDC1A, which do not form a functional laminin α2 and, consequently lack laminins 211/221. It is well accepted by the scientific community that the absence of laminin 211 in the myofiber basement membrane in MDC1A patients causes progressive damage on the myofibers and activates mechanisms of inflammation and fibrosis. However, since infants and mice pups are born with muscle defects, these muscle defects must have arisen during development *in utero*. Hence, we not only pinpoint a critical phase where laminin 211 is essential, but we also trace the onset of the disease in this mouse model during development *in utero*. The study presented in this chapter was published in *Human Molecular Genetics* 26, 2018–2033.

In **chapter 3**, we expand the studies reported in chapter 2 and describe the dynamics of laminin synthesis during skeletal muscle development to understand the contribution of different cells during the assembly of laminin matrices. Our study shows that laminin synthesis is a very complex and dynamic process with contribution of different tissues all along the different phases of myogenesis. Furthermore, muscle stem cells are able to assemble their own laminin niches in the absence of myofiber signals as shown in *Myf5Cre-NICD* fetuses, which do not have any differentiated cells but maintain their muscle stem cells throughout skeletal muscle development (Mourikis et al., 2012a). The work presented in this chapter will be part of a manuscript which is in preparation.

In **chapter 4**, we report the optimization of different techniques to analyze the myogenesis defect described in chapter 2. The results from chapter 2 provide strong evidence implicating laminin 211 as an important regulator of fetal muscle development.

We test the efficacy of two different approaches, microexplant cultures and *in utero* injections of laminin 111, to study the role of laminin signaling in the myofiber basement membrane. Follow up studies with these techniques will be performed in the future.

In the following chapter, **chapter 5**, we extend the study of laminin assembly dynamics to cardiac development. The studies previously reported in the literature are scarce and do not cover the full extent of the different laminin isoforms during cardiac muscle development. We perform an extensive characterization of the different laminin matrices assembled in the cardiac basement membranes and discuss their possible roles. The research presented in this chapter will be part of a manuscript which is in preparation.

Finally, in **chapter 6**, we discuss the main findings described in the previous chapters with an integrative perspective regarding the existing literature. We also highlight the important contribution of this work towards understanding the role of laminin matrices in muscle development.

III. References

Allamand, V. and Guicheney, P. (2002). Merosin-deficient muscular dystrophy, autosomal recessive (MDC1A, MIM#156225, LAMA2 gene coding for α2 chain of laminin). *Eur. J. Hum. Genet.* **10**, 91-94.

Allikian, M. J. and McNally, E. M. (2007). Processing and assembly of the dystrophin glycoprotein complex. *Traffic.* **8**, 177-183.

Amthor, H., Christ, B. and Patel, K. (1999). A molecular mechanism enabling continuous embryonic muscle growth – a balance between proliferation and differentiation. *Development* **126**, 1041-1053.

Amthor, H., Nicholas, G., McKinnell, I., Kemp, C.F., Sharma, M., Kambadur, R. and Patel, K. (2004). Follistatin complexes myostatin and antagonizes myostatin-mediated inhibition of myogenesis. *Dev. Biol.* **270**, 19-30.

Amthor, H., Otto, A., Macharia, R., McKinnell, I. and Patel, K. (2006). Myostatin imposes reversible quiescence on embryonic muscle precursors. *Dev. Dyn.* **235**, 672-680.

Anderson, C., Thorsteinsdóttir, S. and Borycki, A. (2009). Sonic hedgehog-dependent synthesis of laminin α1 controls basement membrane assembly in the myotome. *Development* **136**, 3495-3504.

Andrade, R. P., Pascoal, S. and Palmeirim, I. (2005). Thinking clockwise. *Brain Res. Brain Res. Rev.* **49**, 114-119.

Andrade, R. P., Palmeirim, I. and Bajanca, F. (2007). Molecular clocks underlying vertebrate embryo segmentation: A 10-year-old hairy-go-round. *Birth Defects Res. C. Embryo Today* **81**, 65-83.

Arnold, H. and Braun, T. (1996). Targeted inactivation of myogenic factor genes reveals their role during mouse myogenesis: a review. *Int. J. Dev. Biol.* **40**, 345-363.

Ashby, P. R., Pinçon-Raymond, M. and Harris, A. J. (1993). Regulation of myogenesis in paralyzed muscles in the mouse mutants peroneal muscular atrophy and muscular dysgenesis. *Dev. Biol.* **156**, 529-536.

Askari, J. A., Buckley, P. A., Mould, A. P. and Humphries, M. J. (2009). Linking integrin conformation to function. *J. Cell Sci.* **122**, 165–170.

Aulehla, A. and Herrmann, B. G. (2004). Segmentation in vertebrates: clock and gradient finally joined. *Genes Dev*. **18**, 2060-2067.

Aumailley, M., Bruckner-Tuderman, L., Carter, W.G., Deutzmann, R., Edgar, D., Ekblom, P., Engel, J., Engvall, E., Hohenester, E., Jones, J. C. R. et al. (2005). A simplified laminin nomenclature. *Matrix Biol.* **24**, 326–332.

Bajanca, F., Luz, M., Raymond, K., Martins, G. G., Sonnenberg, A., Tajbakhsh, S., Buckingham, M. and Thorsteinsdóttir, S. (2006). Integrin α6β1-laminin interactions regulate early myotome formation in the mouse embryo. *Development* **133**, 1635-1644.

Barczyk, M., Carracedo, S. and Gullberg, D. (2010). Integrins. *Cell Tissue Res.* **339**, 269–280.

Barrios, A., Poole, R. J., Durbin, L., Brennan, C., Holder, N. and Wilson, S. W. (2003). Eph/Ephrin signaling regulates the mesenchymal-to-epithelial transition of the paraxial mesoderm during somite morphogenesis. *Curr. Biol.* **13**, 1571-1582.

Beauchamp, J. R., Heslop, L., Yu, D. S., Tajbakhsh, S., Kelly, R. G., Wernig, A., Buckingham, M. E., Partridge, T. A. and Zammit, P. S. (2000). Expression of CD34 and Myf5 defines the majority of quiescent adult skeletal muscle satellite cells. *J. Cell Biol.* **151**, 1221-1234.

Behrens, D. T., Villone, D., Koch, M., Brunner, G., Sorokin, L., Robenek, H., Bruckner-Tuderman, L., Bruckner, P. and Hansen, U. (2012). The epidermal basement membrane is a composite of separate laminin- or collagen IV- containing networks connected by aggregated perlecan, but not by nidogens. *J. Biol. Chem.* **287**, 18700-18709.

Ben-Yair, R. and Kalcheim, C. (2005). Lineage analysis of the avian dermomyotome sheet reveals the existence of single cells with both dermal and muscle progenitor fates. *Development* **132**, 689–701.

Bentzinger, C. F., Barzaghi, P., Lin, S. and Ruegg, M. A. (2005). Overexpression of mini-agrin in skeletal muscle increases muscle integrity and regenerative capacity in laminin-α2-deficient mice. *FASEB J.* **19**, 934-942.

Bentzinger, C. F., Wang, Y. X., von Maltzahn, J., Soleimani, V. D., Yin, H. and Rudnicki, M. A. (2013a). Fibronectin regulates Wnt7a signaling and satellite cell expansion. *Cell Stem Cell* **12**, 75-87.

Bentzinger, C. F., Wang, Y. X., Dumont, N. A. and Rudnicki, M. A. (2013b). Cellular dynamics in the muscle satellite cell niche. *EMBO Rep.* **14**, 1062-1072.

Bentzinger, C.F. (2016). Loss of fibronectin from the aged stem cell niche affects the regenerative capacity of skeletal muscle in mice. *Nat. Med.* **22**, 897-905.

Beres, B. J., George, R., Lougher, E.J., Barton, M., Verrelli, B.C., McGlade, C. J., Rawls, A. and Wilson-Rawls, J. (2011). Numb regulates Notch1, but not Notch3, during myogenesis. *Mech. Dev*. **128**, 247-257.

Bernardi, H., Gay, S., Fedon, Y., Vernus, B., Bonnieu, A. and Bacou, F. (2011). Wnt4 activates the canonical β-catenin pathway and regulates negatively myostatin: functional implication in myogenesis. *Am. J. Physiol. Cell Physiol.* **300**, 1122-1138.

Bessho, Y. and Kageyama, R. (2003). Oscillations, clocks and segmentation. *Curr. Opin. Genet. Dev.* **13**, 379-384.

Biben, C. and Harvey, R. P. (1997). Homeodomain factor Nkx2-5 controls left/right asymmetric expression of bHLH gene *eHand* during murine heart development. *Genes Dev.* **11**, 1357-1369.

Biressi, S., Molinaro, M. and Cossu, G. (2007). Cellular heterogeneity during vertebrate skeletal muscle development. *Dev. Biol.* **308**, 281-293.

Bjornson, C. R., Cheung, T. H., Liu, L., Tripathi, P. V., Steeper, K. M. and Rando, T. A. (2013). Notch signaling is necessary to maintain quiescence in adult muscle stem cells. *Stem Cells*, **30**, 232-242.

Boonen, K. J., Rosaria-Chak, K. Y., Baaijens, F. P., van der Schaft, D. W. and Post, M. J. (2009). Essential environmental cues from the satellite cell niche: optimizing proliferation and differentiation. *Am J Physiol Cell Physiol.* **296**, C1338-1345.

Borello, U., Berarducci, B., Murphy, P., Bajard, L., Buffa, V., Piccolo, S., Buckingham, M. and Cossu, G. (2006). The Wnt/-catenin pathway regulates Gli-mediated Myf5 expression during somitogenesis. *Development* **133**, 3723-3732.

Borycki, A. G., Li, J., Jin, F., Emerson, C. P. and Epstein, J. A. (1999). Pax3 functions in cell survival and in pax7 regulation. *Development* **126**, 1665-1674.

Bothe, I., Ahmed, M. U., Winterbottom, F. L., Von Scheven, G. and Dietrich, S. (2007). Extrinsic versus intrinsic cues in avian paraxial mesoderm patterning and differentiation. *Dev. Dyn.* **236**, 2397-2409.

Brack, A. S., Conboy, I. M., Conboy, M. J., Shen, J and Rando, T. A. (2008). A temporal switch from notch to Wnt signaling in muscle stem cells is necessary for normal adult myogenesis. *Cell Stem Cell* **2**, 50-59.

Brancaccio, M., Cabodi, S., Belkin, A. M., Collo, G., Koteliansky, V. E., Tomatis, D., Altruda, F., Silengo, L. and Tarone, G. (1998). Differential onset of expression of α7 and β1D integrins during mouse heart and skeletal muscle development. *Cell Adhes. Commun.* **5**, 195-205.

Brand-Saberi, B., Müller, T. S., Wilting, J., Christ, B. and Birchmeier, C. (1996). Scatter factor/hepatocyte growth factor (SF/HGF) induces emigration of myogenic cells at interlimb level in vivo. *Dev Biol.* **179**, 303-308.

Braun, T., Rudnicki, M. A., Hans-Henning, A. and Jaenisch, R. (1992). Targeted inactivation of the muscle regulatory gene Myf-5 results in abnormal rib development and perinatal Death. *Cell* **71**, 369-382.

Brent, A. E. and Tabin, C.J. (2002). Developmental regulation of somite derivatives: muscle, cartilage and tendon. *Curr. Opin. Genet. Dev.* **12**, 548-557.

Brent, A. E., Schweitzer, R. and Tabin, C.J. (2003). A Somitic compartment of tendon progenitors. *Cell* **113**, 235-248.

Bröhl, D., Vasyutina, E., Czajkowski, M. T., Griger, J., Rassek, C., Rahn, H.P., Purfürst, B., Wende, H. and Birchmeier, C. (2012). Colonization of the satellite cell niche by skeletal muscle progenitor cells depends on Notch signals. *Dev. Cell* **23**, 469-481.

Brunelli, S., Relaix, F., Baesso, S., Buckingham, M. and Cossu, G. (2007). Beta catenin-independent activation of MyoD in presomitic mesoderm requires PKC and depends on Pax3 transcriptional activity. *Dev. Biol.* **304**, 604–614.

Buckingham, M. (2001). Skeletal muscle formation in vertebrates. *Curr. Opin. Genet. Dev.* **11**, 440-448.

Buckingham, M., Bajard, L., Chang, T., Daubas, P., Hadchouel, J., Meilhac, S., Montarras, D., Rocancourt, D. and Relaix, F. (2003). The formation of skeletal muscle: from somite to limb. *J. Anat.* **202**, 59-68.

Buckingham, M. (2006). Myogenic progenitor cells and skeletal myogenesis in vertebrates. *Curr. Opin. Genet. Dev.* **16**, 525-532.

Buckingham, M. and Vincent, S. D. (2009). Distinct and dynamic myogenic populations in the vertebrate embryo. *Curr. Opin. Genet. Dev.* **19**, 444-453.

Buckingham, M. and Rigby, P. W. J. (2014). Gene regulatory networks and transcriptional mechanisms that control myogenesis. *Dev. Cell* **28**, 225-238.

Buckingham, M. and Relaix, F. (2015). Pax3 and pax7 as upstream regulators of myogenesis. *Semin. Cell Dev. Biol.* **44**, 115-125.

Burgess, R., Rawls, A., Brown, D., Bradley, A. and Olson, E. N. (1996). Requirement of the paraxis gene for somite formation and musculoskeletal patterning. *Nature* **384**, 570-573.

Burkin, D. J. and Kaufman, S. J. (1999). The α7β1 integrin in muscle development and disease. *Cell Tissue Res.* **296**, 183-190.

Cachaço, A. S., Chuva De Sousa Lopes, S. M., Kuikman, I., Bajanca, F., Abe, K., Baudoin, C., Sonnerberg, A., Mummery, C. L. and Thorsteindóttir, S. (2003). Knock-in of integrin β1D affects primary but not secondary myogenesis in mice. *Development* **130**, 1659-1671.

Cachaço, A. S., Pereira, C. S., Pardal, R. G., Bajanca, F. and Thorsteinsdóttir, S. (2005). Integrin repertoire on myogenic cells changes during the course of primary myogenesis in the mouse. *Dev. Dyn.* **232**, 1069-1078.

Cai, C. L., Liang, X., Shi, Y., Chu, P. H., Pfaff, S. L., Chen, J. and Evans, S. (2003). Isl1 identifies a cardiac progenitor population that proliferates prior to differentiation and contributes a majority of cells to the heart. *Dev. Cell* **5**, 877-889.

Carmignac, V., Quéré, R. and Durbeej, M. (2010). Proteasome inhibition improves the muscle of laminin α2 chain-deficient mice. *Hum. Mol. Genet.* **20**, 541–552.

Carmignac, V., Svensson, M., Körner, Z., Elowsson, L., Matsumura, C., Gawlik, K. I., Allamand, V. and Durbeej, M. (2011). Autophagy is increased in laminin α2 chain-deficient muscle and its inhibition improves muscle morphology in a mouse model of MDC1A. *Hum. Mol. Genet.* **20**, 4891–4902.

Chakkalakal, J. V., Jones, K. M., Basson, M. A. and Brack, A. S. (2012). The aged niche disrupts muscle stem cell quiescence. *Nature* **490**, 355-360.

Chang, H. Y., Chi, J. T., Dudoit, S., Bondre, C., van de Rijn, M., Botstein, D. and Brown, P. O. (2002). Diversity, topographic differentiation, and positional memory in human fibroblasts. *Proc. Natl. Acad. Sci. U.S.A.* **99**, 12877-12882.

Chargé, S. B. P. and Rudnicki, M. A. (2004). Cellular and molecular regulation of muscle regeneration. *Physiol. Rev.* **84**, 209-238.

Chen, Q., Lin, Tin, T. H., Der, C. J. and Juliano, R. L. (1996). Integrin-mediated activation of mitogen-activated protein (MAP) or extracellular signal-related kinase kinase (MEK) and kinase is independent of ras. *J. Biol. Chem.* **271**, 18122-18127.

Chen, H., Shi, S., Acosta, L., Li, W., Lu, J., Bao, S., Chen, Z., Yang, Z., Schneider, M. D., Chien, K. R. et al. (2004). BMP10 is essential for maintaining cardiac growth during murine cardiogenesis. *Development* **131**, 2219-2231.

Chen, W., Harbeck, M., Zhang, W. and Jacobson, J. R. (2013). MicroRNA regulation of integrins. *Transl. Res.* **162**, 133-43.

Cheng, Y. S., Champliaud, M. F., Burgeson, R. E., Marinkovich, M. P. and Yurchenco, P. D. (1997). Self-assembly of laminin isoforms. *J. Biol. Chem.* **272**, 31525-31532.

Christ, B., Jacob, M. and Jaboc, H. J. (1983). On the origin and development of the ventrolateral abdominal muscles in the avian embryo. An experimental and ultrastructural study. *Anat. Embryol.* **166**, 87-101.

Christ, B., Huang, R. and Scaal, M. (2004). Formation and differentiation of the avian sclerotome. *Anat. Embryol.* 208, 333-350.

Christ, B., Huang, R. and Scaal, M. (2004). Formation and differentiation of the avian sclerotome. *Anat. Embryol*. **208**, 333-350.

Christ, B., Huang, R. and Scaal, M. (2007). Amniote somite derivatives. *Dev. Dyn.* **236**, 2382-2396.

Christoffels, V. M., Habets, P.E., Franco, D., Campione, M., de Jong, F., Lamers, W. H., Bao, Z. E., Palmer, S., Biben, C., Harvey, R. P. and Moorman, A. F. M. (2000). Chamber formation and morphogenesis in the developing mammalian heart. *Dev. Biol.* **223**, 266-278.

Cinnamon, Y., Kahane, N. and Kalcheim, C. (1999). Characterization of the early development of specific hypaxial muscles from the ventrolateral myotome. *Development* **126**, 4305-4315.

Cinnamon, Y., Ben-Yair, R. and Kalcheim, C. (2006). Differential effects of N-cadherin-mediated adhesion on development of myotomal waves. *Development* **133**, 1101-1112.

Cohn, R. D., Henry, M. D., Michele, D. E., Barresi, R., Saito, F., Moore, S. A., Flanagan, J. D., Skwarchuck, M. W., Robbins, M. E., Mendell, J. R., Williamson, R. A. and Campbell, K. P. (2002). Disruption of Dag1 in differentiated skeletal muscle reveals a role for dystroglycan in muscle regeneration. *Cell* **110**, 639-648.

Collins, C. A., Olsen, I., Zammit, P. S., Heslop, L., Petrie, A., Partridge, T. A. and Morgan, J. E. (2005). Stem cell function, self-renewal, and behavioral heterogeneity of cells from the adult muscle satellite cell niche. *Cell* **122**, 289-301.

Colognato, H., Winkelmann, D. A. and Yurchenco, P. D. (1999). Laminin polymerization induces a receptor-cytoskeleton network. *J. Cell Biol.* **145**, 619-631.

Comoglio, P. M., Boccaccio, C. and Trusolino, L. (2003). Interactions between growth factor receptors and adhesion molecules: breaking the rules. *Curr. Opin. Cell Biol.* **15**, 565-571.

Cooley, M. A., Fresco, V. M., Dorlon, M. E., Twal, W. O., Lee, N. V., Barth, J. L., Kern, C. B., Iruela-Arispe, M. L., Argraves, W. S. (2012). Fibulin-1 is required during cardiac ventricular morphogenesis for versican cleavage, suppression of ErbB2 and Erk1/2 activation, and to attenuate trabecular cardiomyocyte proliferation. *Dev. Dyn.* **241**, 303-314.

Cornelison, D. D. W. and Wold, B. J. (1997). Single-cell analysis of regulatory gene expression in quiescent and activated mouse skeletal muscle satellite cells. *Dev. Biol.* **191**, 270-283.

Cornelison, D. D., Filla, M. S., Stanley, H. M., Rapraeger, A. C. and Olwin, B. B. (2001). Syndecan-3 and syndecan-4 specifically mark skeletal muscle satellite cells and are implicated in satellite cell maintenance and muscle regeneration. *Dev. Biol.* **239**, 79-94.

Cossu, G., De Angelis, L., Borello, U., Berarducci, B., Buffa, V., Sonnino, C., Coletta, M., Vivarelli, E., Bouche, M., Lattanzi, L. et al. (2000). Determination, diversification and multipotency of mammalian myogenic cells. *Int. J. Dev. Biol.* **44**, 699-706.

Danen, E. H. and Sonnenberg, A. (2003). Integrins in regulation of tissue development and function. *J. Pathol.* **200**, 471-480.

Delfini, M.C., Hirsinger, E., Pourquié, O. and Duprez, D. (2000). Delta 1-activated notch inhibits muscle differentiation without affecting Myf5 and Pax3 expression in chick limb myogenesis. *Development* **127**, 5213-5224.

Denetclaw, W. F., Christ, J.B. and Ordahl, C. P. (1997). Location and growth of epaxial myotome precursor cells. *Development* **124**, 1601-1610.

Deries, M., Collins, J. J. and Duxson, M. J. (2008). The mammalian myotome: a muscle with no innervation. *Evol. Dev.* **10**, 746-755.

Deries, M., Schweitzer, R. and Duxson, M. J. (2010). Developmental fate of the mammalian myotome. *Dev. Dyn.* **239**, 2898-2910.

Deries, M., Gonçalves, A. B., Vaz, R., Martins, G. G., Rodrigues, G. and Thorsteinsdóttir, S. (2012). Extracellular matrix remodeling accompanies axial muscle development and morphogenesis in the mouse. *Dev. Dyn.* **241**, 350-364.

Deries, M. and Thorsteinsdóttir, S. (2016). Axial and limb muscle development: dialogue with the neighbourhood. *Cell. Mol. Life Sci*. **73**, 4415–4431.

Dietrich, S. (1999). Regulation of hypaxial muscle development. *Cell Tissue Res*. **269**, 175-182.

Diez del Corral, R., Olivera-Martinez, I., Goriely, A., Gale, E., Maden, M. and Storey, K. (2003). Opposing FGF and retinoid pathways control ventral neural pattern, neuronal differentiation, and segmentation during body axis extension. *Neuron.* **40**, 65-79.

Dobaczewski, M., Gonzalez-Quesada, C., Frangogiannis, N. G. (2010). The extracellular matrix as a modulator of the inflammatory and reparative response following myocardial infarction. *J. Mol. Cell. Cardiol.* **48**, 504–511.

Doe, J. A., Wuebbles, R. D., Allred, E. T., Rooney, J. E., Elorza, M. and Burkin, D. J. (2011). Transgenic overexpression of the a7 integrin reduces muscle pathology and improves viability in the dy(W) mouse model of merosin-deficient congenital muscular dystrophy type 1A. *J. Cell. Sci.* **124**, 2287–2297.

Doherty, J. T., Conlon, F. L., Mack, C. P. and Taylor, J. M. (2010). Focal adhesion kinase is essential for cardiac looping and multichamber heart formation. *Genesis* **48**, 492-504.

Domogatskaya, A., Rodin, S. and Tryggvason, K. (2012). Functional diversity of laminins. *Annu. Rev. Cell Dev. Biol.* **28**, 523-553.

Duband, J. L., Dufour, S., Hatta, K., Takeichi, M., Edelman, G. M. and Thiery, J. P. (1987). Adhesion molecules during somitogenesis in the avian embryo. *J. Cell Biol.* **104**, 1361-1374.

Dubrulle, J., McGrew, M. J. and Pourquié, O. (2001). FGF signaling controls somite boundary position and regulates segmentation clock control of spatiotemporal Hox gene activation. *Cell* **106**, 219-232.

Dubrulle, J. and Pourquié, O. (2004). Coupling segmentation to axis formation. *Development* **131**, 5783-5793.

Drake, C. J. and Fleming, P. A. (2000). Vasculogenesis in the day 6.5 to 9.5 mouse embryo. *Blood* **95**, 1671-1679.

Dumont, N. A., Wang, Y. X. and Rudnicki, M. A. (2015). Intrinsic and extrinsic mechanisms regulating satellite cell function. *Development* **142**, 1572-1581.

Dunglison, G. F., Scotting, P. J. and Wigmore, P. M. (1999). Rat embryonic myoblasts are restricted to forming primary fibers while later myogenic populations are pluripotent. *Mech. Dev*. **87**, 11-19.

Durbeej, M. (2010). Laminins. *Cell Tissue Res.* **339**, 259-268.

Duxson, M. J. and Usson, Y. (1989). Cellular insertion of primary and secondary myotubes in embryonic rat muscles. *Development* **107**, 243-251.

Ecob-Prince, M., Hill, M. and Brown, W. (1989). Immunocytochemical demonstration of myosin heavy chain expression in human muscle. *J. Neurol. Sci.* **91**, 71-78.

Engler, A. J., Griffin, M. A., Sen, S., Bönnemann, C. G., Sweeney, H. L. and Discher, D. E. (2004). Myotubes differentiate optimally on substrates with tissue-like stiffness: pathological implications for soft or stiff microenvironments. *J. Cell Biol.* **166**, 877-887.

Ervasti, J. M. and Campbell, K. P. (1993). A role for the dystrophin-glycoprotein complex as a transmembrane linker between laminin and actin. *J. Cell Biol.* **327**, 809-823.

Evans, D., Baillie, H., Caswell, A. and Wigmore, P. (1994). During fetal muscle development, clones of cells contribute to both primary and secondary fibers. *Dev. Biol.* **162**, 348-353.

Frantz, C., Stewart, K. M. and Weaver, V. M. (2010). The extracellular matrix at a glance. *J. Cell Sci.* **123**, 4195–4200.

Fredette, B. J. and Landmesser, L. T. (1991). A reevaluation of the role of innervation in primary and secondary myogenesis in developing chick muscle. *Dev. Biol.* **143**, 19-35.

Fredette, B., Rutishauser, U. and Landmesser, L. (1993). Regulation and activity-dependence of N-Cadherin, NCAM isoforms, and polysialic acid on chick myotubes during development. *J. Cell Biol.* **123**, 1867-1888.

Fukada, S., Uezumi, A., Ikemoto, M., Masuda, S., Segawa, M., Tanimura, N., Yamamoto, H., Miyagoe-Suzuki, Y. and Takeda, S. (2007). Molecular signature of quiescent satellite cells in adult skeletal muscle. *Stem Cells* **25**, 2448-2459.

Fukada, S., Yamaguchi, M., Kokubo, H., Ogawa, R., Uezumi, A., Yoneda, T., Matev, M. M., Motohashi, N., Ito, T., Zolkiewska, A., Johnson, R. L. et al. (2011). Hesr1 and Hesr3 are essential to generate undifferentiated quiescent satellite cells and to maintain satellite cell numbers. *Development* **138**, 4609-4619.

Gallant, N. D., Michael, K. E. and García, A. J. (2005). Cell adhesion strengthening: contributions of adhesive area, integrin binding, and focal adhesion assembly. *Mol. Biol. Cell* **16**, 4329-4340.

Galli, L. M., Willert, K., Nusse, R., Yablonka-Reuveni, Z., Nohno, T., Denetclaw, W. and Burrus, L. W. (2004). A proliferative role for Wnt-3a in chick somites. *Dev. Biol.* **269**, 489-504.

Gawlik, K., Miyagoe-Suzuki, Y., Ekblom, P., Takeda, S. and Durbeej, M. (2004). Laminin α1 chain reduces muscular dystrophy in laminin α2 chain deficient mice. *Hum. Mol. Genet.* **13**, 1775–1784.

Gawlik, K. I., Kerlund, M. A., Carmignac, V., Elamaa, H. and Durbeej, M. (2010). Distinct roles for laminin globular domains in laminin α1 chain mediated rescue of murine laminin α2 chain deficiency. *PLoS ONE* **5**, e11549.

Gawlik, K.I. and Durbeej, M. (2011). Skeletal muscle laminin and MDC1A: pathogenesis and treatment strategies. *Skelet. Muscle* **1**, 9.

Geetha-Loganathan, P., Nimmagadda, S., Huang, R., Christ, B. and Scaal, M. (2006). Regulation of ectodermal Wnt6 expression by the neural tube is transduced by dermomyotomal Wnt11: a mechanism of dermomyotomal lip sustainment. *Development* **133**, 2897-2904.

Geiger, B., Bershadsky, A., Pankov, R. and Yamada, K. M. (2001). Transmembrane extracellular matrix-cytoskeleton crosstalk. *Nat. Rev. Mol. Cell Biol.* **2**, 793-805.

Gilbert, P. M., Havenstrite, K. L., Magnusson, K. E., Sacco, A., Leonardi, N. A., Kraft, P., Nguyen, N. K., Thrun, S., Lutolf, M. P. and Blau, H. M. (2010). Substrate elasticity regulates skeletal muscle stem cell self-renewal in culture. *Science* **329**, 1078-1081.

Gilbert, S. F. (2013). *Developmental biology*. Sunderland, USA: Sinauer Associates, Inc.

Gratchev, A., Guillot, P., Hakiy, N., Politz, O., Orfanos, C. E., Schledzewski, K., and Goerdt, S. (2001). Alternatively activated macrophages differentially express fibronectin and its splice variants and the extracellular matrix protein βIG-H3. *Scand. J. Immunol.* **53**, 386-392.

Gros, J., Scaal, M. and Marcelle, C. (2004). A two-step mechanism for myotome formation in chick. *Dev. Cell* **6**, 875-882.

Gros, J., Manceau, M., Thome, V. and Marcelle, C. (2005). A common somitic origin for embryonic muscle progenitors and satellite cells. *Nature* **435**, 954–958.

Gross, M. K., Moran-Rivard, L., Velasquez, T., Nakatsu, M. N., Jagla, K. and Goulding, M., (2000). Lbx1 is required for muscle precursor migration along a lateral pathway into the limb. *Development* **127**, 413–424

Guicheney, P., Vignier, N., Helbling-Leclerc, A., Nissinen, M., Zhang, X., Cruaud, C., Lambert, J. C., Richelme, C., Topaloglu, H., Merlinin, L. et al. (1997). Genetics of laminin alpha 2 chain (or merosin) deficient congenital muscular dystrophy: from identification of mutations to prenatal diagnosis. *Neuromuscul. Disord.* **7**, 180-186.

Guo, L. T., Zhang, X. U., Kuang, W., Xu, H., Liu, L. A., Vilquin, J. T., Miyagoe-Suzuki, Y., Takeda, S., Ruegg, M. A., Wewer, U. M. and Engvall, E. (2003). Laminin α2 deficiency and muscular dystrophy; genotype-phenotype correlation in mutant mice. *Neuromuscul. Disord.* **13**, 207-215.

Hadchouel, J., Carvajal, J. J., Daubas, P., Bajard, L., Chang, T., Rocancourt, D., Cox, D., Summerbell, D., Tajbakhsh, S., Rigby, P. W. et al. (2003). Analysis of a key regulatory region upstream of the Myf5 gene reveals multiple phases of myogenesis, orchestrated at each site by a combination of elements dispersed throughout the locus. *Development* **130**, 3415-3426.

Harris, A. J., Duxson, M. J., Fitzsimons, R. B. and Rieger, F. (1989). Myonuclear birthdates distinguish the origins of primary and secondary myotubes in embryonic mammalian skeletal muscles. *Development* **107**, 771-784.

Hartley, R. S., Bandman, E. and Yablonka-Reuveni, Z. (1992). Skeletal muscle satellite cells appear during late chicken embryogenesis. *Dev. Biol.* **153**, 206-216.

Helbling-Leclerc, A., Zhang, X., Topaloglu, H., Cruaud, C., Tesson, F., Weissenbach, J., Tomé, F. M., Schwartz, K., Fardeau, M., Tryggvason, K. et al. (1995). Mutations in the laminin α2-chain gene (*LAMA2*) cause merosin-deficient congenital muscular dystrophy. *Nat. Genet.* **11**, 216-218.

Hierck, B. P., Poelmann, R. E., Iperen, L. V., Brouwer, A and Gittenberger-Degroot, A. C. (1996). Differential expression of α6 and other subunits of laminin binding integrins during development of the murine heart. *Dev. Dynam.* **206**, 100-111.

Hinterberger, T. J., Sassoon, D. A., Rhodes, S. J. and Konieczny, S. F. (1991). Expression of the muscle regulatory factor MRF4 during somite and skeletal myofibers development. *Dev. Biol.* **147**, 144-156.

Hirsinger, E., Duprez, D., Jouve, C., Malapert, P., Cooke, J. and Pourquié, O. (1997). Noggin acts downstream of Wnt and Sonic Hedgehog to antagonize BMP4 in avian somite patterning. *Development* **124**, 4605-4614.

Hirsinger, E., Malapert, Pascale., Dubrulle, J., Delfini, M. C., Duprez, D., Henrique, D., Ish-Horowicz, D. and Pourquié, O. (2001). Notch signalling acts in postmitotic avian myogenic cells to control *MyoD* activation. *Development* **128**, 107-116.

Hohenester, E. and Yurchenco, P. D. (2013). Laminins in basement membrane assembly. *Cell Adhes. Migr.* **7**, 56-63.

Hollway, G. and Currie, P. (2005). Vertebrate myotome development. *Birth Defects Res.* **75**, 172-179.

Holmberg, J. and Durbeej, M. (2013). Laminin-211 in skeletal muscle function. *Cell Adh Migr.* **7**, 111-121.

Holowacz, T., Zeng, L. and Lassar, A. B. (2006). Asymmetric localization of numb in the chick somite and the influence of myogenic signals. *Dev. Dyn*. **235**, 633-645.

Holt, K. H., Crosbie, R. H., Venzke, D. P. and Campbell, K. P. (2000). Biosynthesis of dystroglycan: processing of a precursor propetide. *FEBS Lett.* **468**, 79-83.

Horikawa, K., Radice, G., Takeichi, M. and Chisaka, O. (1999). Adhesive subdivisions intrinsic to the epithelial somites. *Dev. Biol*. **215**, 182-189.

Hu, J.K., McGlinn, E., Harfe, B.D., Kardon, G. and Tabin, C. J. (2012). Autonomous and nonautonomous roles of Hedgehog signaling in regulating limb muscle formation. *Genes Dev.* **26**, 2088-2102.

Humphries, J. D., Byron, A. and Humphries, M. J. (2006). Integrin ligands at a glance. *J. Cell Sci.* **119**, 3901-3903.

Hurren, B., Collins, J. J., Duxson, M. J. and Deries, M. (2015). First neuromuscular contact correlates with onset of primary myogenesis in rat and mouse limb muscles. *PLoS One* **24**, e0133811.

Hussain, S. A., Carafoli, F. and Hohenester, E. (2011). Determinants of laminin polymerization revealed by the structure of the α5 chain amino-terminal region. *EMBO Rep.* **12**, 276-282.

Hutcheson, D. A., Zhao, J., Merrell, A., Haldar, M. and Kardon, G. (2009). Embryonic and fetal limb myogenic cells are derived from developmentally distinct progenitors and have different requirements for β-catenin. *Genes Dev.* **23**, 997-1013.

Hutson, M. R. and Kirby, M. L. (2007). Seminars in cell and development biology model systems for the study of heart development and disease cardiac neural crest and conotruncal maldormations. *Semin. Cell Dev. Biol.* **18**, 101-110.

Hynes, R. O. (2002). Integrins: Bidirectional allosteric signaling machines. *Cell* **110**, 673-687.

Ibraghimov-Beskrovnaya, O., Ervasti, J. M., Leveille, C. J., Slaughter, C. A., Sernett, S. W. and Campbell, K. P. (1992). Primary structure of dystrophin-associated glycoproteins linking dystrophin to the extracellular matrix. *Nature* **355**, 696-702.

Ido, H., Harada, K., Futaki, S., Hayashi, Y., Nishiuchi, R., Natsuka, Y., Li, S., Wada, Y., Combs, A. C., Ervasti, J. M. and Sekiguchi, K. (2004). Molecular dissection of the α-dystroglycan – and integrin-binding sites within the globular domain of human laminin-10. *J. Biol. Chem.* **279**, 10946-10954.

Ido, H., Ito, S., Taniguchi, Y., Hayashi, M., Sato-Nishiuchi, R., Sanzen, N., Hayashi, Y., Futaki, S. and Sekiguchi, K. (2008). Laminin isoforms containing the γ3 chain are unable to bind to integrins due to the absence of the glutamic acid residue conserved in the C-terminal regions of the γ1 and γ2 chains. *J. Biol. Chem.* **283**, 28149-28157.

Ingber, D. E. (2006). Mechanical control of tissue morphogenesis during embryological development. *Int. J. Dev. Biol.* **50**, 255–266.

Jejurikar, S. S., Marcelo, C.L. and Kuzon, W. M. Jr. (2002). Skeletal muscle denervation increases satellite cell susceptibility to apoptosis. *Plast. Reconstr. Surg.* **110**, 160-168.

Jones, K.J., Morgan, G., Johnston, H., Tobias, V., Ouvrier, R. A., Wilkinson, I. and North, K. N. (2001). The expanding phenotype of laminin alpha2 chain (merosin) abnormalities: case series and review. *J. Med. Genet.* **38**, 649-657.

Jory, A., Le Roux, I., Gayraud-Morel, B., Rocheteau, P., Cohen-Tannoudji, M., Cumano, A. and Tajbakhsh, S. (2009). Numb promotes an increase in skeletal muscle progenitor cells in the embryonic somite. *Stem Cells* **27**, 2769-2780.

Jung, D., Yang, B., Meyer, J., Chamberlain, J. S. and Campbell, K. P. (1995). Identification and characterization of the dystrophin anchoring site of β-dystroglycan. *J. Biol. Chem.* **270**, 27305-27310.

Kablar, B., Krastel, K., Ying, C., Asakura, A., Tapscott, S. J. and Rudnicki, M. A. (1997). MyoD and Myf-5 differentially regulate the development of limb versus trunk skeletal muscle. *Development* **124**, 4729-4738.

Kablar, B., Asakura, A., Krastel, K., Ying, C., May, L. L., Goldhamer, D. J. and Rudnicki, M. A. (1998). MyoD and Myf-5 define the specification of musculature of distinct embryonic origin. *Biochem. Cell Biol.* **76**, 1079-1091.

Kablar B., Krastel, K., Tajbakhsh, S. and Rudnicki, M. A. (2003). *Myf5* and *MyoD* activation define independent myogenic compartments during embryonic development. *Dev. Biol.* **258**, 307-318.

Kahane, N., Ribes, V., Kicheve, A., Briscoe, J. and Kalcheim, C. (2013). The transition from differentiation to growth during dermomyotome-derived myogenesis depends on temporally restricted hedgehog signaling. *Development* **140**, 1740-1750.

Kanagawa, M., Saito, F., Kunz, S., Yoshida-Moriguchi, T., Barresi, R., Kobayashi, Y. M., Muschler, J., Dumanski, J. P., Michele, D. E., Oldstone, M. B. et al. (2004). Molecular recognition by LARGE is essential for expression of functional dystroglycan. *Cell* **117**, 953-964.

Kawabe, Y., Wang, Y. X., McKinnell, I. W., Bedford, M. T. and Rudnicki, M. A. (2012). Carm1 regulates Pax7 transcriptional activity through MLL1/2 recruitment during asymmetric satellite stem cell divisions. *Cell Stem Cell* **11**, 333-345.

Kassar-Duchossoy, L., Gayraud-Morel, B., Gomès, D., Rocancourt, D., Buckingham, M., Shinin, V. and Tajbakhsh, S. (2004). Mrf4 determines skeletal muscle identity in Myf5:Myod double-mutant mice. *Nature* **431**, 466-471.

Kassar-Duchossoy, L., Giacone, E., Gayraud-Morel, B., Jory, A., Gomès, D. and Tajbakhsh, S. (2005). Pax3/Pax7 mark a novel population of primitive myogenic cells during development. *Genes Dev.* **19**, 1426-1431.

Kelly, A. M. and Zacks, S.I. (1969). The Histogenesis of Rat Intercostal Muscle. *J. Cell Biol.* **42**, 135-153.

Kelly, R. G., Buckingham, M. E. and Moorman, A. F. (2014). Heart fields and cardiac morphogenesis. *Cold Spring Harb. Perspect. Med.* **4**, a015750.

Kikkawa, Y., Hozumi, K., Katagiri, F., Nomizu, M., Kleinman, H.K. and Koblinski, J. E. (2013). Laminin-111-derived peptides and cancer. *Cell Adh. Migr.* **7**, 150-159.

Kim, H., Yoon, C. S. and Rah, B. (1999). Expression of extracellular matrix components fibronectin and laminin in the human fetal heart. *Cell Struct. Funct.* **24**, 19-26.

Kirby, M. L., and Waldo, K (2007). *Cardiac development.* New York, USA: Oxford U Press.

Knöll, R., Postel, R., Wang, J., Krätzner, R., Hennecke, G., Vacaru, A. M., Vakeel, P., Schubert, C., Murthy, K., Rana, B. K., and Bakkers, J. (2007). Laminin-alpha4 and integrin-linked kinase mutations cause human cardiomyopathy via simultaneous defects in cardiomyocytes and endothelial cells. *Circ.* **116**, 515-525.

Kobayashi, Y. M. and Campbell, K. P. (2012). Skeletal Muscle Dystrophin-Glycoprotein Complex and Muscular Dystrophy. In *Muscle: Fundamental Biology and Mechanisms of Disease* (ed. Joseph A. Hill and Eric N. Olson), pp. 935-942. Cambridge: Academic press.

Koshikawa, N., Giannelli, G., Cirulli, V., Miyazaki, K. and Quaranta V. (2000). Role of cell surface metalloprotease MT1-MMP in epithelial cell migration over laminin-5. *J. Cell Biol.* **148**, 615-642.

Kuang, W., Xu, H., Vilquin, J.T. and Engvall, E. (1999). Activation of the *lama2* gene in muscle regeneration: abortive regeneration in laminin alpha2-deficiency. *Lab. Invest.* **79**, 1601–1613.

Kuang, S., Kuroda, K., Le Grand, F. and Rudnicki, M. A. (2007). Asymmetric self-renewal and commitment of satellite stem cells in muscle. *Cell* **129**, 999-1010.

Kumagai, C., Kadowaki, T. and Kitagawa, Y. (1997). Disulfide-bonding between *Drosophila* laminin β and γ chains is essential for alpha chain to form α β and γ trimer. *FEBS Lett.* **412**, 211-206.

Kume, T., Jiang, H., Topczewska, J. M. and Hogan, B. L. (2001). The murine winged helix transcription factors, Foxc1 and Foxc2, are both required for cardiovascular development and somitogenesis. *Genes Dev.* **15**, 2470-2482.

Laprise, P., Vallé, K., Demers, M. J., Bouchard, V., Poirier, E. M., Vézina, A., Reed, J. C., Rivard, N. and Vachon, P. H. (2003). Merosin (laminin-2/4)-driven survival signalling: Complex modulations of Bcl-2 homologs. *J. Cell. Biochem.* **89**, 1115–1125.

Laugwitz, K. L., Moretti, A., Caron, L., Nakano, A. and Chien, K. R. (2008). Islet1 cardiovascular progenitors: a single source for heart lineages? *Development* **135**, 193-205.

Le Grand, F., Jones, A.E., Vanessa, S., Scime, A. and Rudnicki, M. A. (2009). Wnt7a activates the planar cell polarity pathway to drive the symmetric expansion of satellite stem cells. *Cell Stem Cell* **4**, 535-547.

LeBleu, V. S., MacDonald, B. and Kalluri, R. (2007). Structure and function of basement membranes. *Exp. Biol. Med.* **232**, 1121–1129.

Lee, A. S., Harris, J., Bate, M., Vijayraghavan, K., Fisher, L., Tajbakhsh, S. and Duxson, M. (2013). Initiation of primary myogenesis in amniote limb muscles. *Dev. Dyn.* **242**, 1043-1055.

Legate, K. R., Montañez, E., Kudlacek, O. and Fässler, R. (2006). ILK, PINCH and parvin: the tIPP of integrin signalling. *Rev. Mol. Cell Biol.* **7**, 20–31.

Legate, K. R., Wickström, S. A. and Fässler, R. (2009). Genetic and cell biological analysis of integrin outside-in signaling. *Genes Dev.* **23**, 397–418.

Lepper, C., Conway, S. J. and Fan, C. M. (2009). Adult satellite cells and embryonic muscle progenitors have distinct genetic requirements. *Nature* **460**, 627-631.

Lepper, C., Partridge, T. A. and Fan, C. (2011). An absolute requirement for Pax7-positive satellite cells in acute injury-induced skeletal muscle regeneration. *Development* **138**, 3639-3646.

Li, S., Harrison, D., Carbonetto, S., Fässler, R., Smyth, N., Edgar, D. and Yurchenco, P. D. (2002). Matrix assembly, regulation, and survival functions of laminin and its receptors in embryonic stem cell differentiation. *J. Cell Biol.* **157**, 1279-1290.

Li, S., Liquari, P., McKee, K. K., Harrison, D., Patel, R., Lee, S. and Yurchenco, P. D. (2005a). Laminin-sulfatide binding initiates basement membrane assembly and enables receptor signaling in schwann cells and fibroblasts. *J. Cell Biol.* **169**, 179-189.

Li, Z. F., Shelton, G. D. and Engvall, E. (2005b). Elimination of myostatin does not combat muscular dystrophy in dy mice but increases postnatal lethality. *Am. J. Pathol.* **166**, 491-497.

Linask, K. K. (1992). N-Cadherin localization in early heart development and polar expression of Na^+, K^+-ATPase, and integrin during pericardial coelom formation and epithelialization of the differentiating myocardium. *Dev. Biol.* **151**, 213-224.

Linask, K. K., Knudsen, K. A. and Gui, Y. H. (1997). N-cadherin-catenin interaction: necessary component of cardiac cell compartmentalization during early vertebrate heart development. *Dev. Biol.* **185**, 148-164.

Linask, K. K., Ludwig, C., Han, M. D., Liu, X., Radice, G. L, and Knudsen, K. A. (1998). N-cadherin/catenin-mediated morphoregulation of somite formation. *Dev. Biol.* **202**, 85-102.

Linask, K. K., Han, M., Cai, D. H., Brauer, P. R. and Maisastry, S. M. (2005). Cardiac morphogenesis: matrix metalloproteinase coordination of cellular mechanisms underlying heart tube formation and directionality of looping. *Dev. Dyn.* **233**, 739-753.

Lindner, D., Zietsch, C., Becher, P. M., Schulze, K., Schultheiss, H. P., Tchsöpe, C. and Westermann, D. (2012). Differential expression of matrix metalloproteases in human fibroblasts with different origins. *Biochem. Res. Int.* doi: 10.1155/2012/875742.

Lindon, C., Albagli, O., Domeyne, P., Montarras, D. and Pinset, C. (2000). Constitutive instability of muscle regulatory factor Myf5 is distinct from its mitosis-specific disappearance, which requires a D-box-like motif overlapping in the basic domain. *Mol. Cell. Biol.* **20**, 8923-8932.

Linker, C., Lesbros, C., Stark, M. R. and Marcelle, C. (2003). Intrinsic signals regulate the initial steps of myogenesis in vertebrates. *Development* **130**, 4797-4807.

Linker, C., Lesbros, C., Gros, J., Burrus, L. W., Rawis, A. and Marcelle, C. (2005). β-Catenin-dependent Wnt signaling controls the epithelial organization of somites through the activation of *paraxis*. *Development* **132**, 3095-3905.

Lu, P., Takai, K., Weaver, V. M. and Werb, Z. (2011). Extracellular matrix degradation and remodeling in development and disease. *Cold Spring Harb. Perspect. Biol.* **3**, a005058.

Manceau, M., Gros, J., Savage, K., Thomé, V., McPherron, A., Paterson, B. and Marcelle, C. (2008). Myostatin promotes the terminal differentiation of embryonic muscle progenitors. *Genes Dev.* **22**, 668-681.

Marshall, A., Salerno, M.S., Thomas, M., Davies, T., Berry, C., Dyer, K., Bracegirdle, J., Watson, T., Dziadek, M., Kambadur, R., Bower, R. and Sharma, M. (2008). Mighty is a novel promyogenic factor in skeletal myogenesis. *Exp. Cell Res.* **314**, 1013-1029.

Martins, G. G., Rifes, P., Amândio, R., Rodrigues, G., Palmeirim, I. and Thorsteinsdóttir, S. (2009). Dynamic 3D cell rearrangements guided by a fibronectin matrix underlie somitogenesis. *PLoS ONE* **15**, e7429.

Martin-Puig, S., Wang, Z. and Chien, K. R. (2008). Lives of a heart cell: tracing the origins of cardiac progenitors. *Cell Stem Cell* **2**, 320-331.

Matsakas, A., Otto, A., Elashry, M. I., Brown, S. C. and Patel, K. (2010). Altered primary and secondary myogenesis in the myostatin-null mouse. *Rejuvenation Res.* **13**, 717-727.

Mauro, A. (1961). Satellite cell of skeletal muscle fibers. *J. Biophys. Biochem. Cytol.* **9**, 493-495.

McCroskery, S., Thomas, M., Maxwell, L., Sharma, M. and Kambadur, R. (2003). Myostatin negatively regulates satellite cell activation and self-renewal. *J. Cell Biol.* **162**, 1135-1147.

McKee, K. K., Harrison, D., Cappizi, S. and Yurchenco, P. D. (2007). Role of laminin terminal globular domains in basement membrane assembly. *J. Biol. Chem.* **282**, 21437-21447.

McKee, K. K., Capizzi, S. and Yurchenco, P. D. (2009). Scaffold-forming and adhesive contributions of synthetic laminin-binding proteins to basement membrane assembly. *J. Biol. Chem.* **284**, 8984-8994.

McPherron, A.C., Lawler, A. M. and Lee, S.J. (1997). Regulation of skeletal muscle mass in mice by a new TGF-beta superfamily member. *Nature* **387**, 83-90.

Meilhac, S. M., Esner, M., Kelly, R. G., Nicolas, J. F. and Buckingham, M. E. (2004). The clonal origin of myocardial cells in different regions of the embryonic mouse heart. *Dev. Cell* **6**, 685-698.

Meilhac, S. M., Lescroart, F., Balnpain, C. and Buckingham, M. E. (2014). Cardiac cell lineages that form the heart. *Cold Spring Harb. Perspect. Med.* **4**, a013888.

Meinen, S., Lin, S., Thurnherr, R., Erb, M., Meier, T. and Rüegg, M. A. (2011). Apoptosis inhibitors and mini-agrin have additive benefits in congenital muscular dystrophy mice. *EMBO Mol. Med.* **3**, 465–479.

Miyagoe-Suzuki, Y., Nakagawa, M. and Takeda. S. (2000). Merosin and congenital muscular dystrophy. *Microsc. Res. Tech.* **48**, 181–191.

Miyamoto, S., Akiyama, S. K. and Yamada, K. M. (1995). Synergistic roles of receptor occupancy and aggregation in integrin transmembrane function. *Science* **267**, 883-885

Miyamoto, S., Teramoto, H., Gutkind, J. S. and Yamada, K. M. (1996). Integrins can collaborate with growth factors for phosphorylation of receptor tyrosine kinases and MAP kinase activation: roles of integrin aggregation and occupancy of receptors. *J. Cell Biol.* **135**, 1633-1642.

Montarras, D., L'honoré, A. and Buckingham, M. (2013). Lying low but ready for action: the quiescent muscle satellite cell. *FEBS J.* **280**, 4036-4050.

Monsoro-Burq, A. (2005). Sclerotome development and morphogenesis: when experimental embryology meets genetics. *Int. J. Dev. Biol.* **49**, 301-208.

Moore, A. W., McInnes, L., Kreidberg, J., Hastie, N. D. and Schedi, A. (1999). YAC complementation shows a requirement for Wt1 in the development of epicardium, adrenal gland and throughout nephrogenesis. *Development* **126**, 1845-1857.

Moro, L., Venturino, M., Bozzo, C., Silengo, L., Altruda, F., Bequinot, L., Tarone, G. and Defilippi, P. (1998). Integrins induce activation of EGF receptor: role in MAP kinase induction and adhesion-dependent cell survival. *EMBO J.* **17**, 6622-6632.

Mostacciuolo, M. L., Miorin, M., Martinello, F., Angelini, C., Perini, P. and Trevisan, C. P. (1996). Genetic epidemiology of congenital muscular dystrophy in a sample from north-east Italy. *Hum. Genet.* **97,** 277–279.

Mott, J. D. and Werb, Z. (2004). Regulation of matrix biology by matrix metalloproteinases. *Curr. Opin. Cell Biol.* **16**, 558-564.

Mould, A. P., Barton, S. J., Askari, J. A., McEwan, P. A., Buckley, P. A., Craig, S. E. and Humphries, M. J. (2003). Conformational changes in the integrin βA domain provide a mechanism for signal transduction via hybrid domain movement. *J. Biol. Chem.* **278**, 17028-17035.

Mourikis, P., Gopalakrishnan, S., Sambasivan, R. and Tajbakhsh, S. (2012a). Cell-autonomous Notch activity maintains the temporal specification potential of skeletal muscle stem cells. *Development* **139**, 4536-4548.

Mourikis, P., Sambasivan, R., Castel, D., Rocheteau, P., Bizzarro, V. and Tajbakhsh, S. (2012b). A critical requirement for notch signaling in maintenance of the quiescent skeletal muscle stem cell state. *Stem Cells* **30**, 243-252.

Mousavi, K. and Jasmin, B. J. (2006). BDNF is expressed in skeletal muscle satellite cells and inhibits myogenic differentiation. *J. Neurosci.* **26**, 5739-5749.

Munger, J. S., Huang, X., Kawakatsu, H., Griffiths, M. J., Dalton, S. L., Wu, J., Pittet, J., Kaminski, N., Garat, C., Matthay, M. A. et al. (1999). The integrin αvbβ6 binds and activates latent TGFβ1: A mechanism for regulating pulmonary inflammation and fibrosis. *Cell* **96**, 319-328.

Murphy, M. M., Lawson, J. A., Mathew, S. J., Hutcheson, D. A. and Kardon, G. (2011). Satellite cells, connective tissue fibroblasts and their interactions are crucial for muscle regeneration. *Development* **138**, 3625-3637.

Naom, I. S., D'Alessandro, M., Topaloglu, H., Sewry, C., Ferlini, A., Helbling-Leclerc, A., Guicheney, P., Weissenbach, J., Schwartz, K., Bushby, K., Philpot, J., Dubowitz, V. and Muntoni, F. (1997). Refinement of the laminin α2 chain locus to human chromosome 6q2 in severe and mild merosin deficient congenital muscular dystrophy. *J. Med. Genet.* **34**, 99-104.

Nishiuchi, R., Takagi, J., Hayashi, M., Ido, H., Yagi, Y., Sanzen, N., Tsuji, T., Yamada, M. and Sekiguchi, K. (2006). Ligand-binding specificities of laminin-binding integrins: a comprehensive survey of laminin-integrin interactions using recombinant alpha3beta1, alpha6beta1, alpha7beta1 and alpha6beta4 integrins. *Matrix Biol.* **25**, 189-197.

Occhi, S., Zambroni, D., Del, C. U., Amadio, S., Sirkowski, E. E., Scherer, S. S., Campbell, K. P., Moore, S. A., Chen, Z.L., Strickland, S., et al. (2005). Both laminin and Schwann cell dystroglycan are necessary for proper clustering of sodium channels at nodes of ranvier. *J. Neurosci.* **25**, 9418–9427.

Ontell, M. and Kozeka, K. (1984). Organogenesis of the mouse extensor digitorum longus muscle: a quantitative study. *Am. J. Anat.* **171**,149-61.

Orkin, R. W., Gehron, P., McGoodwin, E. B., Martin, G., Valentine, T. and Swarm, R. (1977). A murine tumor producing a matrix of basement membrane. *J. Exp. Med.* **145**, 204-20.

Paige, S. L., Plonowska, K., Xu, A. and Wu, S. M. (2015). Molecular regulation of cardiomyocyte differentiation. *Circ. Res.* **116**, 341-353.

Page-McCaw, A., Ewald, A.J. and Werb, Z. (2007). Matrix metalloproteinases and the regulation of tissue remodelling. *Nat. Rev. Mol. Cell Biol.* **8**, 221-233.

Palmeirim, I., Henrique, D., Ish-Horowicz, D. and Pourquié, O. (1997). Avian *hairy* gene expression identifies a molecular clock linked to vertebrate segmentation and somitogenesis. *Cell* **28**, 639-648.

Patton, B. L., Miner, J. H., Chiu, A. Y. and Sanes, J. R. (1997). Distribution and function of laminins in the neuromuscular system of developing, adult, and mutant mice. *J. Cell Biol.* **139**, 1507-1521.

Patton, B. L. (2000). Laminins of the neuromuscular system. *Microsc. Res. Techniq.* **51**, 247-261.

Patton, B. L., Cunningham, J. M., Thyboll, J., Kortesmaa, J., Westerblad, H., Edström, L., Tryggvason, K. and Sanes, J. R. (2001). Properly formed but improperly localized synaptic specializations in the absence of laminin alpha4. *Nat. Neurosci.* **4**, 597-604.

Porrello, A., Cerone, M. A., Coen, S., Gurtner, A., Fontemaggi, G., Cimino, L., Piaggio, G., Sacchi, A. and Soddu, S. (2000). p53 regulates myogenesis by triggering the differentiation activity of pRb. *J. Cell Biol.* **151**, 1295-1304.

Pourquié, O., Fan, C. M., Coltey, M., Hirsinger, E., Watanabe, Y., Bréant, C., Francis-West, P., Brickell, P., Tessier-Lavigne, M. and Le Douarin, N. M. (1996). Lateral and axial signals involved in avian somite patterning: a role for BMP4. *Cell* **84**, 461-471.

Pownall, M. E., Gustafsson, M. K. and Emerson, C. P. (2002). Myogenic regulatory factors and the specification of muscle progenitors in vertebrate embryos. *Annu. Rev. Cell Dev. Biol.* **18**, 747-783.

Pu, Q., Abduelmula, A., Masyuk, M., Theiss, C., Schwandulla, D., Hans, M., Patel, K., Brand-Saberi, B. and Huang, R. (2013). The dermomyotome ventrolateral lip is essential for the hypaxial myotome formation. *BMC Dev. Biol.* **13**, 41.

Qiao, C., Li, J., Zhu, T., Draviam, R., Watkins, S., Ye, X., Chen, C., Li, J. and Xiao, X. (2005). Amelioration of laminin-α2-deficient congenital muscular dystrophy by somatic gene transfer of miniagrin. *Proc. Natl. Acad. Sci. U.S.A.* **102**, 11999-12004.

Quijano-Roy, S., Sparks, S. E. and Rutkowski, A. (2012). *LAMA2*-Related Muscular Dystrophy. *GeneReviews* 1993-2017.

Rafael, J. A. and Brown, S. C. (2000). Dystrophin and utrophin: genetic analyses of their role in skeletal muscle. *Microsc. Res. Tech.* **48**, 155-166.

Rawlings, J. S., Rosler, K. M. and Harrison, D. A. (2004). The JAK/STAT signaling pathway. *J. Cell. Sci.* **117**, 1281-1283.

Relaix, F., Polimeni, M., Rocancourt, D., Ponzetto, C., Schäfer, B. W. and Buckingham, M. (2003). The transcriptional activator PAX3-FKHR rescues the defects of Pax3 mutant mice but induces a myogenic gain-of-function phenotype with ligand-independent activation of Met signaling in vivo. *Genes Dev.* **17**, 2950-2965.

Relaix, F., Rocancourt, D., Mansouri, A. and Buckingham, M. (2005). A pax3/pax7-dependent population of skeletal muscle progenitor cells. *Nature* **435**, 948-953.

Renshaw, M. W., Ren, X. D. and Schwartz, M. A. (1997). Growth factor activation of MAP kinase requires cell adhesion. *EMBO J.* **16**, 5592-5599.

Reynaud, E. G., Leibovitch, M. P., Tintignac, L. A. J., Pelpel, K., Guillier, M. and Leibovitch, S. A. (2000). Stabilization of MyoD by direct binding to p57Kip2. *J. Biol. Chem.* **275**, 18767-18776.

Rios, A. C., Serralbo, O., Salgado, D. and Marcelle, C. (2011). Neural crest regulates myogenesis through the transient activation of NOTCH. *Nature* **473**, 532-535.

Rocco, M., Rosano, C., Weisel, J. W., Horita, D. A. and Hantgan, R. R. (2008). Integrin conformational regulation: uncoupling extension/tail separation from changes in the head region by a multiresolution approach. *Structure* **16**, 954-964.

Rocheteau, P., Gayraud-Morel, B., Siegl-Cachedenier, I., Blasco, M. A. and Tajbakhsh, S. (2012). A subpopulation of adult skeletal muscle stem cells retains all template DNA strands after cell division. *Cell* **148**, 112-125.

Roediger, M., Miosge, N, and Gersdorff, N. (2010). Tissue distribution of the laminin β1 and β2 chain during embryonic and fetal human development. *J. Mol. Hist.* **41**, 177–184.

Rooney, J. E., Knapp, J. R., Hodges, B. L., Wuebbles, R. D. and Burkin, D. J. (2012). Laminin-111 protein therapy reduces muscle pathology and improves viability of a mouse model of merosin-deficient congenital muscular dystrophy. *Am. J. Pathol.* **180**, 1593-1602.

Rose, O., Rohwedel, J., Reinhardt, S., Bachmann, M., Cramer, M., Rotter, M., Wobus, A. and Starzinski-Powitz, A. (1994). Expression of M-cadherin protein in myogenic cells during prenatal mouse development and differentiation of embryonic stem cells in culture. *Dev. Dyn.* **201**, 245-259.

Rosen, G. D., Sanes, J. R., LaChance, R., Cunningham, J. M., Roman, J. and Dean, D. C. (1992). Roles of the integrin VLA-4 and its counter receptor VCAM-1 in myogenesis. *Cell* **69**, 1107-1119.

Ross, J. J., Duxson, M .J. and Harris, A. J. (1987). Formation of primary and secondary myotubes in rat lumbrical muscles. *Development* **100**, 383-394.

Saga, Y., Miyagawa-Tomita, S., Takagi, A., Kitajima, S., Miyazaki, J. and Inoue, T. (1999). MesP1 is expressed in the heart precursor cells and required for the formation of a single heart tube. *Development* **126**, 3437-3447.

Saga, Y. and Takeda, H. (2001). The making of the somite: molecular events in vertebrate segmentation. *Nat. Rev. Genet.* **2**, 835-845.

Sagar, Pröls, F., Wiegreffe, C. and Scaal, M. (2015). Communication between distant epithelial cells by filopodia-like protrusions during embryonic development. *Development* **142**, 665-671.

Salerno, M.S., Dyer, K., Bracergirdle, J., Platt, L., Thomas, M., Siriett, V., Kambadur, R. and Sharma, M. (2009). Akirin1 (Mighty), a novel promyogenic factor regulates muscle regeneration and cell chemotaxis. *Exp. Cell Res.* **315**, 2012-2021.

Sambasivan, R., Yao, R., Kissenpfenning, A., Van Wittenberghe, L., Paldi, A., Gayraud-Morel, B., Guenou, H., Malissen, B., Tajbakhsh, S. and Galy, A. (2011). Pax7-expressing satellite cells are indispensable for adult skeletal muscle regeneration. *Development* **138**, 3647-3656.

Samsa, L.A., Yang, B. and Liu, J. (2013). Embryonic cardiac chamber maturation: trabeculation, conduction and cardiomyocyte proliferation. *Am. J. Med. Genet. Part C. Semin. Med. Genet.* **163**, 157-168.

Sato, Y., Yasuda, K. and Takahashi, Y. (2002). Morphological boundary forms by a novel inductive event mediated by Lunatic fringe and Notch during somitic segmentation. *Development* **129**, 3633-3644.

Savolainen, S. M., Foley, J. F. and Elmore, S. A. (2009). Histology atlas of the developing mouse heart with emphasis on E11.5 to E18.5. *Toxicol. Pathol*. **37**, 395-414.

Scaal, M., Bonafede, A., Dathe, V., Sachs, M., Cann, G., Christ, B. and Brand-Saberi, B. (1999). SF/HGF is a mediator between limb patterning and muscle development. *Development* **126**, 4885-4893.

Scaal, M. and Christ, B. (2004). Formation and differentiation of the avian dermomyotome. *Anat. Embryol.* **208**, 411-424.

Schiaffino, S. and Reggiani, C. (2011). Fiber types in mammalian skeletal muscles. *Physiol. Rev.* **91**, 1447-1531.

Schienda, J., Engleka, K. A., Jun, S., Hansen, M. S., Epstein, J. A., Tabin, C. J., Kunkel, L. M. and Kardon, G. (2006). Somitic origin of limb muscle satellite and side population cells. *Proc. Natl. Acad. Sci. U.S.A.* **103**, 945-950.

Schittny, J. C. and Yurchenco, P. D. (1990). Terminal short arm domains of basement membrane laminin are critical for its self-assembly. *J. Cell Biol.* **110**, 825-832.

Schnoor, M., Cullen, P., Lorkowski, J., Stolle, K., Robenek, H., Troyer, D., Rauterberg, J. and Lorkowski, S. (2008). Production of type VI collagen by human macrophages: a new dimension in macrophage functional heterogeneity. *J. Immunol.* **180**, 5707-5719.

Schultz, E. (1978). Changes in the satellite cells of growing muscle following denervation. *Anat. Rec.* **190**, 299-311.

Schuster-Gossler, K., Cordes, R. and Gossler, A. (2007). Premature myogenic differentiation and depletion of progenitor cells cause severe muscle hypotrophy in *Delta1* mutants. *Proc. Natl. Acad. Sci. U.S.A.* **104**, 537-542.

Schwartz, M. A. and Simone, D. W. (2008). Cell adhesion receptors in mechanotransduction. *Curr. Opin. Cell Biol.* **20**, 551-556.

Secco, M., Bueno, C., Vieira, N.M., Almeida, C., Pelatti, M., Zucconi, E., Bartolini, P., Vainzof, M., Miyabara, E. H., Okamoto, O. K. and Zatz, M. (2013). Systemic delivery of human mesenchymal stromal cells combined with IGF-1 enhances muscle functional recovery in *LAMA2 dy/2j* dystrophic mice. *Stem Cell Rev.* **9**, 93–109.

Sedmera, D. and Thompson, R. P. (2011). Myocyte proliferation in the developing heart. *Dev. Dyn.* **240**, 1322-1324.

Sengbusch, J. K., He, W., Pinco, K. A. and Yang, J. T. (2002). Dual functions of α4β1 integrin in epicardial development: initial migration and long-term attachment. *J. Cell Biol.* **157**, 873-882.

Serrano, A .L., Baeza-Raja, B., Perdiguero, E., Jardí, M. and Muñoz-Cánoves, P. (2008). Interleukin-6 is an essential regulator of satellite cell-mediated skeletal muscle hypertrophy. *Cell Metab.* **7**, 33-44.

Shea, K. L., Xiang, W., LaPorta, V. S., Licht, J. D., Keller, C., Basson, M. A. and Brack, A. S. (2010). Sprouty1 regulates reversible quiescence of a self-renewing adult muscle stem cell pool during regeneration. *Cell Stem Cell* **6**, 117-129.

Shuai, K. and Liu, B. (2003). Regulation of JAK-STAT signalling in the immune system. *Nat. Rev. Immunol.* **3**, 900-911.

Small, E. M. and Krieg, P. A. (2004). Molecular regulation of cardiac chamber-specific gene expression. *Trends Cardiovasc. Med.* **14**, 13-18.

Smirnov, S. P., McDearmon, E. L., Li, S., Ervasti, J. M., Tryggvason, K. and Yurchenco, P. D. (2002). Contributions of the LG modules and furin processing to laminin-2 functions. *J Biol Chem.* **277**, 18928-18937.

Sonnet, C., Lafuste, P., Arnold, L., Brigitte, M., Poron, F., Authier, F. J., Chrétien, F., Gherardi, R. K. and Chazaud, B. (2006). Human macrophages rescue myoblasts and myotubes from apoptosis through a set of adhesion molecular systems. *J. Cell Sci.* **119**, 2497-2507.

Srivastava, D., Cserjesi, P., Olson, E. N. (1995). A subclass of bHLH proteins required for cardiac morphogenesis. *Science* **22**, 1995-1999.

Stankunas, K., Hang, C. T., Tsun, Z. Y., Chen, H., Lee, N. V., Wu, J. I., Shang, C., Bayle, J. H., Shou, W. Iruela-Arispe, M. L. (2008). Endocardial Brg1 represses ADAMTS1 to maintain the microenvironment for myocardial morphogenesis. *Dev. Cell* **14**, 298-311.

Sternlicht, M. D. and Werb, Z. (2001). How matrix metalloproteinases regulate cell behaviour. *Annu. Rev. Cell Dev. Biol.* **17**, 463–516.

Streuli, C. (1999). Extracellular matrix remodelling and cellular differentiation. *Curr. Opin. Cell Biol.* **11**, 634–640.

Summerbell, D., Ashby, P. R., Coutelle, O., Cox, D., Yee, S. and Rigby, P. W. J. (2000). The expression of *Myf5* in the developing mouse embryo is controlled by discrete and dispersed enhancers specific for particular populations of skeletal muscle precursors. *Development* **127**, 33745-3757.

Suzuki, N., Yokoyama, F. and Nomizu, M. (2005). Functional sites in the laminin alpha chains. *Connect. Tissue Res.* **46**, 142-152.

Swartz, M.E., Eberhart, J., Pasquale, E. B. and Krull, C. E. (2001). EphA4/ ephrin–A5 interactions in muscle precursor cell migration in the avian forelimb. *Development* **128**, 4669–4680.

Tajbakhsh, S., Bober, E., Babinet, C., Pournin, S., Arnold, H. and Buckingham, M. (1996). Gene targeting the *myf-5* locus with *nLacZ* reveals expression of this myogenic factor in mature skeletal muscle fibres as well as early embryonic muscle. *Dev. Dyn.* **206**, 291-300.

Tajbakhsh, S., Borello, U., Vivarelli, E., Kelly, R., Papkoff, J., Duprez, D., Buckingham, M. and Cossu, G. (1998). Differential activation of Myf5 and MyoD different Wnts in explants of mouse paraxial mesoderm and the later activation of myogenesis in the absence of Myf5. *Development* **125**, 4155-4162.

Tajbakhsh, S. and Buckingham, M. (2000). The birth of muscle progenitor cells in the mouse: spatiotemporal considerations. *Curr. Top. Dev. Biol.* **48**, 225-268.

Tajbakhsh, S. (2009). Skeletal muscle stem cells in developmental versus regenerative myogenesis. *J. Intern. Med.* **266**, 372-389.

Talts, J. F., Andac, Z., Göhring, W., Brancaccio, A. and Timpl, R. (1999). Binding of the G domains of laminin α1 and α2 chains and perlecan to heparin, sulfatides, α-dystroglycan and several extracellular matrix proteins. *EMBO J.* **18**, 863-870.

Talts, J. F., Sasaki, T., Miosge, N., Göhring, W., Mann, K., Mayne, R. and Timpl, R. (2000). Structural and functional analysis of the recombinant G domain of the laminin α4 chain and its proteolytic processing in tissues. *J. Biol. Chem.* **275**, 35192-35199.

Taniguchi, Y., Ido, H., Sanzen, N., Hayashi, M., Sato-Nishiuchi, R., Futaki, S. and Sekiguchi, K. (2009). The C-terminal region of laminin β chains modulates the integrin binding affinities of laminins. *J. Biol. Chem.* **284**, 7820-7831.

Tapscott, S.J. (2005). The circuitry of a master switch: Myod and the regulation of skeletal muscle gene transcription. *Development* **132**, 2685-2695.

Thorsteinsdóttir, S., Roelen, B. A., Freund, E., Gaspar, A. C., Sonnenberg, A. and Mummery, C. L. (1995). Expression patterns of laminin receptor splice variants α6Aβ1 and α6Bβ1 suggest different roles in mouse development. *Dev. Dyn.* **204,** 240-58.

Thorsteinsdóttir, S., Deries, M., Cachaço, A.S. and Bajanca, F. (2011). The extracellular matrix dimension of skeletal muscle development. *Dev. Biol.* **354**, 191-207.

Timpl, R., Rohde, H., Robey, P.G., Rennard, S.I., Foidart, J. M. and Martin, G. R. (1979). Laminin – A glycoprotein from basement membranes. *J. Biol. Chem.* **254**, 9933-9937.

Timpl, R., Tisi, D., Talts, J.F., Andac, Z., Sasaki, T. and Hohenester, E. (2000). Structure and function of laminin LG modules. *Matrix Biol.* **19**, 309-317.

Tomé, F. M., Evangelista, T., Leclerc, A., Sunada, Y., Manole, E., Estournet, B., Barois, A., Campbell, K. P. and Fardeau, M. (1994). Congenital muscular dystrophy with merosin deficiency. *Sciences de la Vie* **317**, 351-357.

Townsend, D. (2014). Finding the sweet spot: assembly and glycosylation of dystrophin-associated glycoprotein complex. *Anat. Rec.* **297**, 1694-1705.

Troy, A., Cadwallader, A. B., Fedorov, Y., Tyner, K., Tanaka, K. K. and Olwin, B. B. (2012). Coordination of satellite cell activation and self-renewal by par-complex-dependent asymmetric activation of p38α/β MAPK. *Cell Stem Cell* **11**, 541-553.

Tsiper, M. V. and Yurchenco, P. D. (2002). Laminin assembles into separate basement membrane and fibrillary matrices in Schwann cells. *J. Cell. Sci.* **115**, 1005-1015.

Urciuolo, A., Quarta, M., Morbidoni, V., Gattazzo, F., Molon, S., Grumati, P., Montemurro, F., Tedesco, F. S., Blaauw, B., Cossu, G., et al. (2013). Collagen VI regulates satellite cell self-renewal and muscle regeneration. *Nat. Commun*. **4**, 1964

Vachon, P. H., Loechel, F., Xu, H., Wewer, U. M. and Engvall, E. (1996). Merosin and laminin in myogenesis; specific requirement for merosin in myotube stability and survival. *J. Cell Biol.* **134**, 1483-1497.

van der Flier, A., Gaspar, A. C., Thorsteinsdóttir, S., Baudoin, C., Groeneveld, E., Mummery, C. L. and Sonnenberg A. (1997). Spatial and temporal expression of the β1D integrin during mouse development. *Dev. Dyn.* **210**, 472-486.

Van Ry, P. M., Minogue, P., Hodges, B. L. and Burkin, D. J. (2013). Laminin-111 improves muscle repair in a mouse model of merosin-deficient congenital muscular dystrophy. *Hum. Mol. Genet.* **23**, 383-396.

Vasyutina, E., Stebler, J., Brand-Saberi, B., Schulz, S., Raz, E. and Birchmeier, C. (2005). CXCR4 and Gab1 cooperate to control the development of migrating muscle progenitor cells. *Genes Dev.* **19**, 2187–2198.

Vasyutina, E., Lenhard, D. C., Wende, H., Erdmann, B., Epstein, J. A. and Birchmeier, C. (2007). RBP-J (Rbpsuh) is essential to maintain muscle progenitor cells and to generate satellite cells. *Proc. Natl. Acad. Sci. U.S.A.* **104**, 4443-4448.

Venters, S. J., Thorsteinsdóttir, S. and Duxson, M. J. (1999). Early development of the myotome in the mouse. *Dev. Dyn*. **216**, 219-232.

Venters, S. J. and Ordahl, C. P. (2005). Asymmetric cell divisions are concentrated in the dermomyotome dorsomedial lip during epaxial primary myotome morphogenesis. *Anat. Embryol.* **209**, 449-460.

von der Mark, H., Pöschl, E., Lanig, H., Sasaki, T., Deutzman, R. and von der Mark, K. (2007). Distinct acidic clusters and hydrophobic residues in the alternative splice domains X1 and X2 of α7 integrins define specificity for laminin isoforms. *J. Mol. Biol.* **371**, 1188-1203.

Vincent, S. D. and Buckingham, M. E. (2010). How to make a heart: the origin and regulation of cardiac progenitor cells. *Curr. Top. Dev. Biol.* **90**, 1-41.

von Maltzahn, J., Bentzinger, C. F. and Rudnicki, M. A. (2011). Wnt7a-Fzd7 signalling directly activates the Akt/mTOR anabolic growth pathway in skeletal muscle. *Nat. Cell Biol.* **14**, 186-191.

Waldo, K. L., Hutson, M. R., Stadt, H. A., Zdanowicz, M., Zdanowicz, J. and Kirby, M. L. (2005). Cardiac neural crest is necessary for normal addition of the myocardium to the arterial pole from the secondary heart field. *Dev. Biol.* **281**, 66-77.

Wang, J., Hoshijima, M., Lam, J., Zhou, Z., Jokiel, A., Dalton, N. D., Hultenby, K., Ruiz-Lozano, P., Ross, J. J., Tryggvason, K. (2006). Cardiomyopathy associated with microcirculation dysfunction in laminin α4 chain-deficient mice. *J. Biol. Chem.* **281**, 213–220.

Wang, K., Wang, C., Xiao, F., Wang, H. and Wu, Z. (2008). JAK2/STAT2/STAT3 are required for myogenic differentiation. *J. Biol. Chem.* **283**, 34029-34036.

Wang, Y.X. and Rudnicki, M. A. (2011). Satellite cells, the engines of muscle repair. *Nat. Rev. Mol. Cell Biol.* **13**, 127-133.

Wen, Y., Bi, P., Liu, W., Asakura, A., Keller, C. and Kuang, S. (2012). Constitutive notch activation upregulates pax7 and promotes the self-renewal of skeletal muscle satellite cells. *Mol. Cell. Biol.* **32**, 2300-2311.

Wessels, A. and Pérez-Pomares, J. M. (2004). The epicardium and epicardially derived cells (EPDCs) as cardiac stem cells. *Anat. Rec. A. Discov. Mol. Cell Evol. Biol.* **276**, 43-57.

White, R. B., Biérinx, A. S., Gnocchi, V. F. and Zammit, P. S. (2010). Dynamics of muscle fibre growth during postnatal mouse development. *BMC Dev. Biol.* **10**, 21.

Wigmore, P. M. and Dunglison, G. F. (1998). The generation of fiber diversity during myogenesis. *Int. J. Dev. Biol.* **42**, 117-125.

Wigmore, P. M. and Evans, D. J. R. (2002). Molecular and cellular mechanisms involved in the generation of fiber diversity during myogenesis. *Int. Rev. Cytol.* **216**, 175-232.

Wizemann, H., Garbe, J. H., Friedrich, M. V., Timpl, R., Sasaki, T. and Hohenester, E. (2003). Distinct requirements for heparin and α-dystroglycan binding revealed by structure-based mutagenesis of the laminin α2 LG4-LG5 domain pair. *J. Mol. Biol.* **332**, 635-642.

Wu, S. M., Chien, K. R. and Mummery, C. (2008). Origins and fates of cardiovascular progenitor cells. *Cell* **132**, 537-543.

Xu, R., Chandrasekharan, K., Yoon, J.H., Camboni, M. and Martin, P. T. (2007). Overexpression of the cytotoxic T cell (CT) carbohydrate inhibits muscular dystrophy in the *dy^{W}* mouse model of congenital muscular dystrophy 1A. *Am. J. Pathol.* **171**, 181-199.

Yabluchanskiy, A., Li, Y., Chilton, R. J. and Lindsey, M. L. (2013). Matrix metalloproteinases: drug targets for myocardial infarction. *Curr. Drug Targets* **14**, 276–286.

Yang, S. Y. and Golspink, G. (2002). Different roles of the IGF-I Ec peptide (MGF) and mature IGF-I in myoblast proliferation and differentiation. *FEBS Lett.* **522**, 156-160.

Yee, S. P. and Rigby, P. W. (1993). The regulation of myogenin gene expression during the embryonic development of the mouse. *Genes Dev.* **7**, 1277-1289.

Yin, H., Price, F. and Rudnicki, M. A. (2013). Satellite cells and the muscle stem cell niche. *Physiol. Rev.* **93**, 23-67.

Yoshida-Moriguchi, T., Yu, L., Stalnaker, S. H., Davis, S., Kunz, S., Madson, M., Oldstone, M. B., Schachter, H., Wells, L. and Campbell, K. P. (2010). O-mannosyl phosphorylation of alpha-dystroglycan is required for laminin binding. *Science* **327**, 88-92.

Yu, H. and Talts, J. F. (2003). β1 integrin and α-dystroglycan binding sites are localized to different laminin-G-domain-like (LG) modules within the laminin α5 chain G domain. *Biochem. J.* **371**, 289-299.

Yurchenco, P. D., Tsilibary, E. C., Charonis, A. S. and Furthmayr, H. (1985). Laminin polymerization in vitro. Evidence for a two-step assembly with domain specificity. *J. Biol. Chem.* **260**, 7636-7644.

Yurchenco, P. D. and Cheng, Y. S. (1993). Self-assembly and calcium-binding sites in laminin. A three-arm interaction model. *J. Biol. Chem.* **268**, 17286-17299.

Yurchenco, P. D., Quan, Y., Colognato, H., Mathus, T., Harrison, D., Yamada, Y. and O'Rear, J. J. (1997). The alpha chain of laminin-1 is independently secreted and drives secretion of its beta- and gamma-chain partners. *Proc. Natl. Acad. Sci. USA* **94**, 10189-10194.

Yurchenco, P. D. (2013). Laminins in basement membrane assembly. *Cell Adh Migr.* **7**, 1-8.

Yurchenco, P. D. (2015). Integrating activities of laminins that drive basement membrane assembly and function. *Curr. Top. Membr*. **76**, 1-30.

Zhang, M. and McLennan, I. S. (1995). During secondary myotube formation, primary myotubes preferentially absorb new nuclei at their ends. *Dev. Dyn*. **204**, 168-177.

Zhang, X., Fei, K., Agbas, A., Yan, L., Zhang, J., O'Reilly, Deutzmann, R and Sarras, Jr. (2002). Structure and function of an early divergent form of laminin in hydra: a structurally conserved ECM component that is essential for epitelial morphogenesis. *Dev. Genes Evol.* **212**, 159-172.

Zhou, B., Ma, Q., Rajagopal, S., Wu, S. M., Domian, I., Reviera-Feliciano, J., Jiang, D., von Gise, A., Ikeda, S., Chien, K. R. and Pu, W. T. (2008). Epicardial progenitors contribute to the cardiomyocyte lineage in the developing heart. *Nature* **454**, 109-113.

Zhu, Z. and Miller, J. B. (1997). MRF4 can substitute for myogenin during early stages of myogenesis. *Dev. Dyn.* **209**, 233-241.

CHAPTER 2

Impaired fetal muscle development and JAK-STAT activation mark disease onset and progression in a mouse model for merosin-deficient congenital muscular dystrophy

Impaired fetal muscle development and JAK-STAT overactivation mark disease onset and progression in a mouse model for merosin-deficient congenital muscular dystrophy

Andreia M. Nunes[1,2], Ryan D. Wuebbles[2#], Apurva Sarathy[2#], Tatiana M. Fontelonga[2], Marianne Deries[1], Dean J. Burkin[2] and Sólveig Thorsteinsdóttir[1,3*]

[1]Departamento de Biologia Animal, Centro de Ecologia, Evolução e Alterações Ambientais, Faculdade de Ciências, Universidade de Lisboa, 1749-016 Lisbon, Portugal; [2]Center for Molecular Medicine, University of Nevada School of Medicine, Reno, NV 89557, USA; [3]Instituto Gulbenkian de Ciência, 2780-156 Oeiras, Portugal.

[#]These authors contributed equally

Human Molecular Genetics, **26**, 2018-2033.

Contribution by A.M.N. to this chapter:

	Fig.1	**Fig.2**	**Fig.3**	**Fig.4**	**Fig.5**	**Fig.6**	**Fig.7**	**Fig.S1**	**Writing**
Design and concept	III	III	III	III	III	III	III	III	III
Execution	III	III	III	III	III	III	III	III	
Analysis and interpretation	III	III	III	III	III	III	n.a.	III	

Legend:
n.a.- non-applicable
O- no intervention
I- minor contribution
II- moderate contribution
III- major contribution
Note: Items with major contribution by A.M.N. does not exclude major contributions from other authors.

Contribution by the other authors:

Design and concept: M.D., D.J.B. and S.T.; Execution: A.S. and T.M.F.; Analysis and Interpretation: R.D.W., M.D. and S.T.; Writing: M.D. and S.T.

OXFORD

Human Molecular Genetics, 2017, Vol. 26, No. 11 2018–2033

doi: 10.1093/hmg/ddx083
Advance Access Publication Date: 7 March 2017
Original Article

ORIGINAL ARTICLE

Impaired fetal muscle development and JAK-STAT activation mark disease onset and progression in a mouse model for merosin-deficient congenital muscular dystrophy

Andreia M. Nunes[1,2], Ryan D. Wuebbles[2,†], Apurva Sarathy[2,†], Tatiana M. Fontelonga[2], Marianne Deries[1], Dean J. Burkin[2] and Sólveig Thorsteinsdóttir[1,3,*]

[1]Departamento de Biologia Animal, Centro de Ecologia, Evolução e Alterações Ambientais, Faculdade de Ciências, Universidade de Lisboa, 1749-016 Lisbon, Portugal, [2]Center for Molecular Medicine, University of Nevada School of Medicine, Reno, NV 89557, USA and [3]Instituto Gulbenkian de Ciência, 2780-156 Oeiras, Portugal

*To whom correspondence should be addressed. Tel: +351 217500212; Fax: +351 217500028; Email: solveig@fc.ul.pt

Abstract

Merosin-deficient congenital muscular dystrophy type 1A (MDC1A) is a dramatic neuromuscular disease in which crippling muscle weakness is evident from birth. Here, we use the dy^{W} mouse model for human MDC1A to trace the onset of the disease during development *in utero*. We find that myotomal and primary myogenesis proceed normally in homozygous $dy^{W-/-}$ embryos. Fetal $dy^{W-/-}$ muscles display the same number of myofibers as wildtype (WT) muscles, but by E18.5 $dy^{W-/-}$ muscles are significantly smaller and muscle size is not recovered post-natally. These results suggest that fetal $dy^{W-/-}$ myofibers fail to grow at the same rate as WT myofibers. Consistent with this hypothesis between E17.5 and E18.5 $dy^{W-/-}$ muscles display a dramatic drop in the number of Pax7- and myogenin-positive cells relative to WT muscles, suggesting that $dy^{W-/-}$ muscles fail to generate enough muscle cells to sustain fetal myofiber growth. Gene expression analysis of $dy^{W-/-}$ E17.5 muscles identified a significant increase in the expression of the JAK-STAT target gene *Pim1* and muscles from 2-day and 3-week old $dy^{W-/-}$ mice demonstrate a dramatic increase in pSTAT3 relative to WT muscles. Interestingly, myotubes lacking integrin $\alpha7\beta1$, a laminin-receptor, also show a significant increase in pSTAT3 levels compared with WT myotubes, indicating that $\alpha7\beta1$ can act as a negative regulator of STAT3 activity. Our data reveal for the first time that $dy^{W-/-}$ mice exhibit a myogenesis defect already *in utero*. We propose that overactivation of JAK-STAT signaling is part of the mechanism underlying disease onset and progression in $dy^{W-/-}$ mice.

[†]These authors contributed equally to this work.

Received: August 8, 2016. **Revised:** January 30, 2017. **Accepted:** March 2, 2017

Introduction

Merosin-deficient congenital muscular dystrophy (CMD) type 1A (MDC1A), or laminin-α2 CMD (LAMA2-CMD), is a devastating neuromuscular disease in which patients demonstrate hypotonia from birth. Human MDC1A was initially described by Tomé *et al.* and is caused by mutations in the *LAMA2* gene (1–3), which encodes the laminin α2 chain of laminins 211 and 221 (4). Laminin 211 is the predominant laminin isoform in the basement membrane surrounding adult muscle fibers, while laminin 221 localizes specifically to neuromuscular junctions (5,6). Laminin 211 is crucial for myofiber survival (7,8), and is involved in the regulation of the autophagy-lysosome pathway and the ubiquitin-proteasome system (9,10).

It is generally believed that the absence of laminin 211 around myofibers in MDC1A patients causes a constant stress on these cells, which progressively damages them, inducing muscle wasting, inflammation and fibrosis (11). Since infants are already affected at birth, the muscle weakness underlying the disease must already have arisen during development *in utero*. However, it is unclear when and how disease begins in MDC1A.

Mouse skeletal muscle development starts at E8.5 when Pax3- and/or Pax7-positive muscle stem cells at the edges of the dermomyotome are induced to initiate the myogenic program and differentiate into myotomal myocytes (12–14). The myogenic program involves the expression of one or more of the myogenic regulatory factors (MRFs), the transcription factors Myf5, MyoD, Mrf4 and myogenin (15). From E11.5 until E14.5, these myocytes fuse with differentiating primary myoblasts giving rise to primary (embryonic) myofibers of the trunk muscles, while dermomyotome-derived Pax3-positive cells have migrated and differentiate into the primary myofibers of limbs, tongue and diaphragm (16–20). Subsequently, from E14.5 until birth, Pax7-positive muscle stem cells within the muscle masses undergo a second wave of differentiation into secondary myoblasts. These myoblasts then use the primary myofibers as a scaffold and fuse with each other, generating secondary (fetal) myofibers, and subsequently fuse with both primary and secondary myofibers, increasing their size (17,20). Thus fetal skeletal muscle grows both by addition of new myofibers (hyperplasia) and by fusion of myoblasts to existing myofibers, increasing their size (cell-mediated hypertrophy).

Laminins 111 and 511 are thought to play a role in early stages of myogenesis in the somites (21) and laminins 211, 411 and 511 are found in fetal muscles (5). However, little is known about the exact assembly dynamics and specific roles of the different laminin isoforms during myogenesis. It has been suggested that α4- and α5-laminins can compensate for the absence of α2-laminins during myogenesis *in utero* (5,22), but this hypothesis has not been formally tested.

Here, we perform a detailed analysis of the assembly dynamics of the different laminin isoforms during normal mouse skeletal muscle development. We then use the dy^{W} mouse model for MDC1A to study the effect of laminin α2-chain deficiency on skeletal muscle development *in vivo*. We demonstrate that myotomal and primary myogenesis proceed without defects in $dy^{W-/-}$ embryos. However, during secondary myogenesis, $dy^{W-/-}$ muscles exhibit impaired growth, fail to maintain the normal number of Pax7-positive muscle stem cells and experience a dramatic drop in the number of myogenin-positive myoblasts. This $dy^{W-/-}$ muscle defect correlates with an overactivation of JAK-STAT signaling as well as a dysregulation of Myostatin signaling which we suggest hampers the amplification of the pool of mononucleated muscle cells necessary for cell-mediated hypertrophy of myofibers. We show for the first time that MDC1A starts before birth in $dy^{W-/-}$ mice and that the onset of the disease *in utero* is marked by impaired fetal myogenesis.

Results

Myotomal and primary myogenesis proceed normally in $dy^{W-/-}$ embryos

Our first aim was to detect the stage of MDC1A onset during mouse development. We first characterized myotome development in E10.5 $dy^{W-/-}$ embryos. Immunostaining (for *n* numbers; see Supplementary Material, Tables S1 and S2) with a pan-muscle laminin antibody demonstrates that the laminin matrices lining the dermomyotome and the myotome are normal in $dy^{W-/-}$ embryos (Fig. 1A, A′, C and C′). The mouse *Lama2* gene is normally expressed by myotomal myocytes (Fig. 2D and F) and laminin α2 chain localizes to the myotomal basement membrane in a similar pattern to laminin α1 and α5 chains (Fig. 2A, B, E′ and G′). Laminin α1 and α2 chains are also detected in a patchy pattern among myotomal myocytes (Fig. 2A, E, E′, G and G′) and this pattern is unperturbed in $dy^{W-/-}$ embryos (Fig. 1A, A′, C and C′). Together these observations suggest that the distribution of laminin 111 and 511 is normal in $dy^{W-/-}$ embryos.

Immunostaining for myosin heavy chain (MHC) on sections of E10.5 $dy^{W-/-}$ embryos and their WT littermates shows that myotome morphology and size in $dy^{W-/-}$ embryos is not significantly different from that of WT embryos (Fig. 1A, A″, C, C″ and M; $n = 4$ per genotype). Immunolabeling for Pax3, Pax7 and myogenin did not reveal any differences between WT and $dy^{W-/-}$ embryos (Fig. 1E–G and I–K). TUNEL analysis showed no increase in apoptosis in $dy^{W-/-}$ myotomes (Fig. 1B and D) and phospho-histone 3 (pH3) labeling was similar in WT compared with $dy^{W-/-}$ embryos (Fig. 1H and L). We therefore conclude that myotomal myogenesis proceeds normally in E10.5 $dy^{W-/-}$ embryos.

To analyze if primary myogenesis proceeds normally after E10.5 in $dy^{W-/-}$ embryos, we quantified the total number of primary myofibers in three epaxial deep back muscles (see Materials and Methods) of E17.5 $dy^{W-/-}$ fetuses and their WT littermates, stained with an antibody to slow myosin. This quantification shows that WT and $dy^{W-/-}$ embryos form the same number of primary myofibers (Fig. 1N; $n = 3–6$ per genotype). In fact, our analysis of laminin deposition during primary myogenesis (E11.5–E13.5) in normal embryos supports this hypothesis. Immunostaining with pan-muscle laminin antibody (Fig. 2H and H′) (23,24) and with antibodies for α2 (Fig. 2I), α1 and α5 chains (data not shown) failed to detect a laminin-containing basement membrane around primary myotubes. These results indicate that primary myogenesis is normally laminin independent (see Fig. 3P).

These data show that myotome development and primary myogenesis are not significantly affected in $dy^{W-/-}$ embryos.

Laminins 411 and 511 line myofibers and Pax7-positive cells in fetal $dy^{W-/-}$ muscles

We next determined the normal dynamics of laminin assembly during fetal muscle development by immunohistochemistry. Laminin assembly around myofibers starts at E14.5 (Fig. 3A), i.e. precisely at the beginning of secondary myogenesis (17). In agreement with, and expanding on the data by Patton *et al.* (5), we find that laminin assembly around myofibers involves

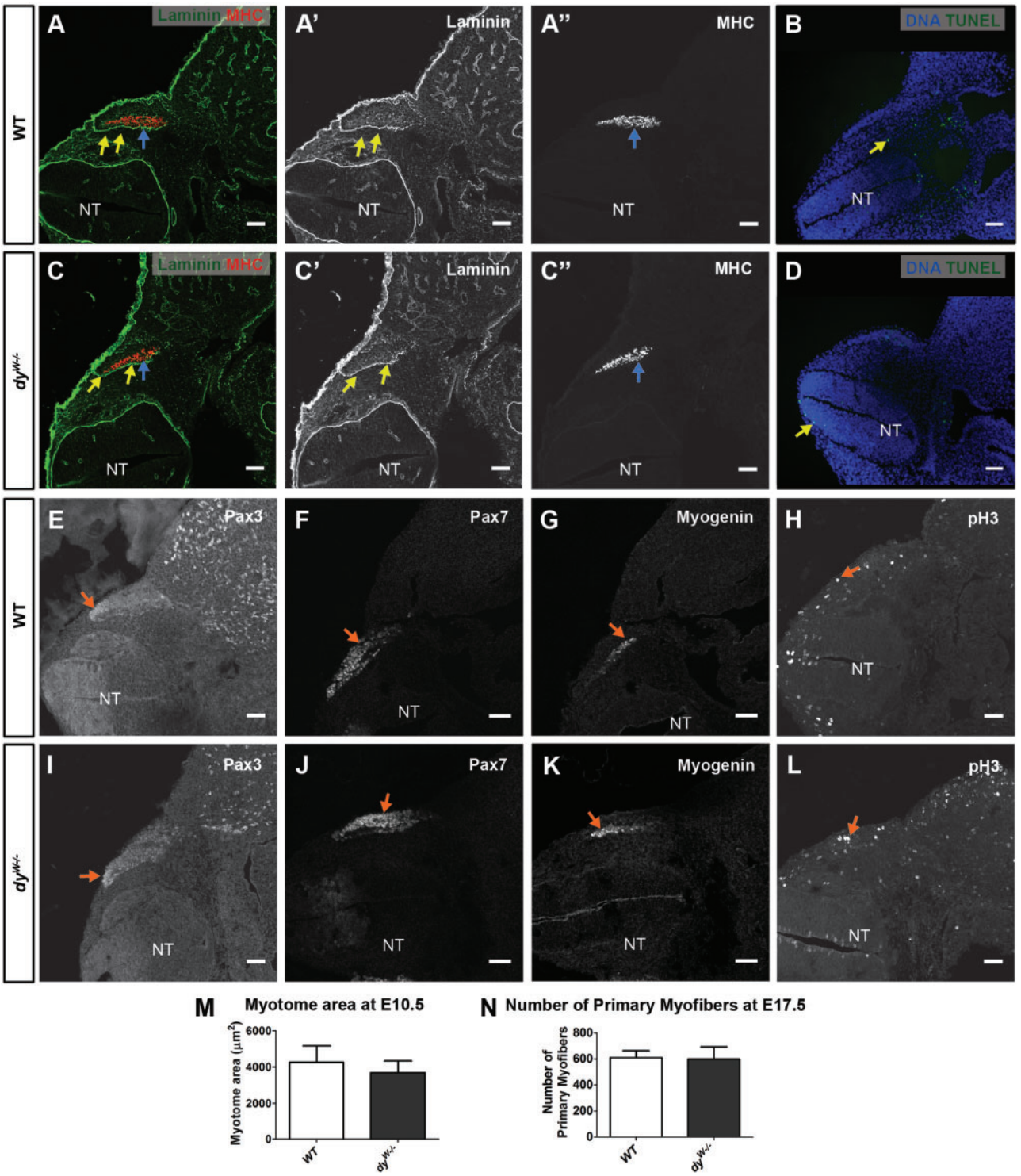

Figure 1. Normal myotomal and primary myogenesis in $dy^{W-/-}$ embryos. Transverse sections of E10.5 WT (**A** and **B**, **E–H**) and $dy^{W-/-}$ embryos (**C** and **D**, **I–L**). (A–A″ and C–C″) Immunohistochemistry for pan-muscle laminin (yellow arrows) and MHC (blue arrows) in WT and $dy^{W-/-}$ embryos. (B and D) Apoptosis (TUNEL assay) in WT and $dy^{W-/-}$ embryos (yellow arrows in B and D). (E–G and I–K) Immunostaining for Pax3 (E and I), Pax7 (F and J) and myogenin (G and K) in WT (arrows in E–G) and $dy^{W-/-}$ (arrows in I–K) embryos. (H and L) pH3 immunostaining (arrows) in WT (H) and $dy^{W-/-}$ (L) embryos. (**M**) Quantification of myotome cross sectional area in E10.5 WT and $dy^{W-/-}$ embryos. (**N**) Quantification of slow-myosin positive myofibers in E17.5 WT and $dy^{W-/-}$ epaxial muscles. Data in M and N are represented as mean ± SEM. See Supplementary Material, Table S2 for *n* numbers. NT, neural tube. Dorsal is on the left. Scale bars: 50 μm.

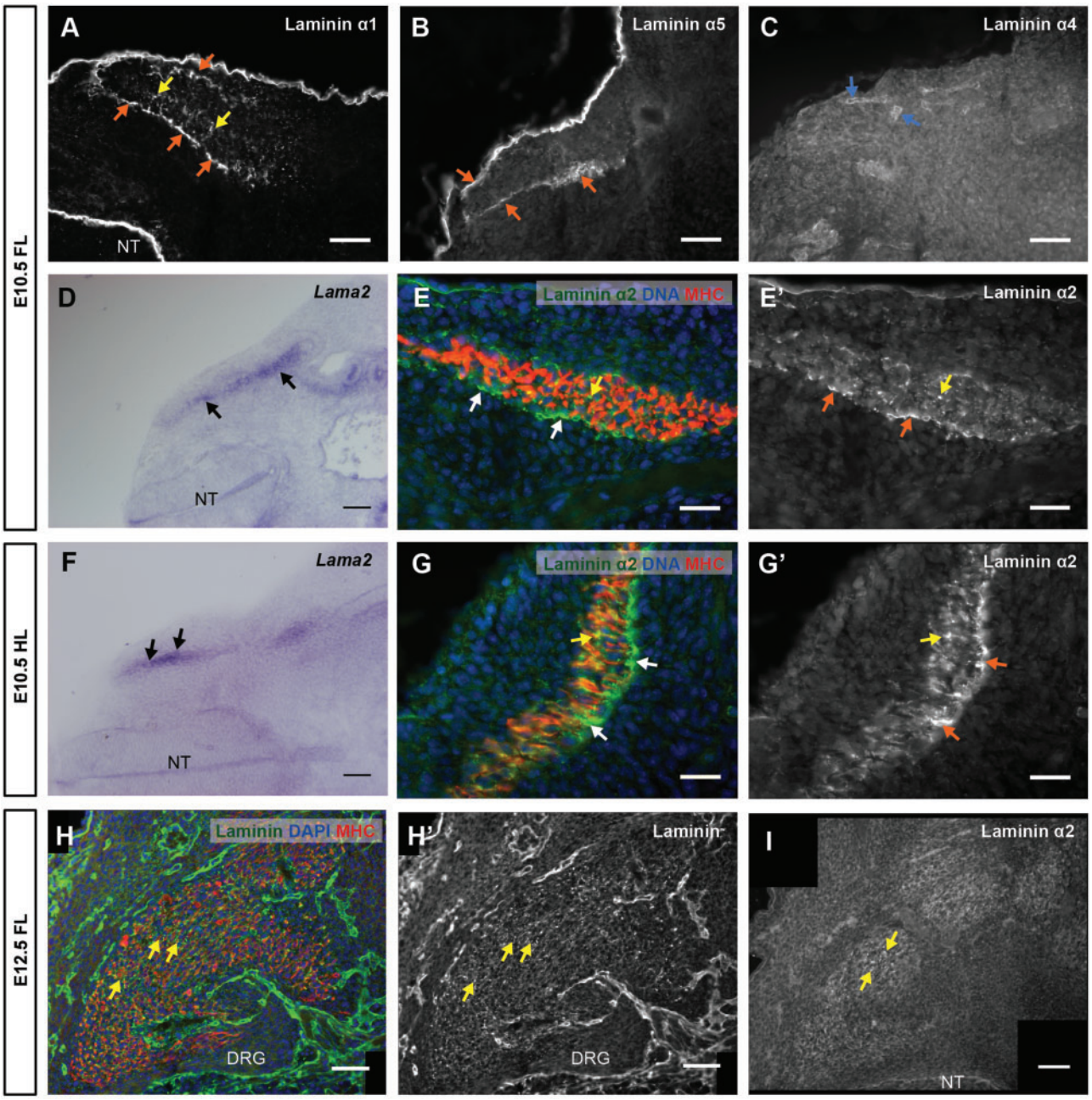

Figure 2. First phase of laminin assembly during mouse myogenesis: the myotome. (**A–G′**) Transverse sections of CD-1 E10.5 embryos at forelimb (A–E′) and hindlimb (F–G′) levels stained by immunofluorescence (A–C, E, E′, G and G′) or by *in situ hybridization* (D and F). (A–C) Immunostaining for laminin α1 (A), α5 (B) and α4 (C) chains. (D and F) *In situ* hybridization for *Lama2*. (E, E′, G and G′) Immunostaining for α2 laminin and MHC with DNA (DAPI) staining (E and G) and grayscale image of α2 laminin immunostaining (E′ and G′). (**H** and **I**) Transverse sections of CD-1 E12.5 embryos at forelimb level stained by immunofluorescence. (H and H′) Immunostaining for laminin (pan-muscle laminin antibody) and MHC, with DNA staining (H), and grayscale image of immunostaining with pan-muscle laminin antibody (H′). (**I**) Immunofluorescence for laminin α2 chain. See Supplementary Material, Table S1 for *n* numbers. FL, Forelimb; HL, Hindlimb; NT, neural tube; DRG, dorsal root ganglia; MHC, myosin heavy chain. Dorsal is on the left, except (G) and (G′) where dorsal is down. Scale bars: 50 μm (A–D,F,H–I); 25 μm (E,E′,G,G′).

laminins containing the α2, α4 and α5 chains (Fig. 3B–D), while laminin α1 is absent (data not shown; see Fig. 4C). The myofiber basement membrane is discontinuous at E14.5 (Fig. 3A–D), but then grows progressively in subsequent stages (E15.5: Fig. 3E–H and M; E17.5: Fig. 3I–L). Pax7-positive muscle stem cells are reported to enter their niche under the myofiber basement membrane at around E16.5 (25,26). Consistent with this notion, we observed a progressive increase in laminin coverage near Pax7-positive cells between E15.5 (Fig. 3N, N′ and N″) and E17.5 (Fig. 3O, O′ and O″). Thus during normal fetal myogenesis, laminins 211, 411 and 511 are gradually assembled around myofibers (see Fig. 3P) and by E17.5 most Pax7-positive muscle stem cells reside underneath the myofiber basement membrane.

It has previously been suggested that laminin α4 and α5 chains may play a role in compensating for the absence of α2 chain laminins during development (5,22). Indeed, at E17.5 these two laminin chains are detected around both WT and $dy^{W-/-}$ myofibers (Fig. 4A, B, E and F). The laminin α1 chain,

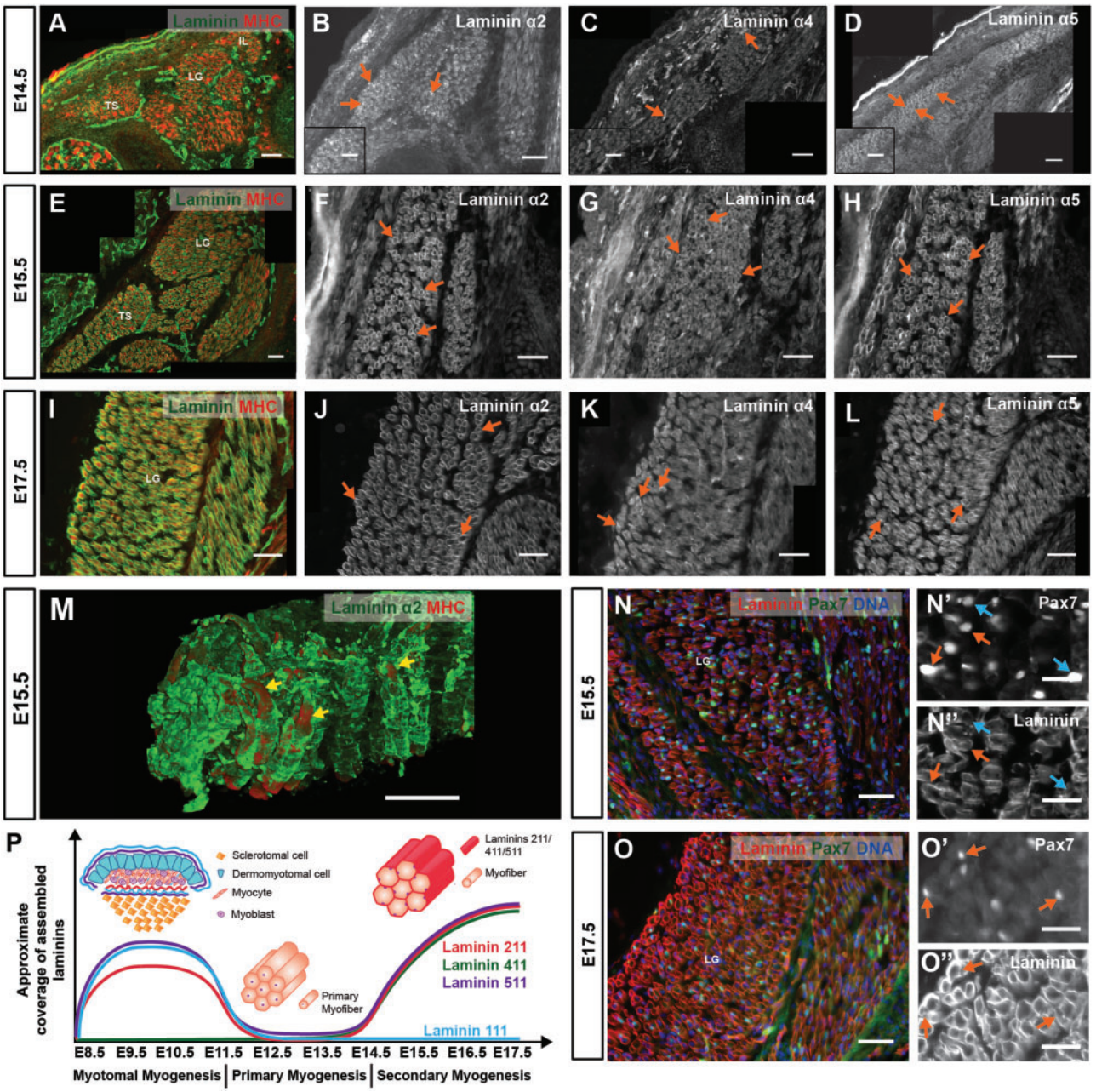

Figure 3. Second phase of laminin assembly during mouse myogenesis: secondary myogenesis. **(A–L)** Transverse sections of CD-1 E14.5 (A–D), E15.5 (E–H) and E17.5 (I–L) fetuses at forelimb level showing epaxial muscles stained by immunohistochemistry for pan-muscle laminin (A, E and I), laminin α2 (B, F and J), α4 (C, G and K) and α5 (D, H and L) chains. **(M)** 3D reconstruction of whole mount E15.5 epaxial muscles showing double immunohistochemistry for laminin α2 and MHC. **(N–O″)** Immunohistochemistry on transverse sections of E15.5 (N and N″) and E17.5 (O and O″) epaxial muscles with pan-muscle laminin and Pax7 antibodies with DNA (DAPI) staining. **(P)** Schematic representation of laminin assembly dynamics over time during myotomal, primary and secondary myogenesis. See Supplementary Material, Table S1 for *n* numbers. TS, transversospinalis; LG, longissimus; IL, iliocostalis; MHC, myosin heavy chain. Dorsal is on the left. Scale bars: 50 μm (A–O); 25 μm (N′, N″, O′ and O″).

normally absent in WT muscles, is not upregulated in fetal $dy^{W-/-}$ muscles (Fig. 4C and G). Thus, in terms of laminin α-chain immunoreactivity, fetal WT and $dy^{W-/-}$ muscles only differ in that the α2 chain is absent in the $dy^{W-/-}$ (see inserts in Fig. 4C and G), as previously reported for adult $dy^{W-/-}$ muscles (27,28). The localization of the α7 subunit of the α7β1 integrin (Fig. 4D and H) and the α-subunit of dystroglycan (Fig. 4I and J), both laminin receptors, is also not affected in $dy^{W-/-}$ when compared with WT fetuses. Double immunostaining for Pax7 and laminins shows that Pax7-positive cells are in close contact with laminin α4 and α5 chains in both WT and $dy^{W-/-}$ muscles (Fig. 4K–N″). Moreover, Pax7-positive cells in $dy^{W-/-}$ muscles at PN2 remain covered by laminins (Fig. 4O, O′ and O″). We conclude that fetal $dy^{W-/-}$ muscles contain laminins 411 and 511 as well as the α7β1 integrin and dystroglycan in a pattern very similar to the one observed in the WT.

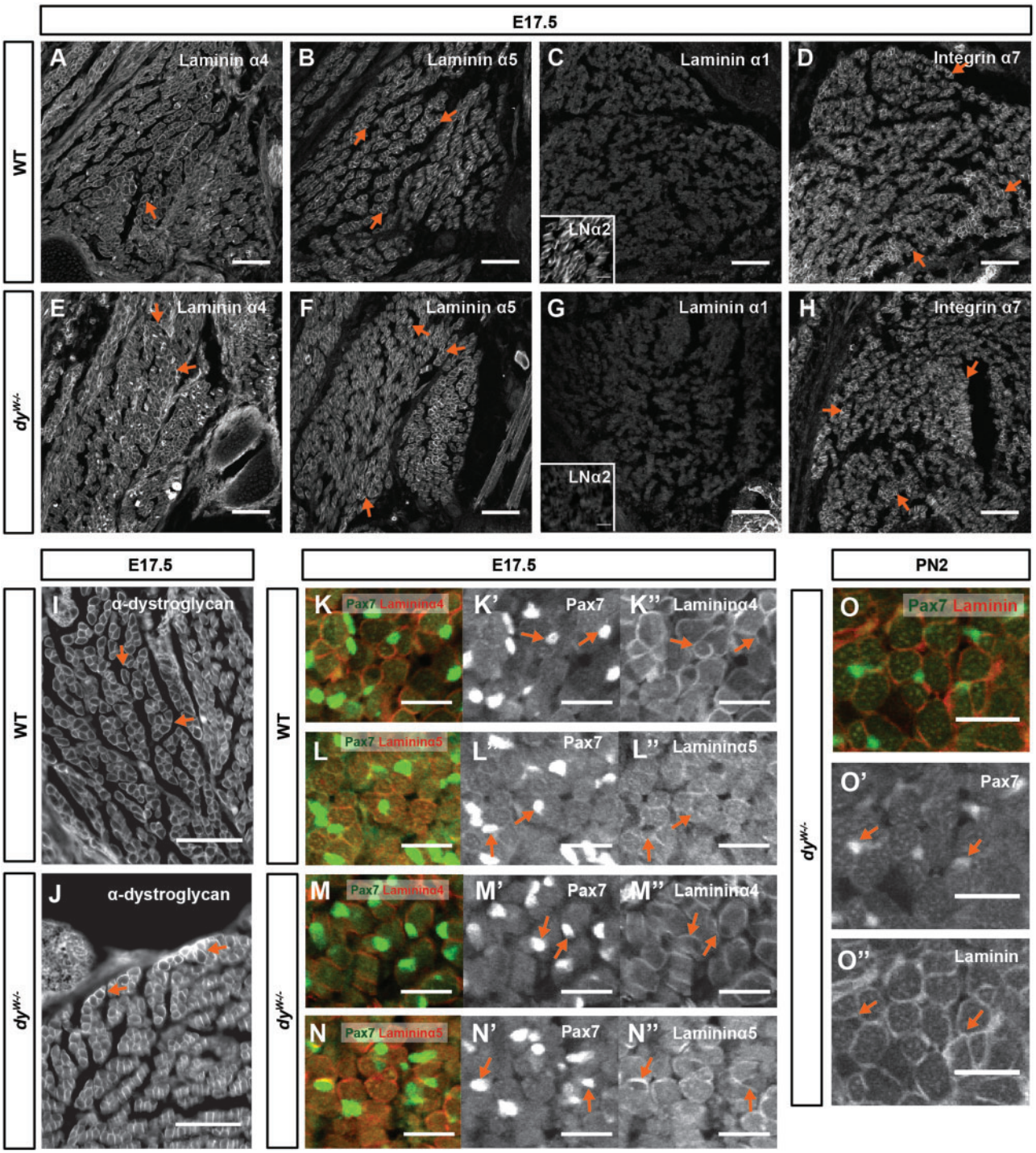

Figure 4. Laminins 411 and 511 line integrin α7β1- and α-dystroglycan-positive myofibers and Pax7-positive cells in $dy^{W-/-}$ muscles. (**A–J**) Immunostaining for laminin α4 (A and E), α5 (B and F), α1 (C and G), α2 (inserts in C and G) chains, integrin α7 subunit (D and H) and α-dystroglycan (I and J) in epaxial muscles of E17.5 WT (A–D and I) and $dy^{W-/-}$ (E–H and J) fetuses. (**K–N″**) Double immunostaining for Pax7 and laminin α4 (K, K″, M and M″) and laminin α5 (M, M″, N, and N″) on transverse sections of epaxial muscles of E17.5 WT (K–N″) and $dy^{W-/-}$ (M–N″) fetuses. (**O–O″**) Double immunostaining for Pax7 and pan-muscle laminin on transverse sections of PN2 $dy^{W-/-}$ epaxial muscles. $n \geq 3$ fetuses/pups per genotype/stage and staining, except for α7 integrin ($n=2$ per genotype) and laminin α2 ($n=1$ per genotype). LNα2, laminin α2. Dorsal is to the left and medial is up. Scale bars: 100 μm (A–J); 50 μm (K–O″).

$dy^{W-/-}$ fetuses display impaired muscle growth

We next asked whether laminins 411 and 511 are able to compensate for the lack of functional laminin 211 during fetal and early postnatal stages of development. To this end we compared the development of $dy^{W-/-}$ muscles with that of WT muscles at E15.5–E18.5 and PN2 (Fig. 5; Supplementary Material, Fig. S1). Overall muscle morphology, as viewed by MHC and pan-muscle laminin immunostaining, appears to be normal in $dy^{W-/-}$ when compared with WT fetuses and PN2 pups (Supplementary

Material, Fig. S1A–J). High-magnification images of pan-muscle laminin staining demonstrate that, despite the absence of laminin 211 in $dy^{W-/-}$ fetuses (insert in Fig. 4G) the pattern of total laminin in WT and $dy^{W-/-}$ fetuses and PN2 pups is indistinguishable (Fig. 5A–J). Measurements of the area of three epaxial muscle groups (transversospinalis, longissimus and iliocostalis; see Materials and Methods) revealed that fetal WT and $dy^{W-/-}$ muscles do not differ in size at E15.5 and E16.5, but that from E17.5 onwards $dy^{W-/-}$ muscles are smaller than WT muscles (Fig. 5K). This difference is significant for E18.5 where $dy^{W-/-}$ muscles have a mean area of 497 170 ± 26 028 μm^2 compared with 607 274 ± 26 626 μm^2 for WT muscles (Fig. 5K; $P = 0.023$; $n = 4$–5 per genotype) and remains significant for PN2 where $dy^{W-/-}$ muscles have a mean area of 707 547 ± 52 802 μm^2 compared with 975 901 ± 56 748 μm^2 for WT muscles (Fig. 5K; $P = 0.021$, $n = 3$–4 per genotype). In spite of this difference in muscle area, the number of myofibers present in WT and $dy^{W-/-}$ fetuses at E15.5–E18.5 does not differ (Fig. 5L) and, although $dy^{W-/-}$ have on average slightly fewer myofibers at PN2, this difference did not reach statistical significance (Fig. 5L; $P = 0.088$; $n = 3$–4 per genotype).

We conclude that although $dy^{W-/-}$ fetuses generate a normal number of myofibers during fetal development, $dy^{W-/-}$ muscles fail to grow normally, being significantly smaller than WT muscles from E18.5 onwards. These results suggest that laminin 211 is essential for the normal growth of fetal muscles and that laminin 411 and 511 are unable to compensate for its absence.

Fetal $dy^{W-/-}$ muscles fail to fully expand their pool of Pax7-positive muscle stem cells and generate fewer differentiated myoblasts

To address the cellular mechanism behind the impaired muscle growth in $dy^{W-/-}$ fetuses, we used immunohistochemistry for Pax7 and myogenin in sections of WT and $dy^{W-/-}$ fetuses and PN2 pups to detect muscle stem cells and differentiated myoblasts, respectively. During normal WT fetal myogenesis, there is a steady increase in the number of Pax7-positive cells in the muscle masses between E15.5 and E17.5 (Fig. 5M; gray line), and the number of Pax7-positive cells stays stable between E17.5 and E18.5 (Fig. 5M; gray line). This occurs even though this pool of cells also feeds into the myogenin-positive pool through differentiation (Fig. 5N; gray line). Quantification of the number of Pax7- and myogenin-positive cells shows that these are at first normal in $dy^{W-/-}$ muscles (Fig. 5M and N; black lines), but between E17.5 and E18.5 there is a dramatic reduction in the number of both Pax7- and myogenin-positive cells in $dy^{W-/-}$ (Fig. 5M and N; black lines) compared with WT muscles (Fig. 5M and N; gray lines). E18.5 $dy^{W-/-}$ fetuses have a mean number of 348 ± 52 Pax7-positive cells per section and thus display a 31% reduction in the number of these cells compared with WT fetuses which have a mean number of 502 ± 39 cells, this difference being statistically significant (Fig. 5M; $P = 0.047$; $n = 5$ per genotype). Thus, whereas E18.5 WT muscles have on average 0.19 Pax7-positive cells/myofiber per section, $dy^{W-/-}$ muscles have 0.13 Pax7-positive cells/myofiber (Supplementary Material, Table S3). E18.5 $dy^{W-/-}$ fetuses show a 47% reduction in the number of myogenin-positive cells compared with WT fetuses, as $dy^{W-/-}$ muscles have an average of 113 ± 12 myogenin-positive cells per section and WT muscles have an average of 212 ± 21 cells and this difference is statistically significant (Fig. 5N; $P = 0.008$; $n = 4$ per genotype). E18.5 WT muscles therefore have an average of 0.08 myogenin-positive cells/myofiber per section, while $dy^{W-/-}$ muscles have only 0.04 myogenin-positive cells/myofiber (Supplementary Material, Table S3). This reduction in the number of Pax7- and myogenin-positive cells in $dy^{W-/-}$ muscles is not due to cell death (Fig. 5O–R), nor to a significant reduction in the number of cells undergoing mitosis (Fig. 5S; $P = 0.515$; $n = 4$–5 per genotype).

In normal WT muscles, the number of Pax7- and myogenin-positive cells goes down between E18.5 and PN2 (Fig. 5M and N; gray lines). Our quantitative data show that the number of Pax7-positive cells in the muscles of $dy^{W-/-}$ PN2 pups is similar to WT pups at PN2 (Fig. 5M; $P = 0.394$; $n = 4$ per genotype), suggesting that the number of Pax7-positive cells diminishes precociously in $dy^{W-/-}$ relative to WT muscles. Furthermore, the number of myogenin-positive cells, although more variable among individuals of both genotypes, is also very similar in $dy^{W-/-}$ relative to WT muscles at PN2 (Fig. 5N; $P = 0.528$; $n = 3$ per genotype). To validate our cell count data at PN2, we isolated PN2 epaxial muscles and assessed Pax7 and myogenin protein levels. Interestingly, Pax7 and myogenin protein levels in $dy^{W-/-}$ PN2 muscles are increased 1.5- and 1.6-fold, respectively, compared with WT pups (Fig. 5T).

Together these data demonstrate that $dy^{W-/-}$ fetal muscles undergo a precocious drop in the number of Pax7- and myogenin-positive cells, which correlates with the significant reduction in cross-sectional area observed in E18.5 $dy^{W-/-}$ muscles. At PN2 the numbers of Pax7- and myogenin-positive cells are similar in WT and $dy^{W-/-}$ muscles and Pax7 and myogenin protein levels are actually increased in $dy^{W-/-}$ relative to WT muscles. However, regardless of this apparent recovery, the difference in cross-sectional area between WT and $dy^{W-/-}$ muscles does not diminish; rather it becomes larger indicating that increased Pax7 and myogenin protein levels does not translate into an actual recovery (Fig. 5K).

$dy^{W-/-}$ muscles display an overactivation of the JAK-STAT signaling pathway

We next applied an RT-qPCR approach to assess for potential changes in the following signaling pathways known to be modulators of muscle growth: Wnt/β-catenin (29,30), Notch (31–34), JAK-STAT (35–37) and Myostatin (GDF8) (38–41). These experiments were done on muscles isolated from E17.5 fetuses, i.e. immediately before $dy^{W-/-}$ muscles are significantly different from WT muscles in terms of a cross-sectional area and the number of Pax7- and myogenin-positive cells.

We did not detect significant differences in transcript levels of the Wnt signaling target genes *Axin2* and *Wisp1* in $dy^{W-/-}$ when compared with WT fetal muscles (Fig. 6A). Transcript levels of the Notch target genes *Dll1*, *HeyL* and *Hey1* were also not different between $dy^{W-/-}$ and WT muscles (Fig. 6B). However, transcripts for the JAK-STAT signaling target gene *Pim1* were significantly increased (Fig. 6C; a 42% increase; $P = 0.007$) in $dy^{W-/-}$ muscles, while *Bcl6* and *Myc* were unchanged (Fig. 6C). Finally, the Myostatin signaling target gene *Akirin1*, which is negatively regulated by Myostatin (42), was significantly increased in $dy^{W-/-}$ compared with WT muscles (Fig. 6D; a 27% increase; $P = 0.027$). *Cdkn1a*, which encodes for p21 and can be regulated by Myostatin signaling (40), demonstrates a slight, but not significant, increase in transcript levels in $dy^{W-/-}$ fetuses (Fig. 6D). Together, these results point to the possibility that an overactivation of the JAK-STAT signaling pathway and a downregulation of the Myostatin signaling pathway in E17.5 $dy^{W-/-}$ muscles may underlie the myogenesis defect identified at E18.5.

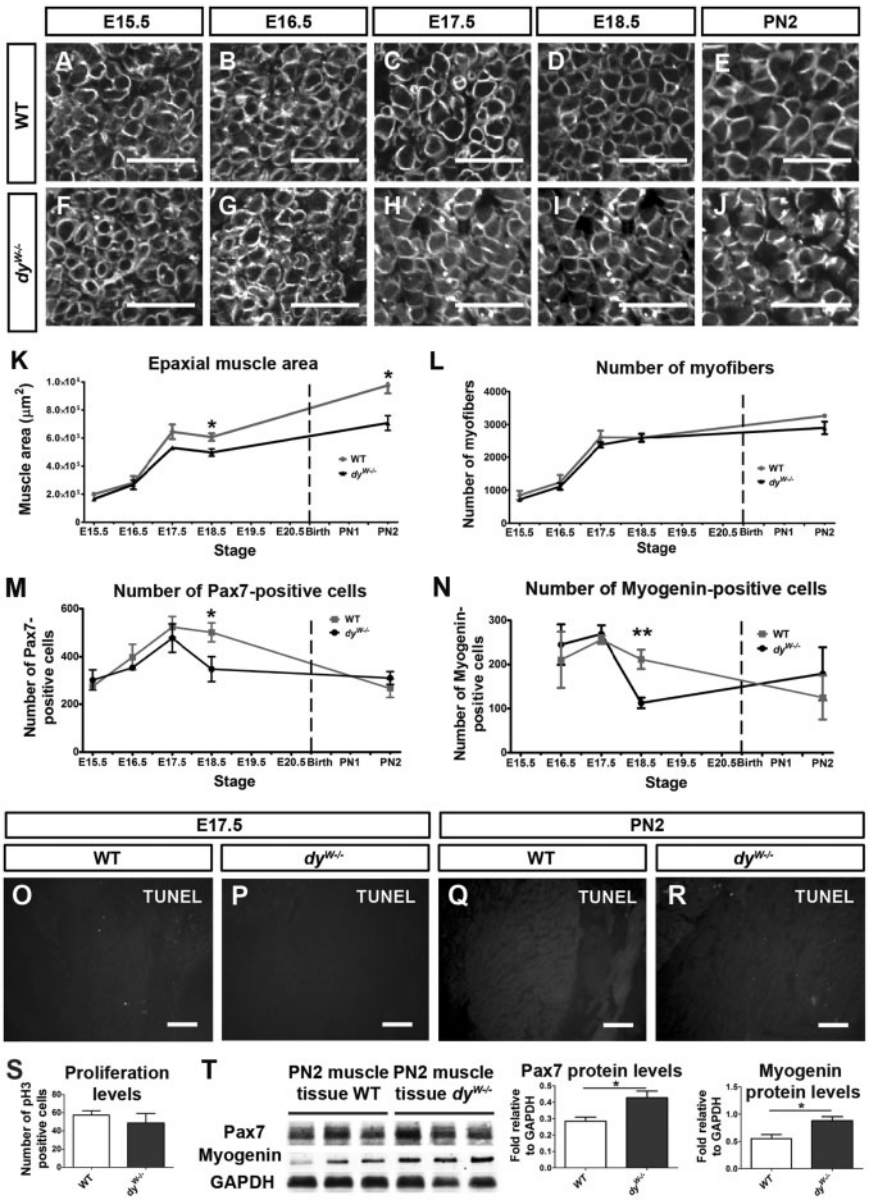

Figure 5. $dy^{W-/-}$ fetuses display a myogenesis defect. (**A–J**) High magnification images of pan-muscle laminin immunostaining on transverse sections of WT (A–E) and $dy^{W-/-}$ (F–J) epaxial muscles at E15.5 (A and F), E16.5 (B and G), E17.5 (C and H), E18.5 (D and I) and PN2 (E and J) showing that fiber shape and laminin coverage is unaffected in $dy^{W-/-}$ compared with WT muscles. (**K**) Graph showing cross sectional area of epaxial WT (gray line) and $dy^{W-/-}$ (black line) muscles from E15.5 to E18.5 and PN2. (**L**) Graph showing myofiber number in the same epaxial muscles from E15.5 to E18.5 and PN2. (**M** and **N**) Graphs showing the quantification of Pax7- (M) and myogenin-positive (N) cells in fetal and PN2 WT (gray lines) and $dy^{W-/-}$ (black lines) epaxial muscles . (**O–R**) TUNEL assay on transverse section of WT (O and Q) and $dy^{W-/-}$ (P and R) muscles at E17.5 (O and P) and PN2 (Q and R). (**S**) Graph showing the number of pH3-positive cells in E17.5 WT and $dy^{W-/-}$ muscles. (**T**) Western blot quantification of Pax7 and myogenin proteins in PN2 WT and $dy^{W-/-}$ muscles. See Supplementary Material, Figure S1 for images of entire composite sections of epaxial muscle groups and Supplementary Material, Table S2 for *n* numbers for (A–S). Data in (K–N), (S and T) is represented as mean ± SEM (*$P < 0.05$; **$P < 0.01$). Scale bars: 50 μm (A–J); 100 μm (O–R).

To test this hypothesis further, we quantified the amount of phosphorylated STAT3 (Tyr 705) (pSTAT3) in E17.5 back muscles using SureFire analysis. This assay revealed that $dy^{W-/-}$ back muscles have, on average, more pSTAT3 compared with control muscles, but this difference was not statistically significant (Fig. 6E; $P = 0.131$; $n = 4$–6 per genotype group). We then isolated protein from the back muscles of PN2 pups and performed Western blot analysis for pSTAT3 (Tyr 705). The results revealed a 3.4-fold and statistically significant ($P = 0.002$) increase in pSTAT3 levels in $dy^{W-/-}$ compared with WT muscles (Fig. 6F). Furthermore, pSTAT3 levels remain significantly higher in 3-week old $dy^{W-/-}$ compared with WT muscles (Fig. 6H; $P = 0.012$). Together, these data demonstrate that $dy^{W-/-}$ muscles display a significant increase in JAK-STAT signaling from very early on, possibly as early as E17.5, and that pSTAT3 activity remains significantly higher in the muscles of 3-week old $dy^{W-/-}$ mice.

Inflammatory cells and fibrotic tissues are known to secrete cytokines that may augment JAK-STAT signaling (43). However, fetal and PN2 $dy^{W-/-}$ muscles were morphologically normal at all stages studied (Fig. 5A–J; Supplementary Material, Fig. S1A–J)

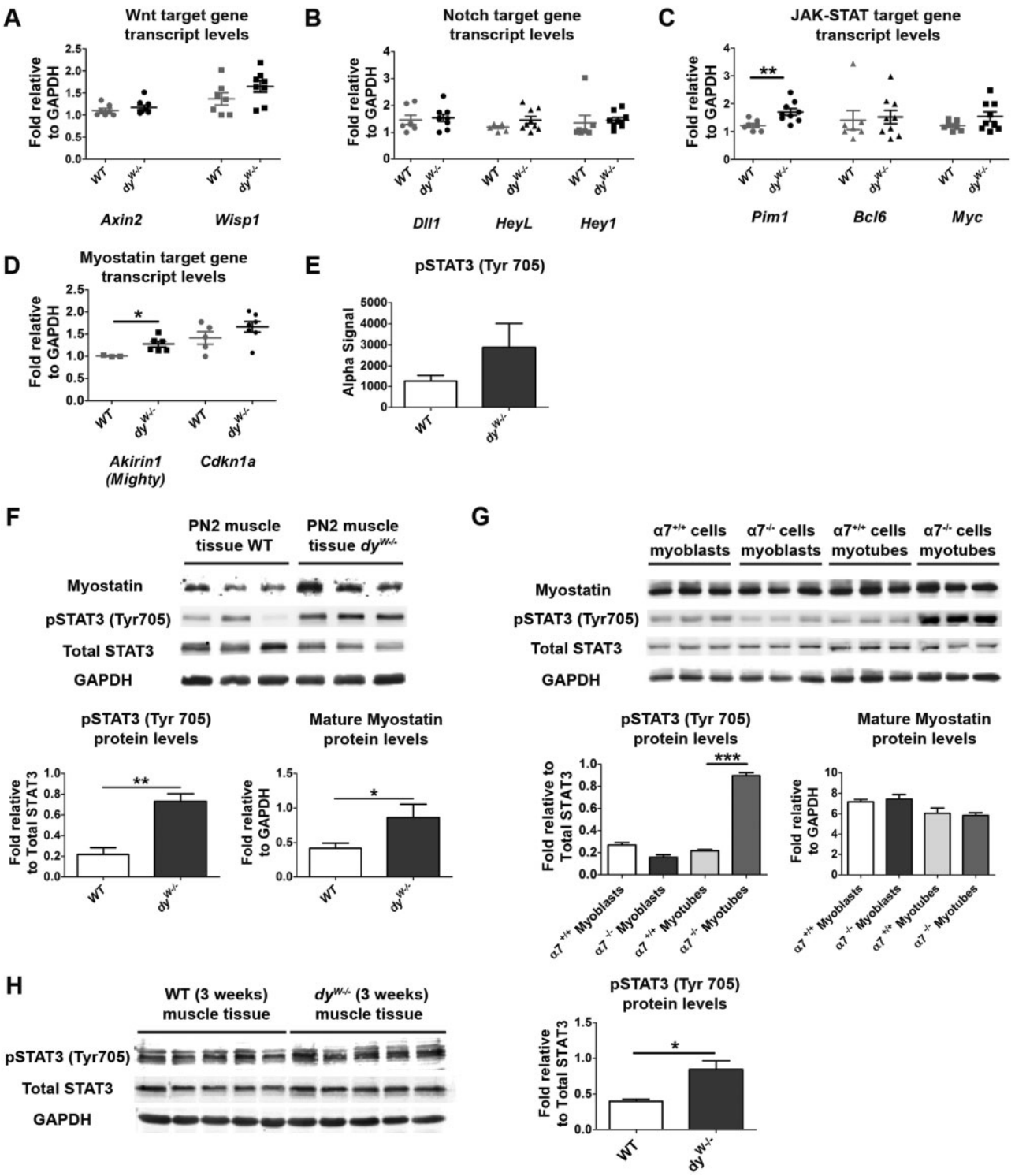

Figure 6. Assessment of the mechanism underlying disease onset in $dy^{W-/-}$ muscles. (A–D) RT-qPCR analysis of the expression of Wnt, Notch, JAK-STAT and Myostatin signaling pathway members and target genes in E17.5 WT and $dy^{W-/-}$ epaxial muscles. (E) SureFire analysis of pSTAT3 (Tyr 705) signal in E17.5 control versus $dy^{W-/-}$ muscles. (F) Western blot analysis of pSTAT3 (Tyr 705) and mature Myostatin in WT and $dy^{W-/-}$ PN2 muscles. (G) Western blot analysis of pSTAT3 and mature Myostatin in cultured $\alpha7^{+/+}$ and $\alpha7^{-/-}$ myoblasts and myotubes. (H) Western blot analysis of pSTAT3 levels in triceps muscle of 3-week old WT and $dy^{W-/-}$ mice. Data represented as mean ± SEM (*P <0.05; **P <0.01; ***P <0.001).

and did not display any infiltration of macrophages at E17.5 or PN2 (as assessed by CD11b immunolabeling; data not shown) nor any increase in Sirius Red staining at PN2 (data not shown). Thus, these results exclude inflammation and fibrosis as the reason for the increased pSTAT3 activity detected in E17.5 and PN2 $dy^{W-/-}$ muscles.

Interestingly, mature Myostatin protein levels were also significantly increased (2.1-fold; $P = 0.049$) in PN2 $dy^{W-/-}$ muscles

when compared with WT (Fig. 6F) indicating that, unlike at E17.5 where our RT-qPCR results indicate a reduction in Myostatin signaling, at PN2 mature Myostatin protein is upregulated in $dy^{W-/-}$ muscles.

Laminin 211 is known to bind to and signal through the α7β1 integrin receptor (44,45). To assess whether the α7β1 integrin modulates the JAK-STAT and/or Myostatin signaling pathways, we measured pSTAT3 and mature Myostatin levels in $\alpha7^{-/-}$ and control $\alpha7^{+/+}$ myoblasts and myotubes. No significant differences were detected between $\alpha7^{-/-}$ and $\alpha7^{+/+}$ myoblasts (Fig. 6G). Mature Myostatin levels were also not significantly different in $\alpha7^{-/-}$ compared with $\alpha7^{+/+}$ myotubes (Fig. 6G). However, pSTAT3 levels were dramatically increased (3.1-fold; $P < 0.0001$) in $\alpha7^{-/-}$ myotubes compared with $\alpha7^{+/+}$ myotubes (Fig. 6G). These results demonstrate that whereas the α7β1 integrin does not appear to affect JAK-STAT signaling in myoblasts, it is a potent negative regulator of JAK-STAT signaling in myotubes.

Together, these results implicate increased pSTAT3 activity in early stages of $dy^{W-/-}$ pathology through a mechanism that seems to involve the α7β1 integrin on myotubes. Moreover, we also provide evidence for a dysregulation of Myostatin signaling in $dy^{W-/-}$ compared with WT muscles as Myostatin signaling is reduced in $dy^{W-/-}$ fetal muscles masses but then mature Myostatin levels are increased in these muscles after birth.

Discussion

MDC1A starts during development *in utero* in the $dy^{W-/-}$ mouse model

Here we reveal for the first time that MDC1A in the $dy^{W-/-}$ mouse starts during development *in utero*. Although laminins containing the α2-chain are first detected during myotome development, this phase of myogenesis proceeds normally in $dy^{W-/-}$ embryos. Laminin 111 and 511 are present during myotome development (this study, 5,21) and we find that both laminin α1 and laminin α2 are detected within the E10.5 myotome, suggesting laminin 111 is able to compensate for the absence of laminin 211 in the myotome. Consistent with this hypothesis, overexpression of a laminin α1 transgene (46) and laminin 111 protein therapy ameliorate pathology in laminin α2-deficient mice (47,48).

Strikingly, primary myogenesis appears to proceed in the total absence of assembled laminins both in trunk and limbs (this study, 23) suggesting that this phase of myogenesis is laminin-independent. Accordingly, we verified that primary myogenesis proceeds normally in $dy^{W-/-}$ embryos.

Laminin assembly around myotubes resumes at E14.5, at the very beginning of secondary (fetal) myogenesis, with the assembly of laminins 211, 411 and 511, but not laminin 111 (this study, 5). We find that these laminins progressively come to line myofibers and Pax7-positive muscle stem cells as they enter their niche at around E16.5 (25,26,49). Fetal myogenesis is characterized by intense muscle growth, which occurs in two ways: (1) by the generation of secondary myofibers (hyperplasia) most of which occurs until E18.0 (26) and (2) through growth of these secondary myofibers, as well as the preexisting primary myofibers, through fusion of myoblasts to these fibers (cell-mediated hypertrophy) (17,20). Our data show that WT and $dy^{W-/-}$ fetuses display similar myofiber numbers. However, our data indicate that between E17.5 and E18.5, $dy^{W-/-}$ fetuses exhibit an impairment in cell-mediated hypertrophy, which is not rescued by the presence of laminins 411 and 511. Our measurements show that the area of $dy^{W-/-}$ muscles is 82% of that of WT muscles at E18.5 and is 75% of WT muscles at PN2, indicating that muscle growth starts lagging behind at E18.5 and that the effect is more pronounced at PN2. Reduced myofiber cross sectional area is indeed one of the hallmarks of disease in $dy^{W-/-}$ animals as the cross-sectional area of triceps brachii myofibers in 5-week old $dy^{W-/-}$ animals is, on average, ∼50% that of same stage WT muscle (47). Moreover, intramuscular injections of laminin 111 into tibialis anterior muscle of 3-week old $dy^{W-/-}$ animals increases the cross sectional area of this muscle by 65% compared with that of PBS injected control $dy^{W-/-}$ animals (48). Together, these observations demonstrate that the presence of laminin 211 (or the closely related laminin 111) acts positively on muscle growth. Here we demonstrate that $dy^{W-/-}$ muscle growth starts lagging behind already *in utero*, before any signs of muscle pathology are detected, which leads us to propose that the onset of MDC1A disease in $dy^{W-/-}$ mice involves a defect in cell-mediated hypertrophy during fetal myogenesis.

Overactivation of JAK-STAT marks $dy^{W-/-}$ disease onset

Our results suggest that the STAT3 signaling pathway is overactivated in $dy^{W-/-}$ muscles and that the link between laminin 211 and STAT3 signaling lies in the α7β1 integrin, since integrin α7-null myotubes *in vitro* show a dramatic upregulation of pSTAT3 compared with control myotubes. It has already been extensively demonstrated that integrin α7β1 signaling plays an important role in disease progression of *Lama2*-deficient mice (7,49,50). Curiously, α7-null myoblasts do not show any increase in pSTAT3. However, myoblasts *in vitro* do not fully represent the diversity of mononucleated muscle cell *in vivo*. Indeed, previous studies have shown that JAK-STAT3 overactivation in satellite cells promotes aging and impairs their expansion during muscle repair (36,37). Thus we cannot exclude the possibility that $dy^{W-/-}$ fetuses display an increased STAT3 phosphorylation in a subset of mononucleated muscle cells. Altogether, these results indicate that a major function of laminin 211 in myofibers is to attenuate STAT3 signaling via the α7β1 integrin.

E18.5 $dy^{W-/-}$ fetal muscles have 31% fewer Pax7-positive cells than WT muscles which demonstrates that these muscles are unable to maintain normal levels of self-renewal of muscle stem cells. We see no indication of cell death, nor differences in pH3-positive cell numbers, excluding increased apoptosis or impaired proliferation as the reason for the drop in Pax7-positive cells. Muscle stem cell amplification is achieved by symmetric divisions of Pax7-positive cells which originate two Pax7-positive stem cells, whereas asymmetric divisions maintain one Pax7-positive stem cell while simultaneously generating a committed cell which later differentiates and fuses with the muscle fiber (51–53). The 3D organization of the myofiber basement membrane favors symmetric divisions of Pax7-positive cells (54). Furthermore, an intact laminin matrix in the Pax7-positive stem cell niche is essential for their self-renewal (55). Thus laminin 211-deficiency is likely to alter the nature of the satellite cell niche as well as its 3D organization. Interestingly, satellite cells cultured on isolated myofibers under conditions that inhibit JAK-STAT signaling show a significant increase in the frequency of symmetric cell divisions and a decrease in asymmetric divisions (36). Thus we suggest a model where altered laminin composition and/or overactivation of JAK-STAT signaling in fetal $dy^{W-/-}$ muscles increases the frequency of asymmetric cell divisions at the expense of symmetric cell divisions, thus leading to a precocious reduction in the

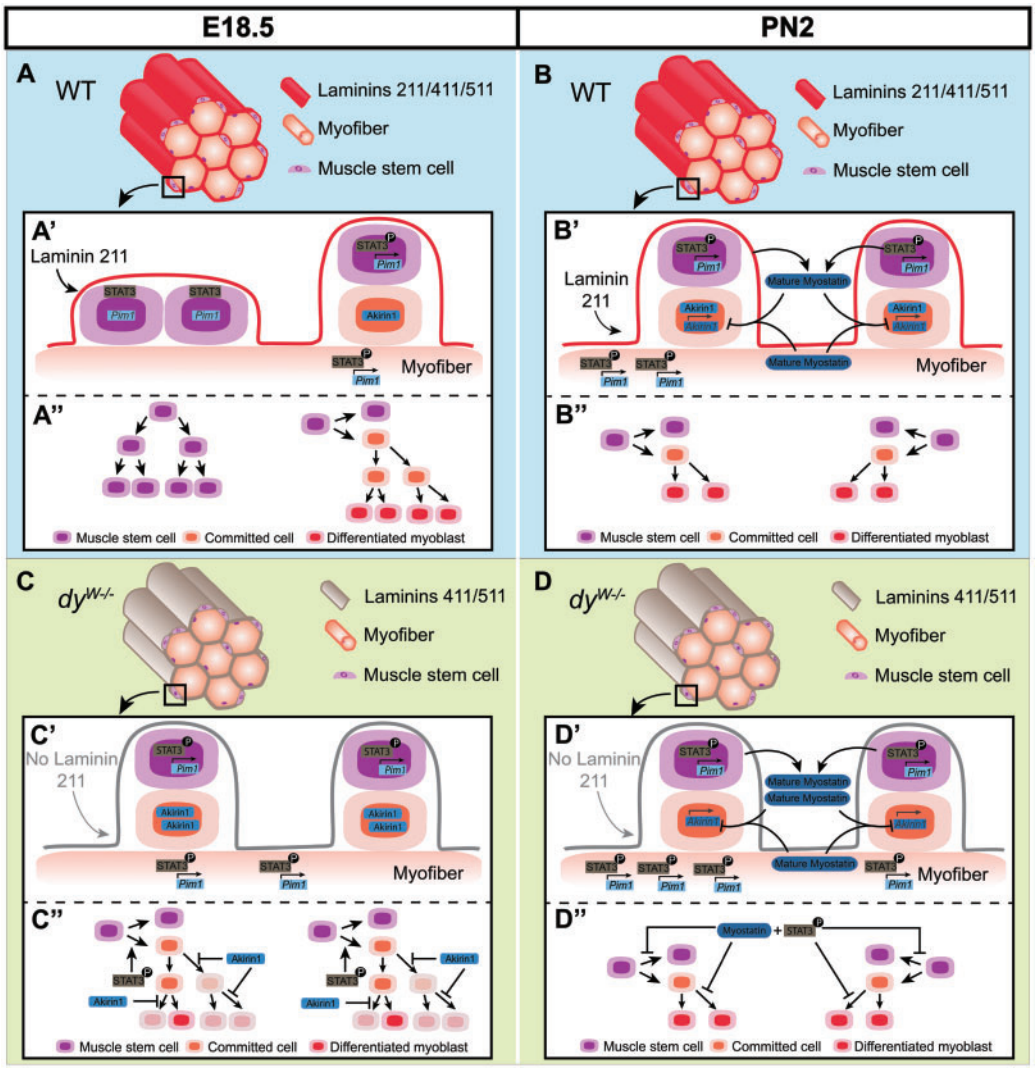

Figure 7. Model illustrating possible mechanism of disease onset during $dy^{W-/-}$ fetal muscle development. Illustration of muscles in normal (WT; **A** and **B**) and *Lama2*-deficient ($dy^{W-/-}$; **C** and **D**) mice at fetal E18.5 (A and C) and postnatal PN2 (B and D) stages. A close-up of the surface of a muscle fiber shows two muscle stem cell division events (A′–D′) and the proposed results of these divisions (A″–D″) in WT (A′, A″, B′ and B″) and $dy^{W-/-}$ (C′, C″, D′ and D″) muscles at E18.5 (A′, A″, C′ and C″) and PN2 (B′, B″, D′ and D″). *Lama2*-deficiency results in a significant reduction in the number of Pax7- and myogenin-positive cells at E18.5 compared with same stage WT muscles. This may occur due to an increase in the frequency of asymmetric cell divisions at the expense of amplifying symmetric divisions (A′ and C′), either because of altered laminin composition (absence of laminin 211) and/or an increase in pSTAT3 activity (A′ and C′). Consequently, E18.5 $dy^{W-/-}$ muscles would have fewer Pax7-positive muscle stem cells than WT muscles (A″ and C″). We further propose that, due to an increased expression of *Aikirin1* (A′ and C′), committed cells in fetal $dy^{W-/-}$ muscles would display impaired expansion capacity, leading to fewer terminally differentiated myoblasts (A″ and C″; shaded cells in C″ would not be generated). Therefore, E18.5 $dy^{W-/-}$ muscles have fewer myogenin-positive, terminally differentiated myoblasts than WT muscles (A″ and C″). In normal postnatal muscle, the frequency of asymmetric cell divisions increases and expansion of muscle stem cells and committed cells decreases. This is illustrated by showing only asymmetric cell divisions in WT (B′ and B″) and $dy^{W-/-}$ muscles (D′ and D″) and fewer cell divisions of committed cells in both WT (B″) and $dy^{W-/-}$ muscles (D″). *Lama2*-deficiency continues to lead to increased levels of pSTAT3 post-natally and in addition leads to the concomitant increase in mature myostatin levels (B′ and D′). Although PN2 $dy^{W-/-}$ muscles are significantly smaller than WT muscles they have similar numbers of stem cells and differentiated cells at this stage (B″ and D″). Thus the rate of asymmetric divisions appears to be similar in WT and $dy^{W-/-}$ PN2 muscles. However, the joint overactivation of JAK-STAT and Myostatin signaling at PN2 could exert a progressive impairment on the division capacity of muscle stem cells and committed cells in $dy^{W-/-}$ individuals (B″ and D″) with consequences for subsequent stages. This effect may later have a negative impact on the regeneration capacity of $dy^{W-/-}$ muscles.

number of Pax7-positive cells in $dy^{W-/-}$ relative to WT muscles (Fig. 7A and C).

Our results also show that E18.5 $dy^{W-/-}$ fetal muscles have an even more dramatic reduction in myogenin-positive cells. This suggests that E18.5 $dy^{W-/-}$ fetal muscles also experience an impaired generation of normal numbers of differentiated and fusion-competent myoblasts. However, increased JAK-STAT signaling leads to an increase in MyoD levels (35–37,56). A possible explanation may lie in the concomitant and significant upregulation of *Akirin1* (*Mighty*) in $dy^{W-/-}$ muscles at E17.5. *Akirin 1* is negatively regulated by Myostatin signaling and is known to activate MyoD in satellite cells (40,42,57). Normally, committed myoblasts can undergo one or two cell divisions before MyoD activates p21, inducing cell cycle exit (58). Interestingly, $Mstn^{-/-}$ fetuses exhibit a drop in the number of Pax7- and myogenin-positive cells at E18.5, which the authors suggest is due to an overactivation of MyoD in committed cells, leading to their faster exit from the cell cycle and formation of

fewer differentiated and fusion-competent cells (41). We thus suggest that the drop in myogenin-positive cells observed in E18.5 $dy^{W-/-}$ muscles may be due to an attenuation of Myostatin signaling which makes committed cells differentiate faster and without significant amplification (Fig. 7A and C).

Taken together we propose a model for MDC1A onset (Fig. 7A and C) where the absence of laminin 211 around fetal myofibers and/or an overactivation of JAK-STAT signaling shift the balance of muscle stem cell divisions to asymmetric divisions, leading to a reduction in the renewal rate of the Pax7-positive muscle stem cell pool. Furthermore, the simultaneous attenuation in Myostatin signaling inhibits the normal amplification of committed cells, leading to a drop in the number of myogenin-positive cells, formation of fewer fusion-competent myoblasts and, consequently, an impairment in fiber growth.

$dy^{W-/-}$ pups start life with significantly smaller muscles and do not possess the machinery to recover their size

In agreement with the situation in human MDC1A patients who have smaller muscles at birth (3), we found that $dy^{W-/-}$ pups are born with significantly smaller muscles than WT pups. Although $dy^{W-/-}$ pups no longer differ from WT pups in the number of Pax7- and myogenin-positive cells, $dy^{W-/-}$ pups have not recovered from the impaired growth during fetal myogenesis. In fact, the apparent recovery of Pax7-positive cell numbers in $dy^{W-/-}$ pups is not due to an increase in Pax7-positive cells in $dy^{W-/-}$ muscles. Rather it is due to a decrease in the number of Pax7-positive cells in WT muscles between E18.5 and PN2. Indeed, a gradual drop in Pax7-positive cell numbers is known to occur during normal postnatal development with the progressive increase in the frequency of asymmetric cell divisions (59). Moreover, muscle stem cells experience a change in identity between fetal and postnatal stages of development, where their capacity for self-renewal goes down while the potency to either differentiate or to recolonize the satellite cell niche increases (60). Our data show that fetal $dy^{W-/-}$ muscles experience a premature decrease in the number of Pax7-positive cells suggesting that they make the transition to a postnatal identity too early.

PN2 pups show a significant increase in pSTAT3 activity (Fig. 7B and D), suggesting that continuous laminin 211-integrin α7β1 signaling is normally required to dampen this signaling pathway. Curiously, in contrast to the situation observed at E17.5 where Myostatin signaling appears to be attenuated, $dy^{W-/-}$ PN2 muscles display higher levels of mature Myostatin compared with WT muscles (Fig. 7B and D). The reason for this is unclear, but a simultaneous increase in pSTAT3 and Myostatin is characteristic of aged muscle, and is thought to be a major factor in the observed loss of regeneration potential during muscle aging (61,62). Consistent with this notion, the muscles of $dy^{W-/-}$ mice have a dramatic reduction in regeneration capacity (48,63).

We therefore propose that $dy^{W-/-}$ muscles display an aged phenotype where, at each time-point from fetal development to adulthood, the muscle environmental cues resemble that of substantially older muscles.

Conclusions

In the present study, we provide the first evidence of *in utero* defects in a mouse model for MDC1A. This marks a paradigm shift in our understanding of MDC1A disease pathogenesis because rather than putting deteriorating muscle fiber health as a first step in the disease, our data demonstrate that the primary defect in $dy^{W-/-}$ mice arises because of impaired in fetal myogenesis. Our results also uncovered the relevance of JAK-STAT and Myostatin pathways in $dy^{W-/-}$ disease onset and progression, which emphasizes the importance of these pathways as targets for future therapies. Taken together, our study provides an important framework for future *in utero* therapies and highlights the necessity for prenatal disease diagnosis and early intervention.

Materials and Methods

Mice and genotyping

dy^{W} mice (gift from Eva Engvall via Paul Martin; The Ohio State University, Columbus, OH, USA) have a *LacZ-neo* cassette inserted in the *Lama2* gene, and homozygous animals produce a small amount of a truncated laminin α2 protein lacking the N-terminal LN domain (27,28). Heterozygous dy^{W} mice were crossed to obtain homozygous $dy^{W-/-}$ mutants and wild-type (WT) controls. Fetuses heterozygous for the dy^{W} allele were indistinguishable from WT controls in all parameters measured (data not shown) and were thus used as controls together with WT fetuses in the SureFire assay. Outbred Charles River CD-1 mice (Envigo, Spain) were used to assess the distribution of laminin variants during normal myogenesis (Figs 2 and 3).

The day of the vaginal plug was designated embryonic day (E) 0.5 and embryos were staged as in Kaufman (64). Anesthetized pregnant females were sacrificed by cervical dislocation, uterine horns removed and placed in cold phosphate buffered saline (PBS) with Ca^{2+} and Mg^{2+} where embryos (E10.5–E13.5) and fetuses (E14.5–E18.5) were dissected out. Post-natal day 2 (PN2) pups were anesthetized by hypothermia and sacrificed by decapitation. Embryos for *in situ* hybridization were collected in PBS.

Embryos, fetuses and pups from heterozygous dy^{W} crossings were genotyped with the following primers: 5′ ACTGCCCTTTC TCACCCACCCTT 3′, 5′ GTTGATGCGCTTGGGACTG 3′ and 5′ GTC GACGACGACAGTACTGGCCTCAG 3′.

All procedures involving mice were performed under two approved protocols: (3/2016) from the Animal Welfare Body of the Faculty of Sciences, University of Lisbon and (000404) from the Institutional Animal Care and Use Committee of the University of Nevada.

Cell culture

Myoblasts isolated previously from gastrocnemius muscles of 10-day old $\alpha7\beta gal^{+/+}$ and $\alpha7\beta gal^{-/-}$ mice (65) were cultured in six-well plates until confluence in Dulbecco's modified Eagle medium (DMEM) (GIBCO) supplemented with 20% fetal bovine serum (Atlanta Biologicals), 0.5% chick-embryo extract (Seralab), 2 mM L-glutamine (GIBCO) and penicillin/streptomycin (100 U/ml; GIBCO) at 37°C with 5% CO_2. Myotubes were obtained by differentiating $\alpha7\beta gal^{+/+}$ and $\alpha7\beta gal^{-/-}$ myoblasts during 5 days in DMEM supplemented with 1% horse serum (Atlanta Biologicals), 2mM L-glutamine (GIBCO) and penicillin/streptomycin (100 U/ml; GIBCO).

In situ hybridization

To determine the mRNA expression pattern of *Lama2* (66), E10.5 embryos were fixed in 4% paraformaldehyde (PFA) in PBS for

whole mount *in situ* hybridization as described previously (66). Briefly, embryos were hybridized overnight at 70°C and probe localization was detected with alkaline phosphatase-conjugated anti-dioxygenin antibodies and NBT/BCIP (Roche) as a substrate. The number of embryos used is listed in Supplementary Material, Table S1.

Immunohistochemistry

Embryos were fixed in 0.2% PFA in 0.12M phosphate buffer (PB) overnight at 4°C. Fetuses and PN2 pups were fixed in 2% PFA in PB for 2 days at 4°C. Embryos, fetuses and PN2 pups were cryo-embedding and 12 μm cryosections were processed for immunohistochemistry essentially as in Bajanca *et al.* (67). However, cryosections of fetuses and PN2 pups were incubated with 0.2% Triton X-100 in PBS for 20 min at room temperature before blocking with 5% bovine albumin serum in PBS. Antigen retrieval was done in E15.5-PN2 tissue by immersing sections in Tris–EDTA (10 mM Tris base, 1 mM EDTA, 0.05% Tween 20) buffer, pH 9.0 at 95°C for 20 min. When staining with monoclonal mouse antibodies, the Mouse-On-Mouse (MOM) kit (Vector Laboratories) was used.

Antibodies used are listed in Supplementary Material, Table S4. The polyclonal antibody against EHS-laminin (i.e. laminin 111) (4) detects all laminins containing α1, β1 or γ1 chains (68). Since all laminin isoforms in skeletal muscle contain at least the γ1 chain, we used this polyclonal anti-laminin antibody to detect all muscle laminins and designate it pan-muscle laminin antibody. TUNEL assay was performed using DeadEnd Fluorometric TUNEL System (Promega). DNA was visualized with 4,6-diamidino-2-phenylindole (DAPI, 5 μg/ml, Sigma). The number of embryos, fetuses and PN2 pups processed for immunohistochemistry and/or TUNEL assay are listed in Supplementary Material, Tables S1 and S2.

Whole mount immunohistochemistry

Whole mount immunohistochemistry was performed as described previously (69). Briefly, dissected fetal back muscles were incubated with primary and secondary antibodies for 2 days at 4°C and were washed for a full day after each antibody incubation. For nuclear staining fetal muscles were incubated with Topro3 (T3605; Molecular Probes; 1:400) and 10 mg/ml ribonuclease A (55674; Calbiochem; 1:100) together with the secondary antibodies. Antibodies used are listed in Supplementary Material, Table S4.

SureFire

AlphaLISA SureFire Ultra kit for p-STAT3 (Tyr705) (ALSU-PST3-A500) was performed according to the manufacturer's instructions (Perkin Elmer). Ten micrograms of protein extract were used per sample for this assay.

Western blotting

Protein extracts were collected in radioimmunoprecipitation assay buffer (RIPA) with 5 mM NaF, 10 mM Na_3VO_4 and a protease inhibitor cocktail (Thermo Scientific; 1:500) and stored at −80°C. After quantification using Pierce BCA protein assay kit (Thermo Scientific), protein extracts were separated with SDS 10 or 12% polyacrylamide gel electrophoresis and transferred to nitrocellulose membranes. Signals were detected using WesternSure™ PREMIUM Chemiluminescent Substract (LICOR) and detection with an Odyssey imaging system (Li-Cor Biosciences). Normalization was performed with glyceraldehyde 3-phosphate dehydrogenase (GAPDH) and/or total STAT3. Quantifications were performed in Fiji (http://fiji.sc/Fiji). Western blots on myoblasts and myotubes were done in triplicate. Muscle tissue from at least 5 PN2 and 3-week old mice per genotype were used. Antibodies used are listed in Supplementary Material, Table S4.

Real time quantitative RT-PCR

RNA was extracted from E17.5 back muscles with Trizol Reagent kit (Ambion, Life Technologies). First-strand cDNA synthesis was performed using the SuperScript III First-Strand Synthesis System for RT-PCR kit (Ambion, Life Technologies). Real-Time qPCR reactions were performed in triplicates with 2× PowerUp SYBR Green Master Mix (Life Technologies) and 500 ng RNA. Transcript levels were normalized against *Gapdh* expession and the fold change was calculated using ΔΔCt method. Primers used are listed in Supplementary Material, Table S5.

Image analysis and quantifications

Sections processed for *in situ* hybridization were photographed using an Olympus DP50 camera coupled to an Olympus BX51 microscope. Sections processed for immunohistochemistry were either imaged with a Hamamatsu Orca R2 camera coupled to an Olympus BX60 fluorescence microscope, or images were acquired on an Olympus IX81 or Leica SPE confocal microscope system. The acquired images were analyzed in Fiji version 1.49 and imported to Amira V.5.3.3 (Visage Imaging, Inc.) software as described previously (69,70).

Transverse sections processed for immunohistochemistry were used for muscle cross-sectional area measurements and quantification of total myofibers, primary myofibers, Pax7- and myogenin-positive cells. To ensure maximum standardization, quantifications were always done in three specific epaxial muscle groups (transversospinalis, longissimus and iliocostalis) at forelimb level and three to five sections per staining and embryo/fetus/PN2 pup were used. Overlapping confocal images covering the three specific epaxial muscles were obtained with a 20× lens and individual images were then stitched together into a large composite image (see Supplementary Material, Fig. S1) using the Fiji plugin Pairwise Stitching (71). Areas were measured using a drawing tool to line the muscles in Fiji and quantifications were performed using Fiji plugin Cell Counter (http://fiji.sc/Cell_Counter). We consider the sum of the number of Pax7- and myogenin-positive cells as a close estimate for the total number mononucleated muscle cells in the muscle masses (Supplementary Material, Table S3) (20). All measurements and counts were done in a blinded fashion.

Statistical analysis

Student's *t*-test was used to test for differences between mRNA, protein or pSTAT3 levels in muscle samples from WT and $dy^{W-/-}$ fetuses and/or PN2 pups, and $\alpha7^{+/+}$ and $\alpha7^{-/-}$ cells, considering $P < 0.05$ as statistically significant. Student's *t*-test was also used to test for differences in the number of Pax7- and myogenin-positive cells in sections of WT and $dy^{W-/-}$ muscles. Finally, differences in muscle cross-sectional area and myofiber numbers were tested using a nested ANOVA where individuals

were nested within genotypes (WT or $dy^{W-/-}$). As described above, all parameters were quantified in stitched composite images of three to five sections per individual, each section covering the same three muscle groups. Each stage was tested separately. Statistical analyses were performed using GraphPad Prism 5 and STATISTICA 12 software.

Supplementary Material

Supplementary Material is available at *HMG* online.

Acknowledgements

We thank Jeff Miner for generously sharing his anti-α5 and anti-α4 laminin antibodies, Madeleine Durbeej for kindly giving the anti-α1 antibody and Patrícia Ybot-Gonzalez for the *Lama2* probe. The MF20, Pax3, Pax7 and IIH6 C4 antibodies were developed by D.A. Fischman, C.P. Ordahl, A. Kawakami and K.P. Campbell, respectively, and were obtained from the Developmental Studies Hybridoma Bank, developed under the auspices of the NICHD and maintained by The University of Iowa, Department of Biology, Iowa City, IA 52242, USA. We also thank Inês Fragata, Jorge Palmeirim and Margarida Bárbaro for help with the statistical analysis, Inês Antunes for help in the laboratory, Patrícia Gomes de Almeida for help with image processing and for critically reviewing the manuscript and all members of our groups for suggestions and constant support.

Conflict of Interest statement. None declared.

Funding

This work was supported by Fundação para a Ciência e a Tecnologia (FCT, Portugal) (project PTDC/SAU-BID/120130/2010, SFRH/BD/86985/2012 scholarship to A.M.N and SFRH/BPD/65370/2009 scholarship to M.D.), Association Française contre les Myopathies (AFM) Téléthon (contract n° 19959), CureCMD, Struggle Against Muscular Dystrophy (SAM), NIH/NIAMS (R01AR064338-01A1), the University of Nevada, Reno (USA) and Mick Hitchcock Scholarship (to A.S. and T.F.).

References

1. Helbling-Leclerc, A., Zhang, X., Topaloglu, H., Cruaud, C., Tesson, F., Weissenbach, J., Tomé, F.M., Schwartz, K., Fardeau, M., Tryggvason, K., *et al.* (1995) Mutations in the laminin α2-chain gene (*LAMA2*) cause merosin-deficient congenital muscular dystrophy. *Nat. Genet.*, **11**, 216–218.
2. Naom, I.S., D'Alessandro, M., Topaloglu, H., Sewry, C., Ferlini, A., Helbling-Leclerc, A., Guicheney, P., Weissenbach, J., Schwartz, K., Bushby, K., *et al.* (1997) Refinement of the laminin α2 chain locus to human chromosome 6q2 in severe and mild merosin deficient congenital muscular dystrophy. *J. Med. Genet.*, **34**, 99–104.
3. Tomé, F.M., Evangelista, T., Leclerc, A., Sunada, Y., Manole, E., Estournet, B., Barois, A., Campbell, K.P. and Fardeau, M. (1994) Congenital muscular dystrophy with merosin deficiency. *C.R. Acad. Sci. III*, **317**, 351–357.
4. Aumailley, M., Bruckner-Tuderman, L., Carter, W.G., Deutzmann, R., Edgar, D., Ekblom, P., Engel, J., Engvall, E., Hohenester, E., Jones, J.C.R., *et al.* (2005) A simplified laminin nomenclature. *Matrix Biol.*, **24**, 326–332.
5. Patton, B.L., Miner, J.H., Chiu, A.Y. and Sanes, J.R. (1997) Distribution and function of laminins in the neuromuscular system of developing, adult, and mutant mice. *J. Cell Biol.*, **139**, 1507–1521.
6. Patton, B.L. (2000) Laminins of the neuromuscular system. *Microsc. Res. Tech.*, **51**, 247–261.
7. Vachon, P.H., Xu, H., Liu, L., Loechel, F., Hayashi, Y., Arahata, K., Reed, J.C., Wewer, U.M. and Engvall, E. (1997) Integrins (α7β1) in muscle function and survival. Disrupted expression in merosin-deficient congenital muscular dystrophy. *J. Clin. Invest.*, **100**, 1870–1881.
8. Laprise, P., Vallé, K., Demers, M.J., Bouchard, V., Poirier, E.M., Vézina, A., Reed, J.C., Rivard, N. and Vachon, P.H. (2003) Merosin (laminin-2/4)-driven survival signalling: complex modulations of Bcl-2 homologs. *J. Cell. Biochem.*, **89**, 1115–1125.
9. Carmignac, V., Svensson, M., Körner, Z., Elowsson, L., Matsumura, C., Gawlik, K.I., Allamand, V. and Durbeej, M. (2011a) Autophagy is increased in laminin α2 chain-deficient muscle and its inhibition improves muscle morphology in a mouse model of MDC1A. *Hum. Mol. Genet.*, **20**, 4891–4902.
10. Carmignac, V., Quéré, R. and Durbeej, M. (2011b) Proteasome inhibition improves the muscle of laminin α2 chain-deficient mice. *Hum. Mol. Genet.*, **20**, 541–552.
11. Gawlik, K.I. and Durbeej, M. (2011) Skeletal muscle laminin and MDC1A: pathogenesis and treatment strategies. *Skelet. Muscle*, **1**, 1–13.
12. Venters, S., Thorsteinsdóttir, S. and Duxson, M.J. (1999) Early development of the myotome in the mouse. *Dev. Dyn.*, **216**, 219–232.
13. Gros, J., Scaal, M. and Marcelle, C. (2004) A two-step mechanism for myotome formation in chick. *Dev. Cell*, **6**, 875–882.
14. Hollway, G. and Currie, P. (2005) Vertebrate myotome development. *Birth Defects Res. C Embryo Today*, **75**, 172–179.
15. Buckingham, M. (2006) Myogenic progenitor cells and skeletal myogenesis in vertebrates. *Curr. Opin. Genet. Dev.*, **16**, 525–532.
16. Cinnamon, Y., Kahane, N. and Kalcheim, C. (1999) Characterization of the early development of specific hypaxial muscles from the ventrolateral myotome. *Development*, **126**, 4305–4315.
17. Biressi, S., Molinaro, M. and Cossu, G. (2007) Cellular heterogeneity during vertebrate skeletal muscle development. *Dev. Biol.*, **308**, 281–293.
18. Deries, M., Schweitzer, R. and Duxson, M.J. (2010) Developmental fate of the mammalian myotome. *Dev. Dyn.*, **239**, 2898–2910.
19. Thorsteinsdóttir, S., Deries, M., Cachaço, A.S. and Bajanca, F. (2011) The extracellular matrix dimension of skeletal muscle development. *Dev. Biol.*, **354**, 191–207.
20. Tajbakhsh, S. (2009) Skeletal muscle stem cells in developmental versus regenerative myogenesis. *J. Intern. Med.*, **266**, 372–389.
21. Bajanca, F., Luz, M., Raymond, K., Martins, G.G., Sonnenberg, A., Tajbakhsh, S., Buckingham, M. and Thorsteinsdóttir, S. (2006) Integrin α6β1-laminin interactions regulate early myotome formation in the mouse embryo. *Development*, **133**, 1635–1644.
22. Ringelmann, B., Ro, C., Hallmann, R., Maley, M., Davies, M., Grounds, M. and Sorokin, L. (1999) Expression of laminin α1, α2, α4, and α5 chains, fibronectin, and tenascin-C in skeletal muscle of dystrophic 129ReJ *dy/dy* mice. *Exp. Cell Res.*, **246**, 165–182.
23. Cachaço, A.S., Pereira, C.S., Pardal, R.G., Bajanca, F. and Thorsteinsdóttir, S. (2005) Integrin repertoire on myogenic

cells changes during the course of primary myogenesis in the mouse. *Dev. Dyn.*, **232**, 1068–1078.
24. Deries, M., Gonçalves, A.B., Vaz, R., Martins, G.G., Rodrigues, G. and Thorsteinsdóttir, S. (2012) Extracellular matrix remodelling accompanies axial muscle development and morphogenesis in the mouse. *Dev. Dyn.*, **241**, 350–364.
25. Kassar-Duchossoy, L., Giacone, E., Gayraud-Morel, B., Jory, A., Gomès, D. and Tajbakhsh, S. (2005) Pax3/Pax7 mark a novel population of primitive myogenic cells during development. *Gen. Dev.*, **19**, 1426–1431.
26. Ontell, M. and Kozeka, K. (1984) Organogenesis of the mouse extensor digitorum logus muscle: a quantitative study. *Am. J. Anat.*, **171**, 149–161.
27. Kuang, W., Xu, H., Vachon, P.H., Liu, L., Loechel, F., Wewer, U.M. and Engvall, E. (1998) Merosin-deficient congenital muscular dystrophy. Partial genetic correction in two mouse models. *J. Clin. Invest.*, **102**, 844–852.
28. Guo, L.T., Zhang, X.U., Kuang, W., Xu, H., Liu, L.A., Vilquin, J.-T., Miyagoe-Suzukic, Y., Takeda, S., Ruegg, M.A., Wewer, U.M. and Engvall, E. (2003) Laminin α2 deficiency and muscular dystrophy; genotype-phenotype correlation in mutant mice. *Neuromuscul. Disord.*, **13**, 207–215.
29. Hutcheson, D.A., Zhao, J., Merrell, A., Haldar, M. and Kardon, G. (2009) Embryonic and fetal limb myogenic cells are derived from developmentally distinct progenitors and have different requirements for β-catenin. *Gen. Dev.*, **23**, 997–1013.
30. Le Grand, F., Jones, A.E., Seale, V., Scimè, A. and Rudnicki, M.A. (2009) Wnt7a activates the planar cell polarity pathway to drive the symmetric expansion of satellite stem cells. *Cell Stem Cell*, **4**, 535–547.
31. Mourikis, P., Gopalakrishnan, S., Sambasivan, R. and Tajbakhsh, S. (2012) Cell-autonomous Notch activity maintains the temporal specification potential of skeletal muscle stem cells. *Development*, **139**, 4536–4548.
32. Schuster-Gossler, K., Cordes, R. and Gossler, A. (2007) Premature myogenic differentiation and depletion of progenitor cells cause severe muscle hypotrophy in *Delta1* mutants. *Proc. Natl. Acad. Sci. U.S.A.*, **104**, 537–542.
33. Vasyutina, E., Lenhard, D.C., Wende, H., Erdmann, B., Epstein, J.A., Birchmeier, C. and Delbru, M. (2007) *RBP-J* (*Rbpsuh*) is essential to maintain muscle progenitor cells and to generate satellite cells. *Proc. Natl. Acad. Sci. U.S.A.*, **104**, 4443–4448.
34. Fukada, S., Yamaguchi, M., Kokubo, H., Ogawa, R., Uezumi, A., Yoneda, T., Matev, M.M., Motohashi, N., Ito, T., Zolkiewska, A., *et al.* (2011) Hesr1 and Hesr3 are essential to generate undifferentiated quiescent satellite cells and to maintain satellite cell numbers. *Development*, **138**, 4609–4619.
35. Wang, K., Wang, C., Xiao, F., W.H. and Wu, Z. (2008) JAK2/STAT2/STAT3 are required for myogenic differentiation. *J. Biol. Chem.*, **283**, 34029–34036.
36. Price, F.D., von Maltzahn, J., Bentzinger, C.F., Dumont, N., Yin, H., Chang, N.C., Wilson, D.H., Frenette, J. and Rudnicki, M. (2014) Inhibition of JAK-STAT signalling stimulates adult satellite cell function. *Nat. Med.*, **20**, 1174–1181.
37. Tierney, M.T., Aydogdu, T., Sala, D., Malecova, B., Gatto, S., Puri, P.L., Latella, L. and Sacco, A. (2014) STAT3 signaling controls satellite cell expansion and skeletal muscle repair. *Nat. Med.*, **20**, 1182–1186.
38. McPherron, C., Lawler, M. and Lee, S.J. (1997) Regulation of skeletal muscle mass in mice by a new TGFβ superfamily member. *Nature*, **387**, 83–90.
39. Thomas, M., Langley, B., Berry, C., Sharma, M., Kirk, S., Bass, J. and Kambadur, R. (2000) Myostatin, a negative regulator of muscle growth, functions by inhibiting myoblast proliferation. *J. Biol. Chem.*, **275**, 40235–40243.
40. McCroskery, S., Thomas, M., Maxwell, L., Sharma, M. and Kambadur, R. (2003) Myostatin negatively regulates satellite cell activation and self-renewal. *J. Cell Biol.*, **162**, 1135–1147.
41. Matsakas, A., Otto, A., Elashry, M.I., Brown, S.C. and Patel, K. (2010) Altered primary and secondary myogenesis in the myostatin-null mouse. *Rejuvenation Res.*, **13**, 717–727.
42. Marshall, A., Salerno, M.S., Thomas, M., Davies, T., Berry, C., Dyer, K., Bracegirdle, J., Watson, T., Dziadek, M., Kambadur, R., *et al.* (2008) Mighty is a novel promyogenic factor in skeletal myogenesis. *Exp. Cell Res.*, **314**, 1013–1029.
43. Harrison, D.A. (2012) The JAK/STAT pathway. *Cold Spring Harb. Perspect. Biol.*, **4**, 1–3.
44. Song, W.K., Wang, W., Foster, R.F., Bielser, D.A. and Kaufman, S.J. (1992) H36-α 7 is a novel integrin α chain that is developmentally regulated during skeletal myogenesis. *J. Cell Biol.*, **117**, 643–657.
45. Hodges, B.L., Hayashi, Y.K., Nonaka, I., Wang, W., Arahata, K. and Kaufman, S.J. (1996) Altered expression of the α7β1 integrin in human and murine muscular dystrophies. *J. Cell Sci.*, **110**, 2873–2881.
46. Gawlik, K., Miyagoe-Suzuki, Y., Ekblom, P., Takeda, S. and Durbeej, M. (2004) Laminin α1 chain reduces muscular dystrophy in laminin α2 chain deficient mice. *Hum. Mol. Genet.*, **13**, 1775–1784.
47. Rooney, J.E., Knapp, J.R., Hodges, B.L., Wuebbles, R.D. and Burkin, D.J. (2012) Laminin-111 protein therapy reduces muscle pathology and improves viability of a mouse model of merosin-deficient congenital muscular dystrophy. *Am. J. Pathol.*, **180**, 1593–1602.
48. Van Ry, P.M., Minogue, P., Hodges, B.L. and Burkin, D.J. (2014) Laminin-111 improves muscle repair in a mouse model of merosin-deficient congenital muscular dystrophy. *Hum. Mol. Genet.*, **23**, 383–396.
49. Gawlik, K., Mayer, U., Blomberg, K., Sonnenberg, A., Ekblom, P. and Durbeej, M. (2006) Laminin α1 chain mediated reduction of laminin α2 chain deficient muscular dystrophy involves integrin α7β1 and dystroglycan. *FEBS Lett.*, **580**, 1759–1765.
50. Doe, J.A., Wuebbles, R.D., Allred, E.T., Ronney, J.E., Elorza, M. and Burkin, D.J. (2011) Transgenic overexpression of the α7 integrin reduces muscle pathology and improves viability in the dyW mouse model of merosin-deficient congenital muscular dystrophy type 1A. *J. Cell Sci.*, **124**, 2287–2297.
51. Kuang, S., Kuroda, K., Le Grand, F. and Rudnicki, M.A. (2007) Asymmetric self-renewal and commitment of satellite stem cells in muscle. *Cell*, **129**, 999–1010.
52. Kuang, S., Gillespie, M.A. and Rudnicki, M.A. (2008) Niche regulation of muscle satellite cell self-renewal and differentiation. *Cell Stem Cell*, **10**, 22–31.
53. Dumont, N.A., Wang, Y.X. and Rudnicki, M.A. (2015) Intrinsic and extrinsic mechanisms regulating satellite cell function. *Development*, **142**, 1572–1581.
54. Webster, M.T., Manor, U., Lippincott-Schwartz, J. and Fan, C.M. (2016) Intravital imaging reveals ghost fibers as architectural units guiding myogenic progenitors during regeneration. *Cell Stem Cell*, **4**, 243–252.
55. Chenette, D.M., Cadwallader, A.B., Antwine, T.L., Larkin, L.C., Wang, J., Olwin, B.B. and Schneider, R.J. (2016) Targeted mRNA decay by RNA binding protein AUF1 regulates adult

muscle stem cell fate, promoting skeletal muscle integrity. *Cell Rep*., **16**, 1379–1390.
56. Serrano, A.L., Baeza-Raja, B., Perdiguero, E., Jardí, M. and Munoz-Cánoves, P. (2008) Interleukin-6 is an essential regulator of satellite cell-mediated skeletal muscle hypertrophy. *Cell Metab*., **7**, 33–44.
57. Salerno, M.S., Dyer, K., Bracegirdle, J., Platt, L., Thomas, M., Siriett, V., Kambadur, R. and Sharma, M. (2009) *Akirin1* (*Mighty*), a novel promyogenic factor regulates muscle regeneration and cell chemotaxis. *Exp. Cell Res*., **315**, 2012–2021.
58. Halevy, O., Novitch, B.G., Spicer, D.B., Skapek, S.X., Rhee, J., Hannon, G.J., Beach, D. and Lassar, A.B. (1995) Correlation of terminal cell cycle arrest of skeletal muscle with induction of p21 by MyoD. *Science*, **267**, 1018–1021.
59. White, R.B., Biérinx, A.S., Gnocchi, V.F. and Zammit, P.S. (2010) Dynamics of muscle fibre growth during postnatal mouse development. *BMC Dev. Biol*., **10**, 21.
60. Tierney, M.T., Gromova, A., Sesillo, F.B., Sala, D., Spenlé, C., Orend, G. and Sacco, A. (2016) Autonomous extracellular matrix remodeling controls a progressive adaptation in muscle stem cell regenerative capacity during development. *Cell Rep*., **14**, 1940–1952.
61. Rossi, G., Antonini, S., Bonfanti, C., Monteverde, S., Vezzali, C., Tajbakhsh, S., Cossu, G. and Messina, G. (2016) Nfix regulates temporal progression of muscle regeneration through modulation of myostatin expression. *Cell Rep*., **14**, 1–12.
62. Snijders, T., Nederveen, J.P., McKay, B.R., Joanisse, S., Verdijk, L.B., van Loon, L.J. and Parise, G. (2015) Satellite cells in human skeletal muscle plasticity. *Front. Physiol*., **6**, 283.
63. Kuang, W., Xu, H., Vilquin, J.T. and Engvall, E. (1999) Activation of the *lama2* gene in muscle regeneration: abortive regeneration in laminin α2-deficiency. *Lab. Invest*., **7**, 1601–1613.
64. Kaufmann, M.H. (1992) *The Atlas of Mouse Development*. Academic Press, San Diego, CA, USA.
65. Rooney, J.E., Gurpur, P.B., Yablonka-Reuveni, Z. and Burkin, D.J. (2009) Laminin-111 restores regenerative capacity in a mouse model for α7 integrin congenital myopathy. *Am. J. Pathol*., **174**, 256–264.
66. Copp, A.J., Carvalho, R., Wallace, A., Sorokin, L., Sasaki, T., Greene, N.D. and Ybot-Gonzalez, P. (2011) Regional differences in the expression of laminin isoforms during mouse neural tube development. *Matrix Biol*., **30**, 301–309.
67. Bajanca, F., Luz, M., Duxson, M.J. and Thorsteinsdóttir, S. (2004) Integrins in the mouse myotome: developmental changes and differences between the epaxial and hypaxial lineage. *Dev. Dyn*., **231**, 402–415.
68. Paulsson, M. (1994) Biosynthesis, tissue distribution and isolation of laminins. In Ekblom, P. and Timpl, R. (eds), *The Laminins*. Harwood Academic Publishers, Amsterdam, pp. 1–26.
69. Gonçalves, A.B., Thorsteinsdóttir, S. and Deries, M. (2016) Rapid and simple method for in vivo ex utero development of mouse embryo explants. *Differentiation*, **91**, 57–67.
70. Rifes, P. and Thorsteinsdóttir, S. (2012) Extracellular matrix assembly and 3D organization during paraxial mesoderm development in the chick embryo. *Dev. Biol*., **368**, 370–381.
71. Preibisch, S., Saalfeld, S. and Tomancak, P. (2009) Globally optimal stitching of tiled 3D microscopic image acquisitions. *Bioinformatics*, **25**, 1463–1465.

Supplementary data

Figure S1- Normal muscle morphology and laminin coverage in *dy*$^{W-/-}$ fetuses and PN2 pups.

Table S1- Number of CD-1 embryos and fetuses used for the immunohistochemistry and *in situ* hybridization experiments.

Table S2- Number of WT and *dy*$^{W-/-}$ embryos, fetuses and PN2 pups used for the immunohistochemistry experiments.

Table S3- Average number of Pax7^{+} and Myogenin^{+} cells during secondary myogenesis.

Table S4- Primary and secondary antibodies used for immunohistochemistry and Western blot.

Table S5- Primers used for RT-qPCR analysis.

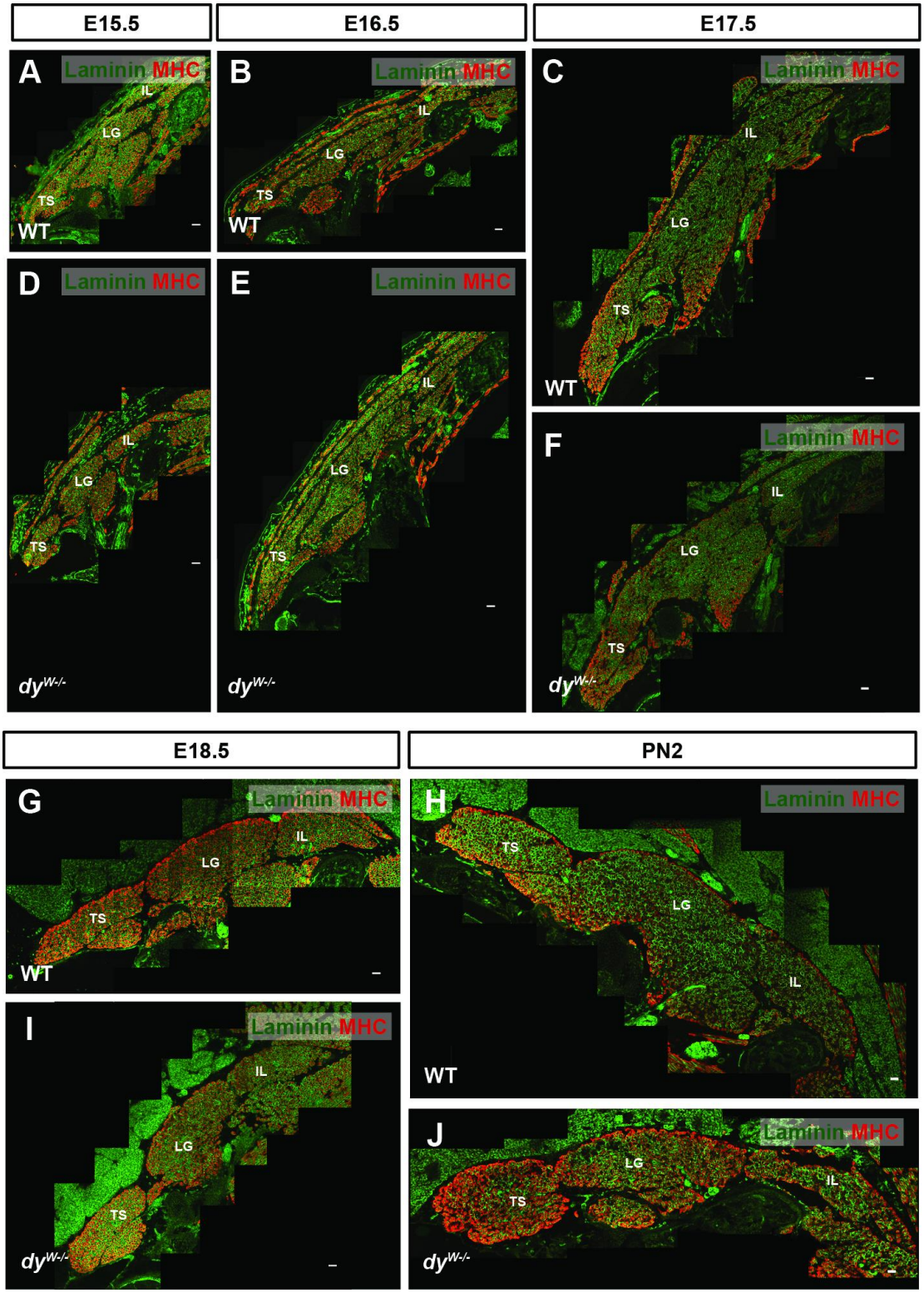

Figure S1 - Normal muscle morphology and laminin coverage in *dy*$^{W-/-}$ fetuses and PN2 pups.

A-J: Double immunostaining for pan-muscle laminin and MHC on transverse sections of WT (A-C, G-H) and *dy*$^{W-/-}$ (D-F, I-J) showing three epaxial muscle groups (TS, LG, IL) at E15.5 (A,D), E16.5 (B,E), E17.5 (C,F), E18.5 (G,I) and PN2 (H,J). Each image in A-J is the result of stitching multiple confocal images of the same section into a large composite image of that section. Muscle morphology and laminin coverage is unaffected in *dy*$^{W-/-}$ compared to WT muscles. **TS:** transversospinalis; **LG:** longissimus; **IL:** iliocostalis. Dorsal is on the left. Scale bars: 50 µm.

Table S1 - Number of CD-1 embryos and fetuses used for the immunohistochemistry and *in situ* hybridization experiments.

Mouse line	Embryonic stage	Staining/ In situ hybridization	Number of embryos/fetuses
CD-1	E10.5	Laminin α1	3
		Laminin α2	3
		Laminin α4	3
		Laminin α5	3
		Lama2	2
	E12.5	Laminin pan	3
		Laminin α2	3
	E14.5	Laminin pan/MHC	3
		Laminin α1	3
		Laminin α2	3
		Laminin α4	3
		Laminin α5	3
	E15.5	Laminin pan/MHC	3
		Laminin α1	3
		Laminin α2	3
		Laminin α4	3
		Laminin α5	3
		Laminin/Pax7	1
		3D Laminin α2/MHC	2
	E17.5	Laminin pan/MHC	3
		Laminin α1	3
		Laminin α2	3
		Laminin α4	3
		Laminin α5	3
		Laminin/Pax7	1

Table S2 - Number of WT and *dy*$^{W-/-}$ embryos, fetuses and PN2 pups used for the immunohistochemistry experiments. Quantitative data were obtained from 3-5 forelimb-level sections of three defined muscles masses, for each staining and embryo/fetus/pup and included individuals from 3-6 litters per stage and staining.

Mouse line	Embryonic stage	Staining	Number of WT embryos/fetuses/ pups	Number of *dy*$^{W-/-}$ embryos/ fetuses/pups
dyW	E10.5	Laminin pan/MHC	4	4
		Pax7	4	4
		Pax3	4	4
		Myogenin	4	4
		Phospho histone 3	2	2
		TUNEL	2	2
	E15.5	Laminin pan/MHC	4	4
		Pax7	3	3
		Myogenin	/	/
	E16.5	Laminin pan/MHC	3	3
		Pax7	3	3
		Myogenin	3	3
	E17.5	Laminin pan/MHC	4	4
		Pax7	3	3
		Myogenin	3	3
		Slow MHC	6	3
		pH3	6	6
		TUNEL	2	2
	E18.5	Laminin pan/MHC	5	4
		Pax7	5	5
		Myogenin	4	4
	PN2	Laminin pan/MHC	4	3
		Pax7	4	4
		Myogenin	3	3
		TUNEL	2	2

Table S3 Average number of Pax7$^+$ and Myogenin$^+$ cells during secondary myogenesis. Average number of Pax7$^+$ and Myogenin$^+$ cells per section (3-5 sections/staining/individual) of transversospinalis, iliocostalis and longissimus muscles and, in brackets, the average number of Pax7$^+$ and Myogenin$^+$ cells per myofiber (Fig. 5L) in WT and *dy$^{W-/-}$* muscles at E15.5, E16.6, E17.5, E18.5 and PN2. Columns 5 and 6 depict an estimate of the total number of mononucleated muscles cells (i.e. Pax7$^+$ plus Myogenin$^+$ cells) and the percentage of those cells that have differentiated (i.e. are Myogenin$^+$).

Embryonic stage	**Genotype**	**Pax7$^+$ cells**	**Myogenin$^+$ cells**	**Pax7$^+$+ Myogenin$^+$ cells (total cells)**	**% of Myogenin$^+$ cells / total cells**
E15.5	WT	277 (0.32/myofiber)	/	/	/
	dy$^{W-/-}$	302 (0.42/myofiber)	/	/	/
E16.5	WT	398 (0.32/myofiber)	211 (0.17/myofiber)	609	35
	dy$^{W-/-}$	355 (0.32/myofiber)	245 (0.22/myofiber)	600	41
E17.5	WT	524 (0.20/nyofiber)	256 (0.09/myofiber)	780	33
	dy$^{W-/-}$	478 (0.20/myofiber)	269 (0.11/myofiber)	747	36
E18.5	WT	502 (0.19/myofiber)	212 (0.08/myofiber)	714	30
	dy$^{W-/-}$	348 (0.13/myofiber)	113 (0.04/myofiber)	461	25
PN2	WT	268 (0.08/myofiber)	125 (0.04/myofiber)	393	32
	dy$^{W-/-}$	311 (0.11/myofiber)	179 (0.06/myofiber)	490	37

Table S4 - Primary and secondary antibodies used for immunohistochemistry and Western blot.

Antibody type	Antibody name	Source	Dilution
Primary antibodies	Laminin polyclonal	Sigma (L9393)	1:400 (IF)
	Laminin α2 (4H8-2)	Sigma (L0663)	1:100 (IF)
	Laminin β1 (LT3)	Abcam (ab4491)	1:100 (IF)
	Laminin γ1 (A5)	Millipore (mab1914P)	1:100 (IF)
	Laminin α5	J. Miner (Gift)	1:800 (IF)
	Laminin α4	J. Miner (Gift)	1:800 (IF)
	Laminin α1	M. Durbeej (Gift)	Supernatant (IF)
	Pax3	DSHB (Pax3)	1:100 (IF)
	Pax7	DSHB (Pax7)	1:50 (IF); 1:250 (WB)
	Myogenin	Santa Cruz Bio (sc-576)	1:100 (IF); 1:200 (WB)
	Myosin Heavy Chain (MHC)	DSHB (MF20)	1:100 (IF)
	Phospho Histone 3 (pH3)	Upstate (s06-570)	1:100 (IF)
	Integrin α7 (C5A)	Ann Sutherland (Gift)	1:100 (IF)
	α-dystroglycan	DSHB (IIH6 C4)	Supernatant (IF)
	Cd11b	BD Bioscience (557672)	1:100 (IF)
	Slow Myosin (1A)	A. J. Harris (Gift)	1:100 (IF)
	Phospho STAT3 (Tyr705)	Cell Signaling (D3A7)	1:1000 (WB)
	Total STAT3	Cell Signaling (79D7)	1:2000 (WB)
	Mature Myostatin	Millipore (AB3239)	1:500 (WB)
	GAPDH	Santa Cruz Bio (sc-20357)	1:1000 (WB)
Secondary antibodies	Alexa Fluor 488-conjugated goat anti mouse IgG F(ab')$_2$ fragments	Life Technologies	1:1000 (IF)
	Alexa Fluor 568-conjugated goat anti rabbit IgG F(ab')$_2$ fragments	Life Technologies	1:1000 (IF)
	Alexa Fluor 488-conjugated goat anti rat IgG F(ab')$_2$ fragments	Life Technologies	1:1000 (IF)
	Goat anti-rabbit-IgG secondary antibody	Li-Cor Biosciences	1:1000 (WB)
	Goat anti-mouse-IgG secondary antibody	Li-Cor Biosciences	1:1000 (WB)
	Anti-rabbit IgG, HRP-linked Antibody	Cell Signaling (7074)	1:2000 (WB)

Table S5 - Primers used for RT-qPCR analysis.

Gene	Forward (5' to 3')	Reverse (5' to 3')
Akirin1	ATCATGCGGCGATACGGGACA	AGTGTACAGCAGCCATCTCTTGA
Axin2	AAGGAGCAGCTCAGCAAAAAGG	TACATGGGGAGCACTGTCTCGT
Bcl6	AAGAGCCATCTGCGCATCCACA	TTCTGGCGCAAATGAAGTCGCA
Cdkn1a	TGTCTGAGCGGCCTGAAGATT	AAGACCAATCTGCGCTTGGAGT
Dll1	AAGCCACGGTCAGGGATACACA	TTCTGTCAGGAATCTCCCCACC
Hey1	AAAATGCTGCACACTGCAGGAG	AGATAACGGGCAACTTCGGCCA
HeyL	ATTGGTCCCCACTGCCTTTGAG	ATCAAAGAACCCTGTGCCACCA
Myc	TAGTGCTGCATGAGGAGACACC	TTGGCAGGGGTTTGCCTCTTCT
Pim1	AAGGGCCAAGTGTTCTTCAGGC	TTCCGGATTTCTTCAAAGGAGGGC

CHAPTER 3

Building laminin matrices during skeletal muscle development

Building laminin matrices during skeletal muscle development

Andreia M. Nunes[1], Inês Antunes[1], André Gonçalves[1], Patrícia Ybot-Gonzalez[2], Marianne Deries[1], and Sólveig Thorsteinsdóttir[1,3]

[1]Centro de Ecologia, Evolução e Alterações Ambientais, Faculdade de Ciências, Universidade de Lisboa, 1749-016 Lisbon, Portugal; [2] Departamento de Pediatria, Hospital Infantil Virgen del Rocio, Sevilla, Spain; [3]Instituto Gulbenkian de Ciência, 2780-156 Oeiras, Portugal

Contribution by A.M.N. to this chapter:

	Fig. 1	**Fig. 2**	**Fig. 3**	**Fig. 4**	**Writing**
Design and concept	III	III	III	II	III
Execution	III	III	III	O	
Analysis and interpretation	III	III	III	III	

Legend:
n.a.- non-applicable
O- no intervention
I- minor contribution
II- moderate contribution
III- major contribution
Note: Items with major contribution by A.M.N. does not exclude major contributions from other authors.

Contribution by the other authors:

Design and concept: M.D. and S.T.; Execution: I.A., A.G. and P.Y.; Analysis and Interpretation: I.A., M.D. and S.T.; Writing: M.D. and S.T.

Building laminin matrices during skeletal muscle development

Andreia M. Nunes[1], Inês Antunes[1], André Gonçalves[1], Patrícia Ybot-Gonzalez[2], Marianne Deries[1], and Sólveig Thorsteinsdóttir[1,3]

[1]Centro de Ecologia, Evolução e Alterações Ambientais, Faculdade de Ciências, Universidade de Lisboa, 1749-016 Lisbon, Portugal; [2] Departamento de Pediatria, Hospital Infantil Virgen del Rocio, Sevilla, Spain; [3]Instituto Gulbenkian de Ciência, 2780-156 Oeiras, Portugal

Abstract

Skeletal muscle fibers are surrounded by a laminin-containing basement membrane essential for skeletal muscle health. During embryonic and fetal development, several laminin isoforms are in contact with myogenic cells, but it is still unclear which cells within the muscle masses produce these different laminins. Here we characterized the laminin expression dynamics throughout mouse myogenesis *in utero* to determine which cells are responsible for producing the laminins. The dermomyotome, the source of skeletal muscle cells, produces laminins 111 and 511 which are deposited in the dermomyotomal basement membrane as well as in the myotomal basement membrane during early stages of myotome myogenesis. Our data also revealed that the myotome synthesizes laminin 211 and 221 which are deposited in its basement membrane. Later on, as the dermomyotome dissociates and muscle progenitor cells enter the myotome, these cells and/or the differentiated myocytes express laminins 111 and 511. The dermomyotomal and myotomal laminin matrices are disassembled and/or degraded during primary myogenesis, but the expression of *Lama2*, *Lama5* and *Lamb1* is maintained within the muscle masses. During fetal myogenesis, both mononucleated cells and myofibers appear to synthesize laminins. Interestingly, our results suggest that the muscle stem cell population in early fetal muscle masses is heterogeneous with regard to its laminin repertoire in that some Pax7-positive cells have no assembled laminin around

them while others have laminins 211, 511 and/or 411. Our results reveal that laminin synthesis and assembly involve cells at multiple stages of myogenic development as well as several different laminin isoforms. This work highlights the need to thoroughly study how this complexity contributes to the development of healthy skeletal muscle.

Key-words: Laminins, Pax3/Pax7-positive muscle stem cells, Myogenesis, Myofibers

Introduction

Skeletal muscles form through a highly coordinated process termed myogenesis. Myogenesis in the body starts at E8.5 in the mouse, when some cells from the dermomyotome are induced by neighboring tissues to activate myogenic regulatory factors (MRFs), transcription factors that initiate the myogenic program, and delaminate from the dermomyotome into the underlying space to constitute the myotome (Venters et al., 1999; Gros et al., 2004; Hollway and Currie, 2005; Buckingham, 2006). In the myotome, these cells divide once or twice before differentiating into myocytes which align and elongate along the rostral-caudal axis. As development proceeds, more Pax3- and/or Pax7- (Pax3/Pax7) positive dermomyotomal cells commit to myogenesis and are progressively added to the myotome where they differentiate contributing to myotomal growth (Venters et al., 1999; Gros et al., 2004; Hollway and Currie, 2005). Pax3/Pax7-positive cells are initially epithelial in the dermomyotome and lined by a laminin-containing basement membrane, but by the end of myotomal myogenesis, the dermomyotome dissociates and proliferating Pax3/Pax7-positive muscle progenitor cells (hereafter designated muscle stem cells) invade the myotomal space (Ben-Yair and Kalcheim, 2005; Kassar-Duchossoy et al., 2005; Relaix et al., 2005; Gros et al., 2005; Thorsteinsdóttir et al., 2011). Between E11.5 and E14.5 some of those muscle stem cells differentiate into myoblasts that fuse with myocytes and/or each other to generate multinucleated primary myotubes (Kelly and Zacks, 1969; Ross et al., 1987; Deries et al., 2010; Thorsteinsdóttir et al., 2011), while others remain as muscle stem cells (Kassar-Duchossoy et al., 2005; Relaix et al., 2005). Then from E14.5 until birth, many Pax7-positive muscle stem cells differentiate into secondary myoblasts which fuse with each other to form the secondary myotubes, and with the primary myotubes and recently formed secondary myotubes to increase their size (Duxson and Usson, 1989; Harris et al., 1989; Biressi et al., 2007; Thorsteinsdóttir et al., 2011). Pax7-positive muscle stem cells

that do not differentiate during fetal myogenesis become the satellite cells of post-natal and adult muscle (Kassar-Duchossoy et al., 2005; Relaix et al., 2005; Tajbakhsh, 2009).

Laminins are major components of basement membranes which surround epithelial, endothelial, muscle, nerve, and fat cells (Thorsteinsdóttir et al., 2011). Laminins are secreted to the extracellular environment as trimers produced by cells which synthesize the three (α, β, γ) chains (Kumagai et al., 1997; Yurchenco et al., 1997; Yurchenco, 2015). Different combinations of 5 α chains, 3 β chains and 3 γ chains generate 16 different laminins, which are named according to their chain composition, e.g. laminin 111 is a trimer of α1, β1 and γ 1 while laminin 211 is composed of α2, β1 and γ1 chains (Aumailley et al., 2005). Up to 8 laminins, namely laminins 111, 121, 211, 221, 411, 421, 511 and 521, are present in skeletal muscle either during development or in adulthood (Durbeej, 2010; Thorsteinsdóttir et al., 2011).

During myotomal myogenesis, two laminin basement membranes are present: the dermomyotome basement membrane that lines the basal side of the dermomyotome; and the myotome basement membrane which separates the myotome from the sclerotome (Bajanca et al., 2006; Deries et al., 2012). The dermomyotome and myotome basement membranes display a similar laminin composition since laminins 111 and 511 are assembled in both (Bajanca et al., 2006). In addition, laminin 211 is assembled among myotomal myocytes and is also incorporated in the myotomal basement membrane (Cachaço et al., 2005; Nunes et al., 2017). Laminins are not assembled during primary myogenesis (Cachaço et al., 2005; Nunes et al., 2017) but during secondary myogenesis, primary and secondary myotubes are progressively surrounded by a basement membrane containing laminins 211, 411 and 511 (Patton et al., 1997; Nunes et al., 2017). Muscle stem cells initially intermingle with myotubes in the muscle masses, but enter their niche under the myotube basement membrane around E16.5 (Ontell and Kozeka, 1984; Kassar-Duchossoy et al., 2005). Muscle stem cells, myoblasts and myotubes are known to interact

with a laminin matrix at most stages of myogenesis, but it is not clear exactly which cells produce these laminin matrices.

Here, we characterized the laminin expression dynamics during myogenesis. We demonstrate that dermomyotomal cells produce their own laminin matrix and provide laminins for the assembly of the myotomal basement membrane during early stages of myotome development. We also show that myotome maturation correlates with laminin synthesis by myotomal myocytes and possibly by that of dermomyotome-derived muscle stem cells invading the myotome as the dermomyotome dissociates. During primary myogenesis, laminin genes are expressed in the muscle masses although no assembled laminins are detected. Finally, we show that mononucleated cells and myotubes both contribute to the laminin matrix within the fetal muscle masses.

Materials and Methods

Mice

Wild-type embryos (E9.5-E13.5) and fetuses (E14.5-E18.5) were obtained from crossings of outbred CD-1 mice (Harlan Interfauna Iberica). The day of the vaginal plug was designated embryonic day (E) 0.5 and embryos were staged as in Kaufman (1992). Isoflurane-anesthetized pregnant females were sacrificed by cervical dislocation.

Myf5$^{Cre/+}$*:R26R*$^{stop\text{-}NICD\text{-}nGFP/+}$ (hereafter abbreviated *Myf5*^{Cre}-NICD) mice express the notch intracellular domain (NICD) under the control of the *Myf5* promoter, which enables the constitutive activation of NICD in muscle stem cells that have, at one point in their lives, activated the *Myf5* gene (Mourikis et al., 2012). *Myf5*^{Cre}-NICD embryos and fetuses do not form the muscles which are dependent on a Myf5-positive cell population and thus maintain a large number of muscle stem cells throughout embryonic and fetal

development (Mourikis et al., 2012). E14.5 *Myf5*^{Cre}-NICD fetuses were a kind gift from Sharaghim Tajbakhsh (Institut Pasteur, Paris, France).

All procedures involving mice were performed under the approved protocol 3/2016 from the Animal Welfare Body of the Faculty of Sciences, University of Lisbon.

In situ hybridization

To determine the mRNA expression pattern of different laminin genes (*Lama1*, *Lama2*, *Lama4*, *Lama5*, *Lamb1*, *Lamb2*), E9.5-E18.5 embryos/fetuses were collected for *in situ hybridization*. E9.5-E12.5 embryos were fixed in 4% paraformaldehyde (PFA) in phosphate buffered saline (PBS) and processed for whole mount *in situ* hybridization as described previously (Copp et al., 2011). Since all muscle laminins contain the γ1 chain, in this study we did not assess the expression of *Lamc* genes. Embryos were permeabilized with 10mg/ml proteinase K (E9.5: 20 minutes; E10.5: 25 minutes; E11.5: 45 minutes; E12.5: 75 minutes) and hybridized with digoxigenin-labelled RNA probes overnight at 70°C. E14.5-E18.5 fetuses were fixed in 4% PFA in PBS for *in situ* hybridization in sections as described previously (Gomes de Almeida et al., 2016). Briefly, sections were incubated with 10 mg/ml proteinase K in PBS for 5 minutes, post-fixed in 4% PFA in PBS for 30 minutes and processed for hybridization overnight at 65ºC. Probe localization was detected with an alkaline phosphate-conjugated anti-digoxigenin antibodies and NBT/BCIP substrate (Roche) in both *in situ* hybridization protocols.

Immunohistochemistry

Embryos and fetuses were processed for cryosectioning and immunostaining as described previously (Bajanca et al., 2004; Nunes et al., 2017). Cryosections were incubated with 0.2% Triton X-100 in PBS for 20 minutes and then incubated with a 5% bovine serum albumin in PBS blocking solution for one hour. Antigen retrieval was done

on sections that were processed for Pax7 detection by immersing them in Tris-EDTA (10 mM Tris base, 1 mM EDTA, 0.05% Tween 20) buffer, pH 9.0 at 95ºC for 20 minutes. The Mouse-On-Mouse (MOM) kit (Vector Laboratories) was used for incubations with mouse monoclonal antibodies. Sections were incubated with primary antibodies overnight at 4ºC and after several washes in PBS they were incubated with secondary antibodies for 1 hour at room temperature. Primary antibodies were: anti-myosin heavy chain (MHC) (1:100; clone MF20 DSHB), anti-EHS laminin (1:400, Sigma), anti-Pax7 (1:50; DSHB), anti-Laminin α2 (1:100; clone 4H8-2 Sigma), anti-Laminin α4 (1:800; gift from Jeff Miner), anti-Laminin α5 (1:800; gift from Jeff Miner), anti-Laminin β1 (1:100; clone LT3 Abcam), anti-Laminin β2 (1:5000; gift from Jeff Miner) and anti-Laminin γ1 (1:100; clone A5 Millipore). The polyclonal antibody against EHS-laminin (i.e. laminin 111) detects all laminins containing α1, β1 or γ1 chains (Paulsson, 1994). Since all muscle laminins contain at least the γ1 chain, we used this polyclonal anti-laminin antibody to detect all muscle laminins and designate it pan-muscle laminin antibody. Secondary antibodies were: $F(ab')_2$-goat anti-Mouse IgG (H+L) cross-adsorbed secondary antibody, Alexa fluor 488 (1:1000; Molecular Probes), $F(ab')_2$-goat anti-rabbit IgG (H+L) secondary antibody, Alexa Fluor 568 conjugate (1:1000; Molecular Probes) and Goat anti-rat IgG (H+L) cross-adsorbed secondary antibody, Alexa Fluor 488 (1:1000; Molecular Probes). DNA was always stained with 4,6-Diamidino-2-phenylindole (DAPI, 5µg/ml, Sigma).

Image analysis and quantifications

Sections processed for *in situ* hybridization were photographed using an Olympus DP50 camera coupled to an Olympus BX51 microscope. Sections processed for immunohistochemistry were imaged with a Hamamatsu Orca R2 camera coupled to an Olympus BX60 fluorescence microscope. Images were analyzed with Fiji version 1.49i.

Results

Dermomyotomal and myotomal cells are major producers of laminins during myotome myogenesis

Previous studies have shown that the dermomyotomal and myotomal basement membranes contain laminins 111 and 511 (Bajanca et al., 2006; Anderson et al., 2009; Nunes et al., 2017). Laminin 211 is found in the myotome basement membrane and among the differentiating myotomal myocytes (Cachaço et al., 2005; Nunes et al., 2017). To determine which cell types produce those matrices, we used *in situ hybridization* in E9.5, E10.5 and E11.5 embryos to determine the expression patterns of the muscle laminin genes (i.e. *Lama* and *Lamb* genes but not *Lamc* genes because all muscle laminins have the γ1 chain) during myotome development. Since different myogenesis phases occur at different axial levels in one single embryo (e.g. Deries et al., 2012), we grouped the analyzed sections into two developmental phases: early myotome (DMM stage 1-2 in Deries et al., 2012) and mature myotome (DMM stage 3-4 in Deries et al., 2012).

Lama1 expression is spatially restricted to the dermomyotome during early myotome development (Fig. 1A) confirming the results of previous studies (Anderson et al., 2009), but as the myotome matures, *Lama1* expression is also detected in the myotome (Fig. 1B). *Lama5* and *Lamb1* are expressed in the dermomyotome (Fig. 1G and I). We also found a signal for *Lamb1* in the early myotome (Fig. 1I; Insert in I). During late myotome development, the *Lama5* and *Lamb1* transcripts becomes enriched to the apical side of dermomyotomal cells and are also present in the myotome (Fig. 1H, J). In contrast, *Lama4* is exclusively expressed by cells in the dermomyotome and is never detected in the myotome (Fig. 1E, F). Laminin α4 protein is only detected in blood vessels at this stage (Nunes et al., 2017) so it is unclear whether *Lama4* mRNA is translated into protein in the dermomyotome. Finally, *Lama2* and *Lamb2* are expressed solely by myotomal cells (Fig. 1C, D, K, L). Immunostaining for laminin β2 chain revealed that it is present in the

basement membrane of the mature myotome (data not shown), which indicates that in addition to laminins 111, 211 and 511, the mature myotomal basement membrane may also contain laminins 121, 221 and/or 521.

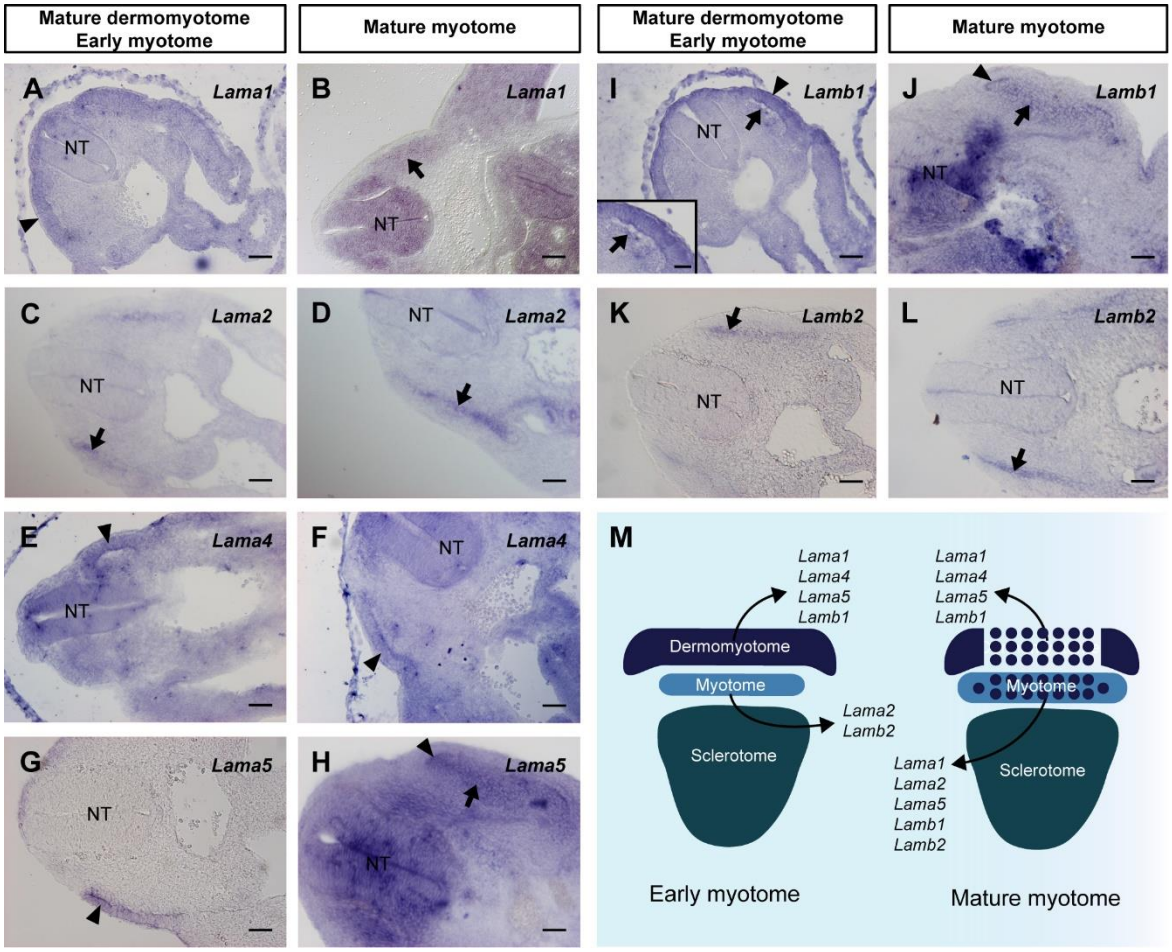

Figure 1- Laminin gene expression during myotome development. (**A, C, E, G, I and K**) Expression of *Lama1* (A), *Lama2* (C), *Lama4* (E), *Lama5* (G), *Lamb1* (I) and *Lamb2* (K) genes during early stages of myotomal development (DMM stages 1-2). The dermomyotome expresses *Lama1* (A, arrowhead), *Lama4* (E, arrowhead), *Lama5* (G, arrowhead) and *Lamb1* (I, arrowhead) genes. The first myocytes of the myotome express *Lama2* (C, arrow), *Lamb1* (I and Insert in I, arrows) and *Lamb2* (K, arrow). (**B, D, F, H, J and L**) Expression of *Lama1* (B), *Lama2* (D), *Lama4* (F), *Lama5* (H), *Lamb1* (J) and *Lamb2* (L) genes during later stages of myotome development (DMM stages 3-4). The dermomyotome maintains the expression of *Lama4* (F, arrowhead), *Lama5* (H, arrowhead) and *Lamb1* (J, arrowhead), while the myotomal cells continue expressing *Lama2* (D, arrow), *Lamb1* (J, arrow) and *Lamb2* (L, arrow). In addition, the mature myotome starts to express *Lama1* (B, arrow) and *Lama5* (H, arrow) (**M**) Schematic representation of laminin expression in early and mature myotome stages. NT, Neural tube. Dorsal is on the left. Scale bars: 50 µm in A-H; 25 µm in insert in I.

Together, our data indicate that there are two distinct phases of laminin production during myotome development (Fig. 1M). Dermomyotomal cells are the main source of laminins 111 and 511, which are assembled in the dermomyotome and myotome basement membranes during early myotome development (Fig. 1M; also see Bajanca et al., 2006; Anderson et al., 2009). Conversely, the early myotomal cells express *Lama2*, *Lamb1* and *Lamb2* genes and appear to contribute the laminins 211/221 which are assembled in the myotome basement membrane (Fig. 1M). During later stages of myotome maturation, when the dermomyotome has started to dissociate, cells in the myotome express a number of laminin genes (Fig. 1M), which means that they may produce as many as 6 different laminins (111, 211, 511, 121, 221 and 521).

Laminin expression dynamics during primary myogenesis

We next sought to determine the laminin expression dynamics during primary myogenesis. Previous studies provided evidence that primary myogenesis proceeds in the absence of assembled laminins as well as in the absence of laminin-binding integrins (Cachaço et al., 2005; Deries et al., 2012; Nunes et al., 2017). *In situ* hybridization in E11.5 embryos revealed that *Lama1* expression is no longer detected in the myotome (Fig. 2A), but *Lama2*, *Lama5* and *Lamb1* transcripts are expressed in the muscle masses undergoing primary myogenesis (Fig. 2B-D). *Lamb2* expression was present in the neural tube but was absent in muscle masses at E11.5 (data not shown). At E12.5, *Lama2* and *Lama5* remain expressed in the epaxial muscle masses (Fig. 2E and F).

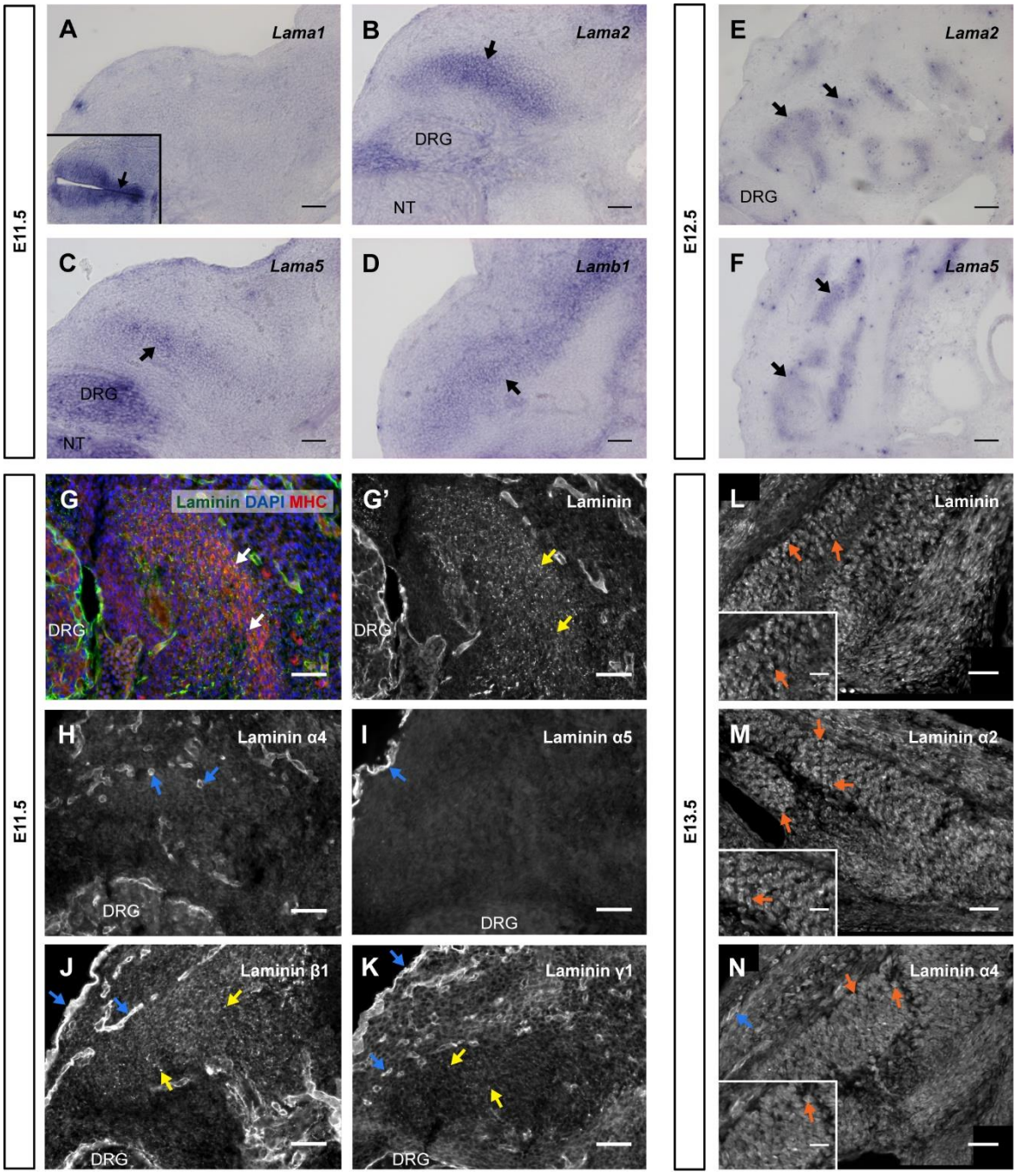

Figure 2- Laminin gene expression and protein localization during primary myogenesis. (**A-D**) *In situ* hybridization on transverse sections of E11.5 embryos at forelimb level showing the epaxial muscle expression of *Lama1* (A), *Lama2* (B), *Lama5* (C) and *Lamb1* (D). *Lama1* is strongly expressed in the neural tube (insert in A, arrow), but it is not expressed in the muscle masses at E11.5 (A). The cells within the muscle masses express *Lama2* (B, arrow), *Lama5* (C, arrow) and *Lamb1* (D, arrow) genes. (**E,F**) *In situ* hybridization on transverse sections of E12.5 epaxial muscles at forelimb level showing the expression of *Lama2* (E) and *Lama5* (F) genes. *Lama2* and *Lama5* are expressed in the epaxial muscles masses at E12.5 (E and F, arrows). **(Continues next page)**

(Continued from previous page) (**G-K**) Transverse sections of E11.5 embryos at forelimb level stained by immunofluorescence. Immunostaining for pan-muscle laminin (green, G and grayscale, G') combined with MHC (red) and DNA staining (blue), and for laminin α4 (H), laminin α5 (I), laminin β1 (J) and laminin γ1 (K) chains. Pan-muscle laminin presents a scattered "spotty" pattern within the muscle (G, white arrows; G', yellow arrows). Laminin α4 and α5 are absent in muscle masses, but enriched in the basement membranes of blood vessels (H, blue arrows) and ectoderm (I, blue arrow), respectively. Laminin β1 and γ1 chains are present in the blood vessels and ectoderm (J and K, blue arrows) and as a dispersed "spotty" pattern in the muscle masses (J and K, yellow arrows). (**L-N**) Transverse sections of E13.5 embryos at the forelimb level stained by immunofluorescence for pan-muscle laminin (L), laminin α2 (M) and laminin α4 (N) chains. Immunolabeling for pan-muscle laminin reveals the presence of laminins around some fibers (L and insert in L, orange arrows). The laminin matrix assembled in the muscle masses at E13.5 is at least composed of laminin α2 (M and insert in M, orange arrows) and laminin α4 (N, orange arrows). Laminin α4 is also detected in the basement membrane of blood vessels (N and insert in N, blue arrow). DRG, Dorsal root ganglia; NT, Neural tube; MHC, Myosin heavy chain. Dorsal is on the left. Scale bars: 50 µm in A-M; 25 µm in inserts in L-N.

Immunostaining for laminin with the pan-muscle laminin antibody in E11.5 embryos reveals a "spotty" pattern within the muscle masses and immunoreactivity with this antibody lines blood vessels and ectoderm (Fig. 2G and G'). This suggests that although laminins are assembled into a matrix in other tissues, they are not assembled in the muscle masses. We next analyzed the presence of different laminin chains in E11.5 muscle masses and found that laminin α4 and α5 chains are present in the basement membranes of blood vessels and ectoderm, respectively (Fig. 2I and H). Laminin α2 was previously detected in a "spotty" pattern within E12.5 muscle masses (Nunes et al., 2017) and we find that laminin α1 displays a similar pattern at E11.5 (data not shown). We further detected the same "spotty" pattern with antibodies against laminin β1 (Fig. 2J) and γ1 (Fig. 2K) chains in E11.5 embryos. These laminin chains are also localized in the basement membranes of blood vessels and ectoderm (Fig. 2J and K). Analysis of later stages of primary myogenesis revealed a few fibers with assembled laminin at E13.5 (Fig. 2L-N; Inserts in L-N; also see Cachaço et al., 2005). Laminin α2 and α4 chains were detected in this newly assembled laminin matrix as well (Fig. 2M and N; Inserts in M and N). These results corroborate previous results which demonstrate that laminin assembly

resumes at the interface between the end of primary myogenesis and the beginning of secondary myogenesis (Nunes et al., 2017).

Together, our data indicate that myogenic cells transcribe laminin genes during primary myogenesis, but laminin proteins are either not secreted or, if they are secreted, they are not assembled into basement membranes. Thus, laminin assembly ceases during this period of myogenesis.

Myofibers and mononucleated cells within the fetal muscle masses build their laminin matrix

Laminin assembly resumes at the beginning of secondary myogenesis with the deposition of laminins 211, 411 and 511 around the sarcolemma of myofibers (Patton et al., 1997; Nunes et al., 2017). We detected *Lama2* and *Lama5* expression in the muscle masses at E14.5 (Fig. 3A and C). Interestingly, *Lama2* and *Lama5* are unevenly expressed within the muscle masses, showing localized patches of intense signal (Fig. 3A and C). No signal for *Lama4* was detected in the muscle masses at this stage (Fig. 3B). Clear expression was, however, encountered in the ventricular myocardium on the same section (insert in Fig. 3B), demonstrating probe efficiency. Immunostaining for laminin β1 and γ1 chains in E14.5 and E15.5 fetuses further supports our previous results suggesting that laminin assembly is in its initial stages at E14.5 (Fig. 3D, E) and by E15.5, assembled laminins are clearly detected in the myofiber basement membrane (Fig. 3I, J; Nunes et al., 2017). It is known that Pax7-positive muscle stem cells enter their niche under the myofiber basement membrane at around E16.5 (Ontell and Kozeka, 1984; Mourikis et al., 2010). Analysis of E17.5 and E18.5 fetuses by *in situ* hybridization revealed that *Lama2* and *Lama5* transcripts at these stages are detected in and near the myofiber nuclei as well

as in mononucleated cells lying immediately adjacent to the myofibers, which may correspond to Pax7-positive muscle stem cells and/or myoblasts (Fig. 3F, G and H).

We next used E14.5 *Myf5*^{Cre}-NICD fetuses in which the transcription of notch intracellular domain (NICD) is under the control of the *Myf5* promoter (Mourikis et al., 2012). Since the majority of muscle stem cells either express or have expressed *Myf5* at some point of their lives (Kuang et al., 2007; Mourikis et al., 2012), their differentiation is blocked by the constitutively expressed NICD and myotubes do not form (Mourikis et al., 2012). It is thus possible to assess which, if any, laminin isoforms are produced by muscle stem cells in the complete absence of myotubes. Immunostaining of adjacent sections for Pax7 and laminin α2 and α5 chains revealed that some, but not all, muscle stem cells are positive for these laminins (Fig. 4A-D). Double labeling for laminin α2 and α5 chains shows that these co-localize around the same cells (Fig. 4E, F-F''), while α4-laminins are only detected in a few Pax7 positive cells (Fig. 4G, H, H'') and in the blood vessels (data not shown). The few Pax7-positive cells which assemble α4-laminins also assemble α2-laminins (Fig. 4G, H-H''), suggesting that these probably assemble α5-laminins as well (Fig. 4I). Strikingly, a considerable number of Pax7-positive cells appear not to produce and/or assemble laminins at this stage, raising the interesting possibility that at E14.5, the muscle stem cell population is a heterogeneous population in terms of its laminin repertoire (Fig. 4I).

Together, our data indicate that both myofibers and Pax7-positive muscle stem cells produce laminins during early stages of fetal myogenesis. In fact, mononucleated muscle cells seem to become major producers of *de novo* laminin during fetal stages.

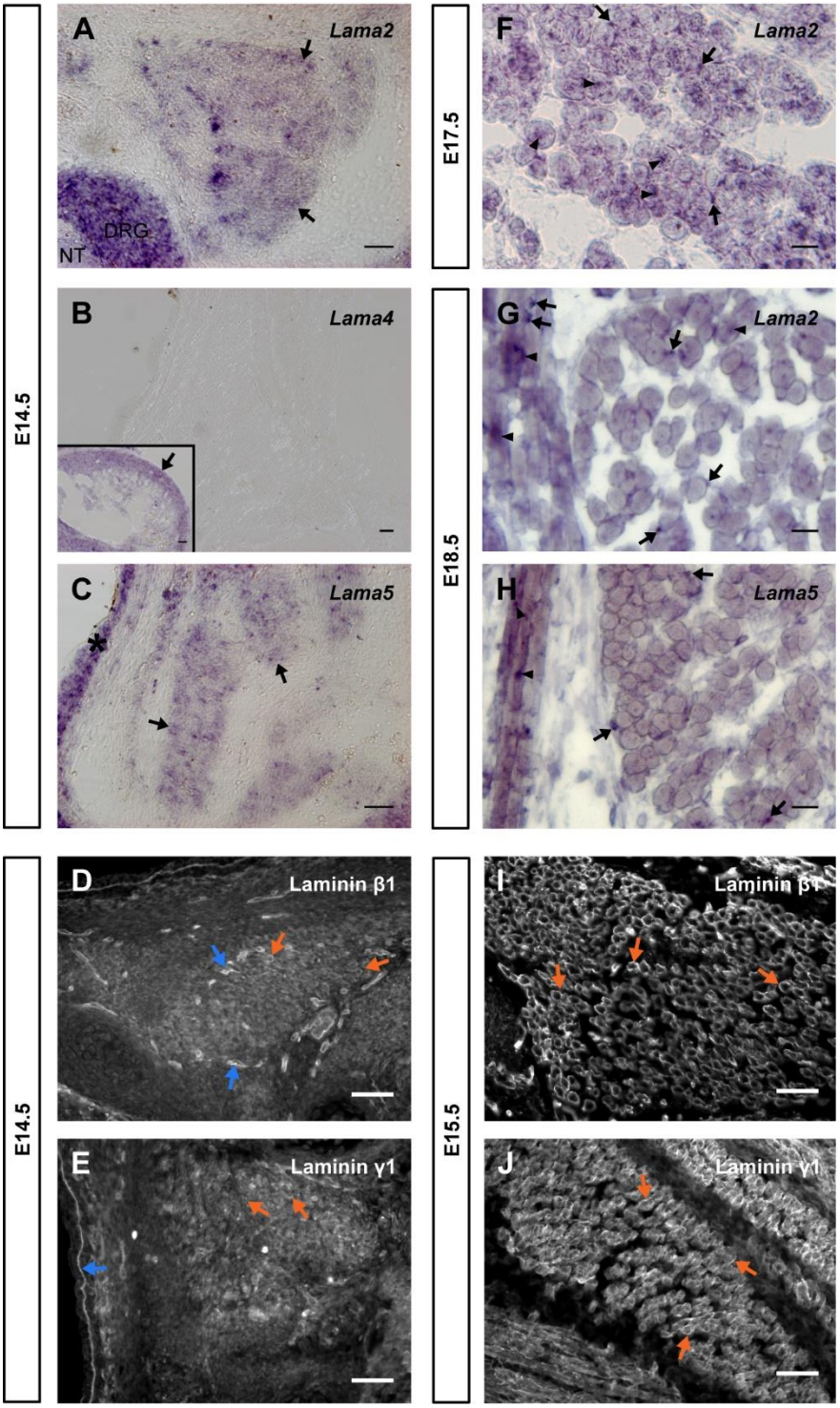

Figure 3- Both myofibers and mononucleated cells within the fetal muscle masses express laminin genes. (**A-C**) Transverse sections of E14.5 fetuses at forelimb level showing epaxial muscles processed for *in situ* hybridization for *Lama2* (A), *Lama4* (B) and *Lama5* (C). *Lama2* is expressed in the dorsal root ganglia (DRG) and in the muscle masses at E14.5 (A, arrows). *Lama4* is strongly expressed in the ventricular myocardium (insert in B, arrow), but it is not expressed in the muscle masses (B). At E14.5 *Lama5* is expressed in muscle masses (C, arrows) and in the epidermis (C, asterisk). **(Continues next page)**

(Continued from previous page) (**D,E**) Transverse sections of E14.5 fetuses at forelimb level showing epaxial muscles stained by immunofluorescence for laminin β1 (D) and laminin γ1 (E). Laminins β1 and γ1 are present around some myofibers (orange arrows) and are enriched around blood vessels (blue arrows in D) and lining the epidermis (blue arrow in E). (**F**) *In situ* hybridizatio*n* for *Lama2* in transverse sections of E17.5 fetuses at the forelimb level reveals the presence of *Lama2* transcripts in the myofiber nuclei (F, arrowheads) and in mononucleated cells beside myofibers (F, arrows). (**G,H**) *In situ* hybridization for *Lama2* (G) and *Lama5* (H) in transverse sections of E18.5 fetuses at forelimb level shows a positive signal in certain regions of the myofibers (arrowheads in G and H respectively). At this stage, *Lama2* and *Lama5* transcripts appear particularly enriched in mononucleated cells immediately adjacent to the myofibers (arrows in G and H respectively). (**I,J**) Transverse sections of E15.5 fetuses at forelimb level showing epaxial muscles stained by immunofluorescence for laminin β1 (I) and laminin γ1 (J). Laminins β1 and γ1 are present around the majority of myofibers (I and J, orange arrows). DRG, Dorsal root ganglia; NT, Neural tube. Scale bars: 50 µm in A-C, D-J; 20 µm in F-H.

Discussion

Building the laminin matrices during myotomal myogenesis: a case of cooperation between the dermomyotome and the myotome

In this study, we analyzed the contribution of cells in the dermomyotome and myotome for the production and assembly of their basement membranes. We uncovered two different phases of laminin production during myotome maturation. Our data indicate that during early myotome development, laminins 111 and 511 are produced by the dermomyotome but are incorporated both into the dermomyotomal and the myotomal basement membranes (Bajanca et al., 2006; Anderson et al., 2009; Nunes et al., 2017). Thus, during these early stages, the myotome apparently gets its laminin 111

and 511 from the dermomyotomal cells. Laminin 211 and 221, on the other hand, seem to be produced by the myotomal myocytes and deposited into the myotomal basement membrane.

During late myotome development, the myotome expands its laminin gene expression profile to include the expression of *Lama1* and *Lama5* and comes to have a more widespread expression of *Lamb1*. This may be part of the myocyte maturation program or, alternatively, the dissociation of the dermomyotome which occurs around the same time (Ben-Yair and Kalcheim, 2005; Kassar-Duchossoy et al., 2005; Relaix et al., 2005; Thorsteinsdóttir et al., 2011), may bring *Lama1*-, *Lama5*- and *Lamb1*-expressing muscle stem cells from the dermomyotome into the myotome. In this latter scenario, differentiated myocytes would continue to synthesize laminins 211/221 while muscle stem cells within the myotome would produce laminins 111 and 511. Experiments combining *in situ* hybridization for laminin genes and immunohistochemistry for Pax3/Pax7 are needed to clarify this issue. Finally, our results revealed that the expression of *Lama4* does not translate into the assembly of α4-laminin matrices in the dermomyotome or myotome (see Nunes et al., 2017). The reason for this is unclear, but the assembly of laminin 411 has been described as a mark of endothelial basement membranes (Yousif et al., 2013). One possibility is that the dermomyotome provides laminin 411 protein to early blood vessels in its vicinity.

Our data suggest that during myotome myogenesis laminin proteins reach target cells through both paracrine and autocrine means as has been demonstrated in other tissues. For instance, laminin secretion and assembly is both an autocrine and a paracrine process during the early development of the neural tube (Copp et al., 2011) and in the assembly of the glomerular basement membrane (Lee et al., 1993). In other cases, such as the development of the retinal and the mammary gland basement membranes, laminin assembly is a paracrine process (Keely et al., 1995; Dong et al., 2002). Based on our results,

we propose that the dermomyotome plays a role in the assembly of the myotomal basement membrane during early stages of myotome development. Later on, the myotome becomes an independent source of laminins, either as a function of a myocyte maturation or due to the activity of dermomyotome-derived muscle stem cells invading the myotome at that same stage.

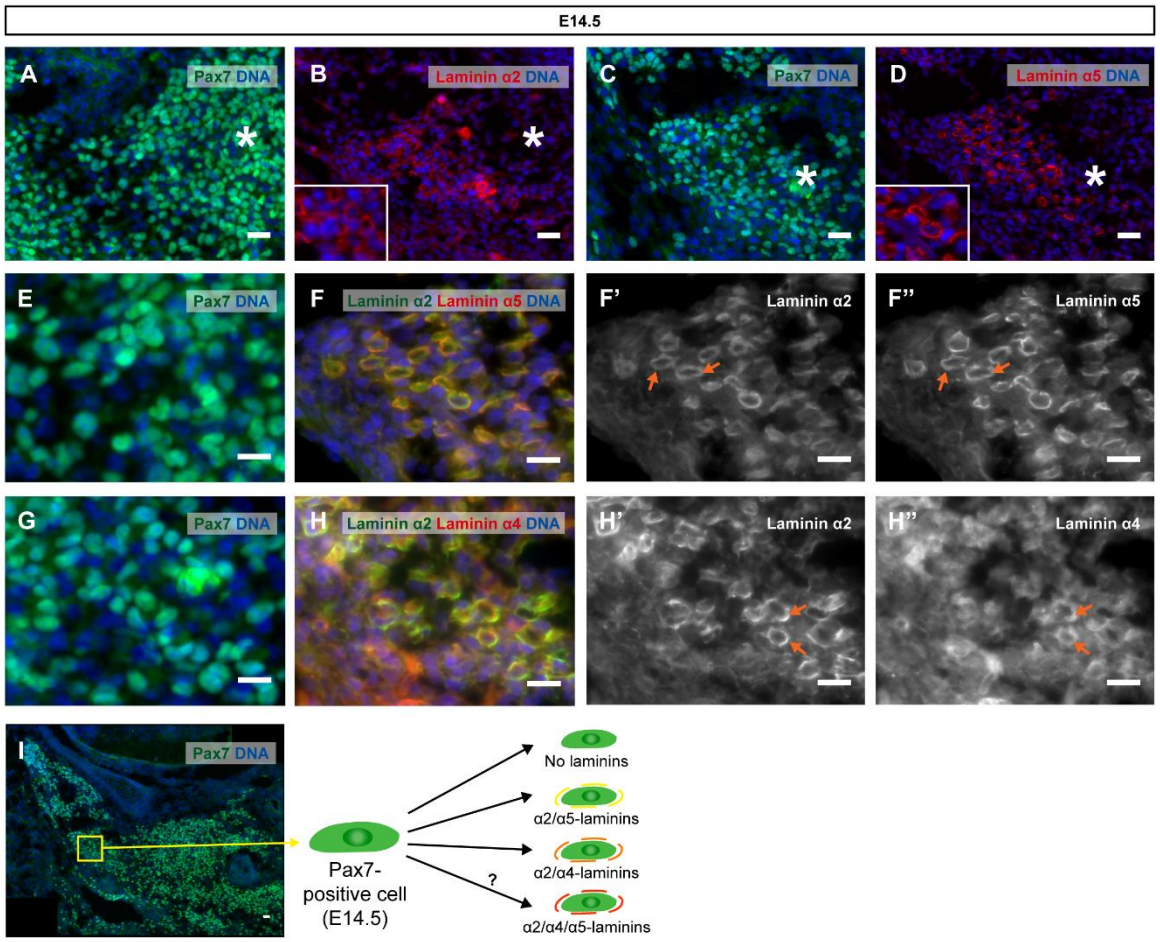

Figure 4- Muscle stem cells build a laminin niche in the absence of myofibers. (**A-H**) Transverse sections showing the presumptive epaxial muscles of E14.5 *Myf5*^{Cre}-NICD fetuses processed for immunofluorescence. Immunostaining for Pax7 (A,C,E,G; green), laminin α2 (B, red; F, green; F', grayscale), laminin α5 (D, F, red; F'', grayscale), laminin α4 (H, red; H'', grayscale) and DNA (A-F, G,H, I, blue). A and B, C and D, E and F, G and H are pairs of adjacent sections to analyze Pax7 positive cells in relation with laminin α2, α5 and α4 chains. Laminins α2 and α5 are not present around all Pax7-positive cells (A-D, asterisks). Double labeling of laminin α2 and α5 reveals that these two α chains mostly co-localize (E-F''; F, F'', orange arrows). Laminin α4 is present in a few Pax7-positive cells and co-localizes with laminin α5 in these cells (G-H''; H', H'', orange arrows). (**I**) Transverse section of E14.5 *Myf5*^{Cre}-NICD fetuses stained for Pax7 (green) and DNA (blue) reveals that the Pax7-positive cell population is spread in the presumptive epaxial muscle masses. Schematic representation of a Pax7-positive cell and its possible laminin niches. Scale bars: 25 µm in A-D, I; 15 µm in E-H''. Inserts are 9x zoomed in.

Primary myogenesis: a laminin independent process?

In agreement with previous work (Cachaço et al., 2005; Deries et al., 2012; Nunes et al., 2017), we found that primary myogenesis proceeds in the absence of assembled laminins. Our results demonstrate that *Lama5* is expressed during primary myogenesis, but this expression does not coincide with laminin α5 synthesis as the muscle masses undergoing primary myogenesis are completely negative for the laminin α5 chain. *Lama2* expression throughout primary myogenesis correlates only with weak "spotty" immunostaining for laminin α2 chain. Laminin α1, β1 and γ1 chains are also found in a faint "spotty" pattern while the α4 chain is completely absent from muscle masses. Intracellular laminin synthesis initially generates β-γ dimers and it is the subsequent addition of the α chain that primes the trimer to be secreted into the extracellular space (Kumagai et al., 1997; Yurchenco et al., 1997; Yurchenco, 2015). It is however not clear whether the "spotty" staining we observed represents *de novo* laminin synthesis.

A possible explanation for the observed "spotty" immunostaining in the trunk muscle masses is that it represents the remnants of the dermomyotomal and myotomal basement membranes, which were disassembled/degraded at the end of myotomal myogenesis (Deries et al., 2012). In support of this hypothesis, limb muscle masses at equivalent stages of myogenesis are completely negative for laminins, except for staining around blood vessels (Cachaço et al., 2005; data not shown). Laminins are known to be remodeled by matrix metalloproteinases (MMP) such MMP2 and MMP14 during adult muscle regeneration (Chen and Li, 2009; Lu et al., 2011; Snyman and Niesler, 2015). MMP14 has been shown to be involved in the processing of laminins 211/221 during muscle regeneration (Ohtake et al., 2006). There are examples of MMP activity generating laminin fragments with biological activity. For example, cleavage of laminin 111 during tumor progression was shown to generate at least four biological active fragments some of which promote angiogenesis and increase the invasion capacity of tumor cells (Kikkawa

et al., 2013). Also, cleavage of laminin 332 releasing a γ2 chain-containing fragment was shown to be important for breast epithelial cell migration (Koshikawa et al., 2000). However, whether the "spotty" laminin pattern observed in trunk muscle masses during primary myogenesis represents laminin fragments with biological activity remains to be addressed.

Another possibility is that the "spotty" pattern represents low levels of *de novo* synthesis without basement membrane assembly. Previous studies have shown that primary myoblasts express considerably lower levels of most of laminin genes assayed when compared to secondary myoblasts (Biressi et al., 2007). Moreover, laminin-binding integrins are downregulated within the muscle masses during these stages (Cachaço et al., 2005; Deries et al., 2012). Laminins and laminin-binding integrins are known to be involved in a bidirectional negative feedback loop mutually downregulating each other's expression at the mRNA and/or protein level (Vachon et al., 1997; Aumailley et al., 2000). For instance, the absence of laminin 211 in *Lama2* deficient skeletal muscle leads to the loss of integrin α7β1 on muscle fibers (Vachon et al., 1997). In another example, the loss of β1-integrins in embryoid bodies was shown to block *Lama1* gene expression and laminin 111 production (Aumailley et al., 2000). Hence, during primary myogenesis, there could be a negative feedback loop where the absence of assembled laminins and consequently laminin signaling through integrins may block integrin membrane localization, which in turn dampens laminin production.

Finally, our data also demonstrates that despite the lack of laminin assembly into a basement membrane surrounding primary myotubes, laminin genes are expressed in the muscle masses during the entire process of primary myogenesis. This suggests that most laminin transcripts are either not translated into protein or laminin trimers are not produced or secreted during primary myogenesis. MicroRNAs are major post-transcriptional regulators and are known to play an important role in the regulation of

skeletal muscle development (Buckingham and Rigby, 2014; Horak et al., 2016; Placoná Diniz and Wang, 2016). During myogenic differentiation, microRNAs are induced by MRFs to block the translation of *Pax3* and *Pax7* transcripts (Buckingham and Rigby, 2014; Horak et al., 2016; Placoná Diniz and Wang, 2016). miR-124 has been reported to target *Lamc1* in the neural tube (Cao et al., 2007) and integrins are also known targets of microRNAs (Chen et al., 2013). Whether microRNAs have a role in regulating laminin matrix assembly is an interesting concept that needs further study. A possible scenario is that laminin gene transcripts are maintained in myogenic cells until the beginning of secondary myogenesis after which their translation is activated, thus enabling the rapid laminin secretion and assembly observed at those stages (Nunes et al., 2017).

Taken together, our results and previous studies strongly suggest that primary myogenesis is a laminin-independent process. The biological reason for this is unclear, but it might be related to the nature of myoblast fusion and myotube formation during primary myogenesis. Primary myogenesis occurs via synchronous fusion of primary myoblasts into primary myotubes (Kelly and Zacks, 1969; Ross et al., 1987; Thorsteinsdóttir et al., 2011), while secondary myogenesis is dependent on primary myotubes to guide the progressive fusion of secondary myoblasts into secondary myotubes. Secondary myotubes are initially formed under the primary myotube basement membrane and once they mature, they detach from the primary and form their own basement membrane (Kelly and Zacks, 1969; Ross et al., 1987; Duxson and Usson, 1989). We thus propose that the formation of primary myotubes does not depend on the interaction with a laminin-containing basement.

Assembly of the laminin matrix during fetal myogenesis: a surprisingly complex crosstalk involving multiple actors

During fetal myogenesis, Pax7-positive cells become localized under the myofiber basement membrane (containing laminin isoforms 211, 411 and 511) at around E16.5 (Patton et al., 1997; Kassar-Duchossoy et al., 2005; Tajbakhsh, 2009; Nunes et al., 2017). Our *in situ* hybridization data indicate that myofibers build their own laminin matrix during the early stages of fetal myogenesis. α4-laminins are the exception as *Lama4* is not expressed within the muscle masses at the beginning of secondary myogenesis, even though it is assembled around blood vessels and some myofibers. We suggest that in a first instance, blood vessels might provide laminin 411 to the myofiber basement membrane (Yousif et al., 2013), but during later stages of fetal myogenesis, fetal myoblasts start expressing *Lama4* (Biressi et al., 2007). We further demonstrate that Pax7-positive cells also contribute to the assembly of laminins. In fact, we found that mononucleated cells appear to be a major source of *de novo* laminins during late fetal myogenesis. Consistent with this hypothesis, secondary myoblasts express high levels of *Itga7* and laminin genes such as *Lama4*, *Lama5*, *Lamb1* and *Lamc1* (Biressi et al., 2007).

Strikingly, our results also revealed that not all Pax7-positive cells at E14.5 produce laminins. It is currently unclear if laminin synthesis in muscle stem cells starts in a subset of Pax7-positive cells but then extends to all such cells during later stages of fetal myogenesis, or whether laminin synthesis is a characteristic of a particular subset of Pax7-positive cells. Indeed, muscle stem cells are a heterogeneous population, which express different levels of *Pax7* and many transiently activate *Myf5* transcription without compromising their stem cell identity (Kuang et al., 2007; Rocheteau et al., 2012). In fact, only 10% of Pax7-positive cells never expressed *Myf5* at some point of their lives (Kuang et al., 2007). Further studies are required to determine whether laminin production varies between different muscle stem cell populations and/or between different stages of fetal

myogenesis. In either case it is clear that laminin assembly within the muscle masses involves several isoforms and multiple cell types.

Conclusions

Our study described the laminin expression dynamics throughout myogenesis and revealed that muscle stem cells, differentiated myocytes and myotubes produce several different laminin isoforms and appear to collaborate to build their laminin matrices through both paracrine and autocrine processes. Thus, the building of a laminin matrix during skeletal muscle development is surprisingly complex, which highlights the need for further studies aimed at analyzing the specific contribution of each actor not only during development, but also during muscle regeneration and disease.

Acknowledgments

We thank Jeff Miner for generously sharing his anti-α5, anti-α4 and anti-β2 laminin antibodies and Shahragim Tajbakhsh and Meryem Baghdadi for kindly providing the *Myf5*^{Cre}-NICD fetuses. The MF20 and Pax7 antibodies were developed by D.A. Fischman and A. Kawakami, respectively, and were obtained from the Developmental Studies Hybridoma Bank, developed under the auspices of the NICHD and maintained by The University of Iowa, Department of Biology, Iowa City, IA52242, USA. This work was supported by Fundação para a Ciência e a Tecnologia (FCT, Portugal) project PTDC/SAU-BID/120130/2010 and Association Française contre les Myopathies (AFM) Téléthon contract nº 19959. A.M.N., A.B.G and M.D. were supported by FCT scholarships SFRH/BD/86985/2012, SFRH/BD/90827/2012 and SFRH/BPD/65370/2009.

References

Anderson, C., Thorsteinsdóttir, S. and Borycki, A. (2009). Sonic hedgehog-dependent synthesis of laminin α1 controls basement membrane assembly in the myotome. *Development* **136**, 3495-3504.

Aumailley, M., Pesch, M., Tunggal, L., Gaill, F. and Fässler, R. (2000). Altered synthesis of laminin 1 and absence of basement membrane component deposition in β1 integrin-deficient embryoid bodies. *J. Cell Sci.* **113** 259-268

Aumailley, M., Bruckner-Tuderman, L., Carter, W.G., Deutzmann, R., Edgar, D., Ekblom, P., Engel, J., Engvall, E., Hohenester, E., Jones, J. C. R. et al. (2005). A simplified laminin nomenclature. *Matrix Biol.* **24**, 326–332.

Bajanca, F., Luz, M., Duxson, M. J. and Thorsteinsdóttir, S. (2004). Integrins in the mouse myotome: developmental changes and differences between the epaxial and hypaxial lineage. *Dev. Dynam.* **231** 402-415.

Bajanca, F., Luz, M., Raymond, K., Martins, G. G., Sonnenberg, A., Tajbakhsh, S., Buckingham, M. and Thorsteinsdóttir, S. (2006). Integrin α6β1-laminin interactions regulate early myotome formation in the mouse embryo. *Development* **133** 1635-1644.

Biressi, S., Molinaro, M. and Cossu, G. (2007). Cellular heterogeneity during vertebrate skeletal muscle development. *Dev. Biol.* **308**, 281-293.

Ben-Yair, R. and Kalcheim, C. (2005). Lineage analysis of the avian dermomyotome sheet reveals the existence of single cells with both dermal and muscle progenitor fates. *Development* **132**, 689–701.

Buckingham, M. (2006). Myogenic progenitor cells and skeletal myogenesis in vertebrates. *Curr. Opin. Genet. Dev.* **16** 525-532.

Buckingham, M. and Rigby, P. W. J. (2014). Gene regulatory networks and transcriptional mechanisms that control myogenesis. *Dev. Cell* **28**, 225-238.

Cachaço, A. S., Pereira, C. S., Pardal, R. G., Bajanca, F. and Thorsteinsdóttir, S. (2005). Integrin repertoire on myogenic cells changes during the course of primary myogenesis in the mouse. *Dev. Dynam.* **232** 1068-1078.

Cao, X., Pfaff, S. L. and Gage, F. H. (2007). A functional study of miR-124 in the developing neural tube. *Genes Dev.* **21,** 531-6.

Chen, X. and Li, Y. (2009). Role of matrix metalloproteinases in skeletal muscle: migration, differentiation, regeneration and fibrosis. *Cell Adh. Migr.* **3**, 337-341.

Chen, W., Harbeck, M., Zhang, W. and Jacobson, J. R. (2013). MicroRNA regulation of integrins. *Transl. Res.* **162**, 133-43.

Copp, A. J., Carvalho, R., Wallace, A., Sorokin, L., Sasaki, T., Greene, N. D. and Ybot-Gonzalez, P. (2011). Regional differences in the expression of laminin isoforms during mouse neural tube development. *Matrix Biol.* **30** 301-309.

Deries, M., Schweitzer, R. and Duxson, M. J. (2010). Developmental fate of the mammalian myotome. *Dev. Dynam.* **239** 2898-2910.

Deries, M., Gonçalves, A. B., Vaz, R., Martins, G. G., Rodrigues, G. and Thorsteinsdóttir, S. (2012). Extracellular matrix remodelling accompanies axial muscle development and morphogenesis in the mouse. *Dev. Dynam.* **241**, 350-364.

Dong, S., Landfair, J., Balasubramani, M., Bier, M.E., Cole, G. and Halfter, W. (2002). Expression of basal lamina protein mRNAs in the early embryonic chick eye. *J. Comp. Neurol.* **447**, 261-273.

Duxson, M. J. and Usson, Y. (1989). Cellular insertion of primary and secondary myotubes in embryonic rat muscles. *Development* **107**, 243-251.

Gomes De Almeida, P. G., Pinheiro, G. G., Nunes, A. M., Gonçalves, A. B. and Thorsteinsdóttir, S. (2016). Fibronectin assembly during early embryo development: A versatile communication system between cells and tissues. *Dev. Dyn.* **245**, 520-535.

Gros, J., Scaal, M. and Marcelle, C. (2004). A two-step mechanism for myotome formation in chick. *Dev. Cell* **6**, 875-882.

Gros, J., Manceau, M., Thome, V. and Marcelle, C. (2005). A common somitic origin for embryonic muscle progenitors and satellite cells. *Nature* **435**, 954–958.

Harris, A. J., Duxson, M. J., Fitzsimons, R. B. and Rieger, F. (1989). Myonuclear birthdates distinguish the origins of primary and secondary myotubes in embryonic mammalian skeletal muscles. *Development* **107**, 771-784.

Hollway, G. and Currie, P. (2005). Vertebrate myotome development. *Birth Defects Res. C. Embryo Today* **75**, 172-179.

Horak, M., Novak, J. and Bienertova-Vasku, J. (2016). Muscle-specific microRNAs in skeletal muscle development. *Dev. Biol.* **410**, 1-13.

Kassar-Duchossoy, L., Giacone, E., Gayraud-Morel, B., Jory, A., Gomès, D. and Tajbakhsh, S. (2005). Pax3/Pax7 mark a novel population of primitive myogenic cells during development. *Gen. Dev.* **19**, 1426–1431.

Kelly, A. M. and Zacks, S. I. (1969). The histogenesis of rat intercostal muscle. *J. Cell Biol.* **42**, 135-153.

Keely, P. J., Wu, J.E and Santoro, S. A. (1995). The spatial and temporal expression of the α2βl integrin and its ligands, collagen I, collagen IV, and laminin, suggest important roles in mouse mammary morphogenesis. *Differentiation* **59**, 1-13.

Kikkawa, Y., Hozumi, K., Katagiri, F., Nomizu, M., Kleinman, H. K. and Koblinski, J. E. (2013). Laminin-111-derived peptides and cancer. *Cell Adh. Migr.* **7**, 150-159.

Koshikawa, N., Giannelli, G., Cirulli, V., Miyazaki, K. and Quaranta, V. (2000). Role of cell surface metalloprotease MT1-MMP in epithelial cell migration over laminin-5. *J. Cell Biol.* **148**, 615-624.

Kaufmann, M. H. (1992). *The atlas of mouse development*. Cambridge, United States: Academic Press.

Kuang, S., Kuroda, K., Le Grand, F. and Rudnicki, M. A. (2007). Asymmetric self-renewal and commitment of satellite stem cells in muscle. *Cell* **129**, 999-1010.

Kumagai, C., Kadowaki, T. and Kitagawa, Y. (1997). Disulfide-bonding between drosophila laminin beta and gamma chains is essential for alpha chain to form alpha beta and gamma trimer. *FEBS Lett.* **412**, 211-206.

Lee, L. K., Pollock, A.S. and Lovett, D. H. (1993). Asymmetric origins of the mature glomerular basement membrane. *J. Cell Physiol.* **157**, 169-177.

Lu, P., Takai, K., Weaver, V.M. and Werb, Z. (2011). Extracellular matrix degradation and remodeling in development and disease. *Cold Spring Harb Perspect Biol.* **3**, a005058.

Mourikis, P., Gopalakrishnan, S., Sambasivan, R. and Tajbakhsh, S. (2012). Cell-autonomous Notch activity maintains the temporal specification potential of skeletal muscle stem cells. *Development* **139**, 4536–4548.

Nunes A. M., Wuebbles R. D., Sarathy A., Fontelonga T. M., Deries M., Burkin, D. J. & Thorsteinsdóttir, S. (2017). Impaired fetal muscle development and JAK-STAT activation mark disease onset and progression in a mouse model for merosin-deficient congenital muscular dystrophy. *Hum. Mol. Genet.* **26**, 2018–2033.

Ontell, M. and Kozeka, K. (1984). Organogenesis of the mouse extensor digitorum logus muscle: a quantitative study. *Am. J. Anat.* **171**,149-61.

Ohtake, Y., Tojo, H. and Seiki, M. (2006). Multifunctional roles of MT1-MMP in myofiber formation and morphostatic maintenance of skeletal muscle. *J. Cell Sci.* **119**, 3822-3832.

Patton, B. L., Miner, J.H., Chiu, A.Y. and Sanes, J. R. (1997). Distribution and function of laminins in the neuromuscular system of developing, adult, and mutant mice. *J. Cell Biol.* **139**, 1507-1521.

Paulsson, M. (1994). Biosynthesis, tissue distribution and isolation of laminins. In *The Laminins* (ed. P. Ekblom and R. Timpl), pp.1–26. Amsterdam: Harwood Academic Publishers.

Placoná Diniz, G. and Wang, D. (2016). Regulation of skeletal muscle by microRNAs. *Compr. Physiol.* **6**, 1279-1294.

Relaix, F., Rocancourt, D., Mansouri, A. and Buckingham, M. (2005). A Pax3/Pax7-dependent population of skeletal muscle progenitor cells. *Nature* **435**, 948-953.

Ross, J. J., Duxson, M. J. and Harris, A. J. (1987). Formation of primary and secondary myotubes in rat lumbrical muscles. *Development* **100**, 383-394.

Snyman, C. and Niesler, C. U. (2015). MMP-14 in skeletal muscle repair. *J Muscle Res Cell Motil.* **36**, 215-225.

Tajbakhsh, S. (2009). Skeletal muscle stem cells in developmental versus regenerative myogenesis. *J. Intern. Med.* **266**, 372–389.

Thorsteinsdóttir, S., Deries, M., Cachaço, A.S. and Bajanca, F. (2011). The extracellular matrix dimension of skeletal muscle development. *Dev. Biol.* **354**, 191-207.

Vachon, P. H., Xu, H., Liu, L., Loechel, F., Hayashi, Y., Arahata, K., Reed, J. C., Wewer, U. M. and Engvall, E. (1997). Integrins (α7β1) in muscle function and survival. Disrupted expression in merosin-deficient congenital muscular dystrophy. *J. Clin. Invest.* **100**, 1870-81.

Venters, S., Thorsteinsdóttir, S. and Duxson, M. J. (1999). Early development of the myotome in the mouse. *Dev. Dynam.* **216**, 219-232.

Yousif, L. F., Di Russo, J. and Sorokin, L. (2013). Laminin isoforms in endothelial and perivascular basement membranes. *Cell Adh. Migr.* **7**, 101-110.

Yurchenco, P. D., Quan, Y., Colognato, H., Mathus, T., Harrison, D., Yamada, Y. and O'Rear, J. J. (1997). The alpha chain of laminin-1 is independently secreted and drives secretion of its beta- and gamma- chain partners. *Proc. Natl. Acad. Sci.* **94**, 10189-10194.

Yurchenco, P. D. (2015). Integrating activities of laminins that drive basement membrane assembly and function. *Curr. Top. Membr*. **76**, 1-30.

CHAPTER 4

Behind the curtain of muscle development:

techniques to unveil the role of laminin 211 during

fetal muscle development

Behind the curtain of muscle development: techniques to unveil the role of laminin 211 during fetal muscle development

Andreia M. Nunes[1,2], Rebecca Evans[2], Marianne Deries[1], Dean J. Burkin[2] and Sólveig Thorsteinsdóttir[1,3]

[1]Centro de Ecologia, Evolução e Alterações Ambientais, Faculdade de Ciências, Universidade de Lisboa, 1749-016 Lisbon, Portugal; [2]Center for Molecular Medicine, University of Nevada School of Medicine, Reno, NV 89557, USA; [3]Instituto Gulbenkian de Ciência, 2780-156 Oeiras, Portugal

Contribution by A.M.N. to this chapter:

	Fig. 1	**Fig. 2**	**Writing**
Design and concept	III	III	III
Execution	III	III	
Analysis and interpretation	III	III	

Legend:
n.a.- non-applicable
O- no intervention
I- minor contribution
II- moderate contribution
III- major contribution
Note: Items with major contribution by A.M.N. does not exclude major contributions from other authors.

Contribution by the other authors:

Design and concept: R.E., M.D., D.J.B. and S.T.; Execution: R.E.; Analysis and Interpretation: M.D., D.J.B. and S.T.; Writing: M.D. and S.T.

Behind the curtain of muscle development: techniques to unveil the role of laminin 211 during fetal muscle development

Andreia M. Nunes[1,2], Rebecca Evans[2], Marianne Deries[1], Dean J. Burkin[2] and Sólveig Thorsteinsdóttir[1,3]

[1]Centro de Ecologia, Evolução e Alterações Ambientais, Faculdade de Ciências, Universidade de Lisboa, 1749-016 Lisbon, Portugal; [2]Center for Molecular Medicine, University of Nevada School of Medicine, Reno, NV 89557, USA; [3]Instituto Gulbenkian de Ciência, 2780-156 Oeiras, Portugal

Abstract

Here we describe two techniques set up to study the fetal muscle defects in the laminin α2-deficient *dy^{W}* mouse model. First, microexplant cultures of wildtype fetal muscles were performed with the objective of developing a protocol to compare the behavior of muscle cells from wildtype and *dy^{W}* muscles *in vitro*. Our preliminary results identified some difficulties with this method: they showed that Pax7-positive cells are not maintained in these cultures and that most cells in the outgrowths appear to be fibroblasts. Nevertheless, this technique can be used to assess the capacity of microexplants to generate Myf5- and MyoD-positive myoblasts. Second, we performed *in utero* injections of laminin 111 with the aim of being able to analyze whether delivery of this laminin isoform, which is very similar to laminin 211, can rescue the phenotype of *dy^{W}* fetuses. Our results show that the surgery and injection protocols do not interfere with normal muscle development. We conclude that this is a promising method to study the role of laminins in fetal muscle development *in vivo*.

Key-words: Microexplant culture, *In utero* injections, Fetal myogenesis, Laminins

Introduction

In vitro cultures of primary myoblasts and myoblast cell lines such as C2C12 have been extensively performed to study myoblast behavior under different culture conditions. However, cell lines and even primary cell cultures do not have the same characteristics as cells within their *in vivo* environment and therefore, cell culture is often not the best way to study *in vivo* behavior. To study muscle development in conditions closer to *in vivo* mouse development, alternative *in vitro* techniques have been developed. For example, young mouse embryo explants (E10.5-E12.5) can be cultured on the top of a filter and grow normally for periods of 6 to 12 hours, allowing for the study of early muscle development (Bajanca et al., 2006; Gonçalves et al., 2016). However, the density and complexity of fetal tissues makes this technique unsuitable to study fetal myogenesis. A microexplant culture system to study fetal muscle development was used to isolate dystrophic *mdx* mouse myoblasts (Smith and Schofield, 1994). This technique involves extracting small muscle tissue samples from fetuses, placing them whole in culture and studying the outgrowth of myogenic cells (Smith and Schofield, 1994). This culture system was later used to generate proliferative myoblasts and study their behavior *in vitro* (Merrick et al., 2007; Merrick et al., 2009; Merrick et al., 2010).

Albeit the important contribution of *in vitro* and *ex vivo* techniques, the fact is that the most reliable way to study any biological process, including muscle development, are *in vivo* techniques. Technically challenging *in vivo* techniques such as *in utero* intracardial embryonic injections (Domínguez-Bendala et al., 2012), *ex vivo* perfusion of mouse placenta (Goeden and Bonnin, 2012) and *in utero* transplantation of hematopoietic cells into fetuses (Nijagal et al., 2011) have been developed and allow for the experimental manipulation of the *in vivo* environment. These are thus promising methods to study fetal muscle development.

We have recently studied muscle development *in utero* in laminin α2-deficient mice (the dy^W mouse; Kuang et al., 1998; Kuang et al., 1999), which display muscle weakness at birth and develop a muscular dystrophy due to the absence of laminin 211. We found that these mice demonstrate an impairment in the growth of fetal muscles, which correlates with an overactivation of STAT3 signaling as well as misregulation of Myostatin signaling (Nunes et al., 2017). Intramuscular and intraperitoneal injections of laminin 111, a laminin isoform that is closely related to laminin 211, has been shown to significantly improve the phenotype and survival of dy^W mice when delivered at 5 weeks of age. Determining whether delivery of laminin 111 during fetal development is able to rescue the fetal myogenesis defects observed previously (Nunes et al., 2017) would provide a valuable assay for the study of this disease in the mouse.

Here we set up two different techniques to study the role of laminin 211 during fetal muscle development, namely the microexplant culture technique and *in utero* injections of laminin 111. Our data reveals that our microexplant culture protocol does not support the maintenance of Pax7-positive cell population, but that it is a potentially useful assay to assess the ability of microexplants to generate myoblast. Our results regarding the *in utero* injections of laminin 111 demonstrate the potential suitability of this method to study the effect of exogenous laminins on fetal myogenesis in dy^W mice.

Materials and Methods

Mice and genotyping

C57BL/6J mice for the microexplant culture experiments were obtained from the Instituto Gulbenkian Ciência animal facility (Oeiras, Portugal).

dy^W mice (gift from Eva Engvall via Paul Martin; The Ohio State University, Columbus, OH, USA) are *Lama2* knock out mice which in homozygosity produce small

amounts of a truncated laminin α2 protein (Kuang et al., 1998; Kuang et al., 1999; Guo et al., 2003). Heterozygous *dy*^{W} mice were crossed to obtain homozygous *dy*$^{W-/-}$ mutants and wildtype (WT) controls for *in utero* laminin 111 injections.

The day of the vaginal plug was designated embryonic day (E) 0.5 and embryos were staged as in Kaufmann (1992). Anesthetized pregnant females were sacrificed by cervical dislocation.

Fetuses from heterozygous *dy*^{W} crossings were genotyped with the following primers: 5' ACTGCCCTTTCTCACCCACCCTT 3', 5' GTTGATGCGCTTGGGACTG 3' and 5' GTCGACGACGACAGTACTGGCCTCAG 3'.

All procedures involving mice were performed under two approved protocols: 3/2016 from the Animal Welfare Body of the Faculty of Sciences, University of Lisbon and 000404 from the Institutional Animal Care and Use Committee of the University of Nevada.

Microexplant culture

The microexplant technique was performed as described previously with minor modifications (Merrick et al., 2010). Briefly, E17.5 and E18.5 fetuses were collected in cold phosphate buffered saline (PBS) with Ca^{2+} and Mg^{2+} and transferred into primary explant culture medium (PECM) as soon as the fetuses were removed from the uterus (PECM: DMEM:F12 medium supplemented with 20% fetal bovine serum (FBS), 2 mM Glutamine and 100U/ml Penicillin/Streptomycin). E17.5 and E18.5 back muscles were isolated and further dissected into small cubes of 0.5 mm^3, termed microexplants. Microexplants were placed in groups of three in a well of a 12-well plate on top of a 0.1% gelatin in PBS-coated coverslip, and then cultured in PECM for 8 days. From the fourth day onwards, 330 µl of medium per well was replaced with the same amount of fresh PECM medium. The

microexplant outgrowths were processed for immunofluorescence on day 8. All quantifications were performed at day 8.

Immunofluorescence

Immunofluorescence on coverslips was performed as described previously (Vaz et al., 2012). Briefly, cells were washed twice in PBS with Ca^{2+} and Mg^{2+}, fixed in 1% paraformaldehyde in PBS for 10 minutes at room temperature and then permeabilized in 0.2% Triton X-100 in PBS for 5 minutes at room temperature. The coverslips were incubated in 2% BSA in PBS for 30 minutes at room temperature for background blocking and then incubated with primary antibodies for 1 hour at room temperature. The cells were washed three times 10 minutes with PBS, incubated with secondary antibodies for 45 minutes at room temperature, followed by washing in PBS. Nuclei were stained with 4', 6-Diamidino-2-Phenylindole, Dihydrochloride (DAPI). The following primary antibodies were used: anti-Pax7 (1:100; DSHB), anti-Myf5 (1:100; Santa Cruz Biotechnology, SC-302), anti-MyoD (1:100; Santa Cruz Biotechnology, SC-760) and anti-vimentin (1:100; DSHB, clone 40E-C). Secondary antibodies were: $F(ab')_2$-goat anti-Mouse IgG (H+L) cross-adsorbed secondary antibody, Alexa fluor 488 (1:1000; Molecular Probes), $F(ab')_2$-goat anti-rabbit IgG (H+L) secondary antibody, Alexa Fluor 568 conjugate (1:1000; Molecular Probes) and $F(ab')_2$-Goat anti-Mouse IgG (H+L) Cross-Adsorbed Secondary Antibody, Alexa Fluor 568.

Immunofluorescence on cryosections was performed essentially as in Nunes et al. (2017). Briefly, fetuses were fixed in 2% paraformaldehyde (PFA) in 0.12M phosphate buffer (PB) for 2 days at 4ºC. Cryosections were incubated with 0.2% Triton-X100 in PBS for 20 minutes at room temperature and treated for antigen retrieval by immersing sections in Tris-EDTA (10 mM Tris base, 1 mM EDTA, 0.05% Tween 20) buffer, pH 9.0 at 95ºC for 20 minutes. Sections were then processed with the Mouse-On-Mouse (MOM) kit

(Vector Laboratories). We used primary antibodies anti-Pax7 (1:50; DSHB) and anti-myosin heavy chain (MHC) (1:100; clone MF20 DSHB). DNA was always stained with 4,6-Diamidino-2-phenylindole (DAPI, 5µg/ml, Sigma).

Image analysis and quantifications

Cell quantifications and the proportion of Myf5 and MyoD-positive cells, with relation to the total number of cells, for microexplant outgrowth were performed in 7-13 images of 846x645 μm^2 using the plugin Cell Counter in Fiji version 1.49i.

Transverse sections from fetuses processed for immunohistochemistry were used for muscle cross-sectional area measurements and quantification of total number of Pax7-positive cells (Nunes et al., 2017). Overlapping confocal images were stitched to include three epaxial muscles (transversospinalis, longissimus and iliocostalis) into a composite image using the Fiji plugin Pairwise Stitching (Preibisch et al., 2009). Quantifications were performed in the three aforementioned epaxial muscle groups at forelimb level in 3-5 sections per staining, using the Fiji plugin Cell Counter (http://fiji.sc/Cell_Counter).

Statistical analysis

Student's *t-test* was used to test for differences in the total number of cells and proportion of Myf5 and MyoD-positive cells between the central region and periphery of the outgrowth. The data for the proportion of Myf5 and MyoD-positive cells was transformed with the arcsine square root function before the *t-test* was applied. We also performed a Student's *t-test* to evaluate differences in muscle cross sectional area and total number Pax7-positive cells in non-injected and laminin 111 injected fetuses.

In utero injections of laminin 111

We performed *in utero* injections as described previously (Nijagal et al.,2011). Fetuses were injected with laminin 111 at E15.5 (see schematic representation in Fig. 2A-C) and collected at E18.5. We made a 1-2 cm incision in the lower abdomen of the pregnant female to expose uterine horns, one at a time. The exposed uterine horn was placed onto cotton swabs and each fetus was injected individually with 5 µl laminin 111 (Invitrogen) (10µg/g) through an intraperitoneal injection. Laminin 111 was previously labeled with DyLight Alexa 488 (Thermo Fisher Scientific) and the delivery of laminin 111 into the peritoneal cavity was confirmed with the IVIS Lumina III In Vivo Imaging System (Perkin Elmer) (data not shown). After the injection of all fetuses, the first uterine horn was placed back into the abdominal cavity and the second uterine horn was exposed to inject the remaining fetuses. During all surgery procedures, fetuses were irrigated with sterile PBS by injecting some PBS on top of each fetus. Injections were made using pulled glass capillaries. Post-surgery care was performed with analgesic treatment. Buprenorphine (0.5 mg/kg) was administered through a sub-cutaneous injection once a day during the 2 days following surgery. This protocol was approved by the University of Nevada (protocol 2014-00404). Controls were same stage fetuses (non-injected fetuses) from a different non-operated female.

Results and Discussion

Microexplant cultures

The microexplant culture system enables the culture of muscle pieces and the study of the developmental capacity of microexplant under different defined conditions through the analysis of outgrowths of mononucleated muscle cells (Merrick et al., 2010).

Therefore, this system could potentially provide an *in vitro* framework to study the *in vitro* behavior of these mononucleated muscle cells from WT versus dy^W muscles.

Our first goal during this work was to test the suitability of microexplant cultures to study fetal muscle development using wildtype fetal muscles. We cultured microexplants collected from C57BL/6J fetuses at E17.5 (Fig. 1A) and E18.5 (Fig. 1B) in primary explant culture medium (PECM) for 8 days. Analysis of E17.5 and E18.5 microexplants at day 8 revealed that they produce outgrowths of equivalent area, suggesting similar outgrowth capacity in culture between explants of these two stages (Fig. 1A and B). We then performed a detailed analysis of E18.5 microexplant outgrowth and verified that the outgrowth has a different cellular organization in the vicinity of the microexplant (central outgrowth) (Fig. 1E, F, G, G', H and H'), when compared to the periphery of the outgrowth (peripheral outgrowth) (Fig. 1I, I', J and J'). Quantifications of total nuclei revealed that, as expected for this type of experiment, cell density is significantly higher in the central outgrowth, when compared to the peripheral outgrowth (*p=0.038*; Fig. 1C).

We then characterized the cell population present in the microexplant outgrowths through immunostaining for Pax7, a marker for muscle stem cells, and the myogenic regulatory factors Myf5 and MyoD, which are markers for committed myoblasts (Buckingham and Rigby, 2014). Immunostaining for Pax7 revealed a complete absence of Pax7-positive cell in the microexplant in both the central (Fig. 1E and E'; compare with negative control in Fig. 1F and F') and peripheral outgrowth (data not shown), indicating that all muscle stem cells differentiated during the culture. Immunostaining of the outgrowths for Myf5 demonstrates that Myf5-positive cells are present in the central (Fig. 1G and G') and in the peripheral (Fig. 1I and I') outgrowth, and that the proportion of Myf5-positive cells is similar in both outgrowths (Fig. 1K). However, the proportion of Myf5-positive cells in the total outgrowth population is very low, only on average 5.6% of

the total number of cells in the peripheral outgrowth and 6.6% in the central outgrowth (Fig. 1K). Interestingly, immunostaining for MyoD indicates that MyoD-positive cells are more numerous in the outgrowths than Myf5-positive cells (Fig. 1H, H', J, and J'). Indeed, on average 28.4 % of the total number of cells in the central outgrowth are MyoD-positive, while only 10.6% are MyoD-positive in the peripheral outgrowth (*p=0.045;* Fig. 1L), suggesting that myogenic cells are more common in the central area of the microexplant outgrowths than in the periphery. Since the central outgrowth is constituted by cells that were maintained for longer in the 3D environment of the microexplant and exited the explant more recently, we propose that these cells are the ones that best represent the myogenic population of the microexplants.

To identify the rest of the population of the cultured microexplant, the presence of fully differentiated myogenic cells was assessed by immunostaining for myosin heavy chain, a marker of differentiated muscle cells. However, no myosin-positive cells were present in the microexplant outgrowths (data not shown) demonstrating that the Myf5/MyoD-positive cells do not terminally differentiate under our culture conditions. Since fibroblast are a common cell type within muscle masses, we next used immunostaining for vimentin, a marker for fibroblasts and fibroblast-like cells, and found that vimentin-positive cells were widespread in the central (Fig. 1D) and peripheral (data now shown) outgrowths. Fibroblasts are known to display a high proliferation capacity in culture in the presence of serum and thus might supplant the less proliferative myogenic cells under our culture conditions.

Together, our data shows that microexplants from fetal muscle generate outgrowths containing myogenic cells, most of which are Myf5- and/or MyoD-positive, but, since the culture medium was supplemented with serum, no myosin-positive myotubes were formed. A problem encountered in our cultures was that growth of myogenic cells is supplanted by fibroblasts, much more so than described previously

(Smith and Schofield, 1994; Merrick et al., 2010). The reason for this is unclear. It is possible that the dissection of deep back muscles brings more connective tissue into the culture than the dissection of limb muscles (Smith and Schofield, 1994; Merrick et al., 2010). Nevertheless, this system may be useful to study the capacity of muscle microexplants from laminin α2-deficient dy^{W} fetuses to generate Myf5-, MyoD- or Myogenin-positive cells when compared to wild-type. Furthermore, it could be used to test the effect of activating or blocking candidate pathways involved in the dy^{W} phenotype (e.g. Nunes et al., 2017) on myogenesis *in vitro*.

An alternative method to the microexplant cultures is the isolation of pure Pax7-positive cell populations and the direct study of these cells. Successful isolation of fetal Pax7-positive cells by fluorescence-activated cell sorting (FACs) has been performed (Tierney et al., 2016). These could be used to perform a transcriptome characterization of $dy^{W-/-}$ and WT Pax7-positive cells or these cells could be plated in culture to assay parameters such as proliferation and differentiation potential and to characterize their behavior in culture, using defined conditions and/or with pharmacological targeting of candidate signaling pathways. The FACS technique is used extensively to study pure cell populations and has provided important insights into the characteristics of these populations and can thus be useful to complement the microexplant approach. Albeit the advantages of studying isolated cell populations, however, caution should be taken with data analysis and interpretation as the cell isolation requires the digestion of muscle tissue, which induces muscle injury, ECM degradation and muscle stem cell activation.

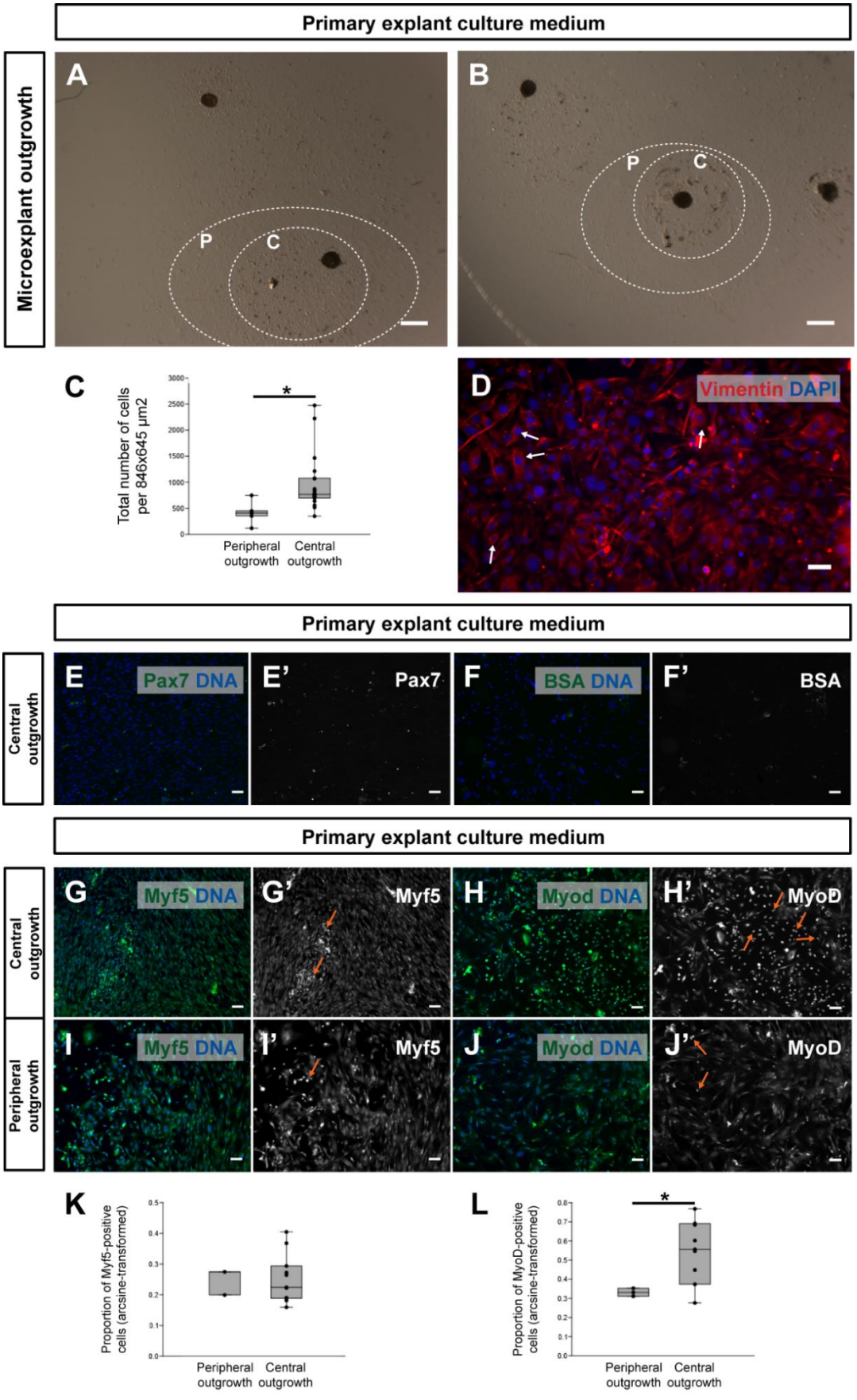

Figure 1- Microexplant cultures of fetal back muscles. (Continues next page)

(Continued from previous page) (**A-B**) Bright field images of E17.5 (A) and E18.5 (B) microexplant outgrowth cultured in primary explant culture medium reveal very similar outgrowth patterns between these stages. (**C**) Graph representing the total number of cells in the microexplant outgrowth reveal significant differences between the number of cells of the central and the peripheral outgrowth (*p=0.038*). (**D**) Immunostaining for Vimentin (red) with DNA (blue) highlights the presence of several Vimentin-positive cells, probably fibroblasts, in the central outgrowth. (**E-J'**) Immunostaining for Pax7 (E; and negative control with BSA instead of antibody, F), Myf5 (G,I) and MyoD (H,J) all in green and combined with DNA staining (blue). They are all displayed in grayscale as well (E',F',G',H',I',J'). (**E-F'**) Immunostaining for Pax7 (E,E') in the central outgrowth reveals the absence of Pax7-positive cells, when compared to negative control with bovine serum albumin (BSA) (F and F'). (**G,G',I,I'**) Immunostaining for Myf5 in the central (G,G') and peripheral (I,I') outgrowth shows that Myf5-positive cells are present in low numbers in the entire outgrowth (G',I', orange arrows). (**H, H', J, J'**) Immunostaining for MyoD in the central (H and H') and peripheral (J and J') outgrowth reveals that MyoD-positive cells are more frequent in the central outgrowth (H', orange arrows) than in the peripheral outgrowth (J', orange arrows). (**K**) Graph showing the proportion of Myf5-positive cells (Y axis shows values obtained after arcsine square root-transformation of proportions) in central and peripheral outgrowths. The proportion of Myf5-positive cells is very low in the entire outgrowth, but the proportion is not different in the central and peripheral outgrowth. (**L**) Graph depicting the proportion of MyoD-positive cells (after arcsine square root-transformation of proportions) in the central and peripheral outgrowths. The proportion of MyoD-positive cells is higher in the central outgrowth population compared to the peripheral outgrowth (*p=0.045*). Scale: 500 µm (A and B) and 50 µm (D-J').

In utero injections of laminin 111

During adult *dy*^{W} muscle development, overexpression of laminin α1 and injection of laminin 111 (which is closely related to laminin 211; see Durbeej, 2010) was shown to provide a protective effect to *dy*$^{W-/-}$ muscle as weekly treatments improve different disease parameters such as the survival rate, muscle strength and regeneration capacity (Gawlik et al., 2004; Gawlik et al., 2010; Rooney et al., 2012; Van Ry et al., 2013). We postulate that laminin 111 might exert the same protective effect during fetal myogenesis if injected before disease onset *in utero*. Laminin 111 is not expressed in skeletal muscle during fetal stages (Patton et al., 1997; Nunes et al., 2017) and therefore, the presence of laminin 111 in the muscle after injection is a proof of injection efficacy. We labelled laminin with the DyLight Alexa 488 kit to assess for laminin 111 in the muscle after injection.

Two litters of E15.5 fetuses from heterozygous *dy*^{W} crossings were injected interperitoneally with laminin 111 (10µg/g) through the uterine horns and the gestation was allowed to proceed until E18.5. Thus, the laminin 111 was delivered before the period between E17.5 and E18.5, during which the *dy*$^{W-/-}$ muscles fail to grow at the WT rate (Nunes et al., 2017). The surgery procedure is schematically illustrated in Fig. 2A-C. Imaging though an IVIS imaging system allowed confirmation of the presence of laminin 111 in the abdominal cavity after injection (data not shown). We then harvested the

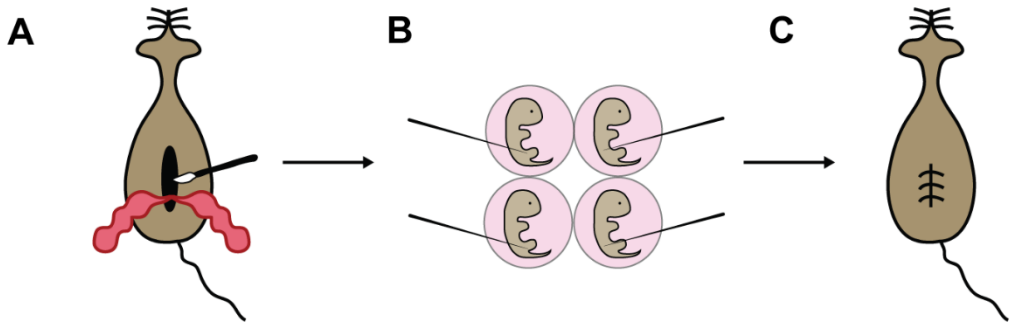

D **Muscle area of injected and non-injected E18.5 epaxial muscles**

	WT E18.5		*dy*$^{W-/-}$ E18.5	
	Non-injected	Injected	Non-injected	Injected
Fetus 1	702181,7	625679,4	422913,7	418398,5
Fetus 2	605702,9	599875,7	534006,8	627131,5
Fetus 3	546337,5		532591,7	
Fetus 4	569502,4		499165,8	
Fetus 5	612643,2			

E **Number of Pax7-positive cells of injected and non-injected E18.5 epaxial muscles**

	WT E18.5		*dy*$^{W-/-}$ E18.5	
	Non-injected	Injected	Non-injected	Injected
Fetus 1	645	566	508	304
Fetus 2	428,8		238,6667	141,3333
Fetus 3	520,25		274	
Fetus 4	439,6667		435,3333	
Fetus 5	474,3333		285	

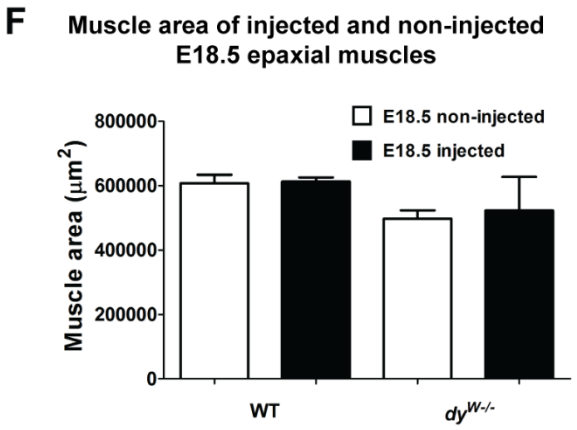

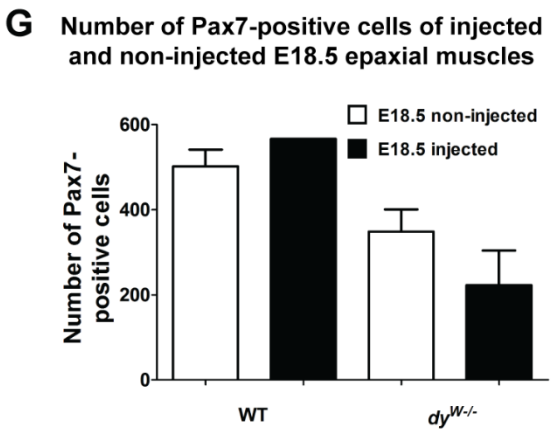

Figure 2- *In utero* injections of laminin 111 into E15.5 fetuses. (**A**-**C**) Schematic representation of the procedure for the *in utero* injections of laminin 111 depicting the abdominal incision to expose the uterine horns (A), intraperitoneal injection of laminin 111 into each fetus (B) and closure of the abdominal incision after the restitution of the uterine horns inside the abdominal cavity (C). (**D**-**G**) Quantifications of muscle area (D) and of Pax7-positive cells (E) and the corresponding graphs (F, G) in E18.5 non-injected and injected fetuses.

fetuses at E18.5. All fetuses survived and n=14 in 17 injected and n=13 in 14 non-injected fetuses, looked developmentally normal and were processed for cryostat sectioning. Quantification of muscle area revealed no significant differences between the injected (n=2) and non-injected (n=5) WT fetuses (Fig. 2D and F), demonstrating that the surgery protocol did not affect normal muscle growth. Of the two laminin 111-injected $dy^{W-/-}$ fetuses, one (fetus 2, Fig. 2D) displays an increased muscle area when compared to $dy^{W-/-}$ non-injected fetuses (n=4), while the other one is very similar to the $dy^{W-/-}$ non-injected fetuses (Fig. 2D) and to $dy^{W-/-}$ fetuses assayed in previous experiments (Nunes et al., 2017). Interestingly, the cross-sectional area of one of the laminin 111-injected $dy^{W-/-}$ fetuses (fetus 2) is within the range of the cross-sectional area of injected and non-injected WT fetuses (Fig. 2D).

We then determined the number of Pax7-positive cells in the injected and non-injected fetuses. No significant differences were found between injected and non-injected fetuses in either WT or $dy^{W-/-}$ muscles (Fig. 2E and G), suggesting that the normal number of Pax7-positive cells is formed during post-injection gestation. It is to be noted that the injected $dy^{W-/-}$ fetus (fetus 2), which displayed a close to normal muscle cross sectional area, presents lower numbers of Pax7-positive cells, when compared to $dy^{W-/-}$ injected and non-injected fetuses (Fig. 2E). The reason for this result is presently unclear. At this stage, more experiments are needed to draw conclusions on the potential beneficial effect of laminin 111 injection into $dy^{W-/-}$ fetuses. Nevertheless, our preliminary experiments demonstrate the feasibility of *in utero* injections as females recover well from surgery, normal fetal development occurs and myogenesis proceed post-injection.

Acknowledgments

We thank Gabriela Rodrigues for her expert advice regarding cell culture procedures. We also thank Jorge Palmeirim for help with the statistical analysis. This work was supported by Fundação para a Ciência e a Tecnologia (FCT, Portugal) (project PTDC/SAU-BID/120130/2010, SFRH/BD/86985/2012 scholarship to A.M.N and SFRH/BPD/65370/2009 scholarship to M.D., Association Française contre les Myopathies (AFM) Téléthon (contract nº 19959), CureCMD, Struggle Against Muscular Dystrophy (SAM), NIH/NIAMS (R01AR064338-01A1).

References

Bajanca, F., Luz, M., Raymond, K., Martins, G. G., Sonnenberg, A., Tajbakhsh, S., Buckingham, M. and Thorsteinsdóttir, S. (2006). Integrin α6β1-laminin interactions regulate early myotome formation in the mouse embryo. *Development* **133**, 1635-1644.

Buckingham, M. and Rigby, P. W. J. (2014). Gene regulatory networks and transcriptional mechanisms that control myogenesis. *Dev. Cell* **28**, 225-238.

Domínguez-Bendala, J., Álvarez-Cubela, S., Nieto, M., Vargas, N., Espino-Grosso, P., Sacher, V. Y., Pileggi, A., García, E., Ricordi, C., Inverardi, L. and Pastori, R. L. (2012). Intracardial embryonic delivery of developmental modifiers in utero. *Cold Spring Harb. Protoc.* **9**, 962-968.

Gawlik, K., Miyagoe-Suzuki, Y., Ekblom, P., Takeda, S. and Durbeej, M. (2004). Laminin α1 chain reduces muscular dystrophy in laminin α2 chain deficient mice. *Hum. Mol. Genet.* **13**, 1775–1784.

Gawlik, K. I., Kerlund, M. A., Carmignac, V., Elamaa, H. and Durbeej, M. (2010). Distinct roles for laminin globular domains in laminin α1 chain mediated rescue of murine laminin α2 chain deficiency. *PLoS ONE* **5**, e11549.

Goeden, N. and Bonnin, A. (2013). Ex vivo perfusion of mid-to-late-gestation mouse placenta for maternal-fetal interaction studies during pregnancy. *Nat. Protoc.* **8**, 66-74.

Gonçalves, A. B., Thorsteinsdóttir, S. and Deries, M. (2016). Rapid and simple method for in vivo ex utero development of mouse embryo explants. *Differentiation* **91**, 57-67.

Guo L. T., Zhang, X. U., Kuang, W., Xu, H., Liu, L. A., Vilquin, J. T., Miyagoe-Suzukic, Y., Takeda, S., Ruegg, M. A., Wewer, U. M. and Engvall, E. (2003). Laminin α2 deficiency and muscular dystrophy: genotype-phenotype correlation in mutant mice. *Neuromuscul. Disord*. **13**, 207–215.

Kaufmann, M. H. (1992). *The Atlas of Mouse Development*. Cambridge, United States: Academic Press.

Kuang, W., Xu, H., Vachon, P. H., Liu, L., Loechel, F., Wewer, U. M. and Engvall, E. (1998). Merosin-deficient congenital muscular dystrophy. Partial genetic correction in two mouse models. *J. Clin. Invest.* **102**, 844-352.

Kuang, W., Xu, H., Vilquin, J.T. and Engvall, E. (1999). Activation of the *lama2* gene in muscle regeneration: abortive regeneration in laminin α2-deficiency. *Lab. Invest.* **7**, 1601-1613.

Merrick, D., Ting, T., Stadler, L. K. J. and Smith J. (2007). A role for Insulin-like growth factor 2 in specification of the fast skeletal muscle fibre. *BMC Dev. Biol.* **7**, 1-16.

Merrick, D., Stadler, L. K. J., Larner, D. and Smith, J. (2009). Muscular dystrophy begins early in embryonic development deriving from stem cell loss and disrupted skeletal muscle formation. *Dis. Model. Mech.* **2**, 374-388.

Merrick, D., Chen, H., Larner, D. and Smith, J. (2010). Adult and embryonic skeletal muscle microexplant culture and isolation of skeletal muscle stem cells. *JoVE* **43**, 374-388.

Nijagal, A., Le, T., Wegorzewska, M. and MacKenzie, T. C. (2011). A mouse model of in utero transplantation. *JoVE* **47**, 1-4.

Nunes A. M., Wuebbles R. D., Sarathy A., Fontelonga T. M., Deries M., Burkin D. J. and Thorsteinsdóttir S. (2017). Impaired fetal muscle development and JAK-STAT activation mark disease onset and progression in a mouse model for merosin-deficient congenital muscular dystrophy. *Hum. Mol. Genet.* **26**, 2018–2033.

Patton, B. L., Miner, J. H., Chiu, A. Y. and Sanes, J. R. (1997). Distribution and function of laminins in the neuromuscular system of developing, adult, and mutant mice. *J. Cell Biol.* **139**, 1507-1521.

Preibisch, S., Saalfeld, S. and Tomancak, P. (2009). Globally optimal stitching of tiled 3D microscopic image acquisitions. *Bioinformatics* **25**, 1463-1465.

Rooney, J. E., Knapp, J. R., Hodges, B. L., Wuebbles, R. D. and Burkin D. J. (2012). Laminin-111 protein therapy reduces muscle pathology and improves viability of a mouse model of merosin-deficient congenital muscular dystrophy. *Am. J. Pathol.* **180**, 1593-1602.

Smith, J. and Schofield, P. N. (1994). The effects of fibroblast growth factors in long-term primary culture of dystrophic (mdx) mouse muscle myoblasts. *Exp. Cell. Res.* **210**, 86-93.

Tierney, M. T., Gromova, A., Sesillo, F. B., Sala, D., Spenle, C., Orend, G. and Sacco, A. (2016). Autonomous extracellular matrix remodeling controls a progressive adaptation in muscle stem cell regenerative capacity during development. *Cell Rep*. **14**, 1940–1952.

Van Ry, P. M., Minogue, P., Hodges, B. L. and Burkin, D. J. (2013). Laminin-111 improves muscle repair in a mouse model of merosin-deficient congenital muscular dystrophy. *Hum. Mol. Genet.* **23**, 383-396.

Vaz, R., Martins, G. G., Thorsteinsdóttir, S. and Rodrigues, G. (2012). Fibronectin promotes migration, alignment and fusion in an in vitro myoblast cell model. *Cell Tissue Res.* **348**, 569–578.

CHAPTER 5

Dynamics of laminin matrices during cardiac muscle development

Dynamics of laminin matrices during cardiac muscle development

Andreia M. Nunes[1], Inês Antunes[1], Ana C. Silva[2], Patrícia Ybot-Gonzalez[3], Marianne Deries[1], Perpétua Pinto-do-Ó[2] and Sólveig Thorsteinsdóttir[1,4]

[1]Centro de Ecologia, Evolução e Alterações Ambientais, Faculdade de Ciências, Universidade de Lisboa, 1749-016 Lisbon, Portugal; [2]Instituto de Investigação e Inovação em Saúde, 4200-135 Porto, Portugal; [3]Departamento de Pediatria, Hospital Infantil Virgen del Rocio, Sevilla, Spain; [4]Instituto Gulbenkian de Ciência, 2780-156 Oeiras, Portugal

Contribution by A.M.N. to this chapter:

	Fig.1	**Fig.2**	**Fig.3**	**Fig.4**	**Fig.5**	**Fig.6**	**Fig.7**	**Fig.8**	**Fig.9**	**Writing**
Design and concept	III	III	III	III	III	III	III	III	III	III
Execution	III	III	III	III	III	III	III	III	III	
Analysis and interpretation	III	III	III	III	III	III	III	III	n.a.	

Legend:
n.a.- non-applicable
O- no intervention
I- minor contribution
II- moderate contribution
III- major contribution
Note: Items with major contribution by A.M.N. does not exclude major contributions from other authors.

Contribution by the other authors:

Design and concept: M.D., P.P. and S.T.; Execution: I.A., A.C.S. and P.Y.; Analysis and Interpretation: M.D., P.P. and S.T.; Writing: M.D. and S.T.

Dynamics of laminin matrices during cardiac muscle development

Andreia M. Nunes[1], Inês Antunes[1], Ana C. Silva[2], Patrícia Ybot-Gonzalez[3], Marianne Deries[1], Perpétua Pinto-do-Ó[2] and Sólveig Thorsteinsdóttir[1,4]

[1]Centro de Ecologia, Evolução e Alterações Ambientais, Faculdade de Ciências, Universidade de Lisboa, 1749-016 Lisbon, Portugal; [2]Instituto de Investigação e Inovação em Saúde, 4200-135 Porto, Portugal; [3]Departamento de Pediatria, Hospital Infantil Virgen del Rocio, Sevilla, Spain; [4]Instituto Gulbenkian de Ciência, 2780-156 Oeiras, Portugal

Abstract

Laminins are major components of basement membranes, which line or surround numerous cell types, including all types of muscle cells. The laminin family is composed of 16 different isoforms. Up to 8 different isoforms are found during the development of skeletal muscle, but much less is known about what isoforms are present during cardiac muscle development and how they are distributed. Here we describe the dynamics of laminin gene expression and laminin isoform deposition during mouse cardiac development, focusing on the maturation of the different cardiac layers along cardiogenesis. A combination of laminins 111/121, 411/421 and 511/521 are present in the cardiac jelly, an extracellular matrix material present at early stages of heart tube development, but only laminin 521 persists in the endocardium-myocardium matrix in late fetal, postnatal and adult stages. The epicardium initially assembles laminins 111 and 511 in the subepicardial matrix, but once trabeculation is concluded, these laminins are gradually replaced by laminin 521. Laminin 211 assembly in the basement membrane of cardiomyocytes starts around E12.5 and by E14.5, laminin 511 also surrounds cardiomyocytes. These laminins are later replaced by laminins 221 and 521, which are maintained in cardiomyocyte basement membrane in the postnatal and adult cardiac

muscle. These data demonstrate that the cardiac laminin matrices are diverse and that their isoform composition changes during development of the heart.

Key-words: Laminins, Heart development, Cardiac jelly, Subepicardial matrix, Cardiomyocyte matrix

Introduction

Contracting cardiac muscle forms early in embryogenesis when the primitive heart tube is established. Cardiac development starts at E7.5 in the mouse when cardiac progenitors become specified to form two cardiogenic fields: the first and second heart field (Yang et al., 2002; Kirby and Waldo, 2007; Wu et al., 2008; Savolainen et al., 2009; Vincent and Buckingham, 2010; Kelly et al., 2014). The heart tube is formed around E8.0, once these cardiogenic fields are brought to the midline with the inward movement of the splanchnic mesoderm during the formation of the foregut pocket (Kirby and Waldo, 2007; Savolainen et al., 2009; Vincent and Buckingham, 2010; Kelly et al., 2014). The heart tube is constituted by two layers at this stage: the myocardium, which comprises the cardiomyocytes with contractile capacity; and the endocardium, that covers the internal wall of the myocardium. These two layers are separated by the cardiac jelly, a layer of extracellular matrix secreted by the myocardium (Kirby and Waldo, 2007; Savolainen et al., 2009). During subsequent stages, from E8.5 until E11.0, the proepicardial cells, which derive from the mesenchyme of the septum transversum, migrate to cover the heart while the heart loops into its final conformation, giving rise to the outermost (third) layer of the heart, the epicardium, (Kirby and Waldo, 2007; Zhou et al., 2008; Vincent and Buckingham, 2010).

The specification of the four heart chambers then starts around E10.5 (Christoffels et al., 2000), while the ventricular myocardium is remodeled into the compact zone and trabeculae (Savolainen et al., 2009; Samsa et al., 2013; Paige et al., 2015). The trabeculation process starts at E9.5 with the emergence of the first trabeculae and then proceeds with further trabeculae growth and maturation until E14.5 (Samsa et al., 2013). The contraction capacity of the myocardial wall resides in the dense compact zone, where the most proliferative cardiomyocytes contribute to the exponential growth of the ventricular wall (Sedmera and Thompson, 2011; Samsa et al., 2013; Paige et al., 2015).

Other developmental programs such as the development of the endocardial cushions, septa and the conduction system occurs simultaneously with chamber specification, thus allowing the proper coordination between electrical stimulation, contractility and blood flow through the different chambers (Kelly et al., 2014). During postnatal development, cardiomyocytes progressively lose their proliferation capacity which is accompanied by a loss in regeneration capacity (Porrello et al., 2011; Ikenishi et al., 2012; Sedmera and Thompson, 2011; Ponnusamy et al., 2016).

Cardiac extracellular matrices form early in cardiac development. Two decades ago, laminins were described in the mouse embryo and were shown to be present in the cardiac jelly and in the cardiomyocyte basement membrane (Little et al., 1989; Nakajima et al., 1997; Kim et al., 1999). Laminins, major components of basement membranes, are trimeric glycoproteins composed of an α, a β and a γ chain, codified by different genes (*Lama*, *Lamb* and *Lamc*). Combinations of different α, β and γ chains generate at least 16 different laminin isoforms (LeBleu et al., 2007; Durbeej, 2010; Yurchenco et al., 2015). The current nomenclature is based on the chain composition, e.g., laminin 111 is composed of α1, β1 and γ1 chains (Aumailley et al., 2005).

mRNA for laminin genes such as *Lama1*, *Lama4* and *Lamb1* are known to be present during fetal cardiac development in the mouse (Hirohata et al., 1997), while *Lama2* expression was detected in postnatal and adult stages (Hirohata et al., 1997). At E10.5, γ1, α1 and α5 are present in the cardiac jelly of atrium and ventricle, and during juvenile cardiac development (4 weeks of age), α2- and α5-laminins were shown to be assembled in the cardiomyocyte basement membrane, while α4-laminins were restricted to the blood vessel basement membrane (Miner et al., 1998; Wang et al., 2006). α5-laminins were shown to be present in the blood vessels as well (Wang et al., 2006). In fact, laminin α4 deficient mice display cardiomyopathy only during adulthood, around 36-40 weeks, suggesting that α5-laminins compensate at least partially for the absence of α4-

laminins (Wang et al., 2006). In *Lama5* null mice, the heart presents a reduction in size of the left ventricle (Miner et al., 1998). There are some reports of MDC1A (Merosin congenital muscular dystrophy type 1A) patients, having dysfunctional or absence of α2-laminins, developing cardiomyopathy (Carboni et al., 2011; Marques et al., 2014) and 30% of patients present left ventricular dysfunction (Gawlik and Durbeej, 2011).

Together, these studies suggest that laminins may play a role during cardiac development. However, a comprehensive and detailed analysis of the spatio-temporal assembly dynamics of the various laminin isoforms during heart development, on which functional studies can build, is still lacking.

Here laminin expression and assembly dynamics during cardiac muscle development were thoroughly studied. The data obtained allowed for the definition of specific spatio-temporal patterns of laminin matrices in the developing cardiac tissue. We demonstrate that laminins 111/121, 411/421 and 511/521 are initially assembled in the cardiac jelly, but in later stages, after cardiac jelly dissociation at E14.5, laminin 521 becomes the main laminin in the endocardium-myocardium basement membrane. We found that laminin 511 appears to be the major laminin in the subepicardial matrix in early stages of cardiac development, but laminin 511 is replaced by laminin 521 during later fetal cardiac development. Finally, we report that laminins 211 and 511 are assembled in the cardiomyocyte basement membrane during trabeculation stages, but these laminins are then replaced by laminin 221 and 521 at the end of fetal development. This cardiomyocyte laminin matrix then further develops into an intricated network during postnatal and adult stages.

Materials and Methods

Mice

Wild-type embryos (E8.5-E12.5), fetuses (E14.5-E17.5) and postnatal day 10 (P10) pups were obtained from crossings of outbred CD-1 mice (Harlan Interfauna Iberica). The day of the vaginal plug was designated embryonic day (E) 0.5 and embryos were staged as in Kaufman (Kaufmann, 1992). Anesthetized pregnant females were sacrificed by cervical dislocation. Adult hearts where retrieved from ~1 year old mice.

All procedures involving mice were performed under the approved protocol 3/2016 from the Animal Welfare Body of the Faculty of Sciences, University of Lisbon.

In situ hybridization

To determine the mRNA expression pattern of different laminin genes (*Lama1*, *Lama2*, *Lama4*, *Lama5*, *Lamb1*, *Lamb2*, *Lamc1*), E9.5 and E10.5 embryos were fixed in 4% paraformaldehyde in PBS (Phosphate Buffered Saline) for whole mount *in situ* hybridization as described previously (Copp et al., 2011). Briefly, embryos were hybridized overnight at 70°C and probe localization was detected with alkaline phosphatase-conjugated anti-dioxygenin antibodies and NBT/BCIP (Roche) as a substrate.

Immunofluorescence

Immunofluorescence on sections and whole mount immunofluorescence were performed as described previously (Gonçalves et al., 2016; Nunes et al., 2017). Adult hearts were fixed in a zinc fixative solution for 24 hours according to the method described previously (Beckstead, 1994) and processed for immunofluorescence on sections. The following primary antibodies were used: anti-myosin heavy chain (1:100; clone MF20

DSHB), anti-Laminin α1 (gift from Madeleine Durbeej), anti-Laminin α2 (1:100; clone 4H8-2 Sigma), anti-Laminin α4 (1:800; gift from Jeff Miner), anti-Laminin α5 (1:800; gift from Jeff Miner), anti-Laminin β1 (1:100; clone LT3 Abcam) anti-Laminin β2 (1:5000; gift from Jeff Miner) and anti-Laminin γ1 (1:100; clone A5 Millipore).

The polyclonal antibody against EHS-laminin, or laminin 111, detects all laminins containing α1, β1 or γ1 chains and for this reason, this antibody was used to detect all laminins except laminins 332, 333, 423 and 523 (Paulsson et al., 1994). We designate it pan-muscle laminin antibody.

Image analysis and quantifications

Sections processed for *in situ* hybridization were photographed using an Olympus DP50 camera coupled to an Olympus BX51 microscope. Sections processed for immunohistochemistry were imaged with a Hamamatsu Orca R2 camera coupled to an Olympus BX60 fluorescence microscope. Whole mount tissue processed for immunohistochemistry was imaged with a Leica SPE confocal microscope system. The acquired images were analyzed in Fiji version 1.49. The confocal images were imported to Amira V.5.3.3 (Visage Imaging Inc.) software and processed as described previously (Gonçalves et al., 2016).

Results

Laminins 111/121, 411/421 and 511/521 are part of the early cardiac jelly and the subepicardial matrix

Our first aim was to characterize the laminin matrices during heart tube elongation and myocardial trabeculation. To accomplish this, we first assessed laminin matrix distribution in E9.5, E10.5, E12.5 and E14.5 embryos/fetuses (Fig. 1 and 2).

In agreement with previous studies, immunostaining for laminin (pan-muscle laminin antibody; refer to Material and Methods for more detail) in E9.5 embryos revealed an early thin myocardium (Fig. 1A, D and F), whose internal wall is covered by laminin (Fig. 1C, E and F; Fig. 2A-B'; also see Nakajima et al., 1997). We find that a laminin matrix is present in the atrial and ventricular cardiac jelly, but, at this stage, it is still a sparse matrix, covering only some patches of the internal wall of the myocardium (Fig. 2A' and B'). The first trabeculae start to protrude from the myocardium at E9.5, while the proepicardial cells start their migration to cover the outer layer of the myocardial (Kirby and Waldo, 2007; Savolainen et al., 2009; Vincent and Buckingham, 2010; Samsa et al., 2013; Paige et al., 2015; also see Fig. 2B). Several trabeculae can be detected in the ventricular myocardial wall by E10.5, when the epicardium is well established (Kirby and Waldo, 2007; Savolainen et al., 2009; Vincent and Buckingham, 2010; Samsa et al., 2014; Paige et al., 2015; also see Fig. 2D). At this stage, we find laminin staining in the newly assembled subepicardial matrix contacting with the outer layer of the atrial (Fig. 2C and C') and ventricular (Fig. 2D and D') myocardium. We also detected laminin immunostaining in the atrial (Fig. 2C and C') and ventricular (Fig. 2D and D') cardiac jelly. Overall, immunostaining of laminin demonstrates a progressive assembly of laminin matrix, between E9.5 and E10.5, in both the cardiac jelly and in the subepicardial matrix (Fig. 2A-D').

During subsequent cardiac development, the trabeculae undergo a maturation process and the compact zone increases massively in size (Kirby and Waldo, 2007; Savolainen et al., 2009; Vincent and Buckingham, 2010; Samsa et al., 2014; Paige et al., 2015; also compare Fig. 2D with 2H). We find laminin in the cardiac jelly and subepicardial matrices in E12.5 embryos (Fig. 2E-F') and E14.5 fetuses (Fig. 2G-H'). Laminin can also be seen in the matrix covering the outer surface of epicardial cells at both stages (Fig. 1E-H'). At E14.5, we further found laminin within the myocardium, probably in the cardiomyocyte basement membrane (Fig. 2H and H'; insert in Fig. 2H').

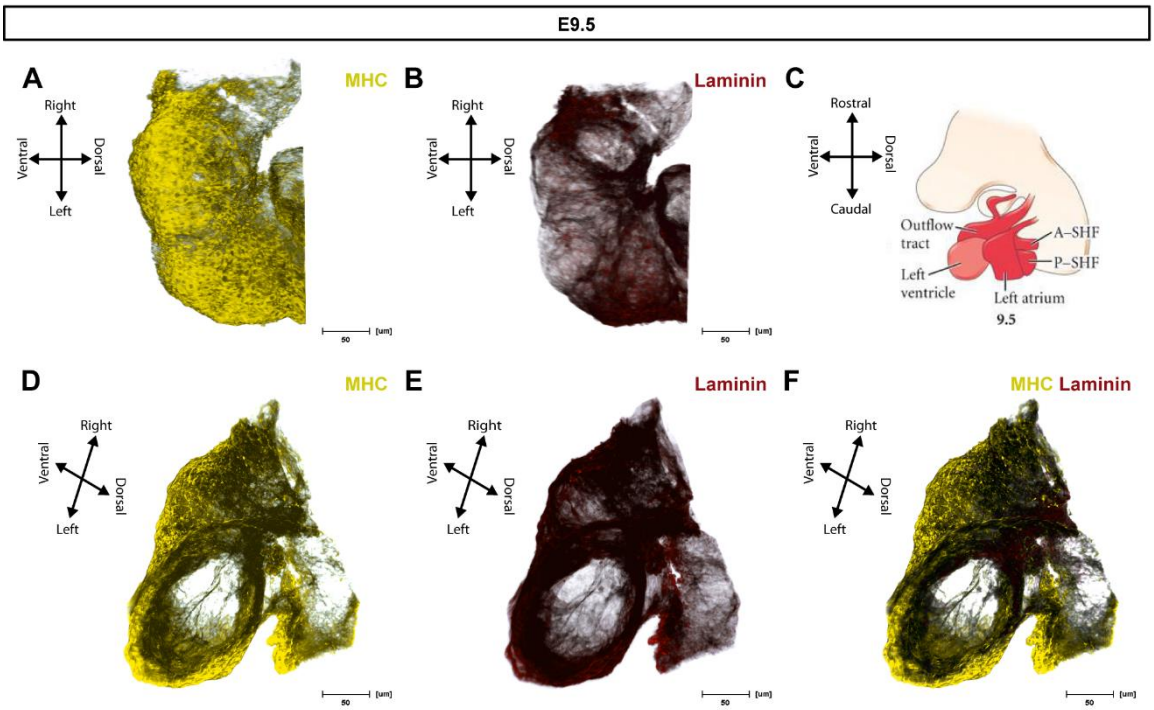

Figure 1- 3D reconstruction of the heart tube and laminin matrix in E9.5 embryos. (**A,B,D-F**) 3D reconstructions of E9.5 hearts stained by immunofluorescence for myosin heavy chain (A,D,F, yellow) and laminin (pan-laminin antibody; B,E,F, red). (**A and B**) Transversal view of myosin heavy chain (A) and laminin (B) immunostaining in 9.5 embryos. (**C**) Schematic representation of the heart tube at E9.5. Adapted from Gilbert, 2013. (**D-F**) Sagittal view of laminin (E,F) and myosin heavy chain immunostaining (D,F). The heart tube is formed by a thin layer of cardiomyocytes lined by laminin along the internal wall. MHC, Myosin heavy chain; A-SHF, Anterior second heart field; P-SHF, Posterior second heart field. Scale bars: 50 µm.

We next sought to understand what laminin isoforms are produced and assembled at the beginning of trabeculation. We first analyzed laminin mRNA expression in E9.5 embryos (Fig. 3). We find that *Lama1* is expressed at low levels in the myocardium (Fig. 3A). *Lama2* appears not be expressed in the heart at these stages, even though a clear signal is detected in the myotome (Fig. 3B; insert in Fig. 3B). *Lama4* and *Lama5* are both expressed in the myocardium (Fig. 3C and D), and *Lama5* is also expressed by endocardial cells (Fig. 3D). We further found that *Lamb1* is expressed in the myocardium and endocardium (Fig. 3E), while *Lamb2* is expressed at low levels in the myocardium, but not in the endocardium (Fig. 3F). We detect *Lamc1* expression mostly in the outer layer of the myocardium and strong *Lamc1* expression is present in the endocardial cells (Fig. 3G). These results suggest that at E9.5 during late stages of heart tube elongation, the endocardial cells are the major producers of laminin 511, whereas the myocardium appears to produce laminins 411/421 and 511/521 and possibly some laminin 111/121 (Fig. 3H). We then analyzed the distribution of different laminin protein isoforms in E9.5 embryos. Our data reveals that laminin α1 (insert in Fig. 3I) is present in the atrial cardiac jelly, while laminin α4 (Fig. 3I and M), α5 (Fig. 3J and N), β1 (Fig. 3K and O) and β2 (Fig. 3L and P) chains are present in the atrial (Fig. 3I-L; insert in Fig. 3I) and ventricular (Fig. 3M-P) cardiac jelly. In addition, we detect laminin α5 and β1 chains in the outer layer of the myocardium (Fig. 3J, K, N and O). We did not detect positive immunostaining for laminin α2 chain in E9.5 hearts (insert in Fig. 3J). Thus, at this stage, our results suggest that the cardiac jelly is formed by a combination of laminins 111/121, 411/421 and 511/521, produced by the myocardium (laminins 111/121, 411/421 and 511/521) and the endocardium (laminin 511 only).

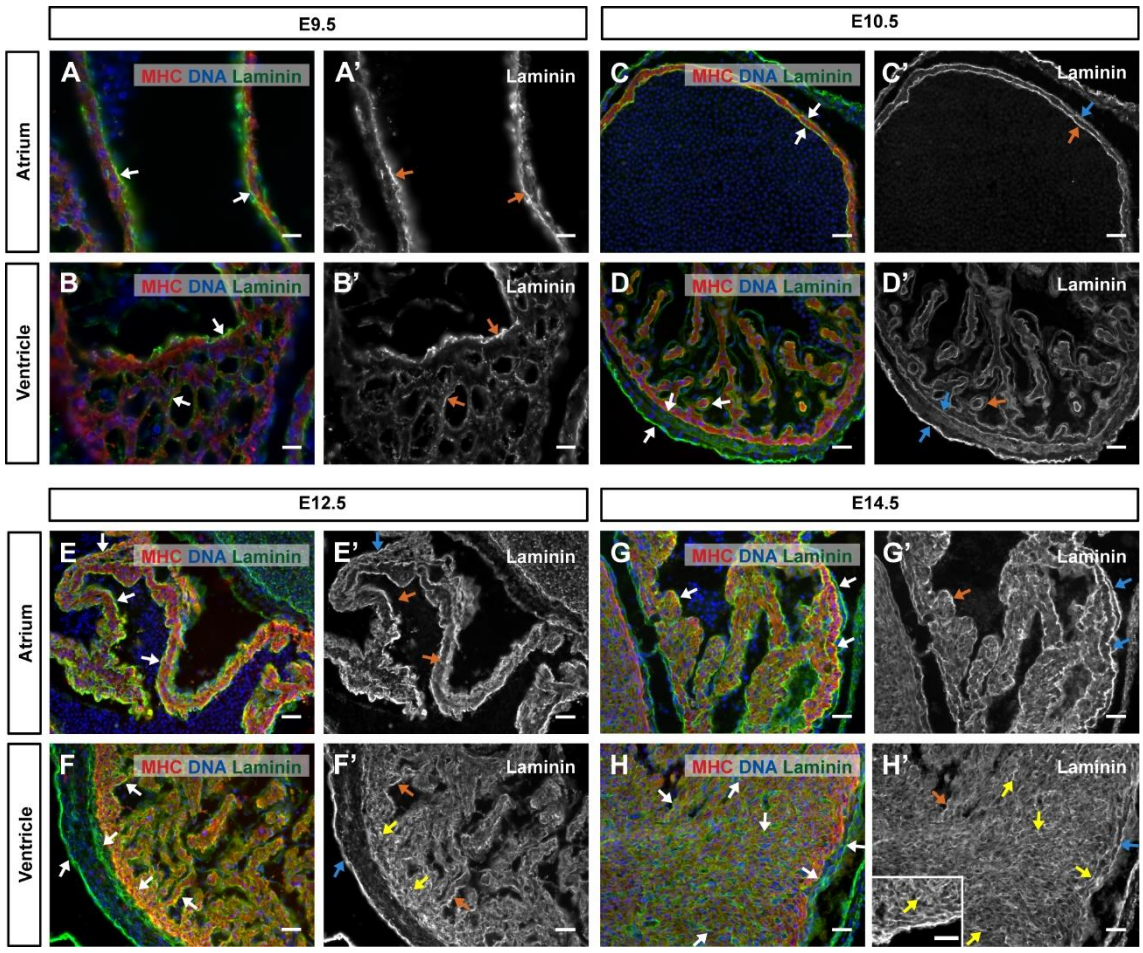

Figure 2- Laminin matrices in embryonic and fetal cardiac development. (**A-H'**) Transverse sections of E9.5 (A-B'), E10.5 (C-D') and E12.5 embryos (E-F'), and E14.5 fetuses (G-H'), stained by immunofluorescence. (A,B,C,D,E,F,G,H) Immunostaining for laminin (pan-laminin antibody; green) and myosin heavy chain (red), with DNA staining (blue) in the atrium (A,C,E,G) and ventricle (B,D,F,H). (A',B',C',D',E',F',G',H') Grayscale for laminin immunostaining in the atrium (A',C',E',G') and ventricle (B',D',F',H'). Laminin is assembled in the cardiac jelly at E9.5 (A and B, white arrows; A' and B', orange arrows), but at E10.5, laminin can also be found in the subepicardial matrix (C,D, white arrows; C',D', blue arrows). Laminin immunoreactivity remains and becomes progressively stronger in the cardiac jelly and in the subepicardial matrix of E12.5 embryos (E,F, white arrows; E',F', orange and blue arrows) and E14.5 fetuses (G,H, white arrows; G',H', orange and blue arrows). Laminin is detected in patches in the basement membrane of ventricular cardiomyocytes for the first time at E12.5 (F, white arrow; F', yellow arrows), and by E14.5, assembled laminin can be clearly detected in the cardiomyocyte basement membrane (H, white arrows; H', yellow arrows; Insert in H', yellow arrow). Arrows: Orange (cardiac jelly/endocardial-myocardial matrix), blue (supepicardial matrix), yellow (cardiomyocyte basement membrane). MHC, Myosin heavy chain. Scale bars: 15 µm (A-B') and 30 µm (C-H').

We next characterized laminin matrices in E10.5 embryos (Fig. 4). At this stage, the epicardium already covers a large portion of the heart (Komiyama et al. 1987; Savolainen et al., 2009). We find that *Lama1* is expressed at high levels in the epicardium, but unlike the case at E9.5 it appears to have been downregulated in the E10.5 myocardium (Fig. 4A). We detect *Lama2* and *Lama4* expression in the myocardium (Fig. 4B and C), but *Lama4* expression in the myocardium is mostly restricted to the atrium (Fig. 4C). Similar to *Lama1*, we found that *Lama5* expression is downregulated in the myocardium between E9.5 and E10.5 but is expressed in the epicardium at E10.5 (Fig. 4D). Lastly, we detect *Lamb2* expression in the atrial and ventricular myocardium, but its expression is stronger in the atrial myocardium (Fig. 4E). Together, these results indicate that at E10.5, the endocardium ceases laminin production, while the forming epicardium produces α1- and α5-containing laminins (Fig. 4F). The myocardium produces laminins 211/221 and 411/421 (Fig. 4F). We then asked where the different laminins are assembled at E10.5 (Fig. 4G-P). Immunostaining for different laminin chains reveals that laminin matrices are generally more developed in the atrium than in the ventricle (Fig. 4G-P), as also suggested by our *in situ* hybridization data (Fig. 4A-E). Indeed, we detect laminin α5 and β1 chains in the basement membrane of the atrial cardiac jelly and subepicardial matrix (Fig. 4H and I), but these are localized mostly in patches in the ventricular matrices (Fig. 4L and M). The exception is laminin α4 chain, which is present in the cardiac jelly in the ventricle, but no immunostaining was detected in the atrium (Fig. 4G and K). Overall, these results suggest that the laminin deposition program advances more slowly in the ventricle when compared to the atrium, the same way the genetic program specifying atria and ventricles is distinct (Small and Krieg, 2004). We also found that laminin β1 chain localizes in the atrial and ventricular cardiac jelly as well as in the subepicardial matrix (Fig. 4I and M), while laminin β2 chain localizes exclusively in the cardiac jelly (Fig. 4J and N). Finally, we identified laminin γ1 chain in the cardiac jelly and subepicardial matrix (Fig. 4Q and R). Although *Lama2* expression was detectable in the myocardium (Fig. 4B), we did not detect

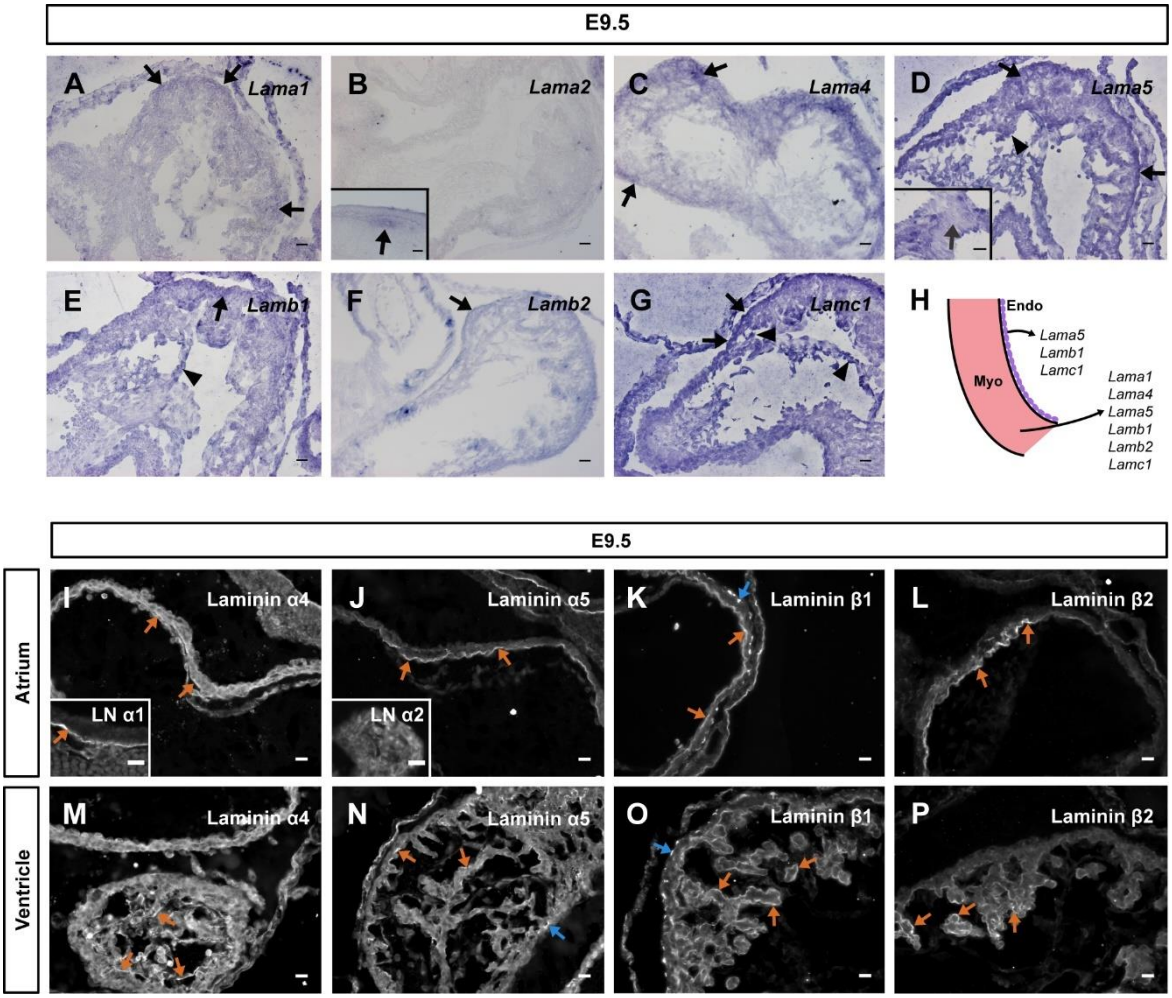

Figure 3- Laminin gene expression and protein localization in E9.5 embryos. (**A-G**) Expression patterns of *Lama1* (A), *Lama2* (B), *Lama4* (C), *Lama5* (D), *Lamb1* (E), *Lamb2* (F) and *Lamc1* (G) genes in E9.5 embryos. The myocardium expresses *Lama1* (A, black arrows), *Lama4* (C, black arrows), *Lama5* (D, black arrows), *Lamb1* (E, black arrow), *Lamb2* (F, black arrow) and *Lamc1* (G, black arrows), while the endocardium expresses only *Lama5* (D, black arrowhead), *Lamb1* (E, black arrowhead) and *Lamc1* (G, black arrowheads). *Lama2* expression is not detected in the heart at this stage (B), but is present in the myotome (insert in B, black arrow). Insert in D indicates an area of the myocardium without expression of *Lama5* (insert in D, gray arrow). (**H**) Schematic representation of myocardium and endocardium depicting what laminin genes are expressed in the heart tube at E9.5. (**I-P**) Transverse sections of E9.5 embryos, stained by immunofluorescence for laminin α1, (insert in I), α4 (I,M), α2 (insert in J), α5 (J,N), β1 (K,O) and β2 (L, P) chains. At E9.5, the cardiac jelly is enriched with laminin α1 (insert in I, orange arrow), α4 (I,M, orange arrows), α5 (J,N, orange arrows), β1 (K,O, orange arrows) and β2 (L,P, orange arrows). Patches of laminin α5 (N, blue arrow) and β1 (K,O, blue arrows) immunostaining can be found in the subepicardial matrix. The cardiac tissue does not stain positive for laminin α2 chain (insert in J). Arrows: Orange (cardiac jelly/endocardial-myocardial matrix) and blue (supepicardial matrix). Myo, Myocardium; Endo, Endocardium. Scale bars: 25 µm (A-G) and 20 µm (I-P, inserts in I,J).

any immunostaining for laminin α2 chain in the E10.5 myocardium (data not shown). In addition, we did not find *Lama1* expression in the myocardium neither the endocardium,

but laminin α1 was previously described in the cardiac jelly (Miner et al., 1998). Together these data indicate that laminin 211/221 production is not yet occurring, but may be about to start. Our data thus suggest that during early stages of myocardium growth and chamber specification, the cardiac jelly is formed by a combination of laminins 111/121,

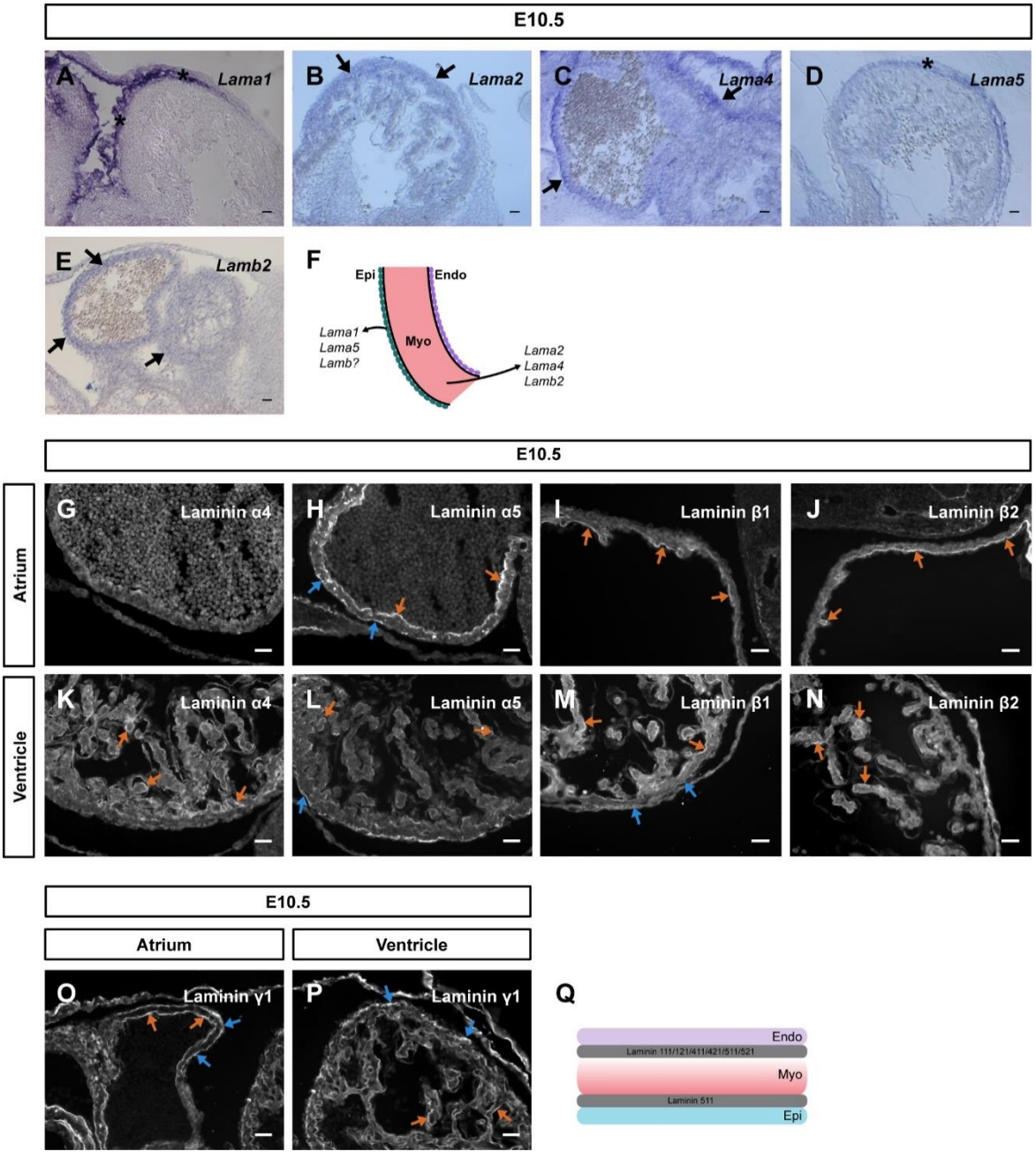

Figure 4- Laminin gene expression and protein localization in E10.5 embryos. (**A-E**) Expression patterns of *Lama1* (A), *Lama2* (B), *Lama4* (C), *Lama5* (D) and *Lamb2* (E) genes in E10.5 embryos. The myocardium now expresses *Lama2* (B, black arrows), *Lama4* (C, black arrows) and *Lamb2* (E, black arrows) genes, whereas the epicardium expresses *Lama1* (A, black asterisks) and *Lama5* (D, black asterisk) genes. **(Continues next page)**

(Continued from previous page) (**F**) Schematic illustration of myocardium and endocardium showing the laminin genes expressed in the heart at E10.5. (**G-P**) Transverse sections of E10.5 embryos, stained by immunofluorescence for laminin α4 (G,K), α5 (H,L), β1 (I,M), β2 (J,N) and γ1 (O,P) chains. The atrial and the ventricular cardiac jelly stain positive for laminin α5 (H,L, orange arrows), β1 (I,M, orange arrows), β2 (J,N, orange arrows) and γ1 (O,P, orange arrows), while the subepicardial matrix is positive for laminin α5 (H,L, blue arrows), β1 (M, blue arrows) and γ1 (O,P, blue arrows). The atrial cardiac jelly does not stain positive for laminin α4 (G), but this laminin chain is detected in the ventricular cardiac jelly (K, orange arrows). (**Q**) Schematic representation of the different cardiac layers and the composition of the cardiac jelly and subepicardial matrix. Arrows: Orange (cardiac jelly/endocardial-myocardial matrix) and blue (supepicardial matrix). Myo, Myocardium; Endo, Endocardium; Epi, Epicardium. Scale bars: 30 μm.

411/421 and 511/521, while the subepicardial matrix is composed exclusively by laminin 511 and that laminins are not yet found surrounding individual cardiomyocytes in the myocardium (Fig. 3Q).

Laminin 211/221, 411/421 and 511/521 compose the cardiac matrices during myocardial trabeculation

We next described laminin assembly dynamics during the later stages of myocardial trabeculation in the ventricle. For this, we analyzed the distribution of different laminin chains in E12.5 embryos and E14.5 fetuses (Fig. 5). Immunostaining for laminin α1 in E12.5 embryos revealed that it is assembled in the cardiac jelly and in the subepicardial matrix (Fig. 5A and E). We find laminin α2 chain in the cardiac jelly and subepicardial matrices in the atrium (Fig. 5B), but did not detect any immunostaining for this laminin chain in the ventricle (Fig. 5F). We also detected some immunostaining for α2 laminin inside the atrial myocardium (Fig. 5B). As was the case for E10.5, we detected weak immunostaining for laminin α4 chain in the atrial cardiac jelly at E12.5 (Fig. 5C). We found clear immunostaining for laminin α4 in the ventricular cardiac jelly and some staining around cardiomyocytes (Fig. 5G). In addition, we find that laminin α5 chain is present in the atrial and ventricular cardiac jelly, but the atrial cardiac jelly appears to

have a more developed laminin matrix than that of the ventricle (Fig. 5D and H). Laminin α5 chain is also present in the subepicardial matrix (Fig. 5D and H). In agreement with the presence of laminin α chains in the cardiac jelly and subepicardial matrices, immunostaining for laminin β chains revealed the presence of laminin β1 and β2 chains in both the cardiac jelly and subepicardial matrix (Fig. 5I-M). However, laminin β2 chain immunostaining in the ventricular subepicardial matrix is weak and patchy (Fig. 5M). We also found that laminin β1 localizes in the matrix surrounding the sarcolemma of ventricular cardiomyocytes (Fig. 5L). Finally, we detect laminin γ1 chain in the cardiac jelly, and in the subepicardial and cardiomyocyte matrices (Fig. 5K and N). Together, these results indicate that a combination of laminins 111/212, 211/221, 411/421 and 511/521 establishes the cardiac jelly at E12.5. Laminins 111, 211 and 511 compose the subepicardial matrix, and laminin 211 (and possibly 411) have started to be assembled in the cardiomyocyte basement membrane (Fig. 5O).

We then analyzed the different laminin niches in E14.5 fetuses at the end of ventricular trabeculation. Since from this stage onwards, we did not detect significant differences between atrial and ventricular laminin matrices, we focused our analysis on the ventricle. The cardiac jelly was described to be digested between E12.5 and E14.5 (Cooley et al., 2012) and thus, we will refer to the laminin matrix in the endocardium-myocardium interface as endocardium-myocardium matrix/basement membrane hereafter. Immunostaining for α1-laminin chain revealed that it is absent from cardiac matrices at E14.5, suggesting that α1-laminin deposition in the cardiac tissue ceases between E12.5 and E14.5 (Fig. 5P). Our results reveal an increase of laminin α2 chain deposition in the endocardium-myocardium matrix and laminin α2 chain is now clearly present in the ventricular cardiomyocyte basement membrane (Fig. 5Q). We detect laminin α4 chain exclusively in the blood vessels scattered throughout the myocardium and in the endocardium-myocardium basement membrane (Fig. 5R). Similar to the pattern observed for the laminin α2 chain, we find that laminin α5 and β1 chains are

present in the cardiomyocyte matrix (Fig. 5S and T). In contrast, laminin β2 chain is mostly localized in the endocardium-myocardium basement membrane around the trabeculae (Fig. 5U). Lastly, we detect laminin γ1 chain in the endocardium-myocardium, subepicardial and cardiomyocyte matrices (Fig. 5V). Our data thus indicate that the endocardium-myocardium matrix is composed of laminins 211/221, 411/421 and

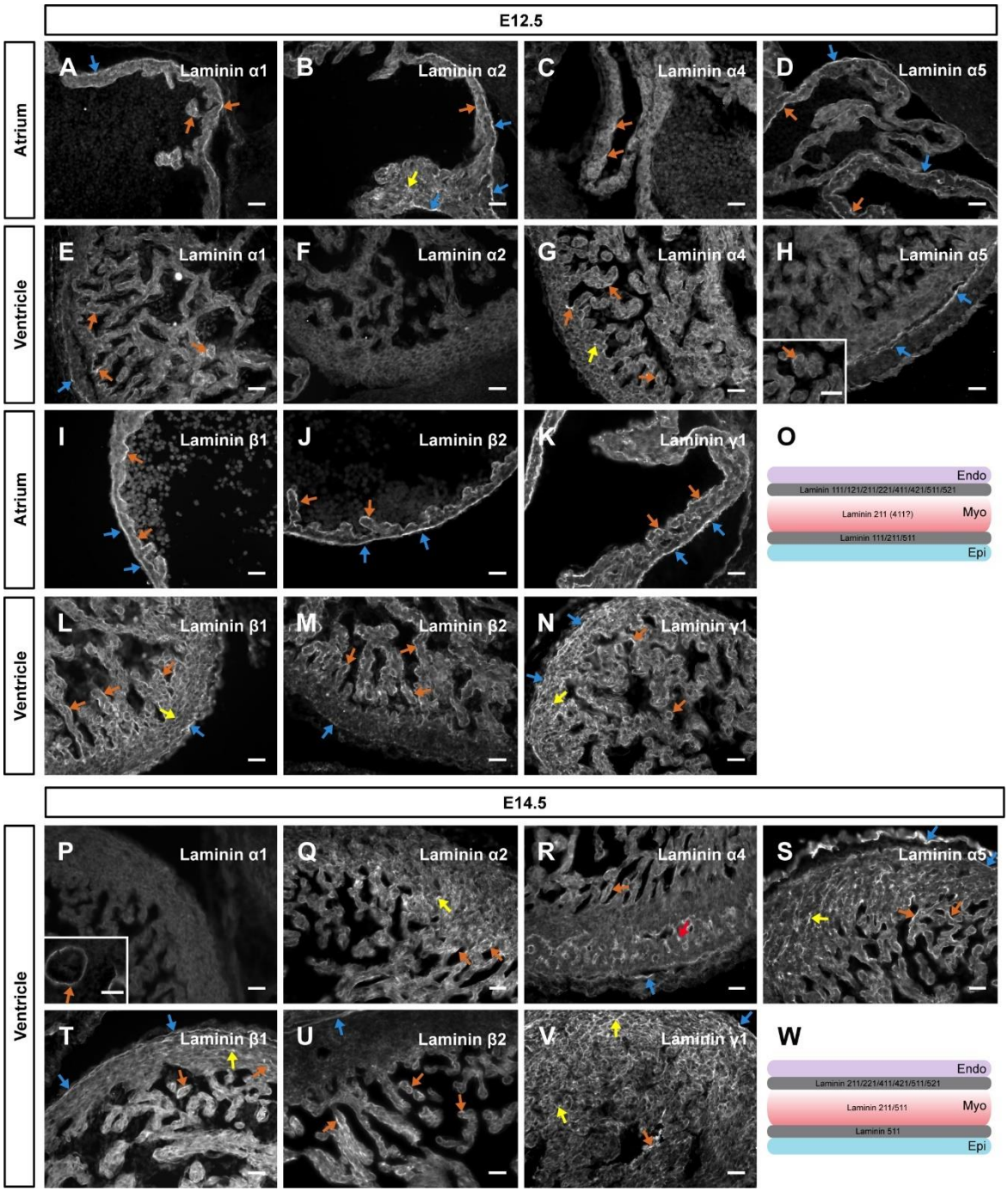

Figure 5- Laminin matrix assembly dynamics in E12.5 and E14.5 hearts. (Continues next page)

(Continued from previous page) (**A-N**) Transverse sections of E12.5 embryos, stained by immunofluorescence for laminin α1 (A,E), α2 (B,F), α4 (C,G), α5 (D, H), β1 (I,L), β2 (J, M) and γ1 (K,N). Laminin α1 (A,E, orange arrows), α4 (C,G, orange arrows), α5 (D, orange arrows; insert in H, orange arrow), β1 (I,L, orange arrows), β2 (J,M, orange arrows) and γ1 (K,N, orange arrows) chains line the internal myocardium wall in the atrial and ventricular cardiac jelly. Laminin α1 (A,E, blue arrows), α5 (D, H, blue arrows), β1 (I,L, blue arrows), β2 (J,M, blue arrows) and γ1 (K, N, blue arrows) chains line the external side of the myocardium, in the subepicardial matrix. Laminin α2 chain is detected in the atrial cardiac jelly (B, orange arrow) and subepicardial matrix (B, blue arrows), but is absent from the ventricular matrices (F). Laminin α2 (B, yellow arrow), α4 (G, yellow arrow), β1 (L, yellow arrow) and γ1 (N, yellow arrow) are now also detected within the myocardium. (**O**) Schematic illustration describing the assembled laminins in the cardiac layers at E12.5. (**P-V**) Transverse sections of E14.5 embryos, stained by immunofluorescence for laminin α1 (P), α2 (Q), α4 (R), α5 (S), β1 (T), β2 (U) and γ1 (V). Laminin α1 chain immunoreactivity is not detected in the heart at this stage, even though positive staining is present in the lungs (insert in P, orange arrow). Laminin α2 (Q, orange arrows), α5 (S, orange arrows), β1 (T, orange arrows), β2 (U, orange arrows) and γ1 (V, orange arrow) are deposited in the endocardium-myocardium basement membrane. Laminin α4 can also be found in the blood vessels (R, red arrow). The cardiomyocyte basement membrane stains positive for laminin α2 (Q, yellow arrow), α5 (S, yellow arrow), β1 (T, yellow arrows) and γ1 (V, yellow arrows). The subepicardial matrix is constituted by laminin α5 (S, blue arrows), laminin β1 (T, blue arrows) and γ1 (V, blue arrows). (**W**) Schematic illustration of laminin matrices composition in the cardiac basement membranes at E14.5. Arrows: Orange (cardiac jelly/endocardial-myocardial matrix), blue (supepicardial matrix) and yellow (cardiomyocyte basement membrane). Myo, Myocardium; Endo, Endocardium; Epi, Epicardium. Scale bars: 30 μm.

511/521, while the subepicardial matrix is composed of laminins 511 (Fig. 5W). The cardiomyocyte basement membrane contains laminins 211 and 511 (Fig. 5W).

Late fetal, postnatal and adult cardiac matrices contain primarily laminins 221 and 521

During late fetal cardiac development, and during subsequent postnatal and adult cardiogenesis, cardiomyocytes gradually reduce and eventually lose their proliferation capacity (Sedmera and Thompson, 2011; Ponnusamy et al., 2016). To characterize the laminin matrices in these stages, we stained E17.5, P10 and adult hearts for different laminin chains (Fig. 6). Immunostaining for laminin (pan-muscle antibody; refer to Material and Methods for more detail) at these stages reveals the presence of well-developed laminin matrices in the endocardium-myocardium and subepicardial basement membranes (Fig. 6A-F', Insert in B, B', D, D', F and F'). We also found that laminin staining is strong in cardiomyocyte basement membranes during these stages (Fig. 6A-F'). We then

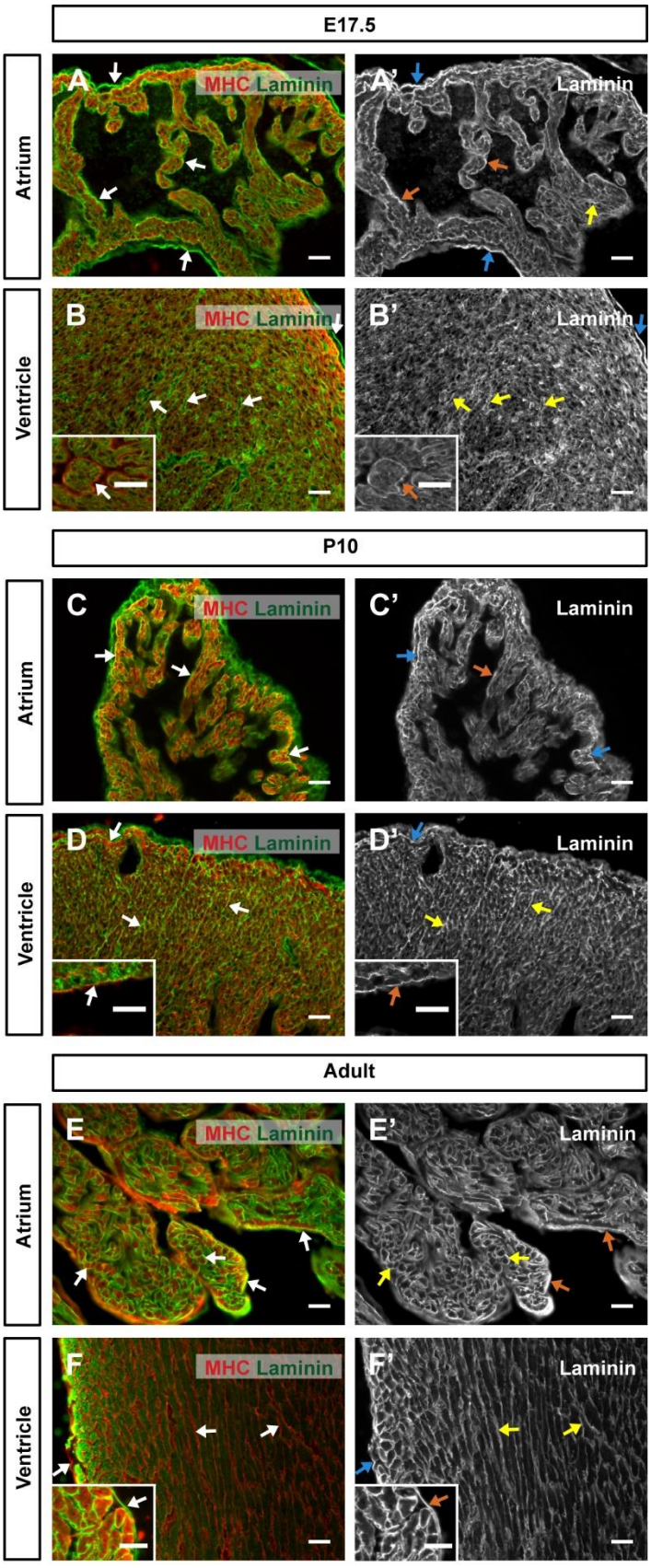

Figure 6- Laminin matrices in late fetal, postnatal and adult cardiac development. (**A-B'**) Transverse sections of E17.5 hearts stained for laminin (A, B, green; pan-muscle antibody) and myosin heavy chain (A,B, red). (A',B') Grayscale for laminin in the atrium (A') and ventricle (B'). Laminin immunoreactivity reveals the presence of laminin matrices in the endocardium-myocardium (A, B, white arrows, insert in B; A', insert in B', orange arrows), cardiomyocyte (A,B, white arrows; A',B', yellow arrows) and subepicardial matrices (A,B, white arrows; A',B', blue arrows). (**C-D'**) Transverse sections of P10 hearts stained for laminin (C,D, green; pan-muscle antibody) and myosin heavy chain (C,D, red). (C',D') Grayscale for laminin in the atrium (C') and ventricle (D'). Laminin matrices are maintained in the endocardium-myocardium (C,D, white arrows, insert in D; C', insert in D', orange arrows), cardiomyocyte (C,D, white arrows; D', yellow arrows) and subepicardial matrices (C,D, white arrows; C',D', blue arrows). (**E-F'**) Transverse sections of adult hearts stained for laminin (E,F, green; pan-muscle antibody) and myosin heavy chain (E,F, red). (E',F') Grayscale for laminin in the atrium (E') and ventricle (F'). Laminin matrices are preserved in the endocardium-myocardium (E,F, white arrows, insert in F; E', orange arrows, insert in F') and subepicardial matrices (E,F, white arrows; F', blue arrow), while the laminin content is increased in the cardiomyocyte basement membrane (E',F', yellow arrows). Arrows: Orange (cardiac jelly/endocardial-myocardial matrix), blue (supepicardial matrix), yellow (cardiomyocyte basement membrane), red (blood vessels). MHC, Myosin heavy chain. Scale bars: 30 µm.

determined the composition of cardiac matrices at E17.5, and found that laminin α2 chain immunostaining is strongest in the cardiomyocyte basement membrane, but also appears to be present in the endocardium-myocardium and subepicardial matrices (Fig. 7A; insert in Fig. 7A). We detect laminin α4 chain in the blood vessel basement membrane and in patches in the endocardium-myocardium matrix (Fig. 7B; insert in Fig. 7B). Immunostaining for laminin α5 chain reveals it is present in the endocardium-myocardium and subepicardial matrices (Fig. 7C; insert in Fig. 7C). We find that a few patches of immunostaining for laminin β1 (insert in Fig. 7D), but most of the E17.5 cardiac tissue is negative for β1 (Fig. 7D). Lastly, we find that laminin β2 (Fig. 7E; insert in Fig. 7E) and γ1 chains are present in the endocardium-myocardium basement membrane (Fig. 7F). We did not find laminin β2 in the subepicardial matrix (Fig. 7W). In addition, we detected laminin γ1 in subepicardial and cardiomyocyte matrices (Fig. 7F). These results suggest that laminins 221, 421 and 521 compose the endocardium-myocardium basement membrane, while the subepicardial matrix is formed by laminins 211 and 511 (Fig. 7G). Laminins 221 and 521 seem to substitute laminins 211 and 511 in the cardiomyocyte basement membrane, respectively (Fig. 7G).

We then analyzed the distribution of different laminin chains in P10 hearts. We find that laminin α2 chain localizes in the endocardium-myocardium, subepicardial and cardiomyocyte matrices (Fig. 7H). At this stage, laminin α4 is no longer detected in the endocardium-myocardium basement membrane and is present exclusively in the blood vessel basement membrane (Fig. 7I). Like laminin α2, laminin α5 chain is mostly found in the subepicardial matrix and in the basement membrane of cardiomyocytes in the compact zone (Fig. 7J). Similar to our data for E17.5, we only detected patches of immunostaining for laminin β1 in the endocardium-myocardium, subepicardial and cardiomyocyte matrices (Fig. 7K, insert in 7K). We find laminin β2 with a more widespread distribution in the endocardium-myocardium, subepicardial and cardiomyocyte basement membranes (Fig. 7L, insert in 7L). These results suggest that laminins 221 and 521 are the

main laminins in the postnatal heart, as they are assembled in the endocardium-myocardium, subepicardial and cardiomyocyte matrices (Fig. 7M).

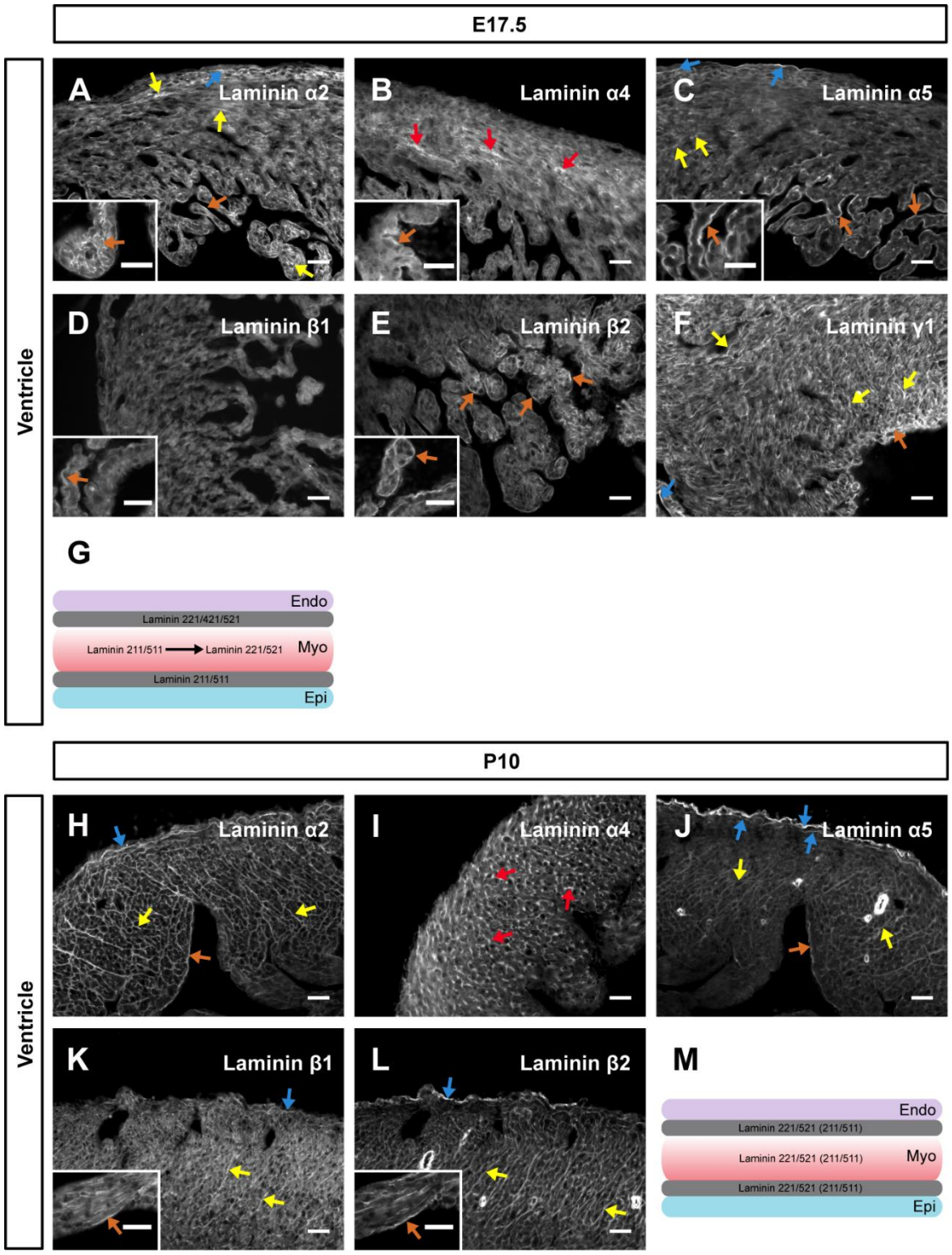

Figure 7- Laminin isoforms in E17.5 and P10 hearts. (Continues next page)

(Continued from previous page) (**A-F**) Transverse sections of E17.5 fetuses stained by immunofluorescence for laminin α2 (A, insert in A), α4 (B, insert in B), α5 (C, insert in C), β1 (D, insert in D), β2 (E, insert in E) and γ1 (F) chains. The cardiomyocyte basement membrane at E17.5 stains positive for laminin α2 (A, yellow arrows) and laminin α5 (C, yellow arrows), but lacks positive staining for laminin β1 (D) and β2 (E). The subepicardial basement membrane contains laminin α2 (A, blue arrow), α5 (C, blue arrows) and γ1 (F, blue arrow), but stains mostly negative for laminin β1 (D) and β2 (E). Immunostaining for laminin α2 (A, insert in A, orange arrows), α5 (C, insert in C, orange arrows), β2 (E, insert in E, orange arrows) and γ1 (F, orange arrow) is observed in the endocardium-myocardium matrix. Laminin α4 is mostly located in the coronary vessels (B, red arrows), but faint immunostaining is also present in the endocardium-myocardium matrix (insert in B, orange arrow). (**G**) Schematic representation depicting the laminin matrices in the cardiac basement membranes at E17.5. (**H-L**) Transverse sections of P10 fetuses stained by immunofluorescence for laminin α2 (H), α4 (I), α5 (J), β1 (K) and β2 (L) chains. The cardiomyocyte and subepicardial matrices stain for laminin α2 (H, yellow and blue arrows, respectively), α5 (J, yellow and blue arrows), β1 (K, yellow and blue arrows) and β2 (L, yellow and blue arrows), while laminin α4 is present only in the blood vessel basement membrane (I, red arrows). The endocardium-myocardium matrix stains for laminin α2 (H, orange arrow), α5 (J, orange arrow), β1 (insert in K, orange arrow) and β2 (insert in L, orange arrow). (**M**) Schematic representation depicting the laminin matrices in the cardiac basement membranes at postnatal day 10. Arrows: Orange (cardiac jelly/endocardial-myocardial matrix), blue (supepicardial matrix), yellow (cardiomyocyte basement membrane), red (blood vessels). Myo, Myocardium; Endo, Endocardium; Epi, Epicardium. Scale bars: 30 µm.

Finally, we find that in the adult, laminin α2 chain is mainly found in the cardiomyocyte matrix (Fig. 8A and E; insert in Fig. 8E) and around smaller cells in close proximity to the cardiomyocytes (Fig. 8A, insert in A). In contrast, laminin α4 chain is detected exclusively in patches of punctuated staining throughout the myocardium, possibly in the blood vessels (Fig. 8B and F, inserts in B and F). We found immunostaining for laminin α5 in the endocardium-myocardium, cardiomyocyte and subepicardial basement membranes (Fig. 8C and G). Immunostaining for laminin β1 chain revealed staining in cardiomyocyte basement membrane in the compact layer (Fig. 8D), but no staining in the trabeculae (Fig. 8H; insert in Fig. 8H). Additionally, we find that laminin β2 chain localizes in the endocardium-myocardium, subepicardial and cardiomyocyte basement membranes (Fig. 8I and J). Together, our data reveals that cardiac laminin matrices in the adult resemble the ones of P10 hearts. However, in the adult, laminin 221 comes to localize exclusively in the cardiomyocyte basement membrane, while laminin

521 becomes the major laminin in the endocardium-myocardium and subepicardial matrices (Fig. 8K).

Discussion

Laminins first appear in the cardiac jelly

In this study, we have characterized the dynamics of laminin matrices throughout cardiac development (Fig. 9). The assembly of laminin matrices in the basement membranes of the heart tube starts as soon as the cardiac jelly forms (Nakajima et al., 1997). Here we demonstrated that the early cardiac jelly contains a number of laminins, first 111/121, 411/421 and 511/521 and later also laminins 211/221 (Fig. 9C-F). Most of these laminins are produced by the cardiomyocytes, but the endocardial cells also appear to synthetize laminin 511. Integrin α6β1 is expressed in the myocardium from E8.5 until the end of trabeculation at around E15.0 (Thorsteinsdóttir et al., 1995; Hierck et al., 1996) and it is thus in a position to mediate the interaction between the cardiomyocytes and the laminin-containing matrices. Integrins are well known mediators of cell migration, differentiation, proliferation and apoptosis (Legate et al., 2006). Therefore, multiple possibilities arise when it comes to the putative effects of integrin α6β1-laminin signaling during heart tube development and trabeculation.

An appropriate cross-talk between endocardium and myocardium is crucial for the development of the coronary vasculature (Wu et al., 2012; Luxán et al., 2016). Notch signaling is one of the master regulators mediating this cross-talk (Samsa et al., 2013; Luxán et al., 2016). *Dll4*, one of Notch ligands, is expressed in the cardiac crescent at the beginning of cardiac development and also in the endocardium during trabeculation (Nimmagadda et al., 2007). Endocardial cells have been shown to give rise to the endothelial layer of the coronary arteries through a developmental process involving

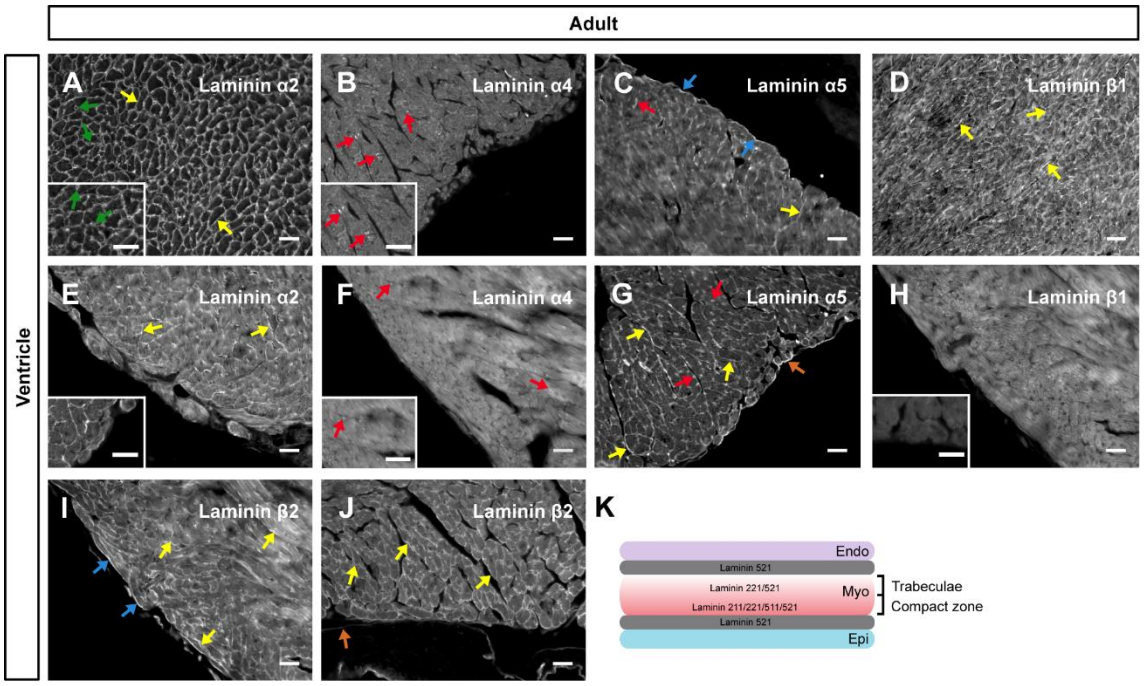

Figure 8- Laminin isoforms in the adult heart. (**A-J**) Transverse sections of adult hearts stained by immunofluorescence for laminin α2 (A,E, insert in E), α4 (B,F), α5 (C,G), β1 (D,H, insert in H) and β2 (I,J) chains. Immunostaining for laminin α2 (A,E, yellow arrows), α5 (C,G, yellow arrows), β1 (D, yellow arrows) and β2 (I,J, yellow arrows) reveals the presence of these laminin chains in the cardiomyocyte basement membrane. Laminin α2 can also be found around smaller cells in close proximity to the cardiomyocytes (A, insert in A, green arrows). Laminin α5 (C,G) and β2 (I,J) also stains positive in the endocardium-myocardium (orange arrows) and subepicardial (blue arrows) basement membranes. Immunostaining for laminin β1 reveals no staining in the cardiac matrices of trabeculae (H). Laminin α4 (B, F, inserts in B,F, red arrows) and α5 (C,G, red arrows) seem to stain positive for blood vessels. (**K**) Schematic illustration of laminin matrices in the adult heart. Arrows: Orange (cardiac jelly/endocardial-myocardial matrix), blue (supepicardial matrix), yellow (cardiomyocyte basement membrane), red (blood vessels). Myo, Myocardium; Endo, Endocardium; Epi, Epicardium. Scale bars: 30 µm.

VEGF secreted by the myocardium and signaling through Vegfr-2 in the endocardium (Liu et al., 2003; Wu et al., 2012). During angiogenesis, *Dll4* expression is induced by laminin111/411-integrin α6β1 signaling (Estrach et al., 2011). The activation of laminin synthesis is induced by VEGF, which is also known to trigger *Dll4* expression in the arterial endothelium (Liu et al., 2003; Stenzel et al., 2011). Thus, it is possible that laminins in the cardiac jelly may be involved in the communication between the endocardium and the myocardium during the development of the coronary vessels. This hypothesis is further supported by the known role of α4- and α5-laminins in the basement membrane of

different types of blood vessels during angiogenesis, including in the coronary vasculature (Wang et al., 2006; Knöll et al., 2007; Yousif et al., 2013).

These findings, together with our results, suggest that laminins 111/121, 211/221, 411/421 and 511/521 have the potential to signal in the cardiac jelly and to mediate the cross-talk between the endocardium and the myocardium during the development of the coronary vasculature. Further studies are needed to better understand whether and how different laminin-integrin interactions affect these and other processes occurring during these stages of cardiogenesis.

The appearance of the third cardiac layer leads to the assembly of the subepicardial matrix

The proepicardium starts to cover the myocardial outer layer at E9.0 and by E11.0, the heart is completely covered by the epicardium (Kirby and Waldo, 2007; Zhou et al., 2008; Vincent and Buckingham, 2010). Our results demonstrate that the myocardium and the epicardium synthesize and assemble laminins in the subepicardial matrix at the beginning of chamber specification and early trabeculation. The subepicardial matrix is formed by at least laminin 511, when the epicardium is first established. The expression of *Lama1* in the epicardium at E10.5 and the presence of laminin 111 in the subepicardial matrix at E12.5 suggest it might be part of subepicardial matrix during trabeculation as well. The epicardial cells play major roles during cardiomyocyte proliferation (Pennisi et al., 2003; Lavine et al., 2005; Takahashi et al., 2014), and some epicardial cells undergo epithelial-to-mesenchymal transition and invade the myocardium to generate part of the coronary vasculature, cardiac fibroblasts and cardiomyocytes (Zhou et al., 2008; Kirby and Waldo, 2007; Katz et al., 2012). We suggest that in the same way as laminins 111 and 511 in the cardiac jelly may play a role during the development of the coronary vasculature,

these same laminins might fulfil a similar role in the epicardial contribution to the coronary vasculature.

The laminin matrix surrounding individual cardiomyocytes appears relatively late in development

Laminin matrices are assembled around all muscle, fat and nerve cells, and line all epithelia and endothelia in the body. The assembly of laminins is the first step in the construction of basement membranes and it is fundamental for the subsequent incorporation of collagen IV in the basement membranes (Smirnov et al., 2002; Li et al., 2002; Tsiper and Yurchenco, 2002; McKee et al., 2007; Yurchenco, 2015). It is interesting to note that embryonic cardiomyocytes do not possess a laminin matrix around them. We

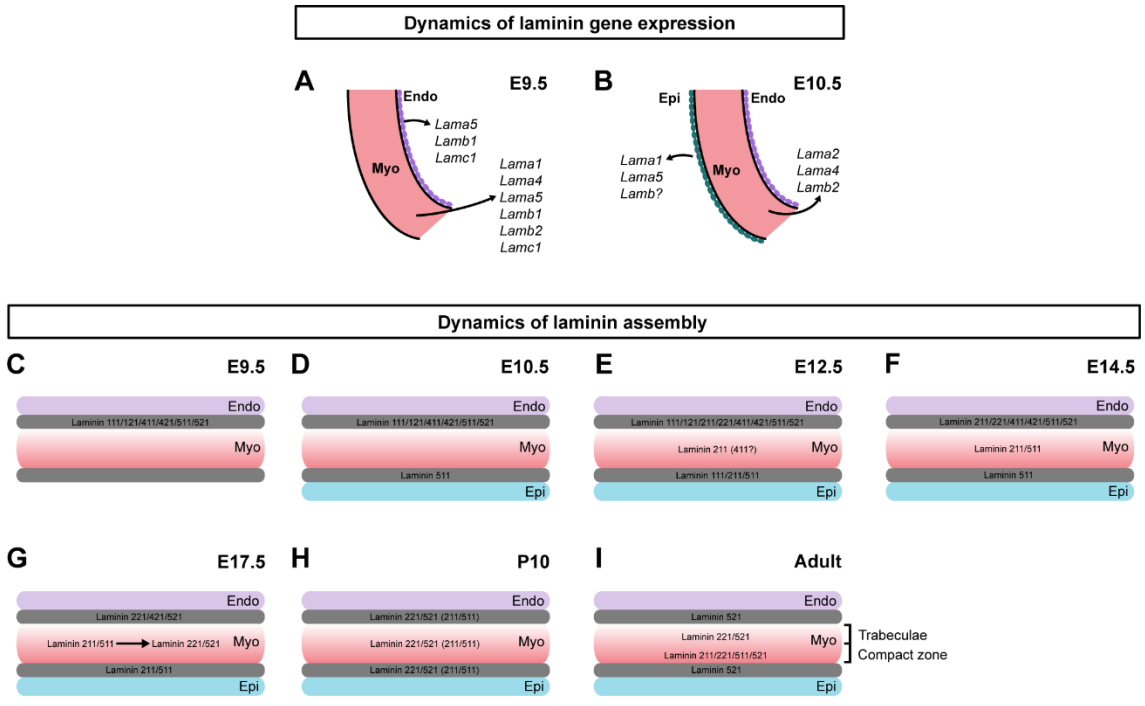

Figure 9- Dynamics of laminin matrices during cardiac development. (**A,B**) Schematic representation depicting the expression of laminin genes in E9.5 (A) and E10.5 embryos (B). (**C-I**) Schematic illustration of laminin matrices in the endocardium-myocardium, cardiomyocyte and subepicardial basement membranes in E9.5 (C), E10.5 (D), E12.5 (E), E14.5 (F), E17.5 (G), P10 (H) and adult (I) stages. Myo, Myocardium; Endo, Endocardium; Epi, Epicardium.

demonstrate for the first time that the cardiomyocyte laminin matrices, laminin 211 (and possibly laminin 411), start to be assembled in the atria at E12.5 and slightly later in the ventricles. Laminin 511 is assembled in the cardiomyocyte basement membrane at E14.5. Therefore, our results suggest that early cardiomyocyte differentiation in the heart tube does not depend on the cardiomyocyte basement membrane. Interestingly, this is a similar situation to what occurs during skeletal muscle development, where primary myogenesis occurs mostly in the absence of laminins and laminins 211, 411 and 511 are assembled from E14.5 onwards (Nunes et al., 2017). One possibility is that during the embryonic stages, the myocardium depends exclusively on signals secreted from the endocardium and epicardium, and/or cues from the cardiac jelly and subepicardial matrix. During the following stages, the myocardium is remodeled into the compact zone and trabeculae (Sedmera and Thompson, 2011; Samsa et al., 2013; Paige et al., 2015), and we suggest that laminin signaling in the cardiomyocyte basement membrane may be important for these processes (Sedmera and Thompson, 2011; Samsa et al., 2013; Paige et al., 2015).

Laminin isoforms change as cardiac development proceeds

Our results revealed that α1- and α2-laminins coexist in the cardiac matrices only for a short period of time. We found that laminin 111 is present in the subepicardial matrix at E12.5, when laminin 211 assembly starts in the cardiomyocyte and subepicardial matrices (Fig. 9). Laminin 111 then becomes undetectable in the cardiac tissue from E14.5 onwards. This shift in laminin dynamics is identical to the one occurring during skeletal muscle development, where a combination of laminins 111/121, 211/221 and 511/521 forms the myotome basement membrane, but only laminins 211, 411 and 511 persist in the myofiber basement membrane during secondary myogenesis (Patton et al., 1997; Nunes et al., 2017). We further find that laminin β1 and β2 chains are both present in the

heart during embryonic and fetal stages, but that the β2 chain becomes more widespread at late fetal and postnatal stages. In agreement with our results, laminin β1 and β2 chains were detected in the cardiomyocyte basement membrane of human embryos of 8/9 gestational weeks (Roediger et al., 2010), which corresponds to Carniege stages 16-19, or about E12.5-E14.0 of mouse development (Hill, 2017).

During later stages of fetal cardiogenesis, between E14.5 and E17.5, laminin 521 appears to progressively substitute laminin 511 in the cardiomyocyte and subepicardial matrices, while laminin 211 is exchanged for laminin 221 in the cardiomyocyte basement membrane (Fig. 9). Our results suggest that even though β1-laminins are detected in late stages of cardiac development, the presence of these laminins in the cardiac laminin matrices decreases as development proceeds. In fact, β2-laminins, namely 221 and 521, become the major assembled laminins in late fetal, postnatal and adult heart. Laminins 211/221 and 511/521 display strong affinity for integrin α7β1 (Timpl et al., 2000; Suzuki et al., 2005; Durbeej, 2010; Holmberg and Durbeej, 2013), which starts being produced in the heart at E17.5 (Brancaccio et al., 1998). α7 protein is, however, not detected by immunohistochemistry at E16.5 or E18.5, but becomes clearly detectable around cardiomyocytes from postnatal P1 onwards (van der Flier et al., 1997) and is a major laminin receptor in adult cardiac muscle (Velling et al., 1996; van der Flier et al., 1997; Brancaccio et al., 1998). Interestingly, the appearance of α7 protein in the myocardium coincides with the substitution of the β1A integrin splice variant by the striated muscle-specific β1D integrin in the cardiomyocyte sarcolemma (van der Flier et al., 1997; Brancaccio et al., 1998). Since the α6-integrin is expressed in the myocardium from E8.5 until E15.0 (Thorsteinsdóttir et al., 1995; Hierck et al., 1996), there seems to be a switch in laminin-binding integrins from α6β1A to α7β1D in late fetal development in parallel with the transition between laminins 211/511 and 221/521 in the cardiac basement membranes. Strikingly, these transitions correlate with the reduction of cardiomyocyte proliferation capacity and loss of regeneration capacity (Porrello et al., 2011; Ikenishi et

al., 2012; Sedmera and Thompson, 2011; Ponnusamy et al., 2016). We thus speculate that laminin 221/521- α7β1D-integrin signaling might have a negative impact on the proliferation of cardiomyocytes.

Finally, our data also unveiled a shift in the assembly of laminins 411 and 511 to laminins 421 and 521 in the basement membrane of blood vessels during late fetal, postnatal and adult cardiogenesis (Fig. 9). Despite the preponderance of β2-laminins during these stages, β1-laminins are still assembled in the cardiac matrices. Our observations are in agreement with the presence of α4 and α5-laminins in the coronary vessels in 4-week-old hearts in the mouse and with the role of these laminins during the development of coronary vasculature (Wang et al., 2006).

Conclusions

Our study is the first to describe the spatio-temporal dynamics of laminin isoform assembly during cardiac development. Here we show that the deposition of different laminin matrices correlates with different cardiac development landmarks such as myocardial trabeculation, the development of the coronary vasculature and cardiomyocyte maturation into post-mitotic cells. The results obtained have raised several interesting questions regarding the role of different laminin isoforms during heart development and can hopefully serve as a basis for future studies.

Acknowledgments

We thank Jeff Miner for generously sharing his anti-α5 and anti-α4 and anti-β2 laminin antibodies, Madeleine Durbeej for kindly giving the anti-α1 antibody. The MF20 antibody was developed by D.A. Fischman and was obtained from the Developmental

Studies Hybridoma Bank, developed under the auspices of the NICHD and maintained by The University of Iowa, Department of Biology, Iowa City, IA52242, USA. This work was supported by Fundação para a Ciência e a Tecnologia (FCT, Portugal) project PTDC/SAU-ORG/118297/2010 and FCT scholarships SFRH/BD/86985/2012 (A.M.N), BI-PTDC/SAU-ORG/118297/2010 (A.M.N and A.C.S.) and SFRH/BPD/65370/2009 (M.D.).

References

Aumailley, M., Bruckner-Tuderman, L., Carter, W.G., Deutzmann, R., Edgar, D., Ekblom, P., Engel, J., Engvall, E., Hohenester, E., Jones, J.C. et al. (2005). A simplified laminin nomenclature. *Matrix Biol.* **24**, 326-332.

Beckstead, J. H. (1994). A simple technique for preservation of fixation-sensitive antigens in paraffin-embedded tissues. *J. Histochem. Cytochem.* **42**,1127-11234.

Brancaccio, M., Cabodi, S., Belkin, A. M., Collo, G., Koteliansky, V. E., Tomatis, D., Altruda, F., Silengo, L. and Tarone, G. (1998). Differential onset of expression of alpha 7 and beta 1D integrins during mouse heart and skeletal muscle development. *Cell Adhes. Commun.* **5**, 193-205.

Carboni, N., Marrosu, G., Porcu, M., Mateddu, A., Solla, E., Cocco, E., Maioli, M.A., Oppo, V., Piras, R. and Marrosu, M.G. (2011). Dilated cardiomyopathy with conduction defects in a patient with partial merosin deficiency due to mutations in the laminin-α2-chain gene: a chance association or a novel phenotype? *Muscle Nerve* **44**, 826-828.

Christoffels, V. M., Habets, P. E., Franco, D., Campione, M., de Jong, F., Lamers, W. H., Bao, Z. E., Palmer, S., Biben, C., Harvey, R. P. and Moorman, A. F. M. (2000). Chamber formation and morphogenesis in the developing mammalian heart. *Dev. Biol.* **223**, 266-278.

Cooley, M. A., Fresco, V. M., Dorlon, M. E., Twal, W. O., Lee, N. V., Barth, J. L., Kern, C. B., Iruela-Arispe, M. L., Argraves, W. S. (2012). Fibulin-1 is required during cardiac ventricular morphogenesis for versican cleavage, suppression of ErbB2 and Erk1/2 activation, and to attenuate trabecular cardiomyocyte proliferation. *Dev. Dyn.* **241**, 303-314.

Copp, A.J., Carvalho, R., Wallace, A., Sorokin, L., Sasaki, T., Greene, N.D. and Ybot-Gonzalez, P. (2011). Regional differences in the expression of laminin isoforms during mouse neural tube development. *Matrix Biol.* **30**, 301-309.

Durbeej, M. (2010). Laminins. *Cell Tissue Res.* **339**, 259-268.

Estrach, S., Cailleteau, L., Franco, C. A., Gerhardt, H., Stefani, C., Lemichez, E., Gagnoux-Palacios, L., Meneguzzi, G. and Mettouchi, A. (2011). Laminin-binding integrins induce Dll4 expression and Notch signaling in endothelial cells. *Circ. Res*. **109**, 172-82.

Gawlik, K.I. and Durbeej, M. (2011). Skeletal muscle laminin and MDC1A: pathogenesis and treatment strategies. *Skelet. Muscle* **1**, 9.

Gilbert, S. F. (2013). *Developmental biology*. Sunderland, USA: Sinauer Associates, Inc.

Gonçalves, A. B., Thorsteinsdóttir, S. and Deries, M. (2016). Rapid and simple method for in vivo ex utero development of mouse embryo explants. *Differentiation* **91**, 57-67.

Hierck, B.P., Poelmann, R. E., Iperen, L. V., Brouwer, A. and Gittenberger-Degroot, A. C. (1996). Differential expression of α6 and other subunits of laminin binding integrins during development of the murine heart. *Dev. Dynam.*, **206**, 100-111.

Hill, M. A. (2017). Embryology Main Page. Retrieved July 1, 2017, from https://embryology.med.unsw.edu.au/embryology/index.php/Main_Page.

Hirohata, S., Kusachi, S., Kondo, J., Sano, I., Murakami, M., Doi, M., Ninomiya, Y. and Tsuji, T. (1997). Laminin α1, α2, α4 and β1 chain mRNA expression in mouse embryonic, neonatal, and adult hearts. *Jpn. Heart J.* **38**, 281-289.

Holmberg, J. and Durbeej, M. (2013). Laminin-211 in skeletal muscle function. *Cell Adh Migr.* **7**, 111-121.

Ikenishi, A., Okayama, H., Iwamoto, N., Yoshitome, S., Tane, S., Nakamura, K., Obayashi, T., Hayashi, T. and Takeuchi, T. (2012). Cell cycle regulation in mouse heart during embryonic and postnatal stages. *Develop. Growth Differ.* **54**, 731–738.

Katz, T. C., Singh, M. K., Degenhardt, K., Rivera-Feliciano, J., Johnson, R. L., Epstein, J. A. and Tabin, C. J. (2012). Distinct compartments of the proepicardial organ give rise to coronary vascular endothelial cells. *Dev. Cell* **22**, 639-50.

Kaufmann, M. H. (1992). *The Atlas of Mouse Development*. Cambridge, USA: Academic Press.

Kelly, R. G., Buckingham, M. E. and Moorman, A. F. (2014). Heart Fields and Cardiac Morphogenesis. *Cold Spring Harb. Perspect. Med*. **4**, a015750.

Kim, H., Yoon, C.S. and Rah, B. (1999). Expression of extracellular matrix components fibronectin and laminin in the human fetal heart. *Cell Struct. Funct.*, **24**, 19-26.

Kirby, M. L. and Waldo, K. (2007). *Cardiac Development.* New York, USA: Oxford University Press.

Knöll, R., Postel, R., Wang, J., Krätzner, R., Hennecke, G., Vacaru, A. M., Vakeel, P., Schubert, C., Murthy, K., Rana, B. K., and Bakkers, J. (2007). Laminin-alpha4 and integrin-linked kinase mutations cause human cardiomyopathy via simultaneous defects in cardiomyocytes and endothelial cells. *Circ.* **116**, 515-525.

Komiyama, M., Ito, K. and Shimada, Y. (1987). Origin and development of the epicardium in the mouse embryo. *Anat. Embryol.* **176**, 183-189.

Lavine, K. J., Yu, K., White, A.C., Zhang, X., Smith, C., Partanen, J., Ornitz, D. M. (2005). Endocardial and epicardial derived FGF signals regulate myocardial proliferation and differentiation in vivo. *Dev. Cell*, **8**, 85-95.

LeBleu, V.S., Macdonald, B. and Kalluri, R. (2007). Structure and function of basement membranes. *Exp. Biol. Med. (Maywood)* **232**, 1121-1129.

Legate, K. R., Montañez, E., Kudlacek, O. and Fässler, R. (2006). ILK, PINCH and parvin: the tIPP of integrin signalling. *Rev. Mol. Cell Biol.*, **7**, 20–31.

Li, S., Harrison, D., Carbonetto, S., Fassler, R., Smyth, N., Edgar, D. and Yurchenco, P.D. (2002). Matrix assembly, regulation, and survival functions of laminin and its receptors in embryonic stem cell differentiation. *J. Cell Biol.* **157**, 1279-1290.

Little, C. D., Piquet, D.M., Davis, L.A., Walters, L. and Drake, C. J. (1989). Distribution of laminin, collagen type IV, collagen type I, and fibronectin in chicken cardiac jelly/basement membrane. *Anat, Rec.* **224**, 417-25.

Liu, Z. J., Shirakawa, T., Li, Y., Soma, A., Oka, M., Dotto, G. P., Fairman, R. M., Velazquez, O. C. and Herlyn M. (2003). Regulation of Notch1 and Dll4 by vascular endothelial growth factor in arterial endothelial cells: implications for modulating arteriogenesis and angiogenesis. *Mol. Cell Biol.* **23**, 14-25.

Luxán, G., D'Amato, G., MacGrogan, D., de la Pompa, J. L. (2016). Endocardial Notch Signaling in Cardiac Development and Disease. *Circ. Res.* **118**, e1-e18.

Marques, J., Duarte, S.T., Costa, S., Jacinto, S., Oliveira, J., Oliveira, M.E., Santos, R., Bronze-da-Rocha, E., Silvestre, A.R., Calado, E. et al. (2014). Atypical phenotype in two patients with LAMA2 mutations. *Neuromuscul. Disord.* **24**, 419-424.

McKee, K.K., Harrison, D., Capizzi, S. and Yurchenco, P.D. (2007). Role of laminin terminal globular domains in basement membrane assembly. *J. Biol. Chem.* **282**, 21437-21447.

Miner, J. H., Cunningham, J. and Sanes, J. R. (1998). Roles for laminin in embryogenesis: exencephaly, syndactyly, and placentopathy in mice lacking the laminin alpha5 chain. *J. Cell Biol.* **143**, 1713-1723.

Nakajima, Y., Morishima, M., Nakazawa, M., Momma, K. and Nakamura, H. (1997). Distribution of fibronectin, type I collagen, type IV collagen, and laminin in the cardiac jelly of the mouse embryonic heart with retinoic acid-induced complete transposition of the great arteries. *Anat. Rec.* **249**, 478-85.

Nimmagadda, S., Geetha-Loganathan, P., Pröls, F., Scaal, M., Christ, B. and Huang, R. (2007). Expression pattern of Dll4 during chick embryogenesis. *Histochem. Cell Biol.* **128**, 147-152.

Nunes, A. M., Wuebbles R. D., Sarathy A., Fontelonga T. M., Deries M., Burkin D.J. and Thorsteinsdóttir S. (2017). Impaired fetal muscle development and JAK-STAT activation mark disease onset and progression in a mouse model for merosin-deficient congenital muscular dystrophy. *Hum. Mol. Genet.* **26**, 2018–2033.

Paige, S. L., Plonowska, K., Xu, A. and Wu, S. M. (2015). Molecular regulation of cardiomyocyte differentiation. *Circ. Res.* **116**, 341-353.

Patton, B. L., Miner, J. H., Chiu, A. Y. and Sanes, J. R. (1997). Distribution and function of laminins in the neuromuscular system of developing, adult, and mutant mice. *J. Cell Biol.* **139**, 1507-1521.

Paulsson, M. (1994). *Biosynthesis, tissue distribution and isolation of laminins. In The Laminin*s, Amsterdam, Netherlands: Harwood Academic Publishers.

Pennisi, D. J., Ballard, V. L. T. and Mikawa, T. (2003). Epicardium is required for the full rate of myocyte proliferation and levels of expression of myocyte mitogenic factors FGF2 and its receptor, FGFR-1, but not for transmural myocardial patterning in the embryonic chick heart. *Dev. Dyn.* **228**, 161–172.

Ponnusamy, M., Li, P.F. and Wang, K. (2016). Understanding cardiomyocyte proliferation: an insight into cell cycle activity. *Cell Mol. Life Sci.* **74**, 1019-1034.

Porrello, E. R., Mahmoud, A. I., Simpson, E., Hill, J. A., Richardson, J. A., Olson, E. N., Sadek, H. A. (2011). Transient regenerative potential of the neonatal mouse heart. *Science* **331**, 1078-1080.

Roediger, M., Miosge, N, and Gersdorff, N. (2010). Tissue distribution of the laminin β1 and β2 chain during embryonic and fetal human development. *J. Mol. Hist.* **41**, 177–184.

Rogers, R. S. and Nishimune, H. (2016). The role of laminins in the organization and function of neuromuscular junctions. *Matrix Biol.*, **57-58**, 86-105.

Samsa, L. A., Yang, B. and Liu, J. (2013). Embryonic cardiac chamber maturation: trabeculation, conduction and cardiomyocyte proliferation. *Am. J. Med. Genet. Part C. Semin. Med. Genet.* **163**, 157-168.

Savolainen, S. M., Foley, J. F. and Elmore, S. A. (2009). Histology atlas of the developing mouse heart with emphasis on E11.5 to E18.5. *Toxicol. Pathol*. **37**, 395-414.

Sedmera, D. and Thompson, R. P. (2011). Myocyte proliferation in the developing heart. Dev. Dyn. **240**, 1322-1324.

Small, E.M. and Krieg, P.A. (2004). Molecular regulation of cardiac chamber-specific gene expression. *Trends Cardiovasc. Med.* **14**, 13-18.

Smirnov, S.P., McDearmon, E.L., Li, S., Ervasti, J.M., Tryggvason, K. and Yurchenco, P.D. (2002). Contributions of the LG modules and furin processing to laminin-2 functions. *J. Biol. Chem.* **277**, 18928-18937.

Stenzel, D., Franco, C. A., Estrach, S., Mettouchi, A., Sauvaget, D., Rosewell, I., Schertel, A., Armer, H., Domogatskaya, A., Rodin, S. et al. (2011). Endothelial basement membrane limits tip cell formation by inducing Dll4/Notch signalling in vivo. *EMBO Rep.* **12**, 1135-1143.

Suzuki, N., Yokoyama, F. and Nomizu, M. (2005). Functional sites in the laminin alpha chains. *Connect. Tissue Res.* **46**, 142-152.

Takahashi, M., Yamagishi, T., Narematsu, M., Kamimura, T., Kai, M. and Nakajima, Y. (2014). Epicardium is required for sarcomeric maturation and cardiomyocyte growth in the ventricular compact layer mediated by transforming growth factor β and fibroblast growth factor before the onset of coronary circulation. *Congenit. Anom.* **54**, 162-171.

Thorsteinsdóttir, S., Roelen, B. A., Freund, E., Gaspar, A. C., Sonnenberg, A. and Mummery, C. L. (1995). Expression patterns of laminin receptor splice variants α6Aβ1 and α6Bβ1 suggest different roles in mouse development. *Dev. Dyn.* **204,** 240-58.

Timpl, R., Tisi, D., Talts, J.F., Andac, Z., Sasaki, T. and Hohenester, E. (2000). Structure and function of laminin LG modules. *Matrix Biol.* **19**, 309-317.

Tsiper, M.V. and Yurchenco, P.D. (2002). Laminin assembles into separate basement membrane and fibrillar matrices in Schwann cells. *J. Cell. Sci.* **115**, 1005-1015.

van der Flier, A., Gaspar, A.C., Thorsteinsdóttir, S., Baudoin, C., Groeneveld, E., Mummery, C.L. and Sonnenberg, A. (1997). Spatial and temporal expression of the β1D integrin during mouse development. *Dev. Dyn.* **210**, 472-486.

Velling, T., Collo, G., Sorokin, L., Durbeej, M., Zhang, H. and Gullberg, D. (1996). Distinct alpha 7A beta 1 and alpha 7B beta 1 integrin expression patterns during mouse development: alpha 7A is restricted to skeletal muscle but alpha 7B is expressed in striated muscle, vasculature, and nervous system. *Dev. Dyn.* **207**, 355-371.

Vincent, S. D., Buckingham, M. E. (2010). How to make a heart: the origin and regulation of cardiac progenitor cells. *Curr. Top. Dev. Biol.* **90**, 1-41.

Wang, J., Hoshijima, M., Lam, J., Zhou, Z., Jokiel, A., Dalton, N. D., Hultenby, K., Ruiz-Lozano, P., Ross, J. Jr., Tryggvason, K. and Chien, K. R. (2006). Cardiomyopathy associated with microcirculation dysfunction in laminin alpha4 chain-deficient mice. *J. Biol. Chem.* **281**, 213-220.

Wu, S. M., Chien, K. R., Mummery, C. (2008). Origins and fates of cardiovascular progenitor cells. *Cell* **132**, 537-542.

Wu, B., Zhang, Z., Lui, W., Chen, X., Wang, Y., Chamberlain, A. A., Moreno-Rodriguez, R. A., Markwald, R. R., O'Rourke, B. P. and Sharp, D. J. (2012). Endocardial cells form the coronary arteries by angiogenesis through myocardial-endocardial VEGF signaling. *Cell* **151**, 1083-1096.

Yang, X., Dormann, D., Münsterberg, A.E. and Weijer, C.J. (2002). Cell movement patterns during gastrulation in the chick are controlled by positive and negative chemotaxis mediated by FGF4 and FGF8. *Dev. Cell* **3**, 425-437.

Yousif, L. F., Di Russo, J. and Sorokin, L. (2013). Laminin isoforms in endothelial and perivascular basement membranes. *Cell Adh. Migr.* **7**, 101-110.

Yurchenco, P.D. (2015). Integrating activities of laminins that drive basement membrane assembly and function. *Curr. Top. Membr.* **76**, 1-30.

Zhou, B., Ma, Q., Rajagopal, S., Wu, S. M., Domian, I., Reviera-Feliciano, J., Jiang, D., von Gise, A., Ikeda, S., Chien, K. R. and Pu, W. T. (2008). Epicardial progenitors contribute to the cardiomyocyte lineage in the developing heart. *Nature* **454**, 109-113.

CHAPTER 6

Discussion

Discussion

This thesis provides a detailed view of laminin isoform diversity throughout striated muscle development, and strengthens the current concept that laminins are not mere static identities in basement membranes, only providing physical support. Rather, the observation that laminin matrices are heterogeneous in terms of isoform content and that they change over development time, provides support for the concept that laminins play an active and important role in cell signaling, which may be isoform specific (Domogatskaya et al., 2012; Aumailley, 2013). Moreover, this thesis demonstrates for the first time that laminin 211 is required during fetal skeletal myogenesis and may thus play specific roles in skeletal muscle development that cannot be compensated for by the other laminins present in the fetal muscles.

In this Chapter, we will discuss the relevance of the results presented throughout this thesis. First, we will focus on the question of laminin diversity, with particular emphasis on muscle development. Then, we will discuss the parallelisms between the laminin matrices in skeletal and cardiac muscles. Finally, we will address some specific points on the potential role of laminin 211 in regulating the identity of muscle stem cells and the potential new avenues for the treatment of MDC1A.

6.1. Laminin diversity during cardiac and skeletal muscle development

Laminins are present in all basement membranes, and are essential components of these matrices. They are the first to be assembled and allow the incorporation of collagen type IV matrices into the nascent basement membrane (Smirnov et al., 2002; Li et al., 2002; Tsiper and Yurchenco, 2002; McKee et al., 2007; Yurchenco, 2015). Other

components such as perlecan and nidogen form bridges between laminin and collagen IV networks, ensuring the proper structure of basement membranes (LeBleu et al., 2007; McKee et al., 2007; Behrens et al., 2012; Hohenester and Yurchenco, 2013). Laminin matrices are major contributors for basement membrane diversity, as the laminin family is composed of at least 16 different isoforms. These different isoforms were described in several tissues such as the vascular and the immune system, the peripheral and central nervous system, and in organs like the pancreas and kidney (Domogatskaya et al., 2012). In this section, we will discuss laminin diversity both in general and from the point of view of striated muscle development.

Laminins have evolved since early animal diversification and are present in both Radiata and Bilateria (Domogatskaya et al., 2012). Diversification of laminin chains has generated a variety of different α, β and γ chains in the vertebrates (Domogatskaya et al., 2012; Fig. 1). Among the described laminin isoforms, up to 8 different laminin isoforms were identified in the embryonic/fetal and adult skeletal muscle in the mouse (Durbeej, 2010; Thorsteinsdóttir et al., 2011). In adult heart, laminins are known to be assembled around cardiomyocytes (Kim et al., 1999). Laminins bind to different receptors such as integrins and dystroglycan via the LG domains in the C-terminal of laminin α chains (Durbeej et al., 2010; Hohenester and Yurchenco, 2013; Yurchenco, 2015). Although laminin β and γ chains affect the binding affinity as well, the underlying mechanism is unknown (Ido et al., 2008; Taniguchi et al., 2009). Not surprisingly, laminin-binding receptors have also evolved since early animal diversification. For instance, dystroglycan originated after the divergence of Ctenophores from Porifera and Eumetazoans (Adams and Brancaccio, 2015), while integrins arose even before the emergence of metazoans

(Johnson et al., 2009). Therefore, the combination of different laminins and laminin-binding receptors has generated an incredible diversity in the possible outcomes of laminin signaling in basement membranes.

During embryonic development, laminins are first assembled in the pre-implantation embryo (Leivo et al., 1980; Thorsteinsdóttir, 1992). Laminin 111 is the most abundant laminin in Reichert's membrane, while laminin 511 is first assembled in the inner cell mass and the earliest embryonic basement membrane (Klaffky et al., 2001; Miner et al., 2004). *Lamc1*-null embryos die before implantation demonstrating that the basement membrane of the inner cell mass is essential for development (Smyth et al., 1999). Even though the dynamics of laminin assembly during embryogenesis has been described in a few cases, such as in the case of intestinal development (Lefebvre et al., 1999), most studies to date have focused on the presence of laminins in the adult, thus underestimating their roles during embryonic development (Nguyen and Senior, 2006; Domogatskaya et al., 2012; Spenlé et al., 2013). In this thesis, we try to fill in the gap in the literature regarding the diversity of laminin matrices during cardiac and skeletal muscle development.

We provide the first comprehensive view of what isoforms are present in the laminin matrices during several different stages of skeletal (**Chapter 2** and **3**) and cardiac (**Chapter 5**) muscle development. In **Chapter 2** and **3**, we demonstrated that cycles of laminin assembly and disassembly define specific microenvironments for myogenic cells at different phases of skeletal muscle development. In **Chapter 5**, we also show that a number of laminin isoforms are present in the matrices of the heart and they display developmentally regulated changes throughout cardiac development. Furthermore, we

illustrate laminin matrix diversity along the development of these muscles and highlight the coexistence of specific laminins in both skeletal and cardiac muscle basement membranes. For instance, we found that laminins 111 and 511 are assembled in the dermomyotome basement membrane, but coexist with laminins 211/221 and/or 121 and

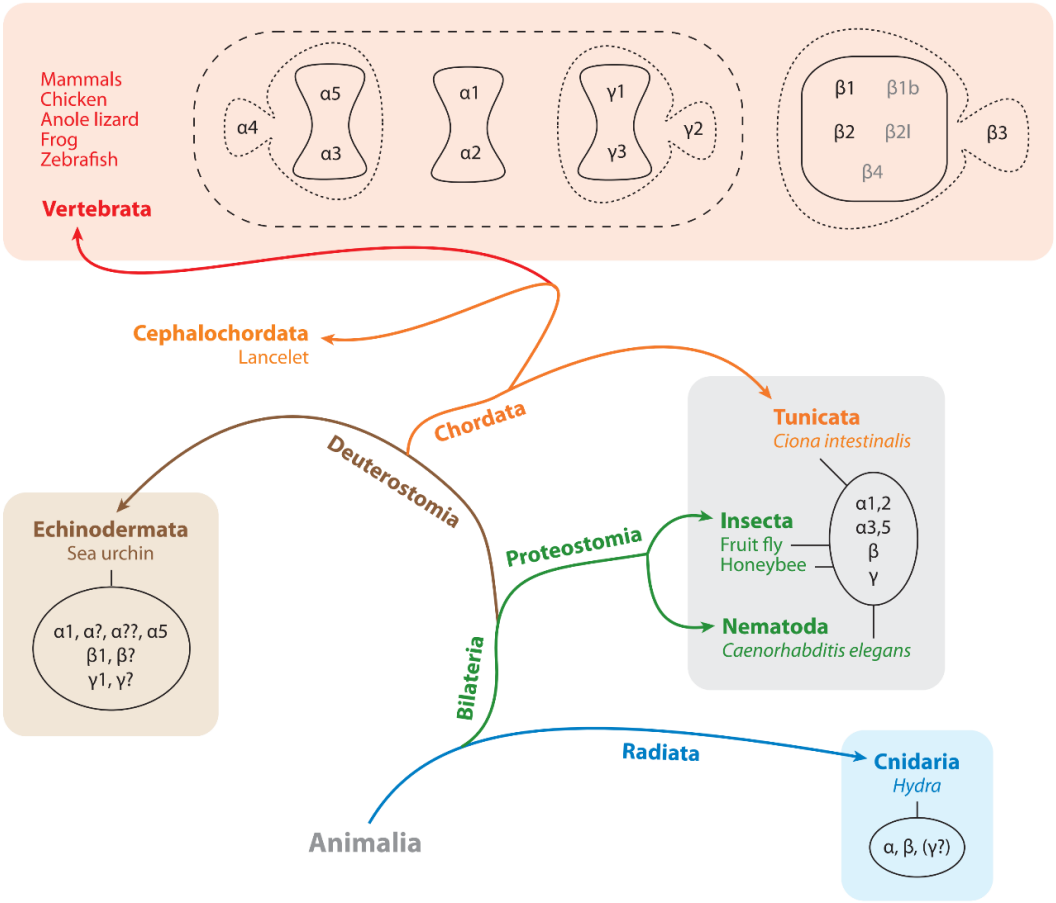

Figure 1- Evolution of the laminin family. Evolutionary tree of the laminin chain family depicting the evolution of different laminin chains along animal diversification. Radiata is represented by *Hydra*, which has only one laminin trimer. Bilateria branch splits into the Protostomia and the Deuterostomia. Protostomia is represented by the insects such as the fruit fly and honeybee and the nematode *Caenorhabditis elegans*, which have two α, one β, and one γ laminin chains that can form two isoforms. Deuterostomia splits into Echinodermata and Chordata. Echinodermata is represented by the sea urchin, which has developed extra α, β, and γ chains. Chordata further splits into Tunicata, Cephalochordata and Vertebrata. Tunicata, represented by the sea squirt, *Ciona intestinalis*, has two α, one β, and one γ laminin chains like the insects and nematodes. The laminin composition in the Cephalochordata (lancelet) is unknown. Vertebrata, represented by mammals, chicken, anole lizard, frog and zebrafish, have five α chains, three β chains and three γ chains. Paralogs were found for laminin β1 and β2 chains (β1b and β2l in gray). No heterodimers with laminin β4 have been described. Evolutionarily conserved protein similarity clusters of laminin chains, are indicated at the top by the solid, dotted, and dashed lines. Adapted from Domogatskaya et al., 2012.

521 in the myotome basement membrane (Table 1A). This suggests simultaneous assembly of laminin isoforms with different combinations of α and β chains. In the

A

	Myotome development		Primary myogenesis			Secondary myogenesis		
	E10.5	E10.5	E11.5	E12.5	E13.5	E14.5	E15.5	E17.5
	DM	M	MF	MF	MF	MF	MF	MF
α1	✓	✓	na	spotty	na	na	na	×
α2	✓	✓	na	spotty	✓	✓	✓	✓
α4	×	×	×	×	✓	✓	✓	✓
α5	✓	✓	×	spotty	na	✓	✓	✓
β1	✓	✓	spotty	na	na	✓	✓	✓
β2	✓	✓	na	na	na	na	na	na
γ1	na	na	spotty	na	na	✓	✓	✓

B

Endocardium-Myocardium basement membrane							
	E9.5	E10.5	E12.5	E14.5	E17.5	P10	Adult
α1	✓	✓	✓	×	na	na	na
α2	×	×	✓	✓	✓	✓	
α4	✓	✓	✓	✓	✓	×	×
α5	✓	✓	✓	✓	✓	✓	✓
β1	✓	✓	✓	✓	×	✓	✓
β2	✓	✓	✓	✓	✓	✓	✓
γ1	na	✓	✓	✓	✓	na	na
Cardiomyocyte basement membrane							
	E9.5	E10.5	E12.5	E14.5	E17.5	P10	Adult
α1	×	×	×	×	na	na	na
α2	×	×	✓	✓	✓	✓	✓
α4	×	×	?	×	×	×	×
α5	×	×	×	✓	✓	✓	✓
β1	×	×	✓	✓	✓	✓	✓
β2	×	×	×	×	✓	✓	✓
γ1	na	×	✓	✓	✓	na	na
Subepicardial basement membrane							
	E10.5	E12.5	E14.5	E17.5	P10	Adult	
α1	×	✓	×	na	na	na	
α2	×	✓	×	✓	✓	×	
α4	×	×	×	×	×	×	
α5	✓	✓	✓	✓	✓	✓	
β1	✓	✓	✓	✓	✓	×	
β2	×	×	×	×	✓	✓	
γ1	✓	✓	✓	✓	na	na	

Table 1- Distribution of laminin chains during the development of skeletal and cardiac muscles. (**A**) Table depicting the presence of different laminin chains during skeletal muscle development. (**B**) Tables representing the distribution of different laminin chains in the endocardium-myocardium, cardiomyocyte and subepicardial basement membranes. DM, Dermomyotome; M, Myotome; na, not assayed; ✓, present; ×, absent; ?, proposed presence.

embryonic cardiac muscle, this diversity is exemplified by the presence of a number of possible combinations, namely laminins 111/121, 211/221, 411/421 and 511/521 in the cardiac jelly (Table 1B).

The fact that different laminins might have evolved and gained distinct functions suggests that this diversity might have accompanied the increasing complexity of skeletal muscle development during evolution. For example, it is interesting to note that the laminin composition of early mouse skeletal muscles is different from that of the zebrafish. During zebrafish development, *Lama2*, *Lamb2* and *Lamc1* are expressed in fast and slow myofibers of trunk muscles, while *Lama4* is expressed in the cells adjacent to the fibers (Sztal et al., 2011). Interestingly, *Lamb1* is expressed only transiently at the onset of myogenesis and *Lama1* and *Lama5* are never expressed in myogenic cells (Sztal et al., 2011). This suggests that laminin 221 is the main laminin in zebrafish trunk muscles, in contrast to the mouse, where a huge diversity of laminins is expressed, assembled, disassembled and assembled again from myotome formation to secondary myogenesis (**Chapter 2** and **3**). In the mouse, laminin 211 is the main laminin in the adult myofiber basement membrane, while laminin 221 is restricted to the specialized neuromuscular junctions (Patton et al., 1997; Patton, 2000; **Chapter 2**). Thus, it appears that in zebrafish, the final skeletal muscle laminin composition is achieved much earlier than in the mouse. This may be because in fish, the myotomes develop directly into the definitive muscles of the adult fish. In contrast, in mammals, the myotomes are transient embryonic structures which later in development, undergo translocation, re-orientation, elongation and cleavage to form the definitive axial muscles (Deries et al., 2010).

When we consider the laminin diversity in the basement membranes highlighted in this thesis, interesting questions arise: What are the functional differences between laminin isoforms? Do some laminins compensate for each other? To answer these questions, a detailed analysis of skeletal and cardiac development in different laminin deficient models is needed. Some possibilities will be discussed in the next section.

6.2. Laminins within skeletal and cardiac muscle tissues

6.2.1. On the specificity of laminin isoforms during cardiac and skeletal muscle development

In **Chapter 2**, **3** and **5**, we performed a thorough description of laminin isoform dynamics in skeletal and cardiac muscles, which unveils both common and distinct patterns for these two types of striated muscles (Table 1). In this section, we will discuss the specificities of laminin signaling in skeletal and cardiac muscles, and the parallelisms between laminin matrices during the development of these muscles.

Different studies have highlighted situations where laminin isoforms compensate for each other and others where the same laminins do not. For instance, laminin 511 compensates for the absence of laminin 111 in early embryonic basement membrane (Miner et al., 2004), but not in the myotomal basement membrane (Anderson et al., 2009), nor in Reichert's membrane (Miner et al., 2004). In the blood vessel basement membrane, α5-laminins were shown to partially compensate for the absence of α4-laminins, and the presence of α5-laminins has been suggested to delay the emergence of cardiac dysfunction in *Lama4* null mice until 36-40 weeks of age (Wang et al., 2006).

Interestingly, in other cases, the absence of certain laminins seems to activate a "back-up system" by increasing the synthesis and assembly of other laminins, although this does not always reflect an effective rescue. This is exemplified in *Lamb2* null mice, where the assembly of β1-laminins is increased in the *Lamb2*$^{-/-}$ synaptic basement membrane, but these mice still display deficient synaptic maturation (Patton et al., 1997).

On the contrary, in the *dy*^{W} *Lama2* deficient mice, it has been suggested that α4- and α5-laminins can compensate for the absence of laminins 211/221 during myogenesis *in utero* (Patton et al., 1997; Ringelmann et al., 1999). However, our study reported in **Chapter 2** challenges this view by demonstrating that *dy*$^{W-/-}$ muscles display a myogenesis defect during fetal myogenesis (**Chapter 2**). This does not exclude the possibility that α4- and α5-laminins may compensate partially for the absence of α2-laminins, for instance, by compensating for the absence of laminin 211 in the myofiber basement membrane. Nonetheless, it clearly shows that they cannot compensate completely. Further studies are necessary to address this hypothesis.

Our results in **Chapter 2** also show that no major myogenesis defects are found during myotome development and that the myotome basement membrane is assembled in the absence of α2-laminins. The absence of laminins 211/221 is probably compensated for by laminin 111 at this stage, which plays a major role in the assembly of the myotome basement membrane (Anderson et al., 2009). In fact, as discussed in **Chapter 2** and **Chapter 4**, laminin 111, which is closely related to laminin 211 (Durbeej, 2010; Domogatskaya et al., 2012), when expressed or delivered to the muscles of *Lama2* deficient mice, is able to significantly improve their phenotype (Gawlik et al., 2004; Rooney et al., 2012; Van Ry et al., 2013). Laminins 111 and 211 not only display similarities

in protein structure but they also bind with similar affinities to the same receptors (Nishimune et al., 2008; Durbeej, 2010). However, laminin 111 is mostly an "embryonic laminin" since it is widely present in basement membranes during embryonic development and often downregulated in adult tissue, such as the case of skeletal muscle (Patton et al., 1997; Ekblom et al., 2003). In addition, the results detailed in **Chapter 2** raise the interesting possibility that laminin 211 is not only important for the maintenance of the post-mitotic myofiber, but also plays an important role in the expansion of Pax7-positive cells. This hypothesis is supported by a previous study showing that injection of laminin 111 in *dyW*$^{-/-}$ adult mice, the protein levels of Pax7 are significantly increased and regeneration capacity is improved (Van Ry et al., 2013). Thus, it is possible that laminins 111 and 211 share the capacity of maintaining the undifferentiated state of Pax7-positive cells, but that laminins 411 and 511 are not able to perform this function.

In **Chapter 5**, we focus our analysis on the thorough description of laminin matrices during cardiac development. Our results demonstrate that the cardiac tissue initially assembles several laminins in the cardiac jelly, but then solely produces laminin 521 in the endocardium-myocardium interface and in the subepicardial matrix. In the cardiomyocyte and subepicardial basement membranes, α2- and α5-laminins coexist during most of cardiac development. Strikingly, MDC1A patients (lacking the α2 laminin chain) rarely develop severe cardiomyopathy (Carboni et al., 2011; Gawlik and Durbeej, 2011; Marques et al., 2014), even though 30% of patients display left ventricle dysfunction (Gawlik and Durbeej, 2011). This suggests that either laminins 211/221 are less important in the cardiomyocyte basement membrane, when compared to their role in the skeletal muscle myofibers, and/or that other laminins compensate. The most probable candidates are

laminins 511 and 521, which coexist with laminins 211 and 221, respectively, throughout cardiac development. The mechanism by which laminins 511 and 521 completely compensate for the absence of laminins 211 and 221 in cardiac muscle is unclear, but it might be related with cardiomyocyte proliferation and maturation requirements. Laminins 111 and 511 might play a role in maintaining the more undifferentiated and proliferative state of cardiomyocytes, which is similar to their role in maintaining the undifferentiated state of cells in the dermomyotome (Bajanca et al., 2006). In contrast, laminins 221 and 521 might be involved in cardiomyocyte maturation. Taking together our results and previous literature, we propose that laminins 511 and 521 might exert a compensatory effect in the absence of laminins 211 and 221, respectively, in cardiac muscle. In skeletal muscle, it is uncertain why laminin 511 is not able to compensate for the absence of laminin 211 while both are present. One possibility is that laminin 511 can compensate for laminin 211 in terms of maintaining myofiber stability as discussed above on this section, but not in the maintenance of Pax7-positive muscle stem cells. Furthermore, laminins 411 and 511 are apparently downregulated around muscle fibers in the adult (Ringelmann et al., 1999) and thus laminin 211 becomes the only laminin isoform present around muscle fibers.

6.2.2. “Skeletal” laminins versus “cardiac” laminins

In spite of their common striated appearance, muscle development and regeneration processes differ substantially between skeletal and cardiac muscle. The development and regeneration of skeletal muscle is dependent on the pool of muscle stem cells, which is maintained throughout development *in utero* and in the adult

(Tajbakhsh, 2009; Lepper et al., 2011; Thorsteinsdóttir et al., 2011). The formation and elongation of the early heart tube is dependent on progenitors from the two heart fields. However, after the heart tube stages, cardiac muscle growth is dependent on cardiomyocyte proliferation (Sedmera and Thompson, 2011). Similarly, cardiac regeneration/repair is dependent on cardiomyocyte proliferation (Beltrami et al., 2001; Senyo et al., 2013). In mammals, cardiomyocyte proliferation progressively decreases during postnatal development (Ikenishi et al., 2012; Sedmera and Thompson, 2011; Ponnusamy et al., 2016), but in lower vertebrates such as the zebrafish, cardiomyocyte proliferation and regeneration capacity is maintained in the adult (Jopling et al., 2010; Kikuchi et al., 2010). To our knowledge there are currently no studies about the specific laminin isoforms that compose the cardiac basement membranes in the zebrafish heart. However, a comparative study into the laminin profile in mouse and zebrafish cardiac muscle might shed some light into the role of different laminin isoforms in the proliferation of cardiomyocytes.

The results detailed in **Chapter 2**, **3** and **5** point for several specificities of laminin matrices in the skeletal and cardiac basement membranes. However, we also found some parallelisms between skeletal and cardiac laminin matrices. Similar to skeletal muscle, we demonstrated in **Chapter 5** that α1- and α2-laminins coexist in the cardiac jelly during early stages of cardiac muscle development (Table 1). Thus, these laminins coexist only during a short period of muscle development in both types of muscle. These results are congruent with the hypothesis that laminin α1 and α2 chains have common functions as described above in section 6.2.1.

We also described the presence of β1-laminins in the dermomyotome basement membrane contacting with Pax3/Pax7-positive cells, and in the myofiber basement membrane lining the Pax7-positive muscle stem cells (**Chapter 3**). Interestingly, the assembly of β1-laminins is also widespread during early stages of cardiogenesis, while β2-laminins are later assembled around the most mature and eventually post-mitotic cardiomyocytes. In skeletal muscle, β1- and β2-laminins are assembled early in the myotomal basement membrane, but then β2-laminins become restricted to the neuromuscular junctions (Patton et al., 1997; Patton, 2000). The reason for this switching from β1- to β2-laminins in cardiac muscle and its developmental consequence is currently not clear. Future studies, as for example studies with knock-in mice where the β1 and β2 chains are conditionally swapped in different subsets of cells, might clarify the relevance of this switch during cardiac muscle development.

6.3. New paths for Merosin-deficient congenital muscular dystrophy type 1A

6.3.1. Insights into the mechanism underlying MDC1A

Merosin-deficient congenital muscular dystrophy type 1A is a severe neuromuscular disease in which muscle weakness is evident from birth. In this thesis, we provide new insights into the mechanism underlying MDC1A onset. The results detailed in **Chapter 2** set a paradigm shift in the understanding of this disease by demonstrating for the first time that MDC1A starts manifesting itself during development *in utero* and involves an impairment in fetal muscle growth. We demonstrate that the impairment in

fetal muscle growth is associated with a decrease in the number of Pax7-positive muscle stem cells and Myogenin-positive cells, suggesting that laminin 211 regulates the expansion and differentiation of Pax7-positive cells. Results detailed in **Chapter 3** raise the possibility that only a subset of Pax7-positive muscle stem cells is capable of producing their own laminin niche. If this is confirmed for more fetal stages than the ones assayed in **Chapter 3**, it is conceivable that these cells would be the most affected by the absence of laminin 211. A recent study has shown that muscle stem cells actively modulate tenascin-C, fibronectin and collagen VI in their ECM microenvironment in a time dependent manner during fetal, postnatal and adult muscle development and the authors suggest that the precise ECM composition of the muscle stem cell niche plays a role in their developmental stage identity (Tierney et al., 2016). We suggest that the absence of laminin 211 during fetal stages might lead to changes in the ECM niche which accelerates the transition of some muscle stem cells from a fetal identity into a postnatal identity. This implies that laminin 211 might function as a cell age identity marker similar to tenascin-C, fibronectin and collagen VI (Tierney et al., 2016).

As discussed in **Chapter 3**, Pax7-positive cells are a heterogeneous population expressing different levels of Pax7 (Rocheteau et al., 2012). Most Pax7-positive cells have activated the *Myf5* gene at some point throughout their lives and only 10% of Pax7-positive cells never expressed *Myf5* (Kuang et al., 2007). Strikingly, in an independent study, another population corresponding to 10% of Pax7-positive cell population was shown to express high levels of Pax7 and to maintain the most basal stem cell identity (Rocheteau et al., 2012). Even though there is no correlation between the described populations in these two studies, it is tempting to speculate that these populations might

constitute a single population of adult “super” muscle stem cells. It would be very interesting to determine if that is so, whether this population is also the one that produces laminins at E14.5 and what role these cells play during fetal development and the onset of MDC1A in *dy*^{W} fetuses.

Further studies are needed to dissect the mechanism by which laminin 211 signals during fetal development. First, it is important to characterize *dy*$^{W-/-}$ Pax7-positive cells by studying the transcriptome of these cells, the capacity of these cells to produce their niche, and their capacity to proliferate and differentiate under the influence of laminin 211 deficient niches. Second, it is important to determine what other signaling pathways are modulated by laminin 211 signaling. Finally, it is also important to study the cross-talk between the fiber and the muscle stem cell in the absence of laminin 211.

6.3.2. What’s next? New avenues for the treatment of MDC1A

Congenital muscular dystrophies comprise a vast group of different pathologies with an estimated prevalence around 7 in 100 000 births (Gawlik and Durbeej, 2011). MDC1A is among the most severe types of congenital muscular dystrophy and accounts for approximately 40% of cases of congenital muscular dystrophy in Europe (Gawlik and Durbeej, 2011). Several treatments have been shown to ameliorate disease pathology in laminin α2-deficient mice (Gawlik et al., 2004; Bentzinger et al., 2005; Qiao et al., 2005; Xu et al., 2007; Doe et al., 2011; Meinen et al., 2011; Rooney et al., 2012; Secco et al., 2013; Van Ry et al., 2013). However, currently there is no available treatment for MDC1A patients.

Laminins 211, 411 and 511 constitute the myofiber basement membrane in fetal muscle, but laminin 211 is the main laminin in the myofiber basement membrane of adult muscle (Patton et al., 1997; **Chapter 2**) since laminins 411 and 511 are absent during postnatal development (Ringelmann et al., 1999). It is generally accepted that the total absence of laminins in the basement membrane causes stress upon the myofiber and leads to the initiation of muscle degeneration (Ringelmann et al., 1999). We suggest that this process follows the primary defect described in **Chapter 2** and exacerbates the primary muscle defect caused by the absence of α2-laminins. Therefore, our study unveils the importance of focusing on the primary defect of myogenesis (i.e. impaired cell-mediated hypertrophy of fetal muscle fibers), rather than directing treatment efforts exclusively to alleviate the degeneration muscle defect. Moreover, this thesis reinforces the need to define the mechanisms underlying the onset and progression of this disease in order to set up combined treatments, as these can tackle not only the degeneration defects arising after birth, but also the primary defect that starts *in utero*.

In **Chapter 4**, we detail the development of different techniques that can possibly be used as tools to study fetal muscle development, including the onset and progression of MDC1A in the *dy*^{W} mouse model. In particular, we highlight the potential of *in utero* injections of laminin 111 to study fetal muscle development *in vivo* and to evaluate the effects of early interventions on MDC1A progression.

Future studies using *in utero* injections of laminin 111 and/or drugs targeting for example JAK-STAT and Myostatin signaling pathways might provide an important insight and open up new avenues for the treatment of patients after birth. Combined treatments targeting the myogenesis defect identified in the fetus, and which we suggest continues

postnatally, as well the subsequent muscle degeneration might prove to be an efficient path to treat patients, particularly in early stages of the disease.

6.4 Final considerations

This thesis provides new insights into laminin diversity during skeletal and cardiac muscle development and reveals the dynamics of assembly and disassembly of laminin isoforms. It further sets a paradigm shift in the understanding of MDC1A, where we demonstrate that the primary defect is a myogenesis defect instead of the classically assumed fibrotic process caused by damage of muscle fibers. We unveil a new role for laminin 211, until now generally accepted as a laminin of "mature and differentiated post-mitotic myofibers", in playing a role in regulating the behavior of Pax7-positive muscle stem cells, which opens new treatment avenues for MDC1A. Furthermore, this thesis provides preliminary work on the development of different techniques to study fetal development of skeletal muscle, which might be useful for a wide range of studies. Overall, this thesis provides a framework to study the role laminins during both skeletal and cardiac muscle development.

6.5 References

Adams, J. C. and Brancaccio, A. (2015). The evolution of the dystroglycan complex, a major mediator of muscle integrity. *Biol. Open.* **28**, 1163-1179.

Anderson, C., Thorsteinsdóttir, S. and Borycki, A. (2009). Sonic hedgehog-dependent synthesis of laminin α1 controls basement membrane assembly in the myotome. *Development* **136**, 3495-3504.

Aumailley, M. (2013). The laminin family. *Cell Adh. Migr.* **7**, 48-55.

Bajanca, F., Luz, M., Raymond, K., Martins, G. G., Sonnenberg, A., Tajbakhsh, S., Buckingham, M. and Thorsteinsdóttir, S. (2006). Integrin α6β1-laminin interactions regulate early myotome formation in the mouse embryo. *Development* **133**, 1635-1644.

Behrens, D. T., Villone, D., Koch, M., Brunner, G., Sorokin, L., Robenek, H., Bruckner-Tuderman, L., Bruckner, P. and Hansen, U. (2012). The epidermal basement membrane is a composite of separate laminin- or collagen IV- containing networks connected by aggregated perlecan, but not by nidogens. *J. Biol. Chem.* **287**, 18700-18709.

Beltrami, A. P., Urbanek, K., Kajstura, J., Yan, S. M., Finato, N., Bussani, R., Nadal-Ginard, B., Silvestri, F., Leri, A. and Beltrami, C. A. (2001). Evidence that human cardiac myocytes divide after myocardial infarction. *N. Engl. J. Med.* **344**, 1750-1757.

Bentzinger, C. F., Barzaghi, P., Lin, S. and Ruegg, M. A. (2005). Overexpression of mini-agrin in skeletal muscle increases muscle integrity and regenerative capacity in laminin-α2-deficient mice. *FASEB J.* **19**, 934-942.

Carboni, N., Marrosu, G., Porcu, M., Mateddu, A., Solla, E., Cocco, E., Maioli, M. A., Oppo, V., Piras, R. and Marrosu, M. G. (2011). Dilated cardiomyopathy with conduction defects in a patient with partial merosin deficiency due to mutations in the laminin-α2-chain gene: a chance association or a novel phenotype?. *Muscle Nerve* **44**, 826-828.

Doe, J. A., Wuebbles, R. D., Allred, E. T., Rooney, J. E., Elorza, M. and Burkin, D. J. (2011). Transgenic overexpression of the α7 integrin reduces muscle pathology and improves viability in the *dy(W)* mouse model of merosin-deficient congenital muscular dystrophy type 1A. *J. Cell. Sci.* **124**, 2287–2297.

Domogatskaya, A., Rodin, S. and Tryggvason, K. (2012). Functional diversity of laminins. *Annu. Rev. Cell Dev. Biol.* **28**, 523-553.

Durbeej, M. (2010). Laminins. *Cell Tissue Res.* **339**, 259-268.

Ekblom, P., Lonai, P. and Talts, J. F. (2003). Expression and biological role of laminin-1. *Matrix Biol.* **22**, 35-47.

Gawlik, K., Miyagoe-Suzuki, Y., Ekblom, P., Takeda, S. and Durbeej, M. (2004). Laminin α1 chain reduces muscular dystrophy in laminin α2 chain deficient mice. *Hum. Mol. Genet.* **13**, 1775–1784.

Gawlik, K.I. and Durbeej, M. (2011). Skeletal muscle laminin and MDC1A: pathogenesis and treatment strategies. *Skelet. Muscle* **1**, 9.

Hohenester, E. and Yurchenco, P. D. (2013). Laminins in basement membrane assembly. *Cell Adhes. Migr.* **7**, 56-63.

Ido, H., Ito, S., Taniguchi, Y., Hayashi, M., Sato-Nishiuchi, R., Sanzen, N., Hayashi, Y., Futaki, S. and Sekiguchi, K. (2008). Laminin isoforms containing the γ3 chain are unable to bind to integrins due to the absence of the glutamic acid residue conserved in the C-terminal regions of the γ1 and γ2 chains. *J. Biol. Chem.* **283**, 28149-28157.

Ikenishi, A., Okayama, H., Iwamoto, N., Yoshitome, S., Tane, S., Nakamura, K., Obayashi, T., Hayashi, T. and Takeuchi, T. (2012). Cell cycle regulation in mouse heart during embryonic and postnatal stages. *Develop. Growth Differ.* **54**, 731–738.

Johnson, M. S., Lu, N., Denessiouk, K., Heino, J. and Gullberg, D. (2009). Integrins during evolution: Evolutionary trees and model organisms. *Biochim. Biophys. Acta.* **1788**, 779-789.

Jopling, C., Sleep, E., Raya, M., Martí, M., Raya, A. and Izpisúa Belmonte, J. C. (2010). Zebrafish heart regeneration occurs by cardiomyocyte dedifferentiation and proliferation. *Nature* **464**, 606-609.

Kikuchi, K., Holdway, J.E., Werdich, A.A., Anderson, R.M., Fang, Y., Egnaczyk, G.F., Evans, T., Macrae, C.A., Stainjer, D.Y. and Poss, K.D. (2010). Primary contribution to zebrafish heart regeneration by gata4(+) cardiomyocytes. *Nature* **464**, 601–605.

Kim, H., Yoon, C.S. and Rah, B. (1999). Expression of extracellular matrix components fibronectin and laminin in the human fetal heart. *Cell Struct. Funct.*, **24**, 19-26.

Klaffky, E., Williams, R., Yao, C. C., Ziober, B., Kramer, R. and Sutherland, A. (2001). Trophoblast-specific expression and function of the integrin α7 subunit in the peri-implantation mouse embryo. *Dev. Biol.* **239**, 161-175.

Kuang, S., Kuroda, K., Le Grand, F. and Rudnicki, M. A. (2007). Asymmetric self-renewal and commitment of satellite stem cells in muscle. *Cell* **129**, 999-1010.

LeBleu, V.S., MacDonald, B. and Kalluri, R. (2007). Structure and function of basement membranes. *Exp. Biol. Med.* **232**, 1121–1129.

Lefebvre, O., Sorokin, L., Kedinger, M. and Simon-Assmann, P. (1999). Developmental expression and cellular origin of the laminin α2, α4, and α5 chains in the intestine. *Dev. Biol.* **210**, 135-150.

Leivo, I., Vaheri, A., Timpl, R. and Wartiovaara, J. (1980). Appearance and distribution of collagens and laminin in the early mouse embryo. *Dev. Biol.* **76**, 100-114.

Lepper, C., Partridge, T. A. and Fan, C. (2011). An absolute requirement for Pax7-positive satellite cells in acute injury-induced skeletal muscle regeneration. *Development* **138**, 3639-3646.

Li, S., Harrison, D., Carbonetto, S., Fässler, R., Smyth, N., Edgar, D. and Yurchenco, P. D. (2002). Matrix assembly, regulation, and survival functions of laminin and its receptors in embryonic stem cell differentiation. *J. Cell Biol.* **157**, 1279-1290.

Marques, J., Duarte, S. T., Costa, S., Jacinto, S., Oliveira, J., Oliveira, M. E., Santos, R., Bronze-da-Rocha, E., Silvestre, A. R. and Calado, E. (2014). Atypical phenotype in two patients with LAMA2 mutations. *Neuromuscul. Disord.* **24**, 419-424.

Meinen, S., Lin, S., Thurnherr, R., Erb, M., Meier, T. and Rüegg, M. A. (2011). Apoptosis inhibitors and mini-agrin have additive benefits in congenital muscular dystrophy mice. *EMBO Mol. Med.* **3**, 465–479.

Miner, J. H., Li, C., Mudd, J. L., Go, G. and Sutherland, A. E. (2004). Compositional and structural requirements for laminin and basement membranes during mouse embryo implantation and gastrulation. *Development* **131**, 2247-2256.

McKee, K. K., Harrison, D., Cappizi, S. and Yurchenco, P. D. (2007). Role of laminin terminal globular domains in basement membrane assembly. *J. Biol. Chem.* **282**, 21437-21447.

Nguyen, N. M. and Senior, R. M. (2006). Laminin isoforms and lung development: All isoforms are not equal. *Dev. Biol.* **294**, 271-279.

Nishimune, H., Valdez, G., Jarad, G., Moulson, C. L., Müller, U., Miner, J. H. and Sanes, J. R. (2008). Laminins promote postsynaptic maturation by an autocrine mechanism at the neuromuscular junction. *J. Cell Biol.* **182**, 1201-1215.

Nunes, A. M., Wuebbles R. D., Sarathy A., Fontelonga T. M., Deries M., Burkin D.J. and Thorsteinsdóttir S. (2017). Impaired fetal muscle development and JAK-STAT activation mark disease onset and progression in a mouse model for merosin-deficient congenital muscular dystrophy. *Hum. Mol. Genet.* **26**, 2018–2033.

Patton, B. L., Miner, J. H., Chiu, A. Y. and Sanes, J. R. (1997). Distribution and function of laminins in the neuromuscular system of developing, adult, and mutant mice. *J. Cell Biol.* **139**, 1507-1521.

Patton, B. L. (2000). Laminins of the neuromuscular system. *Microsc. Res. Techniq.* **51**, 247-261.

Ponnusamy, M., Li, P.F. and Wang, K. (2016). Understanding cardiomyocyte proliferation: an insight into cell cycle activity. *Cell Mol. Life Sci.* **74**, 1019-1034.

Qiao, C., Li, J., Zhu, T., Draviam, R., Watkins, S., Ye, X., Chen, C., Li, J. and Xiao, X. (2005). Amelioration of laminin-α2-deficient congenital muscular dystrophy by somatic gene transfer of miniagrin. *Proc. Natl. Acad. Sci. U.S.A.* **102**, 11999-12004.

Ringelmann, B., Ro, C., Hallmann, R., Maley, M., Davies, M., Grounds, M. and Sorokin, L. (1999). Expression of laminin α1, α2, α4, and α5 chains, fibronectin, and tenascin-C in skeletal muscle of dystrophic 129ReJ dy/dy mice. *Exp. Cell Res.* **246**, 165–182.

Rocheteau, P., Gayraud-Morel, B., Siegl-Cachedenier, I., Blasco, M. A. and Tajbakhsh, S. (2012). A subpopulation of adult skeletal muscle stem cells retains all template DNA strands after cell division. *Cell* **148**, 112-125.

Rooney, J. E., Knapp, J. R., Hodges, B. L., Wuebbles, R. D. and Burkin, D. J. (2012). Laminin-111 protein therapy reduces muscle pathology and improves viability of a mouse model of merosin-deficient congenital muscular dystrophy. *Am. J. Pathol.* **180**, 1593-1602.

Secco, M., Bueno, C., Vieira, N.M., Almeida, C., Pelatti, M., Zucconi, E., Bartolini, P., Vainzof, M., Miyabara, E. H., Okamoto, O. K. and Zatz, M. (2013). Systemic delivery of human mesenchymal stromal cells combined with IGF-1 enhances muscle functional recovery in *LAMA2 dy/2j* dystrophic mice. *Stem Cell Rev.* **9**, 93–109.

Sedmera, D. and Thompson, R. P. (2011). Myocyte proliferation in the developing heart. *Dev. Dyn.* **240**, 1322-1324.

Senyo, S. E., Steinhauser, M. L., Pizzimenti, C. L., Yang, V. K., Cai, L., Wang, M., Wu, T. D., Guerquin-Kern, J. L., Lechene, C. P. and Lee, R. T. (2013). Mammalian heart renewal by pre-existing cardiomyocytes. *Nature* **493**, 433-436.

Smirnov, S. P., McDearmon, E. L., Li, S., Ervasti, J. M., Tryggvason, K. and Yurchenco, P. D. (2002). Contributions of the LG modules and furin processing to laminin-2 functions. *J Biol Chem.* **277**, 18928-18937.

Smyth, N., Vatansever, H. S., Murray, P., Meyer, M., Frie, C., Paulsson, M. and Edgar, D. (1999). Absence of basement membranes after targeting the LAMC1 gene results in embryonic lethality due to failure of endoderm differentiation. *J. Cell Biol.* **144**, 151-160.

Spenlé, C., Simon-Assmann, P., Orend, G. and Miner, J. H. (2013). Laminin α5 guides tissue patterning and organogenesis. *Cell Adh. Migr.* **7**, 90-100.

Sztal, T., Berger, S., Currie, P. D. and Hall, T. E. (2011). Characterization of the laminin gene family and evolution in zebrafish. *Dev. Dyn.* **240**, 422-43.

Tajbakhsh, S. (2009). Skeletal muscle stem cells in developmental versus regenerative myogenesis. *J. Intern. Med.* **266**, 372-389.

Taniguchi, Y., Ido, H., Sanzen, N., Hayashi, M., Sato-Nishiuchi, R., Futaki, S. and Sekiguchi, K. (2009). The C-terminal region of laminin β chains modulates the integrin binding affinities of laminins. *J. Biol. Chem.* **284**, 7820-7831.

Thorsteinsdóttir, S. (1992). Basement membrane and fibronectin matrix are distinct entities in the developing mouse blastocyst. *Anat. Rec.* **232**,141-149.

Thorsteinsdóttir, S., Deries, M., Cachaço, A.S. and Bajanca, F. (2011). The extracellular matrix dimension of skeletal muscle development. *Dev. Biol.* **354**, 191-207.

Tierney, M. T., Gromova, A., Sesillo, F.B., Sala, D., Spenlé, C., Orend, G. and Sacco, A. (2016). Autonomous extracellular matrix remodeling controls a progressive adaptation in muscle stem cell regenerative capacity during development. *Cell Rep.* **14**, 1940–1952.

Tsiper, M. V. and Yurchenco, P. D. (2002). Laminin assembles into separate basement membrane and fibrillary matrices in Schwann cells. *J. Cell. Sci.* **115**, 1005-1015.

Van Ry, P. M., Minogue, P., Hodges, B. L. and Burkin, D. J. (2013). Laminin-111 improves muscle repair in a mouse model of merosin-deficient congenital muscular dystrophy. *Hum. Mol. Genet.* **23**, 383-396.

Wang, J., Hoshijima, M., Lam, J., Zhou, Z., Jokiel, A., Dalton, N. D., Hultenby, K., Ruiz-Lozano, P., Ross, J. Jr., Tryggvason, K. and Chien, K. R. (2006). Cardiomyopathy associated with microcirculation dysfunction in laminin alpha4 chain-deficient mice. *J. Biol. Chem.* **281**, 213-220.

Xu, R., Chandrasekharan, K., Yoon, J.H., Camboni, M. and Martin, P. T. (2007) Overexpression of the cytotoxic T cell (CT) carbohydrate inhibits muscular dystrophy in the *dy^{W}* mouse model of congenital muscular dystrophy 1A. *Am. J. Pathol.* **171**, 181-199.

Yurchenco, P. D. (2015). Integrating activities of laminins that drive basement membrane assembly and function. *Curr. Top. Membr*. **76**, 1-30.